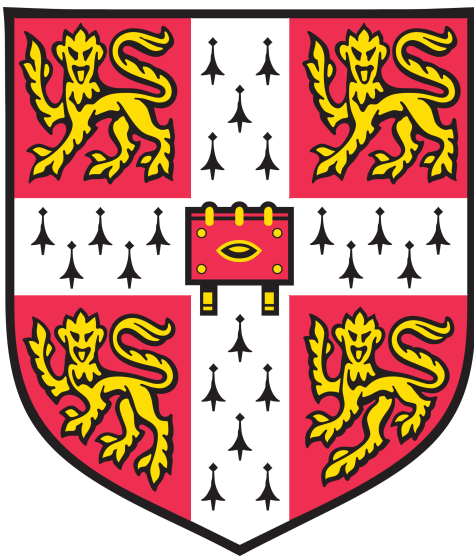# Investigating the calcium wave and actin dynamics at *Drosophila* egg activation

Anna Henrietta York-Andersen

Department of Zoology

St John's College

University of Cambridge

August 2018

This dissertation is submitted for the degree

of Doctor of Philosophy

Abstract

Investigating the calcium wave and actin dynamics at Drosophila egg activation

Anna Henrietta York-Andersen

Egg activation is a series of highly coordinated processes that prepare the mature oocyte for embryogenesis. Typically associated with fertilisation, egg activation results in the resumption of the cell cycle, expression of maternal mRNAs and cross-linking of the vitelline membrane. While some aspects of egg activation, such as initiation factors in mammals and environmental cues in sea animals, have been well-documented, the mechanics of egg activation in many animals are still not well understood. This is especially true for animals where fertilisation and egg activation are unlinked.

In order to elucidate how egg activation is regulated independently of fertilisation, I use *Drosophila melanogaster* as a model system. This insect provides extensive genetic tools, ease of manipulation for experimentation and is amenable for imaging. Through visualisation of calcium, Processing bodies and meiotic spindles, I show that osmotic pressure acts as an initiation cue for the calcium wave and downstream processes, including the resumption of cell cycle and the dispersion of the translational repression sites. I further show that aquaporin channels, together with external sodium ions, play a role in coordinating swelling of the oocyte in response to the osmotic pressure.

I proceed to identify the requirement of internal calcium sources together with a dynamic actin cytoskeleton for a calcium wave to occur. Through co-visualisation of calcium and actin, I provide the first evidence that the calcium wave is followed by a wavefront of non- cortical F-actin at egg activation, which requires the calcium wave. Genetic analysis supports a model where changes in osmotic pressure trigger the calcium wave via stretch- sensitive calcium channels in the oocyte membrane and the calcium wave is relayed by nearby channels via the actin cytoskeleton. My work concludes that the mechanism of egg activation in *Drosophila* is more similar to plants, compared to most vertebrates.

Declaration

The dissertation is the result of my own work and includes nothing which is the outcome of work done in collaboration except declared in the Preface and specified in the text. It is not substantially the same as any that I have submitted, or, being concurrently submitted for a degree or diploma or other qualification at the University of Cambridge or any other University or similar institution except as declared in the Preface and specified in the text. I further state that no substantial part of my dissertation has already been submitted, or, being concurrently submitted for any such degree, diploma or other qualification at the University of Cambridge or any other University or similar institution except as declared in the Preface and specified in the text. It does not exceed the prescribed word limit for the relevant Degree Committee.

Acknowledgements

Contents

Chapter 3 - Establishing the mechanism of the initiation of the calcium wave at *Drosophila* egg activation

Chapter 4 - Investigating the dynamics and function of the actin cytoskeleton at *Drosophila* egg activation

Chapter 5 - Investigating the mechanism of calcium transport at *Drosophila* egg activation

Chapter 6 Investigating mRNA localisation in *Drosophila* embryonic hemocytes   133

Chapter 7 Discussion   154

Chapter 8 References   163

List of figures

List of tables

Abbreviations

AB	Activation buffer
ABP	Actin-binding protein
ADP	Adenosine diphosphate
AP	Anterior-posterior
APC/C	Anaphase-promoting complex
AQP	Aquaporin
ATP	Adenosine triphosphate
ATPase	ATP hydrolase
BAPTA	1,2-bis(o-aminophenoxy)ethane-N,N,N′,N′-tetraacetic acid
Bcd	Bicoid mRNA
CaMKII	Calmodulin-dependent protein kinase II
CaN	Calcineurin
cDNA	Complementary DNA
cGMP	Cyclic guanosine monophosphate
CICR	Calcium-induced calcium release
DEG/ENaC	Degenerin epithelial sodium channel
DIG	Digoxygenin
DNA	Deoxyribonucleic acid
DUOX	NADPH oxidase
eIF	Eukaryotic translation initiation factor
ER	Endoplasmic reticulum
F-actin	Filamentous actin
FRAP	Fluorescence recovery after photobleaching
G-actin	Globular actin
GDP	Guanosine diphosphate
GECI	Genetically encoded calcium indicator
GEF	Guanine nucleotide exchange factor
GFP	Green fluorescent protein
GPCR	G-protein coupled receptor
grk	Gurken mRNA
GTP	Guanosine triphosphate

JNK	c-Jun N-terminal kinase
Hz	Hertz
ICSI	Intracytoplasmic sperm injection
IP$_3$	Inositol 1,4,5-triphosphate
IP3K	Inositol 1,4,5-Triphosphate 3-kinase
l	Litre(s)
LB	Lysogeny broth
M	Milli
M	Molar
M13	Myosin light chain kinase fragment
MAPK	Mitogen-activated protein kinase
MCP	MS2 coat protein
Min	Minute(s)
MPF	Maturation promoting factor
mRNA	Messenger RNA
n	Nano
NA	Numerical aperture
NADPH	Nicotinamide adenine dinucleotide phosphate
NCX	Na$^+$/Ca^{2+} exchanger
nos	Nanos mRNA
osk	Oskar mRNA
Osm	Osmoles
P bodies	Processing bodies
PBS	Phosphate-buffered saline
PBT	PBS and Tween-20
PFC	Posterior follicle cell
PIP$_2$	Phosphatidylinositol 4,5-biphophate
PLC	Phospholipase C
PMCA	Plasma membrane calcium ATPase
RAF	Rapidly accelerated fibrosarcoma
Rho	Ras homologous gene
RNA	Ribonucleic acid
RNAi	RNA interference
RNP	Ribonucleoprotein complex
RPK	Ripped-pocket

RVD	Regularoty volume decrease
RyR	Ryanodine receptor
Sec	Second(s)
SERCA	Sarcoendoplasmic reticulum calcium ATPase
SFK	Src-family protein tyrosine kinase
SH2	Src homology 2
STIM	Stromal-interacting molecule(S)
TRP	Transient receptor potential channel
UAS	Upstream activation sequence
UTR	Untranslated region
UV	Ultraviolet
WASp	Wiskott–Aldrich Syndrome protein
WAVE	WASp family verprolin-homologous protein
YFP	Yellow fluorescent protein
ZBP	Zipcode binding protein
μ	Micro

Chapter 1

General introduction

1.1 Egg activation overview

The mature oocyte is a specialised cell, which is arrested at a specific stage of meiosis and is ready to be fertilised by a parental gamete. Upon fertilisation, the mature oocyte undergoes a series of highly coordinated processes that prepare oocytes for successful embryogenesis. These events are collectively called egg activation. Egg activation is essential for the successful totipotent development of an oocyte, which is ensured by the resumption of the cell cycle, changes in maternal gene regulation and cross-linking of the vitelline membrane (Stricker, 1999; Horner and Wolfner, 2008).

The molecular event that unifies egg activation in all animals is an increase in intracellular calcium (Stricker, 1999). Typically initiating from the point of sperm entry, this calcium increase propagates as a wavefront across an entire oocyte at speeds ranging from 5 to 30µm/s (Jaffe, 2002; Jaffe, 2008; Stricker, 1999). The first calcium wavefront was visualised with aequorin photoprotein in medaka fish eggs (Gilkey et al., 1978). With the development of calcium dyes and genetic tools, the calcium wavefront is now visualised and well-characterised in most animals. The calcium wavefront can take one of two morphological forms: a single wave as documented as in echinoderms, zebrafish, *Xenopus* and cnidarians; or multiple oscillations in ascidian and mammalian eggs (Stricker, 1999). The calcium oscillations in mammalian oocytes have been shown to last for several hours and are required for cell cycle coordination (Miyzaki et al., 1986; Miyazaki et al., 1992; Nagano et al., 1997). Although an increase in calcium at egg activation is a conserved event, the mechanism of the calcium wave or oscillations differs between organisms. This introduction will summarise the key themes relating to egg activation. These include how the fertilisation and non-fertilisation cues initiate events of egg activation, what is the source of calcium and how calcium coordinates the downstream processes after egg activation.

1.2 Fertilisation as an initiation cue of egg activation

The entry of sperm into the female gamete acts as an initiation cue of egg activation in many animals, including ascidians, echinoderms, *Xenopus* and mammals (Stricker, 1999). There are two leading models for fertilisation-induced calcium increase at egg activation: (1) the receptor-binding model; and (2) the soluble-factor model.

1.2.1 Receptor-binding model

The receptor-binding model argues that a calcium increase is initiated by the sperm binding to the plasma membrane of the egg. In order to achieve successful recognition, the egg surface expresses species specific factors to mediate the sperm binding during the acrosomal reaction (Wyrick et al., 1974, Wassaman, 1999). The sperm is hypothesised to bind a surface receptor on the oocyte and to activate the cytoplasmic Phospholipase C (PLC) enzyme, which is known to hydrolyse Phosphatidylinositol 4,5-bisphosphate (PIP_2) into Inositol 1,4,5-trisphosphate (IP_3) (Fukami et al., 2010). IP_3 subsequently binds and activates the IP_3 receptor on the endoplasmic reticulum (ER), releasing intracellular calcium into the cytosol. The PLC is activated by ligand binding to the G-protein coupled receptor (GPCR) and subsequent G-protein translocation (Fukami et al., 2010). GPCR and PLC activation are thought to be key to the calcium release at fertilisation, which is supported by the previous discovery of the potential receptor, Bindin protein, on the plasma membrane of the sea urchin eggs (Foltz and Shilling, 1993). The requirement of the GPCR is further supported by the injection of a guanosine triphosphate (GTP) analogue, which causes calcium oscillations in golden hamster eggs or exocytosis of the cortical granules in sea urchin eggs (Turner et al., 1986; Miyazaki, 1988). Furthermore, intracellular calcium changes are inhibited in the presence of the guanosine diphosphate (GDP) analogue (Turner et al., 1986; Miyazaki, 1988). However, the requirement of the GPCR and PLCβ was later disproved by the evidence that the GDP analogue had non-specific action on other components (Crossley et al., 1991).

3

With the role of PLCβ in question, new data from starfish and sea urchins indicated that, in fact, sperm binding causes the activation of PLCγ via Src-family protein tyrosine kinase (SFK). This was supported by the injection of PLCγ or SFK interfering SH2 domains into starfish and sea urchin eggs, which prevented a calcium increase at fertilisation (Abassi et al., 2000; Runft et al,. 2004). SFK was suggested to up-regulate PLCγ activity to hydrolyse PIP_2 into IP_3, and to mediate a calcium increase at fertilisation (Shearer et al., 1999, Jaffe et al., 2001; Runft et al., 2004). Altogether, the requirement of SFK and PLCγ was shown to be essential in sea urchin, zebrafish, starfish and ascidian oocytes (Carroll et al., 1997, Runft et al., 1999, Shearer et al., 1999; Kinsey et al., 2003). Despite this research, the identity of the receptor on the plasma membrane of these oocytes remains unknown, and hence the receptor-binding model remains controversial in the fertilisation field .

1.2.2 Soluble-factor model

While PLCγ plays an important role at fertilisation in some animals, it does not explain how fertilisation is directly linked to a calcium increase at egg activation. Compared to sea urchin oocytes, the injection of inhibitory SH2 domains did not block fertilisation in frogs or mammals (Mehlmann et al., 1998; Runft et al., 1999; Mehlmann and Jaffe 2005). Data from these model systems has led to a soluble-factor model, which argues that the fusion of a sperm to an egg results in the translocation of a soluble-factor into the cytoplasm of an egg (Runft et al., 2002; Whitaker, 2006; Miyazaki, 2006; Whitaker, 2008). The first experiments in establishing this model involved the injection of mammalian sperm extracts into the eggs, causing calcium oscillations in human, hamster and mouse oocytes (Swann, 1990; Homma and Swann, 1994; Swann 1996). Similar observations were also made in invertebrate animals, where sperm extract were able to activate Nemertean worm and ascidian oocytes (Stricker et al., 1996; McDougall et al., 2000). Together, these findings led to the conclusion that the presence of a sperm soluble-factor is able to initiate an increase in intracellular calcium and egg activation. Analysis of rabbit sperm indicated trypsin and temperature dependancy, leading to the proposal that the sperm factor was a protein (Stice and Robl, 1990). The requirement of a soluble-factor was further

supported by the observation that intracytoplasmic sperm injection (ICSI) from a single sperm cell caused calcium oscillations in human oocytes (Tesarik et al., 1994). The calcium oscillations are disrupted when sperm binds to the egg, but is not able to fuse to the membrane in mouse (Kaji et al., 2000). Furthermore, the injection of somatic cell extracts into mammalian eggs did not cause calcium oscillations (Jones et al., 2000). Together, these data argue that upon the egg-sperm fusion, a sperm soluble protein translocates into the egg's cytoplasm and initiates calcium oscillations in mammalian oocytes.

Purification and cloning experiments in mouse oocytes identified the factor as a sperm-specific isoform of PLC, known as PLC zeta (Saunders et al., 2002). The depletion of PLC zeta in sperm extracts inhibits the calcium oscillations at fertilisation (Saunders et al., 2002). The role of PLC zeta to initiate the calcium oscillations has been demonstrated further by the injection of either the protein or RNA into mouse, pig, cow and human oocytes (Saunder et al, 2002; Kouchi et al., 2004; Rogers et al., 2004; Ross et al., 2008; Ito and Kashiwazaki 2012; Nomikos et al., 2013). PLC zeta is a unique isoform of PLC as it was shown to initiate IP_3 production at resting calcium levels of 100nM (Nomikos et al., 2015). The function of PLC zeta is thus proposed to be due to the four EF-hands, X-Y catalytic and C2 domains in the protein (Nomikos et al., 2011). This data argues that the EF-hands bind calcium ions, and the X-Y catalytic domains bind PIP_2.

PLC zeta is enriched within the sperm at the site of sperm-oocyte contact and fusion (Fujimoto et al., 2004; Heytens 2009; Escoffier et al., 2016). However, in comparison to other isoforms, PLC zeta is not localised at the plasma membrane (Yu et al., 2012). There is no PLC zeta null mouse line available, but genetic knock-down using the PLC zeta RNAi line expressed in males causes disrupted and reduced calcium oscillations at fertilisation (Knott et al., 2005). To date, how PLC zeta mediates an efficient increase in the calcium oscillations at mammalian fertilisation is not clear.

In summary, the soluble-factor hypothesis is the predominant model to explain how fertilisation acts as the initiation cue of a universal calcium increase at egg activation with evidence from both vertebrate and invertebrate model systems. The fertilisation causes an increase in IP_3 and subsequent release of

intracellular calcium that propagates across the oocyte in the form of a single wave or oscillations.

1.3 Non-fertilisation initiation cues of egg activation

While fertilisation is the initiation cue of egg activation in many organisms, in some animals egg activation is independent of fertilisation. Models of non-fertilisation initiation cues include changes in the external environment or the application of physical stress on the plasma membrane of the oocyte.

1.3.1 Changes in the external environment as the initiation cue of egg activation

The ionic composition of the external solution has been shown to be important in starfish *Asterina pectinifera* (Kishimoto et al., 1998; Harada et al., 2003). *Ex vivo* studies in these eggs proved the requirement of external sodium ions for the resumption of meiosis (Harada et al., 2003). Sodium is hypothesised to activate the sodium/hydrogen antiporter channel in the oocyte, facilitating the export of hydrogen ions across the plasma membrane. This results in an increase of intracellular pH and the subsequent resumption of the cell cycle. The composition of the external ionic solution has been shown to be important in another marine animal, shrimp *Siconia ingentis,* where egg activation requires the presence of magnesium ions in seawater (Lindsay et al., 1992). Interestingly, the exposure to oxygen in the air results in the resumption of meiosis in the oocytes of stick insects *Catrausius morosus* (Went, 1982). These examples show that changes in the external environment are capable of initiating the downstream events of egg activation independent of fertilisation.

1.3.2 Physical stress on the membrane as the initiation cue of egg activation

Another cue to initiate egg activation is the application of physical stress on the plasma membrane of an oocyte. Data supporting this model predominantly comes from parthenogetic insects, such as *Pimpla turionellae* (wasp), where egg activation was observed when the egg was squeezed through a polythene capillary (Went and Krause 1973; Went and Krause 1974). This physical stress is proposed to displace the maternal nucleus and to drive the resumption of the cell cycle. Parthenogetic activation was achieved when the unactivated eggs of *Drosophila mercatorum* were placed and passed through *Drosophila hydei* oviduct, suggesting that the pressure from the genital ducts is required for egg activation (Beck and Gloor, 1979; Went 1982).

The tension in the plasma membrane can also be initiated from within the egg, rather than from the external environment. The osmotic pressure model contends that the osmotic flow into the egg results in tension on the membrane and in stretching of cytoskeletal components of the egg. This change in pressure subsequently causes the calcium influx via mechanosensitive channels. The model is supported by experiments in which the addition of hypotonic solution results in egg activation of dragonfly, mayfly, turnip sawfly and yellow fever mosquito (Sawa and Oishi, 1989; Tojo and Machida, 1998; Watanabe et al., 1999, Yamomoto et al., 2013). The mosquito oocytes undergo a visible morphological darkening, which is thought to be associated with the increased production and cross-linking of the endochorion at egg activation (Li, 1994; Li and Li, 2006). The oocytes are thought to be kept in the meiotically-arrested state in the ovaries to prevent parthenogenetic activation (Yamomoto et al., 2013). Together, there is substantial data arguing that the physical pressure stimulus is able to activate eggs in many insects.

1.4 The source of calcium at egg activation

Calcium ions are a key second-messenger in many biological systems. Calcium mediates various downstream processes, including tissue contraction in

muscles, firing of action potentials in neurones, cell death and protein expression (Berridge 2000, Clapham 2007, Bootman et al., 2012). The basal calcium concentration in cells is approximately 100nM, compared to the typical extracellular concentration of 1µM. Any increase in intracellular calcium is highly coordinated, as prolonged exposure to calcium can result in cell death (Rinton et al., 2008; Celsi et al., 2009). Importantly, cells cannot produce calcium ions and therefore have to mediate the calcium influx from intracellular stores via calcium channels (Chapter 5), or the extracellular environment.

1.4.1 The role of IP$_3$ receptor at egg activation

The ER is a dynamic intracellular store, from which the calcium release is mediated by either the Ryanodine (RyR) or IP$_3$ receptors (Meldolesi, 2001; Berridge, 2002). The activation of these channels, by the ligand and calcium binding, results in an intracellular calcium increase, which propagates across a cell in a calcium-induced calcium release (CICR) manner. At egg activation, the calcium increase predominantly comes from the ER via the IP$_3$-mediated pathway. The first experiment, where purified IP$_3$ was injected into sea urchin eggs, showed a calcium wave and other hallmarks of egg activation (Whitaker and Irvine, 1984; Swann and Whitaker, 1986). The calcium release was also initiated by IP$_3$ injection into hamster eggs (Miyazaki, 1988). The inhibition of mammalian type 1 IP$_3$ receptor by the injection of an antibody in the same eggs resulted in no calcium oscillations (Miyazaki et al., 1993). Since then, IP$_3$ was shown to be a key molecule to induce calcium release at fertilisation in many eggs, including frogs, starfish and ascidians (Stricker, 1999). The proposed mechanism for the calcium release at fertilisation includes the upregulation of IP$_3$ production, IP$_3$ and calcium binding to the IP$_3$ receptor, and subsequent calcium release and propagation via a CICR mechanism (the mechanism of calcium signalling is discussed in greater detail in the Chapter 2 introduction).

1.4.2 The role of RyR at egg activation

There is also evidence that RyR contributes to the calcium release in sea urchin oocytes, as well as in ascidian and mammals oocytes (Galione et al., 1993; Lee et al., 1993; Ayabe et al., 1995; Grumetto et al., 1997; Russo et al., 1996, Wilding and Dale, 1998). Previous studies have shown that the activation of RyR, by caffeine or ryanodine stimulation, results in calcium release in echinoderm and fish eggs (Galione et al., 1993; Fluck et al., 1999; Lee et al., 1993; Santella et al., 1999; Stricker 1999). The potential cues for RyR are cyclic ADP ribose and nitric oxide, where cyclic ADP ribose was shown to induce calcium release in echinoderm eggs (Galione et al., 1993 Santella et al., 1999). The nitric oxide increase was shown to be associated with sea urchin egg activation (Kuo et al., 2000), and is thought to be linked with the cGMP pathway (Willmott et al., 1996). Overall, RyR is thought to provide a contributory calcium release alongside the IP$_3$-mediated calcium release in some eggs.

Data from all these systems strongly support the conclusion that the calcium influx from internal and external environments are not mutually exclusive. For example, in Mollusca and Nemerteans the initial calcium influx from the extracellular environment allows the propagation of the calcium wavefront via CICR (Stricker, 1996; Deguchi et al., 1996; Stricker, 1999). The external calcium also plays a role in supporting prolonged calcium oscillations by refilling the internal calcium stores in mammalian eggs (Igusa and Miyazaki, 1983; Kline and Kline, 1992; Miyazaki, 1995). In summary, an increase in intracellular calcium at egg activation is sustained by both internal and external calcium sources.

1.5 Resumption of the cell cycle in the mature oocyte

One key aspect of egg activation is the resumption of the cell cycle, which prepares the oocyte to enter embryogenesis. After the oocyte has undergone maturation, the oocyte is paused in development. Waiting for fertilisation, this arrest is ensured by an increased activity of the maturation promoting factor (MPF), which consists of a regulatory subunit Cyclin B1 and a catalytic subunit

Cdk1 (Doree and Hunt, 2000). The arrest has been shown to occur at different stages of meiosis depending on the organism. In most insect, mollusc and ascidian eggs, arrest is at metaphase I of meiosis (King, 1970; Dupre et al., 2011); mammalian and frog eggs at the metaphase II of meiosis (Fan and Sun, 2004); echinoderm and cnidarian eggs at the G1 stage of mitosis concomitant with the timing of the pronuclei formation (Dupre et al., 2011).

The key step to reverse the meiotic arrest is an increase in intracellular calcium at egg activation (reviewed in Horner and Wolfner, 2008). This resumption is mediated by the activation of anaphase-promoting complex (APC/C), which degrades the Cyclin B1 complex. Although APC/C function is well-documented, it is not quite clear how an increase in calcium is linked to APC/C activity at egg activation. One hypothesis is that calcium results in the activation of the downstream effector calmodulin-dependent protein kinase II (CaMKII), which modulates the activity of APC/C (Lorca et al., 1993; Tatone et al., 2002; Markoulaki et al., 2004).

Mammals encode four isoforms of CaMKII, including α, β, δ and γ (Ma et al., 2015). Compared to other isoforms, CaMKII γ has been shown to be essential for egg activation in mouse eggs (Backs et al., 2010). Experiments that use pharmacological or genetic   techniques to remove CaMKII result in the disruption of egg activation (Colonna et al., 1997; Galicano et al., 1997; Backs et al., 2010), and eggs fail to inhibit the activity of MAPK and Cdk1/Cyclin B, and thus remain arrested in meiosis. It is hypothesised that an increase in CaMKII activity leads to destruction of Emi2, and subsequent activation of APC/C. Together, these data support a model where a calcium increase coordinates the resumption of meiosis via the activation of APC/C at egg activation.

Another way calcium has been hypothesised to mediate the resumption of meiosis is via Calcineurin (CaN), a phosphatase linked to calcium and calmodulin activity. It was shown to be important in *Drosophila* and *Xenopus* oocytes at egg activation (Takeo et al., 2006; Horner et al., 2006; Mochida and Hunt, 2007). CaN exhibits an increase in activity similar to CaMKII at egg activation, prior to the degradation of Cyclin B (Nishiyama et al., 2007). Previous work has shown that frog eggs lacking CaN activity at egg activation

have elevated levels of Cyclin B and are unable to exit the meiotic arrest (Nishiyama et al., 2007). It is proposed that CaN acts on numerous downstream effectors, including a binding APC/C factor Cdc20 and others (Mochida and Hunt, 2007). Together, this conserved increase in activity of CaMKII and CaN, via calcium, is hypothesised to lead to full activation of APC/C and the resumption of the cell cycle at egg activation.

1.6 Modification to the outer coverings of the oocyte at egg activation

The modification in the outer layer of the oocyte is an important feature of egg activation. By providing a more stable and turgid eggshell, this aspect of egg activation prevents polyspermy and supports the early development of the egg. Calcium is known to be responsible for modifying the outer layer of the oocyte. There are two main mechanisms to modify the outer layer of an oocyte: (1) cortical granule exocytosis; and (2) cross-linking of eggshell.

1.6.1 Cortical granule exocytosis at egg activation

Most oocytes are known to have cortical granules within 0.1-1µm of the plasma membrane (Schuel, 1985; Shapiro et al., 1989). These granules are filled with enzymes such as glycosides and proteases. At egg activation, the cortical granules undergo translocation and fusion with the oocyte's plasma membrane, releasing the granular content into the perivitelline space (Tahara et al., 1996). This process is known as cortical granule exocytosis. Evidence that this process hardens the exterior of the oocyte comes from sea urchin or some mammalian oocytes, where peroxidase-type enzyme is released and cross-links the tyrosine residues in the membrane (Gulyas, 1979; LaFleur et al., 1998). Another key function of the enzymes is to cleave any remaining sperm proteins from the vitelline membrane or zona pellucida, thus preventing polyspermy.

Cortical granule exocytosis is mediated by an increase of intracellular calcium at egg activation, which can be prevented by the injection of calcium chelators into the oocyte (Kline and Kline, 1992). This process is hypothesised to involve

SNARE and synaptotagmin proteins, which are known to be modulated by calcium (Clapman et al., 1995; Clapman, 2002). Further evidence argues for the involvement of synaptotagmin in sea urchin eggs, where the visualisation of this factor showed that synaptotagmin 1 localises to the scattered cortical granules in a developing oocyte or at the cortex in the mature oocyte (Leguia et al., 2006). Immunolocalisation and Western blotting techniques have shown that Synaptotagmin plays a role in mediating the fusion of the cortical granules at sea urchin egg activation (Leguia et al., 2006). Thus, cortical granule exocytosis is an important and common mechanism to modify the outer layer of the oocyte at egg activation.

1.6.2 Cross-linking of the eggshell at egg activation

The other modification of the plasma membrane at egg activation involves the cross-linking of the eggshell layer. These changes have been shown to be mediated by a protein EGG-3 in *C.elegans* oocytes (Maruyama et al., 2007). Visualisation and knock-down studies have shown that EGG-3 recruits other factors, such as MBK-2 and CHS-1, which together form a network of proteins to increase stability of the outer eggshell layer (Maruyama et al., 2007).

Drosophila is another organism that is known to cross-link the chorion at egg activation (Waring, 2000; Horner et al., 2008). Previous work has shown that the chorion production can be induced by the application of hydrogen peroxide, suggesting the requirement of a peroxidase enzyme (Mindrinos et al., 1980). In addition, Nudel protease mutant flies fail to undergo covalent cross-linking, suggesting that Nudel might be required for the cross-linking of the chorion (LeMosy and Hashimoto, 2000). Overall, the cortical granule exocytosis and cross-linking of the outer layer are each essential processes that occur at egg activation.

1.7 Focus and outline of my PhD

It is evident that egg activation is an indispensable event in the development of any organism. The role of egg activation has been well-documented in many models systems, including worms, frogs, sea urchins and mammals (Stricker, 1999). Despite extensive research in these systems, the mechanism and the function of egg activation in insects is poorly understood. *Drosophila* has been a favoured model system for many decades to study early developmental events due to extensive availability of genetic tools, the practicality of fly husbandry and the short life cycle of the organism. My PhD will focus on using *Drosophila* as a model system to provide a better understanding of the mechanism of egg activation.

My PhD work firstly attempts to address the mechanisms of the initiation, propagation and recovery of the calcium wave. I test the requirement of calcium channels, the models of the initiation and the source of calcium. My work highlights a link between intracellular calcium changes and the hallmark downstream processes of egg activation: the resumption of the cell cycle, the translation of the maternal mRNA and changes in cytoskeletal dynamics. My work provides further evidence as to how egg activation occurs in *Drosophila,* which highlights more similarities with plants as compared to most vertebrates.

The structure of this PhD thesis will be:

Chapter 1 - General introduction

Chapter 2 - Materials and methods

Chapter 3 - Establishing the mechanism of the initiation of the calcium wave at *Drosophila* egg activation

Chapter 4 - Investigating the dynamics and function of the actin cytoskeleton at *Drosophila* egg activation

Chapter 2

Materials and methods

2.1 Fly husbandry

The fly stocks were raised on Iberian recipe fly food at 18°C, 21°C or 25°C. The stocks were kept in vials and flipped every 3-4 weeks. To expand stocks for experiments, the flies were transferred to bottles containing Iberian recipe fly food, and flipped as required. For dissection of the mature oocytes, female flies were fattened with additional yeast and water for 36-48 hours at 25°C.

2.2 Fly strains

The following fly strains were used for this project:

	Fly line	Genotype	Bloomington number/ Reference
1	MyrGCaMP5	UASt-MyrGCaMP5/Tm3	Melom et al., 2013
2	GCaMP3	matalpha-GAL4::VP16; UASp-GCaMP3/cyo	Kaneuchi et al., 2015
3	Tubulin-GaL4	tub-GAL4VP16 ; Sco/cyo	Lee et al., 1999
4	OregonR		
5	Water-witch RNAi	y1 sc* v1; P{TRiP.HMC03264}attP2	51503
6	Water-witch mutant	y1 w67c23; P{EPgy2}mRpS9EY20195 wtrwEY20195	22370
7	Ripped-pocket RNAi	y1 sc* v1; P{TRiP.HMS01973}attP40	39053
8	Painless mutant	w*; P{EP}painEP2251	31432
9	Trpm mutant	y1 w67c23; P{EPgy2}TrpmEY01618/cyo	15365
10	IP$_3$ mutant	w*; ltp-r83Asv35/TM6B, Tb1	30740
11	IP$_3$ mutant	w*; ltp-r83Aka901/TM6B, Tb1	30741
12	Prip mutant	y1; P{SUPor-P}PripKG08662	14750
13	Prip RNAi	y1 sc* v1; P{TRiP.GLC01619}attP2	44464
14	Prip RNAi	y1 v1; P{TRiP.HMC03097}attP40	50695
15	SERCA mutant	SERCAKum170/CyO	26700
16	F-tractin (2nd chromosome)	w*; P{UASp-F-Tractin.tdTomato}15A/SM6b; MKRS/TM2	58989
17	F-tractin (3rd chromosome)	w*; snaSco/CyO; P{UASp-F-Tractin.tdTomato}10C/TM2	58988
18	Lifeact - mCherry	w;;UAS-lifeact::mCherry	A. Rosdal (Isabel Palacios)
19	Ressille::GFP	w;Resille::GFP/CyO;MKRS/TM6b	Maik Drechsler
20	ER marker	(1)G0320::YFP	Lye et al., 2014
21	Mitochondria marker	mRpS9::YFP	Lye et al., 2014
22	Golgi marker	YFP::Rab6	62544
23	Sarah mutant	sarah A108/Tm3	Mariana Wolfner
24	Sarah mutant	sarah A426/Tm3	Mariana Wolfner
25	Act42A MS2	UASp-actin42AMS2/TM3 Sb	Daniel St Johnston
26	MCP-GFP	P[w+ UASt MCP-GFP] 8c / CyO	Liz Gavis
27	Hemocyte marker	srp-GAL4, UAS-GFP; crq-GAL4, UAS-GFP	Helen Skaer
28	P body marker	Me31B::GFP	Nakamura et al., 2001
29	Prip deficiency	Df(2R)BSC160/CyO	9595
30	IP$_3$ RNAi	P{TRiP.HMC03351}attP40	51795
31	IP$_3$ RNAi	P{TRiP.GLC01786}attP40	51686

Table 2.1. The list of *Drosophila* fly lines used in this project.

2.3 Preparation of mature oocytes for live imaging

The mature oocytes were dissected from fattened fly ovaries using a probe and fine tweezers (Fine Science tools) as described previously (Weil et al., 2012). The mature oocytes were teased out of the ovary taking care not to puncture the eggs. The oocytes were placed in series 95 halocarbon oil on 22x40 or 22x50 cover slips. The oocytes were aligned parallel to each other with a probe to maximise the acquisition area for imaging. A crosshair was drawn around the sample for ease of location once on the scope. Excess ovarian tissue was removed with a probe. The oocytes were left to settle for 10-15 minutes before imaging. The protocol was adopted from *York-Andersen et al., 2016, JoVE*.

2.4 *Ex vivo* egg activation, solutions and pharmacological treatments

The mature oocytes were activated *ex vivo* using activation buffer (AB): 260mOsm (3.3 mM NaH_2PO_4, 16.6 mM KH_2PO_4, 10 mM NaCl, 50 mM KCl, 5% polyethylene glycol 8000, 2 mM $CaCl_2$, brought to pH 6.4 with a 1:5 ratio of NaOH:KOH) (Mahowald et al., 1983). Schneider's Insect Medium (Sigma-Aldrich) was used as a control solution. The oil displacement was achieved by the addition of one or two drops of the solution to the sample by a glass pipette (York-Andersen et al., 2016).

For osmolarity experiments, sucrose (Sigma-Aldrich) was directly dissolved into distilled water and the osmolarity was measured by an osmometer (Loser Osmometer MOD200Plus). The osmolarity range used was 0-570 mOsm. NaCl and KCl were used at a concentration of 25-100mM. LiCl was used at the final concentration of 100mM. The stock solutions of Thapsigargin, Cytochalasin-D and Latrunculin-A were dissolved in ethanol, and then added to AB to achieve the required final concentration. BAPTA, Sodium Orthanovanadate and Phalloidin were directly dissolved into AB.

	Pharmacological agent	Function	Final concentration	Company/Reference
1	BAPTA	Calcium chelator	10mM	Sigma
2	Thapsigargin	SERCA inhibitor	10µM	Sigma
3	Sodium Orthanovanodate	ATPase inhibitor	10mM	Sigma
4	Cytochalisin-D	Actin-capping agent	10µg/ml	Sigma
5	Phalloidin	Actin-stabilising agent	1:2000	Roche
6	Latrunculin-A	G-actin binding agent	10µg/ml	Isa Palacios Lab

Table 2.2 The list of pharmacological agents and final concentrations used in this project.

2.5 Heat shock treatment

The mature oocytes were dissected onto a 22 x 40 cover slip. The cover slip was placed on the heat block for 10-40 minutes at 40°C. Alternatively, the whole fly was placed into the 1.5ml eppendorf tube in the hot-water bath at 40°C for 40 minutes. After incubation of a whole fly, the mature oocytes were dissected onto the cover slip for imaging as described above.

2.6 Imaging

The protocol was adapted from *York-Andersen et al., 2016*. Time-series of the calcium wave at *ex vivo* activation were acquired with an inverted Leica SP5, under 20x 0.7 NA Oil immersion objective with acquisition parameters for 488 excitation and 500-570nm emission, 400Hz. Similar settings were used for: (1) F-tractin and Lifeact, for 561 excitation and 570-700nm emission, 400Hz; and (2) P bodies, for 488 excitation of 500-570nm, 200Hz. The Z-stack was taken from the shallowest visible plane of the oocyte and was acquired at 2µm per frame, 40µm deep, with a total of 20 scans per frame. The first two Z-stacks were acquired before the addition of AB and the rest of Z-stacks were acquired for a total time of 20 minutes. The time-series were presented as maximum projections of 40µm, unless stated otherwise. (York-Andersen et al., 2016).

Fluorescence recovery after photobleaching (FRAP) (Lippincott-Schwartz et al., 2001) was carried out on the cortex of the mature oocyte using a UV laser on the Olympus FV3000 microscope for 15 seconds. The photo-bleached area was

approximately 30µm x 10µm. The fluorescence recovery was recorded using the Olympus FV3000 for 20 minutes, with acquisition parameters for 488 excitation of 500-570nm, 400Hz.

All hemocyte images were acquired with an inverted Leica SP5 Confocal microscope under a 63x 1.4NA immersion objective at zoom 3.3. Acquisition parameters included two channels with emissions collection spectrums of 500-565nm and 570-655nm,1024x1024 and 10Hz, which were kept constant. The time-series were acquired at a single plane. All the acquired images were analysed with FIJI (Image J) and Affinity Designer.

2.7 Embryo collection and fixation

For embryo collection, 100-150 flies were placed in a large plastic cage with a yeasted apple juice agar plate placed at the bottom. Embryos were collected overnight at room temperature. The plate with fresh yeast was replaced on a daily basis. Embryos were washed with water into the plastic sieve and collected with a paint brush. Embryos were then dechorionated for 2-3 minutes in 50% bleach, rinsed with water to remove the bleach and carefully dried with a tissue at the bottom of the sieve (Kiehart et al., 2007). For live imaging, the embryos were placed directly on a 20x50 coverslip and covered with series 700 halocarbon oil.

Otherwise, embryos were fixed with 500µl of 4% paraformaldehyde (Sigma) and 500µl of heptane in 1.5ml eppendorf tube, and left on the rotator for 15 minutes (PTR-35 360° vertical multi-function rotator, Thomas Scientific). The bottom phase was then carefully removed and 500µl of methanol was added to the same eppendorf tube with embryo samples. Excess solution was removed from the tube and was washed with 1ml of 0.1% PBST for 30 minutes.

For some experiments, the fixation protocol was modified: (1) to contain 15% of sucrose added to 2% paraformaldehyde, compared to 4% paraformaldehyde only (Hollenbeck et al., 1987; Campbell and Holt, 2001); (2) length of fixation with 4% paraformaldehyde was reduced to 1 or 5 minutes; (3) all the stages of the protocol were carried out at 4°C.

2.8 Design of anti-sense and sense probes

Bacteria with required cDNA plasmids was acquired from the *Berkeley Drosophila Genome Project - Drosophila Gold Collection* (Table 2.3) kept at -80°C and grown in 5ml of standard Lysogeny broth (LB) medium (Bertani, 1951) in 10ml plastic tube with Ampicillin (1:1000) (Sigma-Aldrich) or Chloramphenicol (1:2000) (Sigma-Aldrich). The bacterial colony was picked with a disinfected 200µl pipette tip and placed into prepared LB medium. The tube with bacteria was left overnight in the shaker at 37°C. After the incubation, the bacterial solution was centrifuged at 13000 rpm for 10 minutes and the supernatant was removed.

cDNA was purified using a New England Biolab plasmid purification kit (T1010S). cDNA was then precipitated using a standard protocol from *Green and Sambrook, 2016.* To generate a linear cDNA for anti-sense and sense probes, the reaction mix contained: 1µl of enzymatic buffer (New England BioLabs); 1µl of the desired restriction enzyme (Table 2.4) (New England BioLabs); 1µg of cDNA; and the rest of the volume was matched with ultra pure water to give a total volume of 10µl. The linearisation reaction mix was left to incubate at 37°C for 2 hours. The cDNA was then purified with the Zymo Research DNA concentrator kit (D4003). The probe was labelled with DIG-RNA labelling kit for 2 hours, which included 700-1000ng purified cDNA template, 2µl 10x Transcription Buffer (Roche), 2µl DIG RNA labelling mix (Sigma-Aldrich), 2µl SP6, T7 or T3 RNA polymerase (Thermo Fisher Scientific) and 1µl of Protector RNase inhibitor (Sigma-Aldrich).

Gene name	Plate number	Well number	Gene number	Transcript ID	Clone ID	Vector	Antibiotic	Insert size
actin-42A	AU.66	18	CG12051	A	LD18090	pBS SK-	Amp	1645
actin-79B	AU.63	13	CG7478	A	GH04529	pOT2	Chlor	1542
actin-87E	AU.47	96	CG18290	A	RE14441	pFlc-1	Amp	1582
SCAR	AU.39	87	CG4636	A	SD02991	pOT2	Chlor	2308

Table 2.3 The list of cDNA used in this project from the *Berkeley Drosophila Genome Project - Drosophila Gold Collection.*

Gene name	Reverse (antisense) promoter	Restriction enzyme for antisense probe	Forward (sense) promoter	Restriction enzyme for sense probe
actin-42A	T7	EcoRI	T3	XhoI
actin-79B	SP6	EcoRI	T7	XhoI
actin-87E	T3	XhoI	T7	BamHI
SCAR	SP6	EcoRV	T7	XhoI

Table 2.4 The list of restriction enzymes used to design antisense and sense mRNA probes for *in situ hybridisation*.

2.9 *In situ hybridisation*

The protocol for in situ hybridisation was adapted from *Lecuyer et al., 2008*. Following embryo collection and fixation protocol from the section 2.6, embryos were treated with proteinase K (Roche) at 1:2000 dilution in 1ml 1xPBS and 0.1%Tween-20 solution (PBT) for 2 minutes at room temperature and then the reaction was stopped with 2 mg/ml glycine (Sigma-Aldrich) in PBT. The embryos were then fixed in 4% paraformaldehyde for a further 10 minutes and subsequently washed five times with 1ml PBT 2 minutes per wash. Embryos were then hybridised with a probe (1:20) in hybridisation buffer 100µl overnight at 55°C. Subsequent washes were performed with hybridisation buffer for 3 x 20 minutes at room temperature and then 3 x 20 minutes with PBT. The samples were incubated with anti-Digoxigenin-AP for 2-3 hours (conjugated to alkaline phosphatase) (1:2000) (Sigma-Aldrich) and then washed with PBT for 3 x 10 minutes. Embryos were then transferred to a siliconised watch glass 2cm x 2cm and incubated with Fast Red tablets solution (1 Fast Red tablet fully dissolved in 2ml 0.1M Tris pH 8) (Sigma-Aldrich). The solution was added to cover the embryos and the signal was developed in darkness for 30-60 minutes. Excess solution was removed and the embryos were transferred to be mounted on a slide with 15µl ProLong Gold Antifade Mountant (Thermo Fisher Scientific) and a 20 x 20 cover slip. The edges were secured with nail polish. The slides were left overnight at 4°C.

2.10 Antibody staining of embryonic hemocytes

Embryos were incubated with the primary goat anti-GFP (1:500) (Abcam, Ab6673) in PBT for 2-3 hours at room temperature. If the *in situ hybridisation* had to be performed alongside antibody staining of hemocytes, primary goat anti-GFP antibody was added together with anti-Digoxigenin-AP (section 2.9). Embryos were then washed with PBT 5 x 5 minutes. Subsequently, embryos were incubated with chicken anti-goat (488) secondary antibody (1:200) (Thermo Fisher Scientific) in PBT for 1 hour at room temperature.

2.11 Quantifications and statistical tests

The calcium wave data was analysed statistically using Fisher's exact test with P-values based on previous statistics from the Wolfner lab ($P<0.05$ considered significantly different) (Kaneuchi et al, 2015). The spindle dimensions and calcium recovery time were quantified and statistically analysed using an unpaired T-test with $p<0.05$ values showing significant difference. The number of asterisks represents the P-value: (*) $P \leq 0.05$; (**) $P \leq 0.01$; (***) $P \leq 0.001$.

F-tractin and photo-bleached area mean fluorescence intensity were quantified using Fiji tool (mean pixel value). A box of the same area was used to measure intensity at the anterior and posterior poles to avoid any dark unrepresentative areas. The values were then plotted over time in seconds.

mRNA enrichment in embryonic hemocytes was quantified by comparing antisense and sense images. Visible clumps of mRNA were identified and the number of pixels were counted within hemocytes. The particles of three pixels or less were excluded from the quantifications.

Chapter 3

Establishing the mechanism of the initiation of the calcium wave at *Drosophila* egg activation

3.1 Introduction

3.1.1 Chapter overview

Drosophila early development is divided into several stages: (1) the formation of the germarium; (2) selection of the oocyte; (3) early-mid oogenesis and (4) late oogenesis. These processes will be discussed in this introduction, which will provide a better understanding of how *Drosophila* form a mature oocyte that is able to undergo egg activation. Furthermore, this section will highlight the molecular processes that are associated with *Drosophila* egg activation, compare the differences between *in vivo* and *ex vivo* experimental approaches and discuss the current models on how egg activation is initiated in *Drosophila*.

3.1.2 Formation of the germarium

Drosophila early development occurs in the female reproductive machinery, which is composed of two ovaries, common and lateral oviducts, seminal receptacle, spermatheca, accessory gland and uterus (Hughes et al., 2018). The ovary consists of approximately 12-16 ovarioles, with the germarium at the anterior half of the ovary, and the egg chambers undergoing development towards the posterior end of the ovary (Figure 3.1A) (reviewed in Kirilly and Xie, 2007). The germarium is considered as the starting point of *Drosophila* oogenesis, with the stem cells in the anterior dividing asymmetrically to produce a daughter germ stem cell and a cystoblast (Lin and Spradling, 1993). The cystoblast subsequently undergoes four mitotic divisions to produce 16 cells, which arrest at prophase I (Lin and Spradling, 1993; Page and Hawley, 2001; Resnick et al., 2009). The 16 cells undergo incomplete cytokinesis and are connected by actin-rich cytoplasmic bridges known as ring canals (Figure 3.1B). The number of ring canals differs between the cells. The first two cells generated have four ring canals, one of which is selected to become an oocyte.
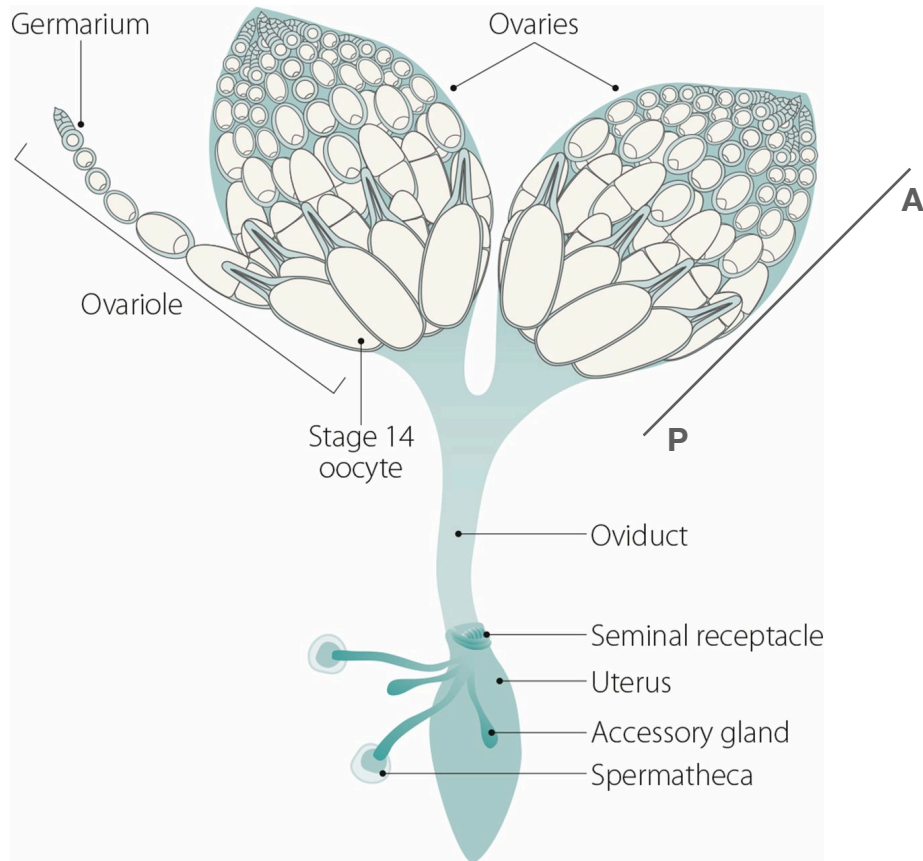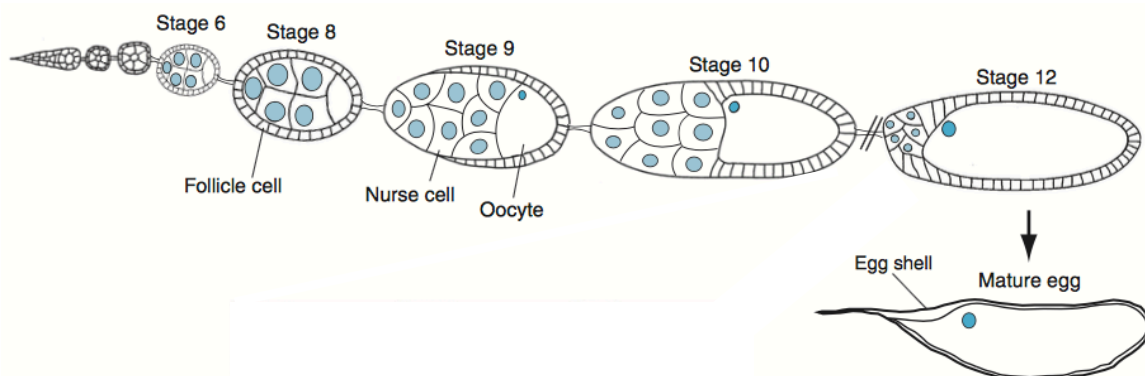
Figure 3.1. *Drosophila* oogenesis and female reproductive system.
(A) *Adapted from Hughes et al., 2018. Drosophila* female reproductive machinery is composed of two ovaries, two lateral oviducts joined into one common oviduct, seminal receptacle, uterus, accessory gland and spermatheca. The anterior of the ovary contains younger stages of egg chambers in the germarium, with older stages closer to the posterior of an ovary. Stage 14 oocytes are located near the entrance to the lateral oviduct with their posterior poles pointing towards the oviduct.
(B) *Adapted from Becalska and Gavis, 2009. Drosophila* oogenesis is divided into 14 morphological stages. The nurse cells nuclei are represented in blue. The nurse cells and the oocyte are encompassed by an epithelial monolayer of follicle cells. The final stage of oogenesis is referred as stage 14.

3.1.3 Selection of the oocyte

The specification and selection of the oocyte is not a well-understood process, but is suggested to depend on the intrinsic polarity of the fusome, a cellular structure that interconnects the cells via the ring canals (Lin and Spradling, 1995; Mckeavin, 1997; de Cuevas and Spradling, 1998). It is proposed that the fusome organises the polarity of the microtubule cytoskeleton and becomes separated between all cells within a cyst. The pro-oocyte that inherits the most fusome material is likely to be specified as the oocyte. Further work has highlighted the requirement of Egalitarian and Bicaudal-D proteins in the oocyte selection, as the mutants of these factors form cysts with 16 nurse cells without the oocyte (Bolivar et al., 2001). These factors are hypothesised to aid the oocyte selection by the organisation of the microtubule cytoskeleton (Bolivar et al., 2001). The final product of this process results in the specification of one oocyte, with the remaining 15 cells adopting the fate of the nurse cells. The oocyte undergoes budding off at the posterior of the germarium and marks the beginning of oogenesis.

3.1.4 *Drosophila* early-mid oogenesis

After leaving the germarium surrounded by somatic follicle cells, the egg chamber undergoes coordinated development, which is classified by 14 morphological stages of oogenesis: early oogenesis (stage 1-6); mid-oogenesis (stage 7-10); late oogenesis (stage 11-14) (Weil, 2014). The egg chamber consists of the oocyte, 15 nurse cells and follicle cells. Nurse cells play an essential role in producing maternal transcripts and proteins to support an embryo until the activation of the zygotic genome (Lasko, 2012). Follicle cells form a protective monolayer of epithelial cells around the egg chamber and play a role in patterning of the embryonic axes (Wu et al., 2008).

One of the key events in early oogenesis is the localisation of *gurken (grk)* mRNA to the posterior pole of the oocyte. This localisation has been shown to occur by the action of dynein on the microtubule cytoskeleton (Gonzalez-Reys et al., 1995; Duncan and Warrior, 2002; Januschke et al., 2006). Once localised,

grk mRNA is translated to Grk protein and is secreted across the membrane to signal on the follicle cells at the posterior pole (Peri et al., 1999; Chang et al., 2008). The follicle cells that receive Grk protein acquire their fate to become the posterior follicle cells (PFC) at stage 6 of oogenesis (Neuman-Silberberg and Schupbach, 1993; Gonzalez-reys et al., 1995). Following the differentiation, PFCs send an unknown signal back and induce re-organisation of the microtubule cytoskeleton in the oocyte, with minus-ends originating from the oocyte posterior and plus-ends protruding into the nurse cells (Gonzalez-Reys and St Johnston, 1998). This results in the migration of the nucleus and re-localisation of *grk* mRNA to the dorsal-anterior corner of the oocyte, which is a key step in dorsal-ventral axis patterning (Neuman-Silberberg and Schupbach, 1993; Gonzalez-Reys et al., 1995; Zhao et al., 2012). The microtubule re-polarisation also establishes a microtubule network which facilitates mRNA active transport from the nurse cells into the oocyte from stage 7 onwards (Saxton, 2001; Weil et al., 2006; Zimyanin et al., 2008).

During mid-oogenesis (7-10a), *oskar (osk)* mRNA becomes localised at the posterior pole (Kim-Ha et al., 1991; Zimyanin et al., 2008). The visualisation of *osk* mRNA by *in situ hybridisation* in wild-type and various mutant backgrounds have shown that *osk* mRNA is responsible for mediating the anterior-posterior patterning, which includes localisation of *nanos (nos)* mRNA and the formation of the pole plasm at the posterior pole (Ephrussi et al., 1991; Rongo et al., 1995; Vanso and Ephrussi, 2002). Visualisation of *osk* mRNA using the MS2-system in live oocytes has shown that *osk* undergoes active movement in both direction on the microtubules via dynein and kinesin motors, which results in "Biased Random Walk" of *osk* to the posterior pole (Zimyanin et al., 2008). The posterior localisation is also ensured by a variety of factors, including Tropomyosin II, Barentsz and Staufen (Ephrussi et al., 1991; Micklem et al., 2000; Zimyanin et al., 2008).

In comparison to the active transport of *grk* and *osk*, pharmacological studies have shown that *nos* mRNA becomes localised at the posterior by passive-diffusion and an actin entrapment mechanism (Forrest and Gavis, 2003). However, this process is considered inefficient as approximately 96% of *nos* mRNA become degraded during embryogenesis (Bergsten and Gavis, 1999).

nos mRNA plays an important role in the formation of the pole plasm, which specifies the germline lineage in flies (Ephrussi et al., 1991; Trcek et al., 2015) . In contrast to *osk, grk* and *nos*, the majority of *bicoid (bcd)* mRNA is localised to the anterior of the oocyte during late oogenesis from stage 10b-14 (Weil et al., 2006). *bcd* mRNA is transported on the microtubule tracks by a dynein motor and becomes anchored by the actin cytoskeleton at the end of oogenesis (Weil et al., 2006). Genetic studies have shown that this localisation requires direct and indirect factors, including Swallow, Exuperantia and Staufen (St Johnston et al., 1989; Weil et al., 2010). Co-visualisation and pharmacological studies have shown that *bcd* mRNA, together with a direct factor Staufen, is transported on the microtubules and localised to the anterior of the oocyte (Weil et al., 2006). The mutant background of an indirect factor Swallow has been shown to result in mislocalisation of *bcd* mRNA in mid-oogenesis, but not directly involved in transport of *bcd* (Weil et al., 2010). It is hypothesised that Swallow is instead involved in modulating the cortical actin cytoskeleton at the membrane, thus indirectly coordinating *bcd* localisation at the anterior (Weil et al., 2010). Together, these findings highlight the importance of mRNA localisation at the anterior and posterior poles of the oocyte in setting up future embryonic axes of the *Drosophila* oocyte.

3.1.5 *Drosophila* late oogenesis and morphology of the mature oocyte

Towards the completion of oogenesis, nurse cells extrude their cytoplasm into the oocyte in the coordinated process called nurse cell dumping and subsequently undergo programmed cell death (King, 1970; Spradling 1993; Peterson and McCall, 2013). Although this mechanism is not fully-understood to date, it is proposed that nurse cell death is mediated by redundant interactions between apoptosis, cell autophagy and programmed necrosis (Cummings and King, 1970; McCall, 2004; Bass et al., 2009). By the last stage of oogenesis, the nurse cell nuclei are degraded, resulting in a mature oocyte surrounded by a layer of the follicle cells (stage 14 egg chamber) (Figure 3.2).

The follicle cells play an important role in the formation of numerous structures characteristic of the mature oocyte: (1) perivitelline membrane; (2) outer

eggshell layer chorion; (3) dorsal appendages; and (4) micropyle (Figure 3.2). During late oogenesis, the follicle cells are responsible for building a protective layer for the oocyte, which consists of the perivitelline membrane and the outer chorion layer (King, 1970; Mahowald and Kambysellis, 1980). The follicle cells secrete a vast number of factors into the extracellular matrix via the vitelline body vesicles, which coordinate production of the outer layer of a mature oocyte (Margaritis et al., 1980; Margaritis, 1985; Cavaliere et al., 2008). As the perivitelline membrane surrounds the oocyte by stage 14, it forms a perivitelline space between the oocyte and itself (Figure 3.2). The composition of the perivitelline space in the oocyte is currently unknown, but has been shown to consist of different ions, including calcium, in the early *Drosophila* embryo (Van der Meer and Jaffe, 1983).

In addition, the specialised type of follicle cells, roof and floor cells, are responsible for the formation of the dorsal appendages (breathing tubes) at the anterior pole of an oocyte (Ward and Berg, 2005). These cells become specified earlier in oogenesis by Grk protein, which upregulates RAS/RAF/MAPK pathways (Perri et al., 1999). Immunostaining and visualisation data have shown that these epithelial cells subsequently undergo extensive morphogenetic movements, resulting in the elongated tubule formation of the dorsal appendages (Ward and Berg, 2005). A different population of the follicle cells, known as border cells, undergo centripetal movement towards the anterior pole of an egg chamber and form a micropyle, a site of the sperm entry (Montell et al, 1992; Montell et al., 2012). Previous work has shown that the laser ablation of the border cells disrupts the micropyle at the anterior (Montell et al., 1992). Further experiments have shown that overexpression of the factors in JNK pathway, such as *puckered,* in non-differentiated follicle cells, results in the formation of the micropyle-like structure (Suzanne et al., 2001). Therefore, the follicle cells adopt different fates depending on the signal they receive and coordinate development of many essential structures within an oocyte to support early embryogenesis.

With the removal of nurse cells and the coordinated events of the follicle cells, the final product of oogenesis is a mature oocyte located at the posterior of the

ovaries near the entrance to the lateral oviduct, awaiting to undergo egg activation (Figure 3.1 A).
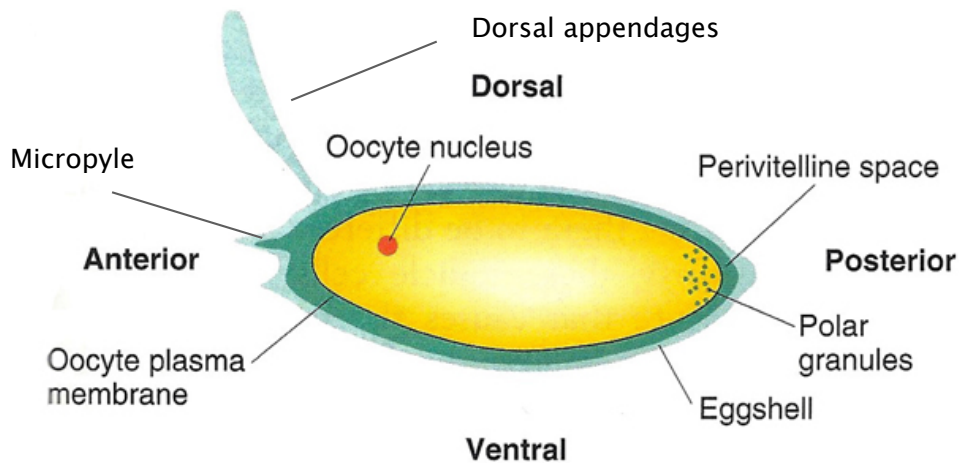
Figure 3.2. *Drosophila* **mature oocyte morphology.**
Adapted from Biol 202 notes, lecture 21, 2013. Drosophila mature oocyte (stage 14) is encompassed perivitelline space, formed by the perivitelline membrane (darker green). The outer layer is the chorion eggshell (lighter green). The micropyle and the dorsal appendages are at the anterior of the oocyte. The oocyte nucleus (red) is arrested at the Metaphase I and is located near the cortex towards the dorsal appendages.

3.1.6 Resumption of the cell cycle at *Drosophila* egg activation

In *Drosophila*, egg activation is independent of fertilisation, and occurs in the female oviduct at ovulation (Doane, 1960; Heifeitz et al., 2001). Prior to egg activation, *Drosophila* developmental arrest at metaphase I of meiosis, otherwise known as oocyte maturation, depends on the elevated activity of Cdk1/Cyclin B (Von Stetina et al., 2008). This is evidenced by oocytes that lack Cdk1, or co-regulators of Cdk1, which exhibit disrupted meiotic maturation (Xiang et al., 2007; Von Stetina et al., 2008). The resumption of meiosis occurs at egg activation and is coordinated by the degradation of Cyclin B, which is a conserved event in most of the eggs (Swan and Schupbach, 2007). Previous work has shown that oocytes that are unable to degrade Cyclin B do not resume meiosis and remain arrested in metaphase I (Swan and Schupbach, 2007). The degradation of Cyclin B is mediated by APC/C, which is activated by a factor called Cortex Cdc20, a specific oocyte isoform (Pesin and Orr-Weaver, 2007). However, APC/C does not become activated in the mutants of *Drosophila* calcipressin, Sarah, and the oocytes are only able to progress up to

anaphase I, suggesting a link with calcium signalling at egg activation (Takeo et al., 2006; Horner et al., 2006).

3.1.7 mRNA translation at *Drosophila* egg activation

Another essential process of egg activation is the translation of maternal mRNAs (Stricker, 1999; Weil et al., 2008). It was shown that *Drosophila* mature oocytes are pre-loaded with maternal transcripts of 55% of the genome, many of which become translated within 30 min of deposition, suggesting a major translational activation upon egg activation (Tadros et al., 2007, Horner and Wolfner, 2008). Previous work has also shown that the number of ribosomes increases by approximately 20% following egg activation (Mahowald et al., 1983). The examples of maternal transcripts that become translated at egg activation include *bcd, hunchback, torso, smaug and string* (Tadros and Lipshitz, 2005; Tadros et al., 2007).

bcd mRNA is usually found to be localised to sites of translational repression called Processing bodies (P bodies) (Weil et al., 2012). These sites are known to lack ribosomes and to consist of numerous factors that repress the translation of mRNA. Using super-resolution microscopy, *bcd* was shown to be enriched in P bodies, but become released and translated in early embryogenesis (Weil et al., 2012). Upon egg activation, *bcd* mRNA becomes translated and forms a morphogen gradient opposing a gradient of Nanos protein emanating from the posterior, which establishes the anterior-posterior axis of the future embryo (Gregor et al., 2007; Lipshitz, 2009; Sprirov et al., 2009). It is well-understood that egg activation acts as a signal to initiate the translation of many transcripts (Tadros and Lipshitz, 2005). It has been suggested that calcium might be key in mediating this translation at egg activation as *Sarah* mutants fail to translate *bcd* at egg activation (Horner et al., 2006).

3.1.8 The visualisation of the calcium wave at *Drosophila* egg activation

Despite decades of research, an increase in intracellular calcium in the mature oocyte had not been documented until recently. Similar to other model systems, *Drosophila* egg activation is associated with an increase of intracellular calcium, which takes a form of a single wavefront (York-Andersen et al., 2015; Kaneuchi et al., 2015). The presence of the calcium wave at egg activation has been visualised in *ex vivo* dissected mature oocytes. The *ex vivo* activation is achieved by the application of hypotonic solution, called activation buffer (AB) (Mahaowald et al., 1983; York-Andersen et al., 2016), which results in the morphological changes associated with *Drosophila* egg activation, such as swelling and increased cross-linking of the vitelline membrane (Mahowald et al., 1983). The *in vivo* visualisation of the calcium wave in the oviduct of a fly was also attempted and showed an intracellular calcium increase in the mature oocyte (Kaneuchi et al., 2015). However, this approach was found to be not optimal as the anaesthetic agent "FlyNap" was used and resulted in the "unnatural" relaxation of the oviduct muscles. It was also challenging to visualise an *in vivo* increase in calcium as the fly twitched its abdomen. Therefore, the *ex vivo* egg activation was found to be a more suitable experimental approach to investigate the mechanism of the calcium increase in the *Drosophila* mature oocyte.

This calcium wave typically starts from the posterior pole of the mature oocyte and has a speed of around 1.5 µm/sec (York-Andersen et al., 2015). The calcium wave was initially visualised by the injection of calcium dyes, conjugated to fluorophores. The mature oocytes were activated *ex vivo* using AB. Ratiometric imaging showed the initiation and propagation of the calcium wave from the posterior pole upon the addition of AB (York-Andersen et al., 2015). However, this visualisation approach was not sustainable to perform further studies due to the leakage of the cytoplasm at the point of the injection.

Therefore, I utilised a less invasive approach by visualising calcium increase with a genetically encoded calcium indicator (GECI). Previous work has developed a new calcium genetic sensor GCaMP, which is composed from a circularly permutated EGFP, myosin light chain kinase fragment (M13) and a

calcium-binding protein Calmodulin (Figure 3.3) (Nakai et al., 2001). Upon an intracellular calcium increase, Calmodulin binds calcium ions and induces GCaMP to undergo a conformational change, resulting in an excitable fluorescence state (Nakai et al., 2001). Random-site mutagenesis has allowed the development of newly improved GCaMP lines in different tissues with higher calcium sensitivity and a high signal-to-noise ratio (Chen et al., 2013; Yang et al., 2018).

There are two GCaMP lines that have been used to visualise the calcium wave at *Drosophila* egg activation (Kaneuchi et al., 2015; York-Andersen et al., 2015). One of them being Myristoylated GCaMP5 (MyrGCaMP5), which is associated with the plasma membrane due to the myristoylation modification (Melom et al., 2013). MyrGCaMP5 was originally designed to be expressed in the somatic nervous system under the GaL4 promoter (Melom et al., 2013). However, MyrGCaMP5 was expressed in the germline and was found to be optimal for visualising the calcium wave at *Drosophila* egg activation (York-Andersen et al., 2015). At the same time, the Wolfner Lab developed a new recombined form of GCaMP3 that is specifically expressed in the fly germline under the germline-specific GaL4 promoter (Kaneuchi et al., 2015). Both of the indicators were compared and showed a similar calcium wave at egg activation. Therefore, for the purpose of this project, I used both of the constructs to visualise the calcium
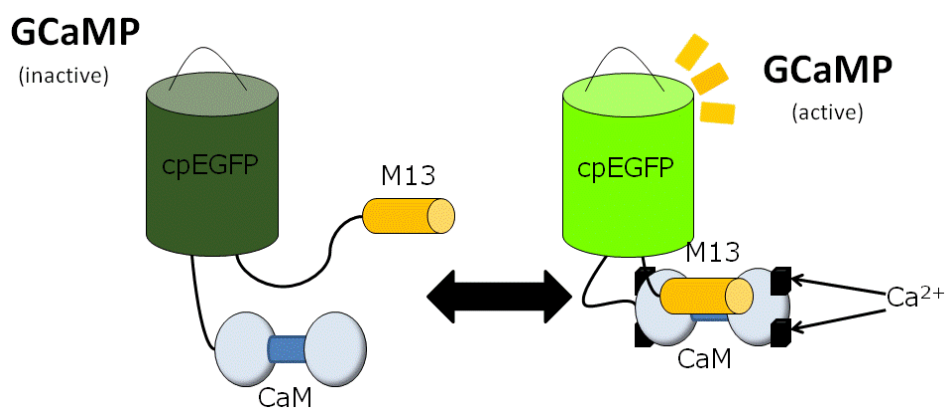
Figure 3.3. Diagram of GCaMP structure and conformational change.
Adapted from Iino Laboratory website (Oda et al., 2011; Satoh et al., 2014). GCaMP in inactive state is composed from a circularly permutated EGFP (cpEGFP) (dark green), myosin light chain kinase fragment (M13) (yellow) and a calcium-binding protein Calmodulin (blue). Upon an increase in calcium, Calmodulin binds calcium and undergoes a conformational change, which results in M13 binding and excited stage of cpEGP.

wave at egg activation depending on the experimental design, such as the genetic set-up.

3.1.9 The models for egg activation initiation in *Drosophila*

Similarly to other insects, egg activation in *Drosophila* is independent of fertilisation and was shown to occur during passage through the oviduct (Doane, 1960). There are two models in the field for *Drosophila* egg activation: (1) the physical pressure model; and (2) the osmotic pressure model. The physical pressure model proposes that the pressure exerted by the oviduct on the mature oocyte results in egg activation. The evidence supporting this hypothesis originated when the physical pulling on the dorsal appendages resulted in the resumption of the cell cycle (Endow and Komma, 1997). The model was further supported by experiments in which application of hydrostatic pressure on *ex vivo* oocytes resulted in increased cross-linking of the outer membrane tested by resistance to bleach (Horner and Wolfner 2008; Sartain and Wolfner 2013). However, my previous work has shown that physical pressure on its own is not a sufficient trigger for *Drosophila* egg activation, as suction pressure on the posterior pole did not result in any intracellular calcium changes (York-Andersen et al., 2015).

The osmotic pressure model proposes that the mature oocyte uptakes the fluid from the epithelial oviduct, which results in the oocyte swelling. This model was supported by observations that the oocytes are visibly dehydrated whilst in the ovaries, but undergo an increase in volume by the time they are deposited. In addition, the exposure of isolated mature oocytes to the external hypotonic solutions causes them to swell and initiate the calcium wave (Mahowald et al., 1983; York-Andersen et al., 2015; Kaneuchi et al., 2015). My previous work supports this model, as when the mature oocytes are exposed to distilled water, rapid swelling is observed and an increase in intracellular calcium from all over the cortex is evident (York-Andersen et al., 2015). The initiation mechanism of *Drosophila* egg activation remains unestablished. This chapter will focus on further exploring this model.

3.2 Aims of this chapter

1. **To establish the potential initiation cue of *Drosophila* egg activation.**

2. **To address whether the calcium wave depends on the extracellular ionic composition.**

3. **To establish the potential source of calcium at *Drosophila* egg activation.**

3.3 Results

3.3.1 Calcium wave phenotypes at *Drosophila* egg activation

Depending on the experimental design, the calcium waves can exhibit different phenotypes, which I classified as a full wave, partial wave, cortical increase or no wave. The "full wave" phenotype describes the calcium wave that initiates from the posterior pole and propagates across an entire oocyte (Figure 3.4A, 3.5A). This is a wild-type phenotype of the calcium wave, which is observed in 85% of the mature oocytes at *ex vivo* egg activation. In contrast, the "partial wave" phenotype describes the calcium wave that initiates from the posterior, but does not propagate across the entire oocyte and/or recovers prematurely (Figure 3.4B, 3.5B). This phenotype happens in 5% of the wild-type experiments. The "cortical increase" is classified by an increase of calcium from all round the cortex, rather than in a wavefront manner (Figure 3.4C, 3.5C). This phenotype was originally observed when the oocytes were activated with distilled water (York-Andersen et al., 2015). The "no wave" phenotype, which describes an absence of the calcium wave is observed in 10% of the wild-type experiments. (Figure 3.4D, 3.5D). I use this classification of the calcium wave phenotype, because it helps to quantify and analyse the mechanism of the calcium wave in a consistent manner across different experimental approaches.
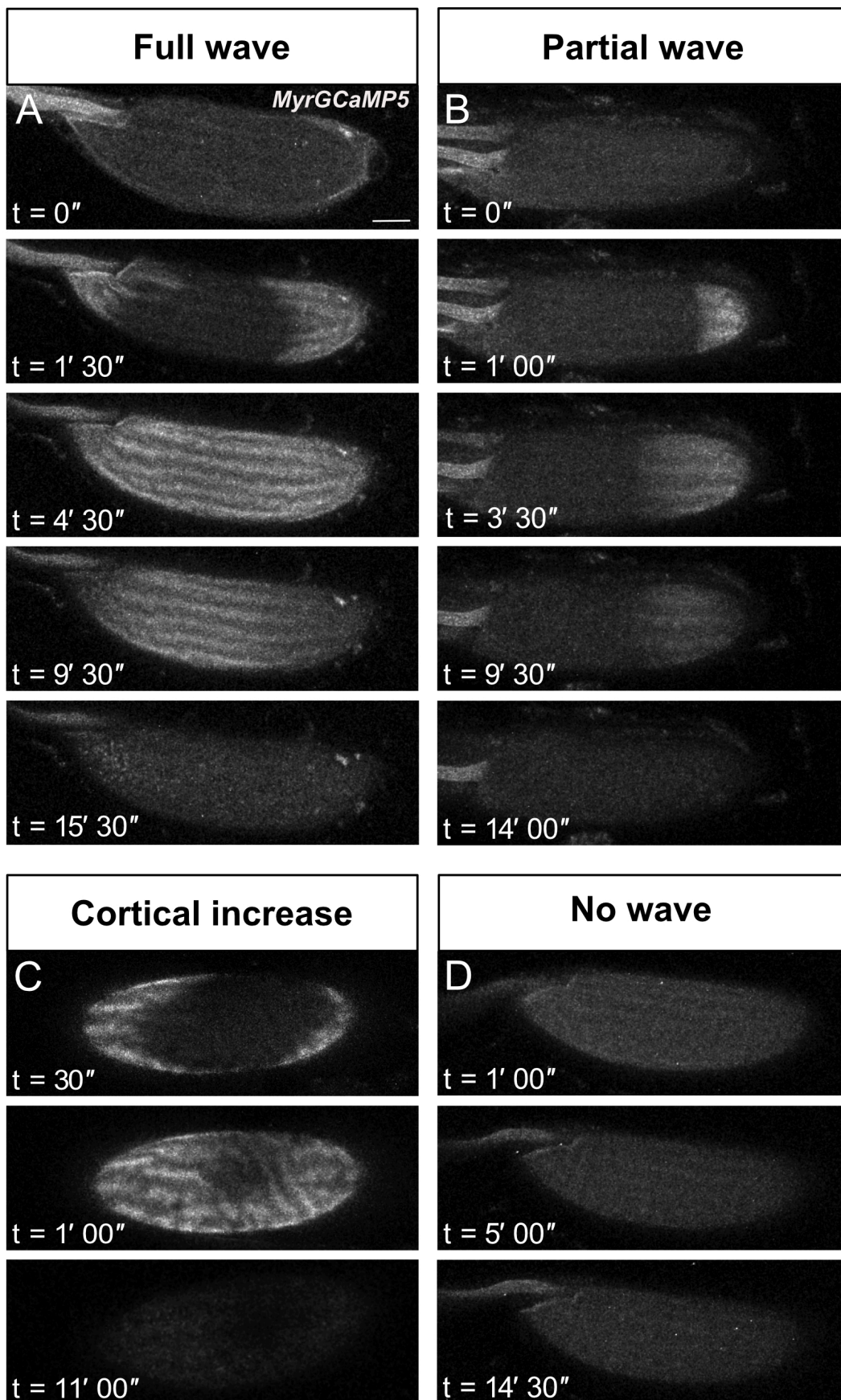
Figure 3.4. Calcium wave phenotypes in the *Drosophila* mature oocyte.
(A-D) Time-series of *ex vivo* mature oocytes expressing UAS-myrGCaMP5 following the addition of AB. (A) shows a full calcium wave; (B) shows a partial calcium wave; (C) shows a cortical calcium increase; (D) shows no calcium wave phenotype. Scale bar 60µm. Maximum projection = 40µm.
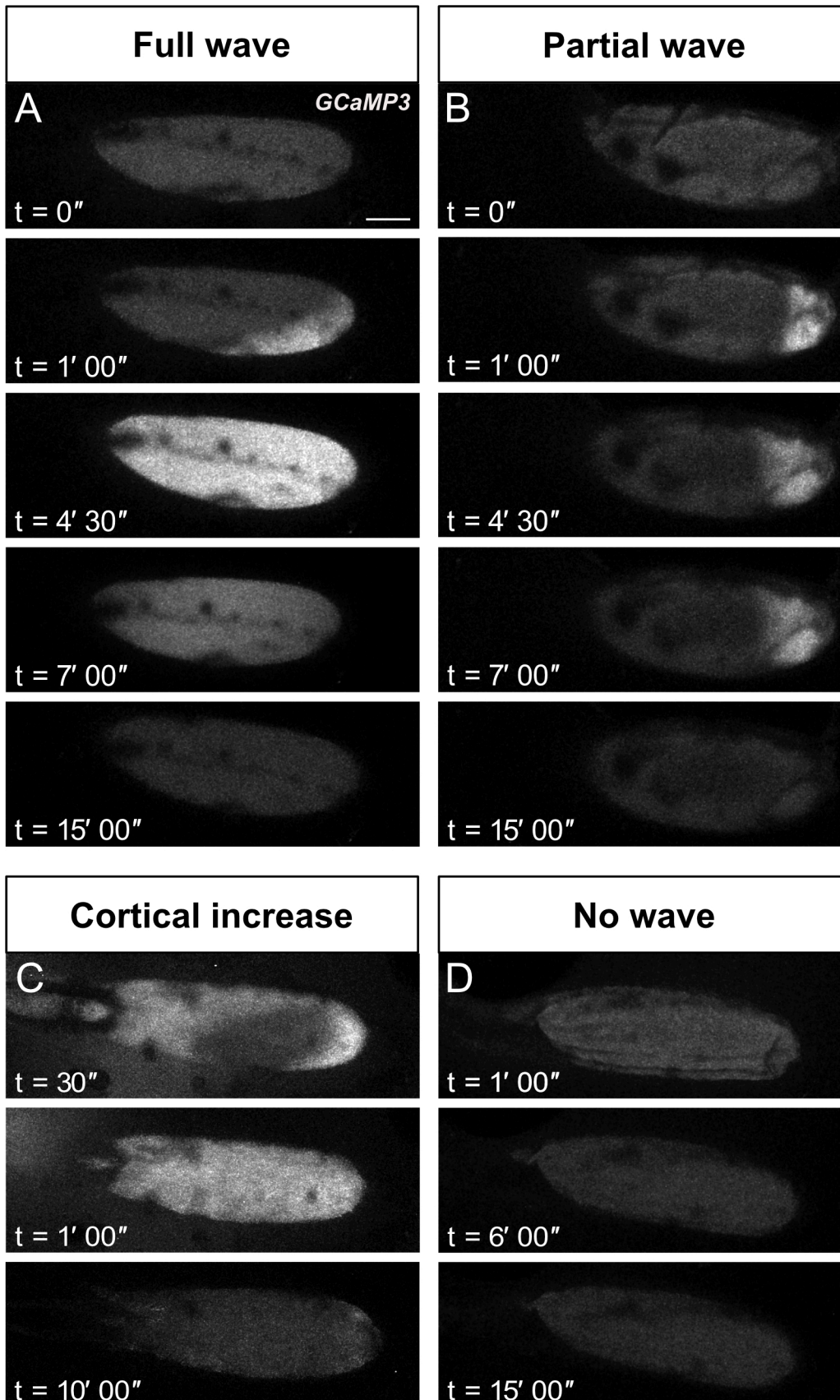
Figure 3.5. Calcium wave phenotypes in the *Drosophila* mature oocyte.
(A-D) Time-series of *ex vivo* mature oocytes expressing UAS-GCaMP3 following the addition of AB. (A) shows a full calcium wave; (B) shows a partial calcium wave; (C) shows a cortical calcium increase; (D) shows no calcium wave phenotype. Scale bar 60µm. Maximum projection = 40µm.

38

3.3.2 Swelling is required for the calcium wave initiation and propagation

My previous work has shown that physical pressure applied to the posterior pole is not sufficient to initiate the calcium wave (York-Andersen et al., 2015). This evidence, together with the observation that the mature oocytes appear dehydrated whilst in the ovary, but are swollen by the time they are deposited, suggests that swelling might play a role in the initiation and the propagation of the calcium wave at egg activation. In order to test this hypothesis, a 125 μm diameter tube was used to secure the anterior half of the mature oocyte, with the posterior pole being exposed. Upon the addition of AB, the calcium wave initiated as normal from the posterior, but did not propagate past the tube (Figure 3.6, n=15). Similarly, when the whole oocyte was placed in the tube, the calcium wave did not initiate upon the addition of AB (data not shown). The calcium wave normally encompasses the whole oocyte by 3.5 minutes, but in this case the wave did not propagate until the tube was removed. This suggests that swelling is required for the initiation and propagation of the calcium wave.
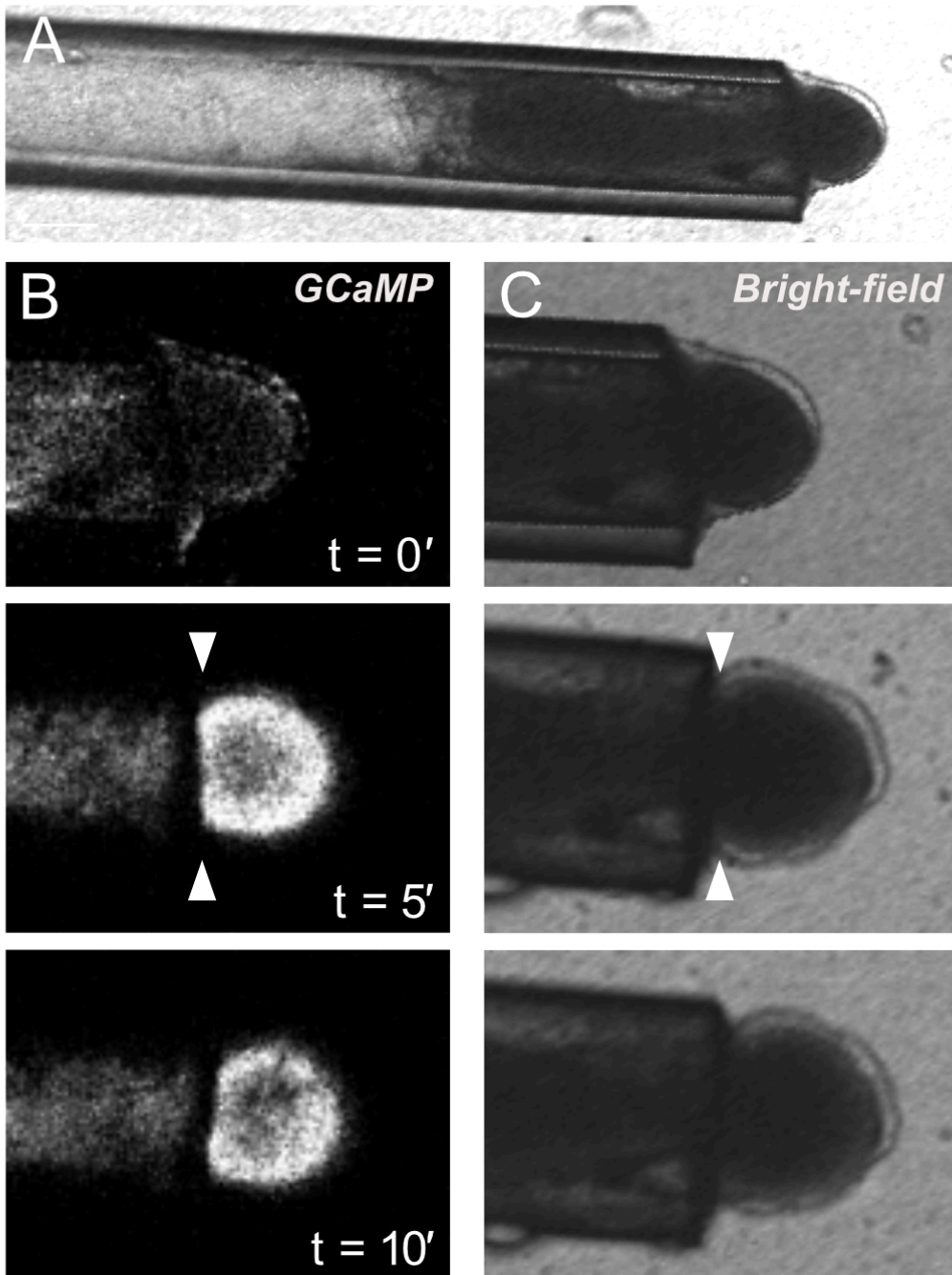
Figure 3.6 Inhibition of swelling results in the perturbed propagation of the calcium wave.
(A) Bright-field image of an *ex vivo* mature oocyte, expressing UAS-myrGCaMP5, placed in a 125 μm diameter tube. (B-C) Time-series of the same oocyte in the tube, with half of the posterior pole exposed to AB. The calcium wave initiates normally, but does not propagate past the point of the tube after 10 minutes. Scale bar 60μm. Single plane.

3.3.3 Osmotic pressure initiates the calcium wave in *Drosophila* mature oocytes

The above evidence is indicative of the requirement of swelling for the calcium wave to occur at egg activation. It is possible that, once the mature oocyte leaves the ovary and enters the oviduct, the oocyte uptakes the oviduct fluid and undergoes swelling. To test whether or not the uptake of external fluid could act as an initiation cue for the calcium wave at egg activation, *ex vivo* mature oocytes were treated with a water and sucrose solution of the same solute content as AB, measured in osmolarity (260mOsm). Sucrose is highly soluble in water and is neutrally charged, which makes it a suitable candidate for varying the osmolarity of the solution. Upon observation, the oocytes exhibited a similar proportion of the calcium wave phenotypes to AB (Figure 3.7A), suggesting that water and sucrose solution of the osmolarity 260mOsm is sufficient to cause the calcium wave at egg activation.

To further test whether the osmolarity of an external solution is important for the initiation of the calcium wave, mature oocytes were exposed to water and sucrose solutions of different osmolarities. Upon the addition of solution to the oocytes, the calcium wave phenotypes were analysed and quantified. The highest number of full calcium waves of 81% was observed at 300 mOsm, with this number declining rapidly by 573 mOsm (Figure 3.7B, blue). The highest proportion of the "cortical increase" was detected at 0 mOsm (Figure 3.7B, green). The number of oocytes with a "cortical increase" went down as the solute concentration increased (Figure 3.7B, green). The "partial" and "no wave" calcium phenotypes became more predominant with an increase in the osmolarity. This suggests that the solution of 450mOsm and higher is unable to support a calcium wave at *Drosophila* egg activation. Together, these findings suggests that the external osmolarity can impact the initiation of the calcium wave at egg activation.
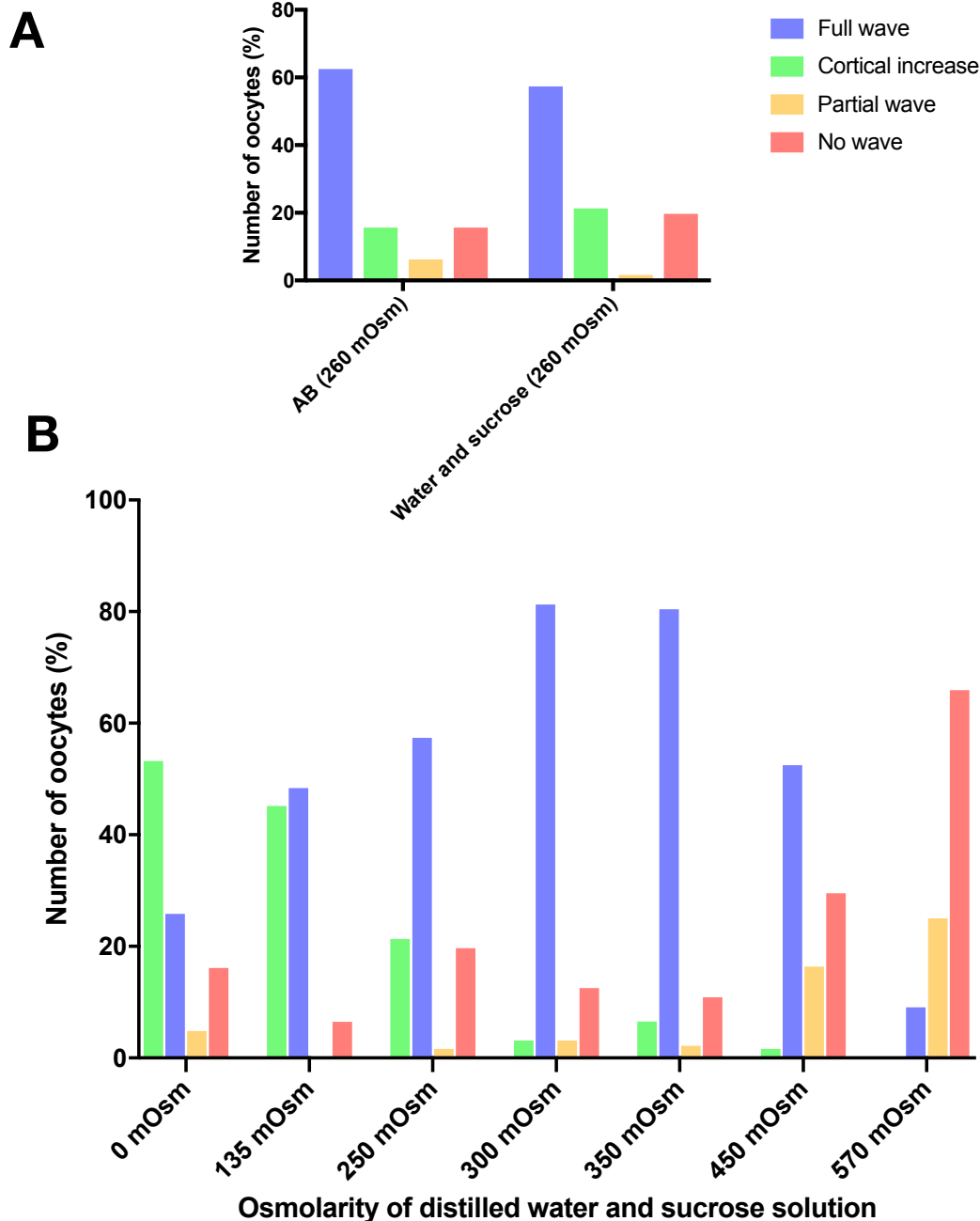
Figure 3.7 Quantification of the calcium wave phenotypes upon treatment with a solution of distilled water with sucrose.
The graph shows that AB, or water and sucrose, of 260mOsm result in a similar percentage distribution of the calcium wave phenotypes. Full wave (blue), cortical increase (green), partial wave (yellow) and no wave phenotype (red). (B) The graph shows the number of the mature oocytes activated with water and sucrose solution only, with a range of osmolarities from 0-570 mOsm. The number of full waves increases from 0mOsm, peaks at 300 mOsm and then decreases with an increase in osmolarity. The proportion of eggs that burst peaks at 0mOsm and then decreases with increase in osmolarity. The proportion of a partial wave increases with increase in osmolarity. The proportion of no wave increases with an increase in osmolarity. 300-350 mOSm is an optimal osmolarity of an external solution to cause the initiation and propagation of the calcium wave. n = 30 of oocytes per osmolarity. This data was analysed statistically using Fisher's exact test with $P<0.05$ considered significant. The proportion of full calcium waves observed at 300mOsm is significantly higher ($P<0.02$) than full waves at all measured osmolarities, except 350mOsm. The proportion of bursts observed at 0mOsm is significantly higher ($P<0.01$) than bursts at all measured osmolarities, except 135mOsm. The proportion of partial waves observed at 570mOsm is significantly higher ($P<0.01$) than partial waves at all measured osmolarities, except 450mOsm. The proportion of no waves observed at 570mOsm is significantly higher ($P<0.001$) than no waves at all measured osmolarities. *In collaboration with Part II student 2015-2016 Alex Berry.*

42

3.3.4 Osmotic pressure results in the metaphase I to anaphase I spindle transition

The meiotic spindle structure and dynamics have been well-characterised at *Drosophila* egg activation (Page and Orr-Weaver, 1997, Endow and Komma, 1997, Heifeitz et al., 2001). In a non-activated oocyte, the spindle is parallel to the cortex and is generally near the base of the dorsal appendages at the anterior pole. Previous work has shown that, upon egg activation, the meiotic spindle undergoes a dynamic morphological change within 10 minutes (Endow and Komma, 1997). This change involves contraction and an initial pivoting of the spindle and is indicative of the resumption of the cell cycle at *Drosophila* egg activation (Endow and Komma, 1997).

To address whether osmotic pressure results in the morphological change in the spindle associated with the resumption of the cell cycle, the meiotic spindle was visualised using Jupiter-mCherry and the mature oocytes were incubated with distilled water and sucrose at 260mOsm. Before activation, the spindle is of an ellipse shape (n=15) (Figure 3.8A-E), with a dark region in the middle, where the DNA is likely to reside. Upon addition of AB, or distilled water and sucrose, the spindle became more rounded with a significant increase in width (Figure 3.8B,D,G), which is indicative of spindle contraction at anaphase I. When treated with a control solution, Schneider's Insect medium, the spindles did not undergo any morphological change (Figure 3.8E-G).

In order to quantify this morphological change, the spindle width and length were measured before and after 10 min of activation. The width was measured at the widest point - halfway through the spindle length. Upon addition of AB or water and sucrose, the spindle length did not show any significant change and remained approximately 12µm, whereas the width increased by about 70% (2.1µm) (Figure 3.8G). Together, this evidence supports that osmotic pressure caused by distilled water with sucrose of 260mOsm results not only in the initiation of the calcium wave, but also in meiotic spindle transition to anaphase I.
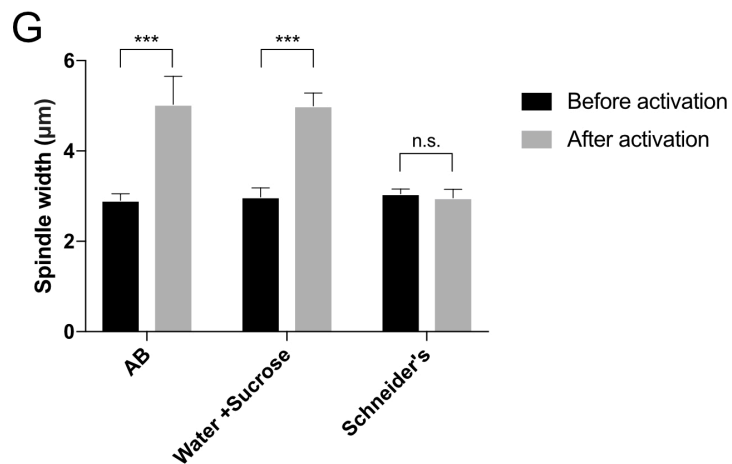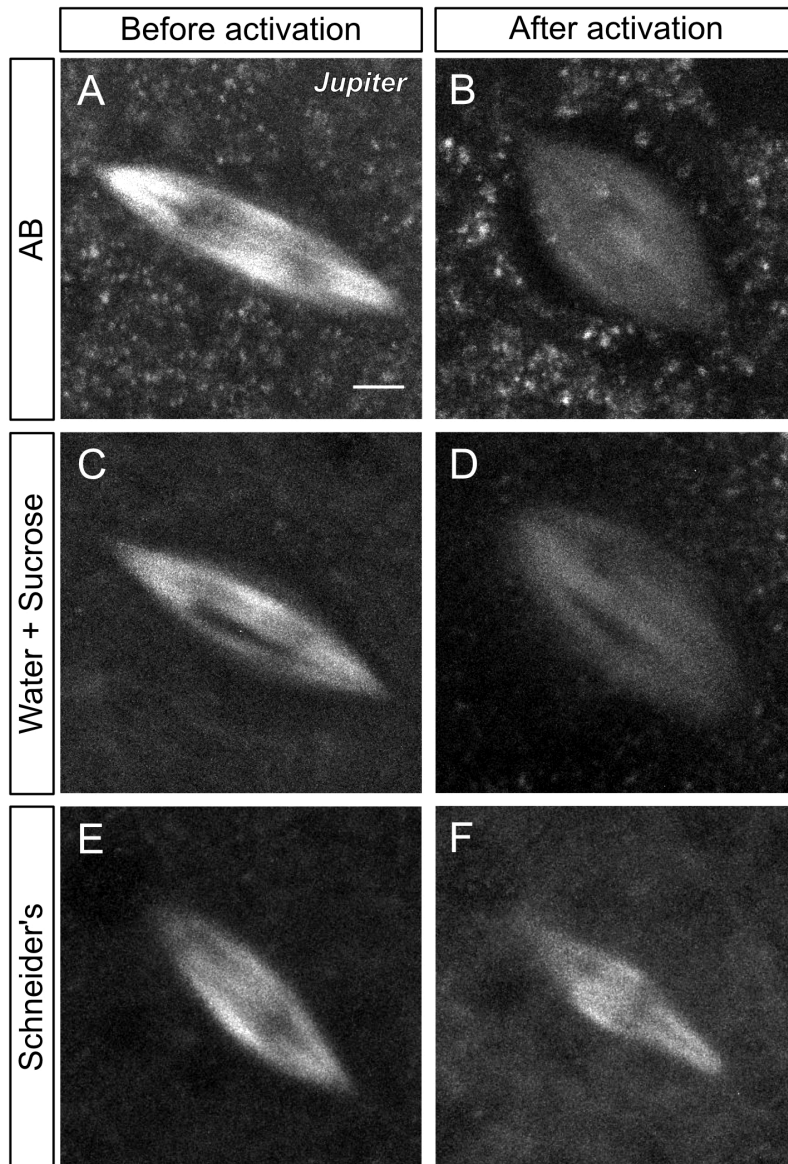
Figure 3.8. Meiotic spindle undergoes increase in a width upon osmotic pressure.
Mature oocytes expressing Jupiter::mCherry.The spindle shows a significant increase in a width by 70% upon addition of AB (A-B) or distilled water and sucrose (C-D) (260mOsm). The spindle width does not change upon the addition of Schneider's medium (E-F). Scale bar 2μm. Max projection 3μm. (G) The spindle width shows a significant increase after 10 minutes of egg activation by about 2.1 μm (70%), when the oocyte is treated with AB or distilled water with sucrose (260mOsm). No significant changes are observed with Schneider's incubation.

3.3.5 Osmotic pressure results in the dispersion of P bodies in *Drosophila* mature oocytes

My previous work has shown that P bodies are present uniformly in the *Drosophila* mature oocyte, resembling granular distribution (Weil et al., 2012; York-Andersen et al., 2015). Upon egg activation, this distribution becomes dispersed and is thought to release mRNAs from the P bodies and allow for their translation (Weil et al., 2012; York-Andersen et al., 2015). However, the cue of P bodies' dispersion remains unknown. To understand whether it is osmotic pressure that results in the dispersion of P bodies at *Drosophila* egg activation, the mature oocytes were treated with water and sucrose solution of a similar osmolarity to AB. Upon the addition of the solution, the mature oocytes swelled, as expected, and showed dispersion of P bodies (Figure 3.9). This suggests that osmotic pressure results in the dispersion of P bodies, a possible mechanism for the initiation of maternal transcripts at egg activation. It appears that external solution with a minimal content of ions and of osmolarity range 250-350mOsm is sufficient to cause the calcium wave at *Drosophila* egg activation and some downstream processes.
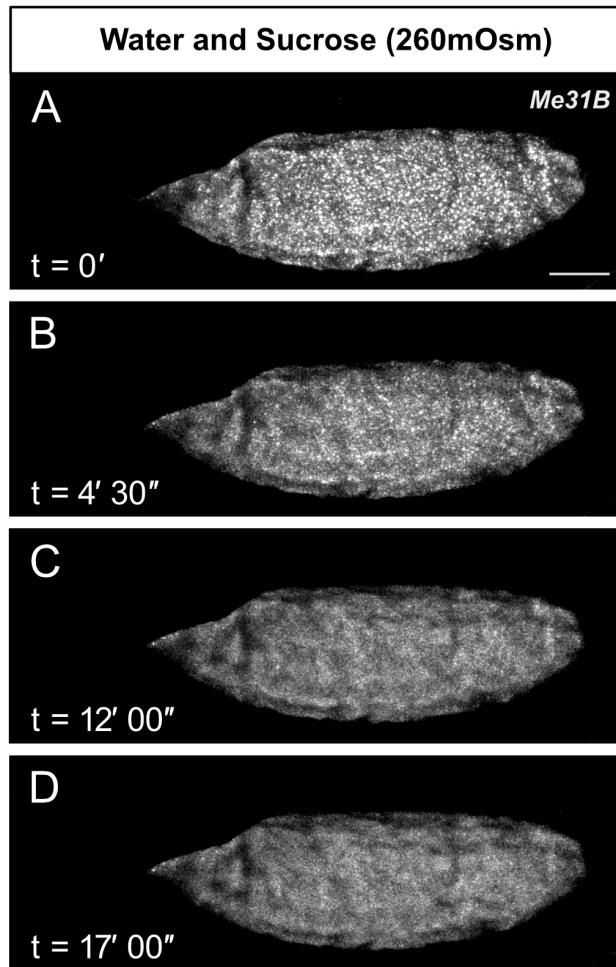
Figure 3.9. P bodies disperse upon the addition of water and sucrose of a similar osmolarity to AB.
(A-D) Time-series of *ex vivo* mature oocytes expressing Me31B::GFP following the addition of water and sucrose (260mOsm). P bodies disperse after 4 min 30 sec. Scale bar 60μm. Maximum projection = 40μm.

3.3.6 High ratio of sodium ions is non-facilitatory of the calcium wave

To test whether the external solution of a certain osmolarity range is sufficient to initiate the calcium wave in the mature oocyte, Schneider's control medium was diluted to the same osmolarity as AB (260mOsm). Upon addition of Schneider's medium, the mature oocytes swelled as expected, but did not show any calcium wave (n=46/53, 87%) (Figure 3.10A). These findings were unexpected and contradictory to the osmotic pressure model.

In order to better understand this finding, the recipe of Schneider's medium was analysed and it was noted that Schneider's has a higher ratio of sodium ions to potassium ions (5:1) compared to AB ratio (1:5). To investigate whether it is the high content of sodium ions that is resulting in no calcium wave, the mature oocytes were incubated with NaCl (50mM, 260mOsm). Upon addition of the solution, the oocytes swelled, but did not show a calcium response of any phenotype (Figure 3.10B). Similar results were observed with other high sodium content solutions, such as Acidic Tyrode solution (260mOsm) (solution used to activate mammalian eggs (Yamatoya et al., 2010) and Isolation buffer (260mOsm) (control solution) (data not shown).

To test whether it is the presence of sodium ions, or the aforementioned ratio between potassium and sodium ions that has an effect on the calcium wave at egg activation, the mature oocytes were treated with NaCl solution of different concentrations (260mOsm) alongside solutions containing different ratios of sodium to potassium. Upon the addition of NaCl, the oocytes swelled as normal, but the calcium wave was only present in approximately 5% of the eggs, compared to the wild-type of 85% (Figure 3.11A). This suggests that the presence of sodium in the external solution is inhibitory to the calcium wave at egg activation. This inhibitory affect was off-set by the presence of potassium ions at 25:75 Na:K ratio (Figure 3.11B). Therefore, the interplay between sodium and potassium in the external solution plays a role at *Drosophila* egg activation. It is possible that the ratio of sodium and potassium ions in the external solution plays a role in mediating a change in the membrane potential, which has been shown to associate with egg activation in other organisms (Stricker, 1999).
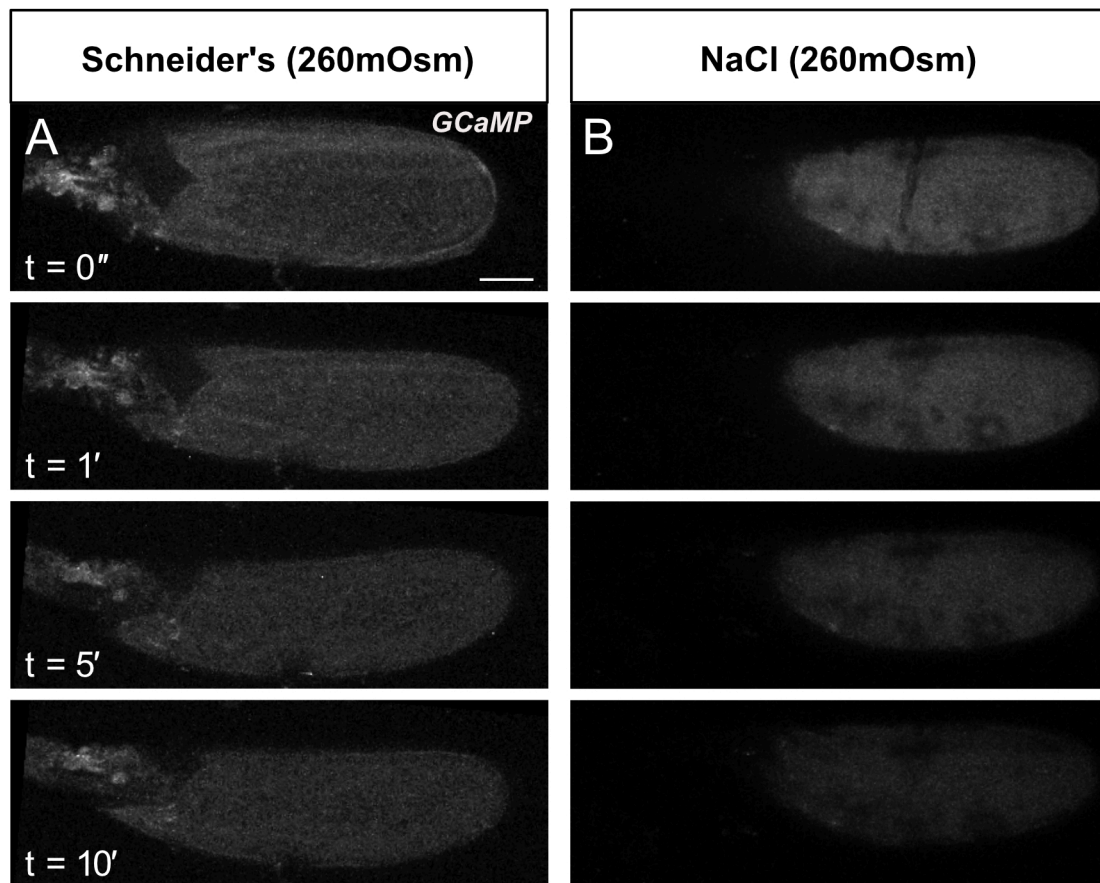
Figure 3.10. Diluted Schneider's Insect medium and NaCL do not result in the calcium wave in the mature oocyte.
(A-B) Time-series of *ex vivo* mature oocytes expressing UAS-myrGCaMP5 following the addition of (A) diluted Schneider's Insect medium (260mOsm) and (B) NaCl (50mM, 260mOsm). Both oocytes swell but there is no increase in the calcium levels. Scale bar 60μm. Maximum projection = 40μm.

A
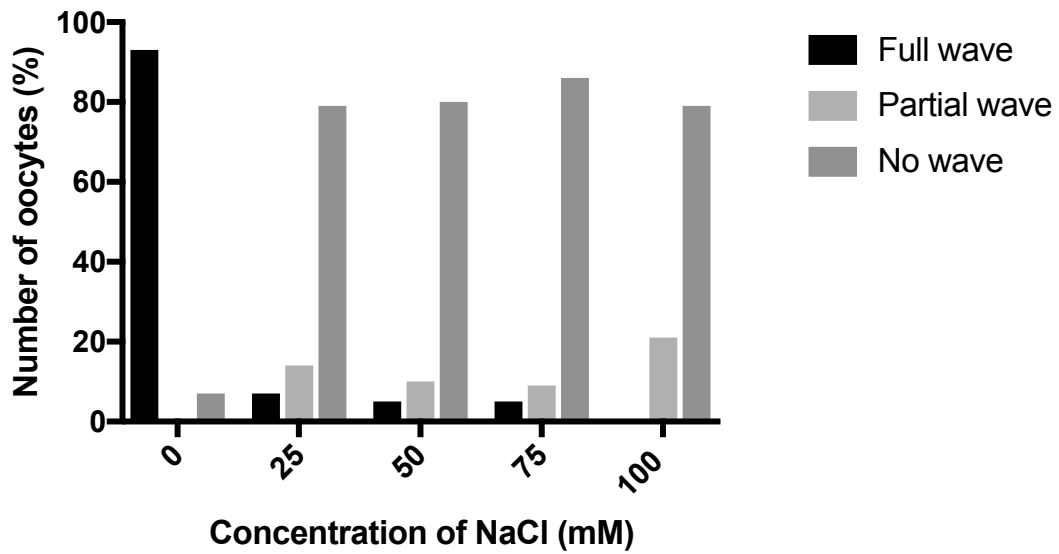
B
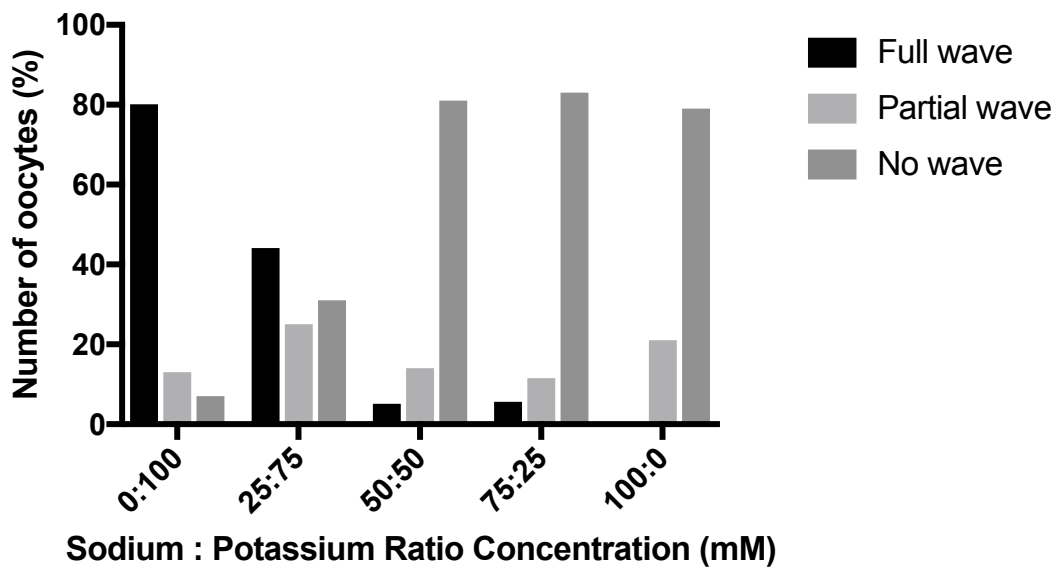
Figure 3.11. Sodium or high ratio of sodium ion solutions inhibit the calcium wave at egg activation.
(A) The graph show the calcium wave presence in the mature oocytes treated with NaCl at different concentrations. The NaCl is inhibitory to the calcium wave at 25mM-100mM concentrations. (B) The graph shows the presence of the calcium wave in NaCl and KCl solution. The presence of the calcium wave decreases from 50:50 sodium : potassium solution to about 5%, as observed with NaCl only. n=30 for each treatment.

3.3.7 Aquaporin channels are required for water homeostasis at egg activation

The intracellular water levels have to be maintained to ensure the optimal environment for biological functions. To do this, cells mediate water transport via the lipid bilayer and/or water-pore channels aquaporins. The aquaporins are known to coordinate rapid uptake or export of water molecules (Verkman, 2011; Verkman et al., 2014). Since my data suggests that the osmotic pressure acts as an initiation cue of *Drosophila* egg activation, I next tested the requirement of aquaporins in mediating water entry in the mature oocyte.

In order to investigate whether the aquaporins are required for the swelling of the mature oocyte at egg activation, I tested the effect of the broad aquaporin channel antagonist, copper sulphate (Verkman et al., 2014). Upon the addition of the AB with copper sulphate, the mature oocytes swelled, but did not show the calcium wave in ~ 70% of the eggs (n=44) (Figure 3.12B). This finding suggests that the aquaporin channels are not essential for swelling to occur, but are required for the calcium wave initiation.

There is only one aquaporin channel Prip that is known to be expressed in the ovarian tissue (*Drosophila* Fly Atlas). To investigate the role of Prip at *Drosophila* egg activation, the presence of the calcium wave was tested in the homozygous mutant background of Prip. Since the homozygous mutant was lethal, I tested the requirement of Prip using knock-down tools in heterozygous deficiency or mutant backgrounds. There is currently only one RNAi line available for the germline knock-down of Prip (BL50695), and one for the germline and somatic Prip (BL44464). Upon the addition of AB, the number of oocytes with the calcium wave significantly decreased to 50% in the germline knockdown over the deficiency or mutant (Figure 3.12B, n=25 (P=0.014) and n=18 (P=0.001) respectively). A similar significant decrease was also observed with only one copy knock-down of both somatic and germline Prip (BL44464) (Figure 3.12B, n=13). Interestingly, the most extreme phenotype was observed in homozygous BL44464 RNAi background, where the ovaries did not form at all and exhibited severely disrupted phenotype (Figure 3.12A).

To further understand why the disruption of Prip results in a reduced number of the calcium waves, I investigated the morphology of the *ex vivo* mature oocytes with depleted Prip background. I found that about 50% of the oocytes burst or had cytoplasm leaking within 1.5 minutes after the addition of AB (n=123), compared to 3% bursts in wild-type oocytes. Some burst eggs were still able to show the calcium wave. This significant difference in bursts is likely indicative of a requirement for Prip in mediating water homeostasis during swelling at egg activation.
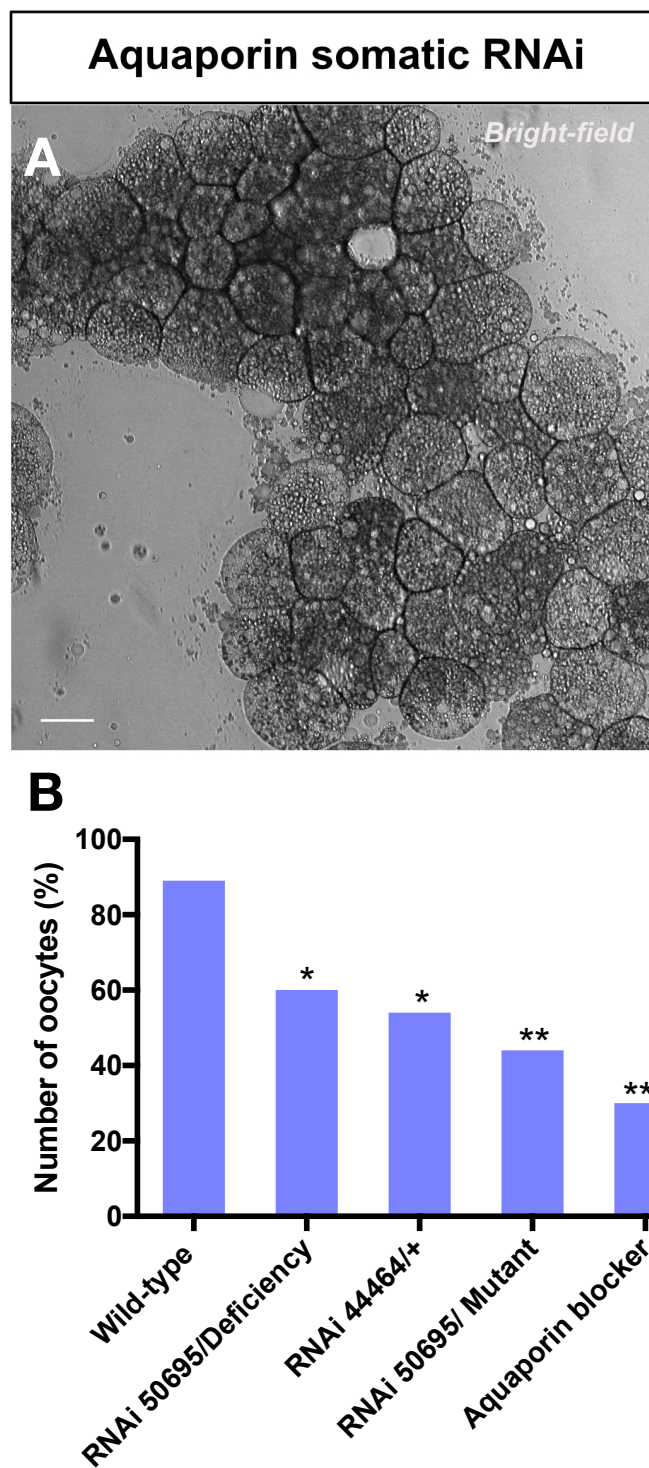
Figure 3.12. Aquaporin is required for the calcium wave at egg activation.
(A) The bright-field image of the disrupted *Drosophila* ovary in the homozygous RNAi background, with the depletion of both the somatic and the germline tissues (n=5). The ovaries exhibit a vesicle phenotype. Scale bar 100μm. Single plane. (B) The graph shows the presence of the calcium wave in the aquaporin depleted backgrounds. The calcium wave number is significantly reduced in RNAi over aquaporin deficiency or mutant (P=0.014 and P=0.001 respectively). The aquaporin pharmacological blocker results in a significant decrease to approximately 30% (P=0.0001) (Fisher's Exact Test).

3.3.8 External calcium is not required for the initiation and propagation of the calcium wave at *Drosophila* egg activation

In many animals, external calcium is required for the calcium rise at egg activation (Stricker, 1999). To test whether external calcium is required for the calcium wave at egg activation in *Drosophila*, *ex vivo* mature oocytes were treated with AB containing a calcium chelator BAPTA. These oocytes exhibited swelling and a full calcium wave in 89% of experiments (n=19) (Figure 3.13). Both the phenotype and percentage of calcium waves is similar in oocytes treated with AB. These findings suggest that external calcium is not required for the calcium wave initiation and propagation at egg activation.

However, this contradicts data from another lab (Kaneuchi et al., 2015), where oocytes, pre-treated with high sodium hypertonic solution before activating them with AB, did not show a calcium wave in the presence of BAPTA. These differences in the results may be due to aspects of the protocol used for activation. Pre-incubation of the oocytes may result in BAPTA getting into the oocytes and depleting the intracellular calcium stores, or the control solution affecting the timing of the calcium wave. I believe that my approach is better, because the mature oocytes are treated with calcium depleted AB with no incubation time. My data suggests that the calcium wave initiation and propagation is mediated by the release of intracellular calcium into the mature oocyte at egg activation.
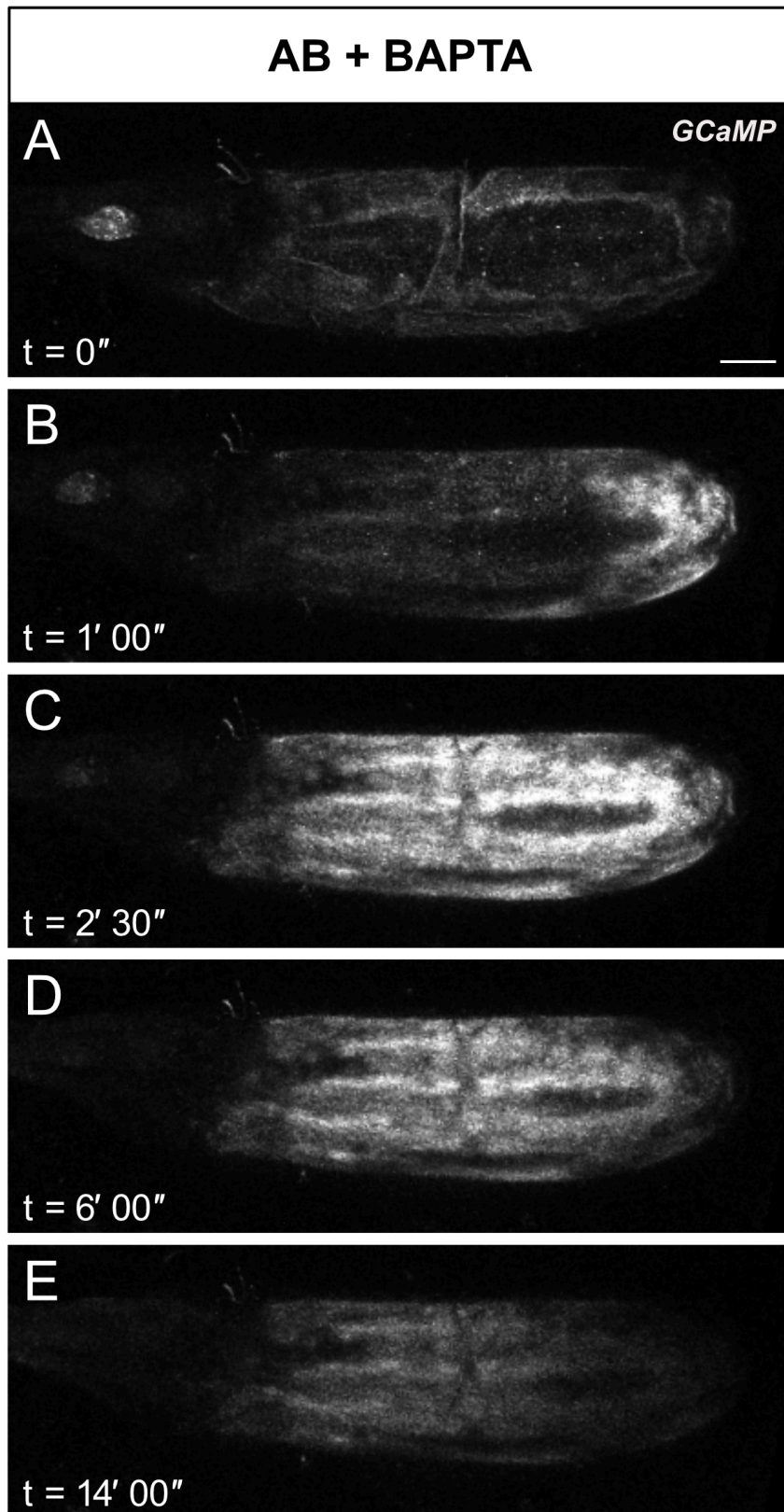
Figure 3.13. External calcium is not required for the initiation and propagation of the calcium wave at egg activation.

(A-E) Time-series of *ex vivo* mature oocyte expressing UAS-myrGCaMP5 following the addition AB and BAPTA. (B) Shows the calcium wave initiating from the posterior pole (t=1′00″), fully propagating across entire the oocyte (t=2′30″) and followed by the recovery (t=14′). Scale bars 60µm. Maximum projection = 40µm.

3.3.9 Golgi is enriched at the posterior pole of the *Drosophila* mature oocyte

The osmotic pressure model suggests that the posterior pole is the site that is exposed to the oviduct fluid first, and hence initiates the calcium wave from the posterior pole. However, this cannot explain my *ex vivo* data, where the calcium wave starts predominately from the posterior pole (~70%) in oocytes dissected into oil and treated with AB. This *ex vivo* data suggests that the posterior pole is able to initiate the calcium wave at egg activation independent of the oviduct tissue.

A possible hypothesis is that the posterior pole in enriched with organelles that act as internal storage of calcium ions. These include the endoplasmic reticulum (ER), mitochondria and golgi. To investigate whether there is a particular distribution of these organelles in the mature oocyte, I utilised protein traps YFP::Rab6 to visualise the golgi, mRpS9::YFP to visualise the mitochondria and I(1)G0320::YFP to visualise the ER (Lye et al., 2014; Dunst et al., 2015). The ER and mitochondria showed a uniform distribution in the mature oocyte (Figure 3.14C,F and Figure 3.14B,E respectively). In contrast, the golgi showed an enrichment at the posterior pole (Figure 3.14A,D). This enrichment seemed to concentrate in the follicle cells in particular (Figure 3.14D). This suggests a potential role of the posterior follicle cells in the initiation of the calcium wave at egg activation. Upon the addition of AB, the golgi remains enriched at the posterior pole, but becomes more dispersed after about 10 minutes (Figure 3.15). It is possible that the golgi enrichment at the posterior of the mature oocyte may support the initial calcium influx or pre-load the perivitelline space with the required levels of calcium for egg activation.
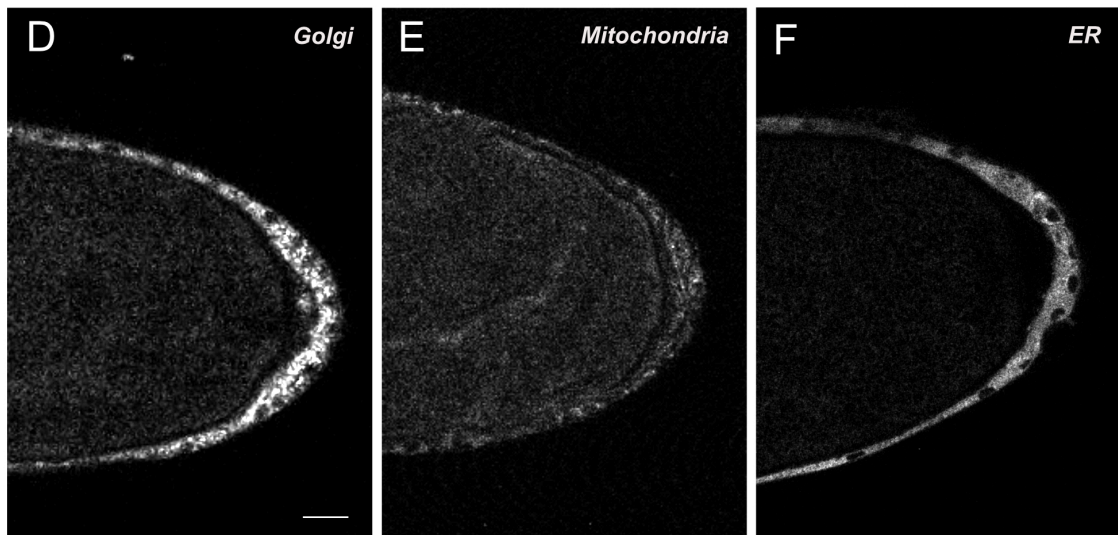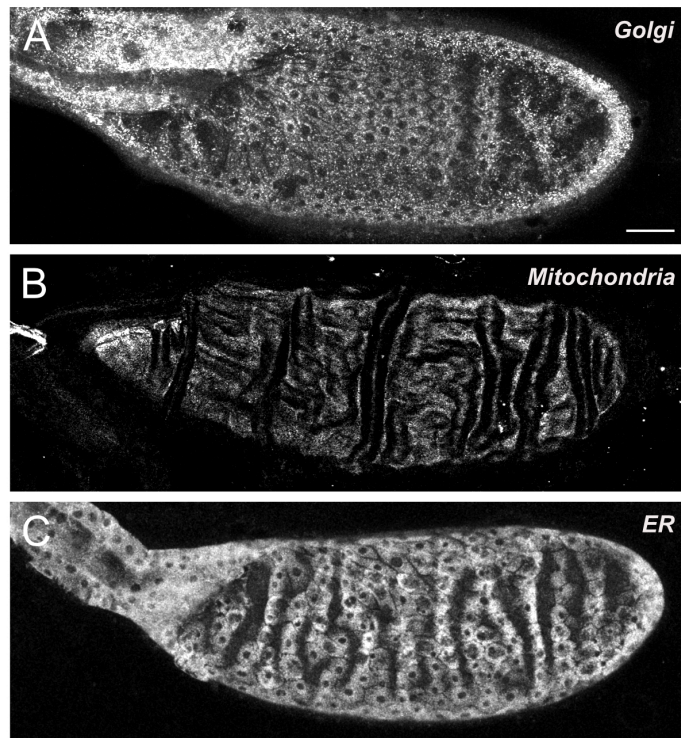
Figure 3.14. Golgi, but not ER or mitochondria, is enriched at the posterior pole in the oocyte.

(A,D) The Golgi is labelled with YFP::Rab6; (B,E) mitochondria with mRpS9::YFP; (C,F) ER with I(1)G0320::YFP. Scale bars 60μm. The Golgi is enriched at the posterior pole (A,D). The ER is present in the posterior follicle cells, but it not enriched, compared to the Golgi (C,F). The mitochondria shows a wrinkled distribution (B), and does not show any particular enrichment (B, E). The bright spot at the anterior is auto fluorescence from the dorsal appendages (B). (A-C) Maximum projection = 40μm. Scale bar 60μm (D-F) Single plane. Scale bar 40μm.
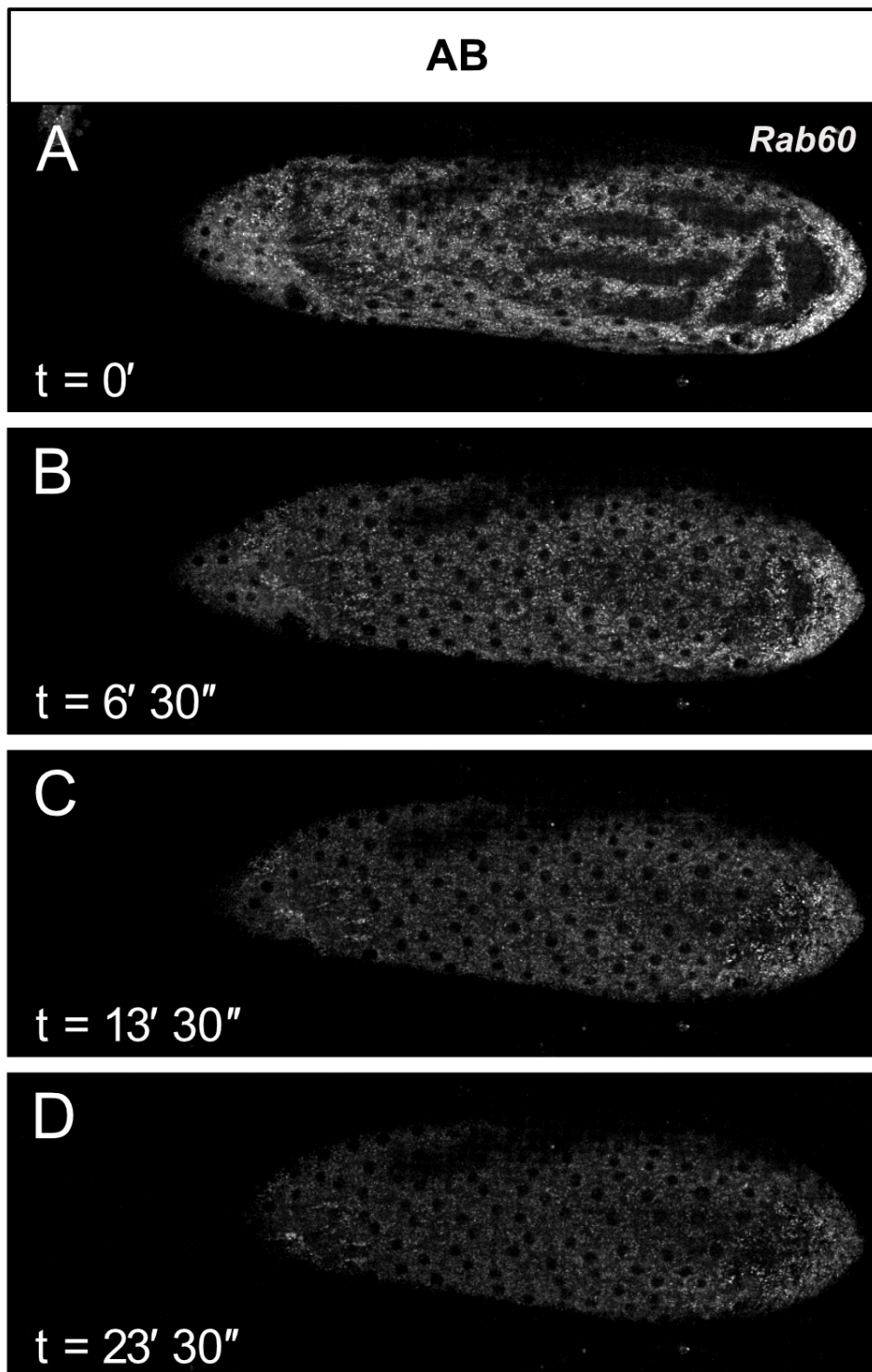
Figure 3.15. The Golgi is enriched at the posterior and disperses at egg activation.
(A-D) Time-series of *ex vivo* mature oocyte expressing YFP::Rab6 following the addition AB.
(A-D) shows the enrichment of Golgi at the posterior pole that disperses by t=23′30″. Scale
bars 60µm. Maximum projection = 40µm.

3.3.10 Posterior follicle cells are required for the initiation of the calcium wave from the posterior pole

One of the features of the posterior pole is the presence of the posterior follicle cells (PFCs). PFCs are essential for symmetry breaking in the oocyte to generate the anterior-posterior (AP) axis (Neuman-Silberberg and Schupbach, 1993; Gonzalez-reys et al., 1995). To investigate whether AP polarity plays a role in the initiation of the calcium wave at *Drosophila* egg activation, I tested the mature oocytes mutant for Gurken (Grk), which is required for the specification and differentiation of PFCs (reviewed in Roth and Lynch, 2009). These oocytes do not polarise and show two poles morphologically similar to each other. Upon the addition of AB, the mutant Grk oocytes swelled and showed a calcium wave at egg activation (Figure 3.16, n=10). However, the calcium wave initiated from the anterior and posterior poles at equal frequencies (Figure 3.16). This suggests that the polarity of the oocyte set by the Grk signal is required for the calcium wave initiation from the posterior pole at *Drosophila* egg activation.
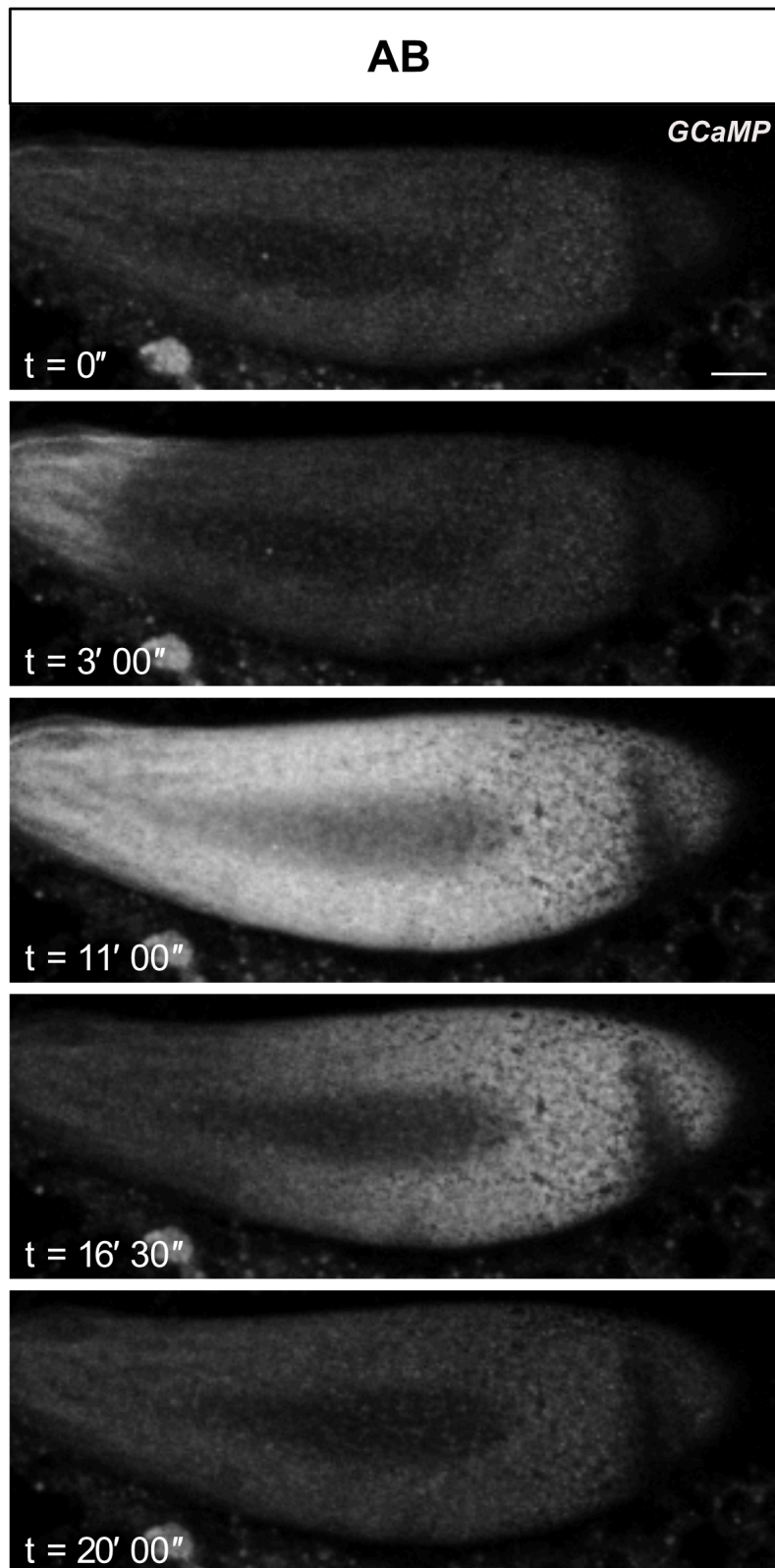
Figure 3.16. Calcium wave initiates from the anterior pole in mature oocytes lacking the anterior-posterior polarity.
Time-series of *ex vivo* mature oocytes expressing UAS-myrGCaMP5 in the Gurken depleted background. Following the addition of AB, the oocyte swells normally, but the calcium wave initiates from the anterior pole in 50% of the cases (n=10). Scale bar 60µm. Maximum projection = 40µm.

3.4 Discussion

This chapter shows that the osmotic pressure acts as an initiation cue for the calcium wave at *Drosophila* egg activation and is sufficient to cause the downstream processes of egg activation. I show that the ionic composition of the external solution and the polarity of the oocyte are important for the calcium wave initiation, whilst the presence of external calcium is not. I provide evidence for the role of aquaporins in water homeostasis in the *Drosophila* mature oocyte undergoing egg activation. Finally, I show that the golgi is enriched at the posterior pole of the mature oocyte.

3.4.1 Cell volume change and osmoregulation mechanisms

My data shows that the osmotic pressure initiates the calcium wave at *Drosophila* egg activation. I hypothesise that once the oocyte enters the oviduct, it is most likely exposed to the epithelial fluid, which is lower in osmolarity compared to the cytoplasm of an egg. The oocyte uptakes the fluid and undergoes swelling, which results in membrane tension, the rearrangement of the actin cytoskeleton (Chapter 4), the activation of the mechanosensitive channels (Chapter 5) and the calcium influx. The mature oocyte is likely to mediate cell volume change by pumping water out and exporting solutes out of the cytoplasm, in a similar process to other systems. However, the mechanism of this process remains elusive.

To mediate this change in volume, it is possible that the mature oocyte senses a difference in intracellular osmolarity and activates downstream processes to withstand the osmotic pressure, a response known as the regulatory volume decrease (RVD). In order to decrease its volume, a cell needs to reduce the number of intracellular solute molecules, which ensures the export of water. For example, RVD is known to activate the Na-K-2Cl co-transporter, and/or the Na/H exchanger, in response to the osmotic pressure in many cells (Hall et al 1995; Hall et al., 1996). These channels facilitate the export of potassium and chloride ions, thus decreasing the solute concentration. Therefore, the *Drosophila* mature oocyte could also export potassium and chloride ions to keep the

volume of the oocyte at physiological levels. Genetic manipulation of these channels should clarify their role at egg activation.

Apart from regulating potassium and chloride concentrations, the RVD has also been shown to result in an increase in intracellular calcium following osmotic stress in many cells, including intestinal epithelial cells, human osteoblast-like cells, rat astrocytes, and cancer cell lines (O'Connor and Kimelberg, 1993; Sauer et al., 1998; MacLeod and Hamilton, 1999; Weskamp et al., 2000; Shen et al., 2001). The general mechanism that is suggested to cause this calcium increase is via the mechanosensitive channels able to regulate calcium influx or potassium export. It is also hypothesised that other cells might sense an increase in cell volume via intracellular solute sensors, membrane-bound sensors or cytoskeletal sensors (Kultz and Burg, 1998). Hence, it is possible that the *Drosophila* mature oocyte undergoes tension in the lipid bilayer, which results in the reorganisation in the cortical actin cytoskeleton and transcriptional upregulation in response to prolonged osmotic stress at egg activation. Future work should focus on measuring the osmolarity of the oocyte and the oviduct fluid. The extraction of which proved quite challenging so far, because of the difficulties in getting a sufficient amount of the fluid to assess its osmolarity. This finding would provide further support for the osmotic pressure for the initiation of *Drosophila* egg activation.

3.4.2 Aquaporin requirement in water homeostasis

Aquaporin channels have been identified in many model systems, including yeast, bacteria, plants and mammals (Magni et al., 2006). The aquaporins have been shown to be involved in many cellular functions, such as cell migration, neuroexcitation, cell proliferation, epithelial fluid transport and brain swelling (Verkman 2011). For example, knock-out studies in mice have indicated the requirement of the aquaporin 1 (AQP1) for fluid absorption in the kidney proximal tubule (Schnermann et al., 1998) and AQP5 for secretion of saliva (Ma et al., 1999). Interestingly, AQP1 was also shown to be involved in cancer cell migration (Saadoun et al., 2005) with the localisation of the protein to the

leading edge of the migrating cell (Papadopoulos et al., 2008; Loitto et al., 2009), proposing a mechanism for localised volume change.

In *Drosophila,* aquaporin channels are also known to mediate water homeostasis. There are seven aquaporin channels that are present in the *Drosophila* genome (*Drosophila* FlyAtlas). However, it is not well-understood whether aquaporins also mediate water homeostasis in other fly tissues, including the *Drosophila* egg chamber. My findings suggest that the aquaporin Prip is required for successful *Drosophila* egg activation and initiation of the calcium wave. The significant increase in the number of oocytes bursting in the aquaporin depleted background is indicative of the aquaporin requirement in mediating water homeostasis. Since aquaporins are able to transport water in both directions, it is likely that Prip pumps water out of the activated egg to maintain physiological levels of fluid inside the oocyte without causing a burst. The observation that some oocytes did not burst or showed a calcium wave can be explained by possible residual levels of Prip after knock-down. The most severe phenotype was observed with the knock-down of Prip in somatic and germline tissues together. Previous *in situ hybridisation* experiments have highlighted the presence of Prip in the follicle cells in the *Drosophila* mature oocyte (Arbeitman et al., 2004). The follicle cells are somatic epithelial cells with their apical membranes orientated towards the oocyte. Therefore, it is possible that the presence of Prip in the follicle cells is required for the water transport at egg activation. Interestingly, Prip was also expressed in the oviduct, which could point towards a mechanism of oviduct fluid production. Together, it is clear that Prip plays a role at *Drosophila* egg activation whether expressed in the somatic or germline tissues.

3.4.3 The source of calcium at *Drosophila* egg activation

Calcium waves at egg activation can be mediated by intracellular and/or external calcium sources (Stricker, 1999). In *Drosophila*, my data has shown that the external calcium is not required for the calcium wave initiation and propagation at egg activation. This points towards the need for intracellular stores to mediate the calcium wave. The possible intracellular stores are the

ER, golgi, mitochondria and perivitelline space. If the ER is responsible for the calcium influx at egg activation, the possible calcium channels to mediate this influx are RyR and IP$_3$ receptors. RyR is not expressed in the *Drosophila* ovaries (*Drosophila* Fly Atlas), and a possible involvement of the IP$_3$ receptor will be discussed in the next chapter. However, IP$_3$ is unlikely to mediate the calcium wave as it is broken down at a much faster rate, than the propagation speed of the calcium wave (Wang et al., 1995). Therefore, the calcium wave is unlikely to be mediated by the calcium release from the ER.

In contrast, golgi has been shown to play an active role in calcium signalling (reviewed in Pizzo et al., 2011). The primary role of golgi is to modify and to sort proteins for trafficking. Its role as a calcium store has emerged with the invention of the golgi-specific aequorin, which showed that there is high concentration of calcium ions inside the golgi (Pinton et al., 1998). Golgi was shown to have similar properties to the ER in the timing of the calcium release, but differs with a much faster calcium sequestration nature (Missiaen et al., 2004). Golgi was also shown to express IP$_3$ receptors similar to the ER, which release calcium into the cytoplasm (Yoshimoto et al., 1990; Pinton et al., 1998, Lin et al., 1999; Surroca and Wolff 2000). This calcium release is counteracted by the calcium sequestration in an ATP-dependent manner back into golgi and is mediated by SERCA and SPCA pumps (Pinton et al., 1998; Lin et al., 1999; Baelen et al., 2003). These findings primarily come from cultured cells, and a direct physiological role of golgi in the calcium release is not well-understood. In *Drosophila*, golgi might also act as an intracellular calcium store in the mature oocyte at egg activation. My findings have shown that golgi is enriched in PFCs of the mature oocyte. However, the enrichment does not prove the requirement, and further work should test knock-down lines or pharmacological inhibitors, to understand the role of golgi at egg activation.

The perivitelline space is another, and in my opinion the most likely, source of intracellular calcium at egg activation. The perivitelline space lies between the plasma membrane of the oocyte and the perivitelline membrane. The composition of the perivitelline space in the egg chamber is currently unknown, but has been shown to consist of different ions, including calcium in the early *Drosophila* embryo (Van der Meer and Jaffe, 1983). It is possible that the

63

perivitelline space is pre-loaded with calcium during oogenesis. As the mature oocyte undergoes swelling, the activation of the mechanosensitive channels can mediate the calcium influx from the perivitelline space at egg activation (mechanosensitive channels are discussed in the Chapter 5). Calcium could also be pumped back into the perivitelline space (discussed in the Chapter 5), explaining the presence of calcium in early embryogenesis. The future focus should be to assess the role and composition of the perivitelline space in the mature oocyte, possibly by chemical degradation of the perivitelline membrane.

3.4.4 The importance of the osmotic pressure at *Drosophila* egg activation

From my data, it is evident that the osmotic pressure acts as an initiation cue of the calcium wave at *Drosophila* egg activation. My working model proposes that, once the oocyte enters the oviduct, it is exposed to a hypotonic solution that results in the swelling of the oocyte. This swelling results in increased membrane tension and the opening of mechanosensitive channels. The channels coordinate the calcium influx from the perivitelline space. Golgi might pre-load the perivitelline space with the required calcium ions.

It is interesting that egg activation is independent of fertilisation in *Drosophila*, compared to other animals. It is possible that, as the fertilised eggs develop in the environment, egg activation needs sufficient time to prepare the oocyte. For example, egg activation would ensure that the oocyte had sufficient time to produce the chorion shell to withstand the external environment once deposited. Alternatively, egg activation might prepare the cytoplasm of the oocyte to ensure an accessible environment for the sperm entry from the spermatheca.

Overall, the application of osmotic or mechanical pressure seems to be a common initiation cue in insects. Understanding this mechanism may improve the reproduction of many insects, or in contrast, may introduce a new form of insecticide, specifically targeting egg activation in parasitic insects that act as vectors of infections, like malaria.

Chapter 4

Investigating the dynamics and function of the actin cytoskeleton at *Drosophila* egg activation

4.1 Introduction

4.1.1 Overview of the chapter

The actin cytoskeleton is a major cellular network that regulates many biological processes, including cell division, directed cell migration, intracellular trafficking and cell shape changes (Dominguez and Holmes, 2011). The actin cytoskeleton is an ideal candidate to mediate various downstream processes due to its polymeric nature, intrinsic polarity and vast number of binding partners. Although these properties have been extensively studied in many model systems, the dynamics and function of the actin cytoskeleton at egg activation is not fully-understood. This introduction will discuss the mechanism of actin polymerisation and the role of the actin cytoskeleton during the early development of organisms, in particular its role at egg activation.

4.1.2 The general structure and function of the actin cytoskeleton

Actin is composed of globular-actin (G-actin) monomers, which are 43 kDaltons in size (343 amino acids). G-actin monomers bind to each other at the nucleation point to form a polymeric filamentous actin (F-actin) at a 166 degree angle (Holmes et al., 1990; Kabsch et al., 1990), giving it an appearance similar to the DNA double-helix molecule. The actin polymer is polarised and has two dynamically different ends, one barbed and one pointed (Pollard 1983, Pollard et al., 2000). The actin filament undergoes elongation at the barbed end and dissociation at the pointed end (Woodrum et al. 1975). These differences at the polarised ends can result in a treadmilling effect, which provide free monomers for polymerisation of actin. The G-actin monomers are found in the ATP-bound form, which is hydrolysed to ADP in filamentous actin. ATP hydrolysis is not essential for the monomers to bind, but was shown to increase the efficiency of the monomers attachment at the barbed end of the filament (Blanchoin and Pollard, 1999; Blanchoin and Pollard, 2002). Together, these events result in the formation of F-actin.
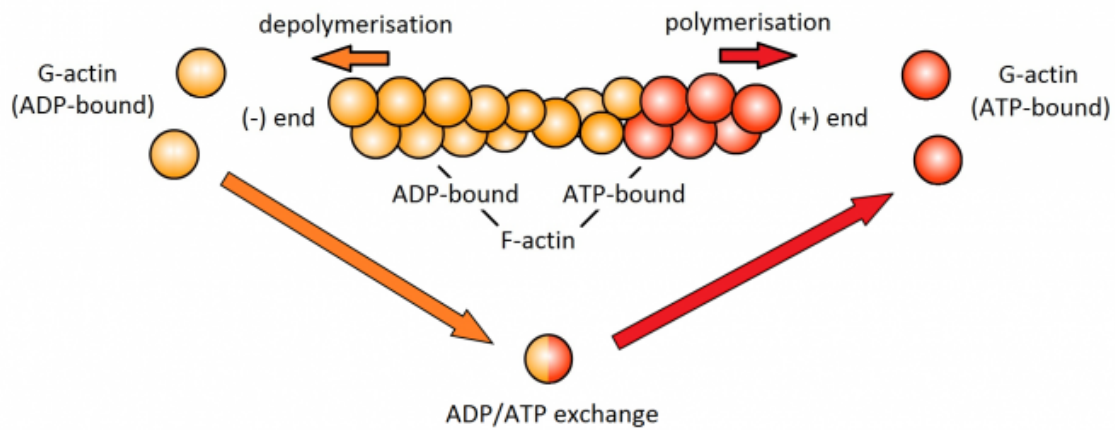
Figure 4.1. Summary of F-actin polymerisation from G-actin monomers.
Adapted from Wirth Lab and SMA Support UK Website. G-actin monomers bind each other to form polarised F-actin with plus and minus ends. G-actin monomers undergo ATP/ADP exchange, with ATP-bound G-actin associating with the plus end of F-actin and ADP-bound G-actin with the minus end of F-actin.

F-actin was shown to form a variety of morphological networks, including branched, cross linked, parallel and anti-parallel bundles (reviewed Blanchoin et al., 2014). These formations assemble depending on the G-actin monomer availability and the presence of actin-binding proteins (ABP), such as the Arp2/3 complex and WAVE family complex, which together coordinate the formation of the branched F-actin (Machesky et al., 1994; Mullins et al., 1997; Mullins et al., 1998). The branched F-actin is commonly formed in the leading edge of the migrating cells, providing mechanical force and contractions that pull a cell forward (Machesky et al., 1994; Mullins et al., 1997; Mullins et al., 1998).

Non-branched F-actin forms parallel or anti-parallel actin bundles which are usually found in stress fibers or filopodia (Vignjevic et al., 2003; Barral and Martin, 2011). These bundles are formed and organised by formins and Eva/ Vasp protein complexes (Haviv et al., 2006; Dominguez, 2010; Breitsprecher et al., 2011). The F-actin bundles can result in the formation of thin protrusions within the plasma membrane. Cofilin is another example of an ABP that binds to the ADP-actin and modulates the dissociation of actin monomers from the pointed end (Pavlov et al., 2007). Together, these factors and others coordinate the actin architecture in a highly temporal and spatially regulated manner.

4.1.3 The role of the actin cytoskeleton in the acrosome reaction prior to egg activation

One major role of the actin cytoskeleton in early development is the fusion of the sperm and egg gametes to result in successful fertilisation. The binding between the sperm and the egg results in the breakdown of the zona pellucida in mammals. (Brucker and Lipford, 1995). In the sperm, prior to this reaction, F-actin undergoes depolymerisation, which is hypothesised to enable the outer acrosomal membrane and the overlying plasma membrane to come into close proximity and fuse (Breibart et al., 2005). The sperm head is filled with G-actin monomers which rapidly polymerise, aided by profilin, during the acrosome reaction to allow sperm membrane protrusion towards the egg (Breibart et al., 2005). Pharmacological treatments and visualisation of calcium have shown that the sperm binding to the plasma membrane in mammals results in an intracellular calcium increase at the tip of the sperm, which is thought to activate protein kinase A pathway and actin polymerisation during the acrosome reaction (Heras et al., 1997; Cohen et al., 2004; Breibart et al., 2005, Pelletan et al., 2015).

In sea urchins, purification studies have identified Bindin protein in the sperm head that binds the actin-based microvilli structures on the membrane of an egg (Summers and Hylander 1975; Glabe and Vacquier et al., 1978; Schatten and Hulser 1983). Apart from the acrosome reaction, the binding of the sperm to the egg membrane has been shown to induce the aggregation of actin filaments at the entry point of the sperm in sea urchin oocytes (Terasakki, 1996). Immunofluorescence and electron microscopy observations have shown that this actin polymerisation results in the formation of a cytoplasmic bridge which mediates the transfer of the sperm nucleus into an oocyte (Tilney and Jaffe, 1980; Gundersen et al., 1986). Similar actin structures, fertilisation cones, were identified by phalloidin staining in starfish oocytes (Puppo et al., 2008). The pharmacological induction of multiple actin cones was shown to result in polyspermy (Puppo et al., 2008). Together, these experiments suggest that the actin cytoskeleton is essential for successful fertilisation and transfer of paternal pronuclei.

4.1.4 The role of the actin cytoskeleton at egg activation

Egg activation triggers ordered signalling processes, including cytoskeletal rearrangements, to prepare an egg for embryogenesis (Horner and Wolfner, 2008). Cytoskeletal dynamics have been studied at this stage of development in a few model systems, with some of the most extensive research in starfish. Early ultrastructural analysis of the cultured starfish oocytes have shown that the cortex of an oocyte is composed of F-actin and microvilli filled with actin filaments, which become shorter at egg activation (Hirai and Shida 1979; Longo et al. 1995). More recently live imaging of F-actin has shown the centripetal movement associated with the internalisation of a sperm in starfish (Puppo et al., 2008; Vasilev et al., 2012). Interestingly in ascidian oocytes, the wave of myosin-dependent cortical contraction was observed at egg activation (McDougall and Sardet, 1995). Injection of membrane dyes has indicated that the endoplasmic reticulum accumulates at the vegetal pole following this contraction (Speksnijder et al., 1993), possibly to support further calcium oscillations. In *Xenopus* eggs*,* visualisation of actin with Lifeact and Utrophin *in vivo* actin marker revealed a "wave" of cortical F-actin at egg activation (Bement et al., 2015). This points towards conserved wave-like F-actin dynamics at egg activation. It was further demonstrated by live imaging and overexpression experiments that starfish and frog oocytes both exhibited a Rho-activity wave, where Rho activity up regulates F-actin polymerisation, but F-actin subsequently inhibits Rho (Bement et al., 2015). Both of these waves were suggested to be regulated by Cdk1 and Rho-GEF Ect2, and thus are thought to be linked to the regulation of the cell cycle. Research on actin waves is limited as the field has primarily focused on calcium signalling, and there is less data exploring actin dynamics at egg activation.

4.1.5 The role of the actin cytoskeleton in cortical granule exocytosis after egg activation

Cortical granule exocytosis is one of the essential downstream processes of egg activation which acts as a slow-block to polyspermy (Liu et al., 2011). In mature oocytes, the actin cytoskeleton acts as a physical barrier to the

exocytosis of cortical granules. Following egg activation, actin rearrangement facilitates the release of the cortical granules (Vitale et al., 1991; Trifaro et al., 1992). Ultrastructural analysis of the cortex and live imaging of F-actin in starfish oocytes have demonstrated that the microvilli decrease their length allowing the cortical granules to move to the plasma membrane at egg activation (Santella et al., 1999). Furthermore, when mouse oocytes are incubated with an inhibitor of actin depolymerisation, it results in an increase of polyspermy (McAvey et al., 2002). This has led to a model proposing F-actin depolymerisation as a mandatory step in the release of cortical granules and a slow-block to polyspermy following egg activation (Lelkes et al., 1986; Muallem et al., 1995).

4.1.6 Calcium signalling and actin rearrangement at egg activation

It is hypothesised that an increase in intracellular calcium at egg activation results in the rearrangement of the actin cytoskeleton. This has been supported by evidence from starfish oocytes, where a pharmacologically-induced calcium increase resulted in the depolymerisation of cortical actin and the parallel polymerisation of cytosolic actin (Vasilev et al., 2012). In contrast, the pharmacological disruption of a calcium increase has been shown to result in the perturbed actin cytoskeleton, which fails to display the centripetal movement of F-actin (Vasilev et al., 2012). Further evidence has shown that the actin depolymerisation, in turn, results in the calcium influx and subsequent cortical granule exocytosis in the starfish oocyte (Lim et al., 2002). In *Drosophila* oocytes, the single calcium wave was perturbed when actin was inhibited with Cytochalasin D (actin polymerisation inhibitor) (York-Andersen et al., 2015). These findings suggest a model where calcium and actin display a co-regulatory relationship at egg activation, which is not fully-understood.

4.1.7 Visualisation of the actin cytoskeleton in *Drosophila* egg chamber

The actin cytoskeleton distribution has been well-studied during early *Drosophila* development. Throughout *Drosophila* oogenesis, actin plays a role

70

in tissue morphogenesis, signalling cascades, localisation of mRNAs and maintaining the integrity of the cortex (Wang and Riechmann, 2007; Weil et al., 2008 Spracklen et al., 2014). The actin distribution has been extensively visualised using fixed tissue and genetically-encoded markers (the summary of which is provided in Table 1) (Cavaliere et al., 2008). To test for function, pharmacological inhibitors, such as Cytochalisin D, Latrunculin-A and Phalloidin have been added to oocytes to disrupt actin. These inhibitors have unique properties that allow for different experimental tests. For example, Cytochalasin-D acts by binding to the growing end of F-actin filaments and preventing addition of G-actin monomers (Lin and Lin, 1979; Brown and Spudich, 1979; Grumet and Lin, 1980; MacLean-Fletcher and Pollard, 1980). Phalloidin is a stabilising actin agent, from a class of phallotoxins isolated first from mushrooms, known to bind actin filaments with a higher affinity than the actin monomers (Copper, 1987). Therefore, these drugs are commonly used to study actin dynamics.

Drosophila mature oocytes were shown to display a uniform distribution of F-actin around the cortex (Cavaliere et al., 2008) and to have G-actin monomers in the cytoplasm (personal communication). Past work has potentially identified the requirement of dynamic actin at *Drosophila* egg activation (York-Andersen et al., 2015), however, a detailed study is sorely lacking. Therefore, the focus of this chapter is to understand the dynamic changes of actin at *Drosophila* egg activation.

Actin Markers	Fluorophore	Expression	Construct	Type of actin	Dispersion of actin (initial)	Actin increase after dispersion	Reference
Moesin	GFP	Protein trap	GFP sequence 238 amino acids conjugated with a C-terminus Moesin tail, which consists of extended helical regions and an actin-binding site.	Cortical actin	Yes	No	Edwards et al., 1997
Moesin	mCherry	UASp	DNA encoding mCherry and the actin-binding domain of Drosophila Moesin (C-terminal 137 residues)	Cortical actin	Yes	No	Millard and Martin 2008
F-tractin	ddTomatoe	UASp	N-terminus 1-66 amino acids of rat IP3K actin-binding domain fused to a fluorophore	F-actin	Yes	Yes - wavefront from posterior	Johnson and Schell, 2009
Lifeact	mCherry	UASp	First 17 amino acids of yeast Abp 140 protein	G-actin + F-actin	Yes	Yes - wavefront from posterior	Riedl et al., 2008
Utrophin	GFP	Endogeneous promoter	calponin homology domains of human ubiquitous dystrophin	F-actin	Yes	Can't observe	Burkel et al., 2007
Utrophin	GFP	UASp	Human Utrophin residues	F-actin	Yes	Can't observe	Rauzi et al., 2010

Table 4.1.Summary of genetically-encoded actin markers used in *Drosophila in vivo* imaging

4.2 Aims of this chapter

1. To determine to what extent the actin cytoskeleton undergoes a dynamic change at *Drosophila* egg activation.

2. To address whether the actin cytoskeleton depends on the changes in intracellular calcium at *Drosophila* egg activation.

3. To investigate whether the calcium wave depends on the actin cytoskeleton at *Drosophila* egg activation.

4.3 Results

4.3.1 Visualisation of Moesin at *Drosophila* egg activation

In order to test if cortical actin undergoes a rearrangement at *Drosophila* egg activation, I used a genetically-encoded actin marker GFP-Moesin (Table 1) (Edwards et al., 1997). This genetically-encoded marker belongs to the ERM (ezrin, radixin, moesin) family that is known to promote cortical actin assembly and to link transmembrane proteins with the F-actin cytoskeleton (Fievet et al., 2007). This construct consists of a GFP sequence of 238 amino acids conjugated to the C-terminus tail of Moesin (Turunen et al., 1994).

Before activation, Moesin showed a cortical distribution across the entire oocyte (n=15) (Figure 4.2A) (this is shown as a stack, so the image looks as though actin is in the centre, but is actually cortical). However, this distribution became less ordered and more diffuse 3 minutes after the addition of AB (Figure 4.2A). Taken together with my finding that osmotic pressure is required for egg activation to occur (Chapter 3), I hypothesise that cortical actin detects swelling of the oocyte as it generates membrane tension. Therefore, cortical actin can act as an osmosensor and relay a change in the oocyte volume via downstream signalling cascades.

4.3.2 Visualisation of F-tractin at *Drosophila* egg activation

To further verify the hypothesis that actin undergoes a rearrangement at *Drosophila* egg activation, I tested a different genetically-encoded actin indicator F-tractin. Comprised of the N-terminus of Inositol 1,4,5-Triphospate 3-kinase (IP3K) actin-binding domain fused to a fluorophore (Table 1) (Schell et al., 2001), F-tractin has been shown to closely correlate with phalloidin staining (Schell et al., 2001; Spracklen et al., 2014).

In contrast to GFP-Moesin, activation of egg chambers, expressing F-tractin-tdTomato, showed an increase in F-tractin fluorescence starting from the posterior pole (Figure 4.2B) (n=20). The increase propagated across the oocyte

to the anterior pole in a wavefront manner and subsequently recovered after approximately 16 minutes (Figure 4.2B). This wavefront exhibited similar dynamics to the calcium wave previously characterised: the actin wavefront initiated from the posterior pole, traversed the oocyte at approximately 1.5 µm/sec and took 12 minutes to recover following the initiation. Interestingly, this F-tractin wavefront initiated at 5 minutes 30 seconds after addition of AB, on average 4 minutes after the calcium wave. This suggests that F-actin is possibly regulated downstream of the calcium wave. In some experiments, I observed a second increase in F-tractin initiating approximately 25 minutes after the addition of AB (data not shown) that also propagated across the oocyte from the posterior pole in a wavefront manner. The physiological significance of this second wavefront is not clear, but I hypothesise that it could ensure re-organisation of actin following egg activation.

4.3.3 Visualisation of Lifeact at *Drosophila* egg activation

One possibility is that the F-tractin wavefront represents an IP3K activity instead of actin. This is due to the F-tractin structure, containing the actin-binding domain from IP3K (Schell et al., 2001). In order to verify that there is an actin wavefront associated with *Drosophila* egg activation, I tested Lifeact, another genetically-encoded construct that has been shown to label actin *in vivo* in many model systems (Riedl et al., 2008; Bement et al., 2015) This construct consists of the first 17 amino acids of yeast Abp140 protein fused to GFP (Riedl et al., 2008).

Prior to activation, the mature oocytes expressing Lifeact-mCherry showed a uniform cortical distribution, similar to GFP-Moesin and F-tractin-tdTomato (Figure 4.2A-C). At activation, Lifeact showed an initial dispersion that was followed by an increase in fluorescence from the posterior pole that propagated across the oocyte in a wavefront manner and recovered within 12 minutes of the initiation (Figure 4.2C). The average speed of Lifeact wavefront was 1.5 µm/sec (n=10), similar to F-tractin. Together, these observations suggests that there is a non-cortical F-actin wavefront that is associated with *Drosophila* egg activation. As the Lifeact and F-tractin wavefronts are consistent, I conclude that

they represent a wave of F-actin rather than IP3K activity. In this chapter, F-tractin and Lifeact are used interchangeably to visualise and analyse the non-cortical wavefront.

The visualisation of Moesin, F-tractin and Lifeact at egg activation suggests two different F-actin populations in the mature *Drosophila* oocyte: (1) cortical and (2) non-cortical wave. At the onset of egg activation, the cortical F-actin undergoes rearrangement in the form of dispersion (Figure 4.2A). This is then followed by the non-cortical F-actin wavefront starting from the posterior pole (Figure 4.2A-B). However, it is still not clear whether these cortical and non-cortical actin dynamics are dependent on the calcium wave at egg activation.
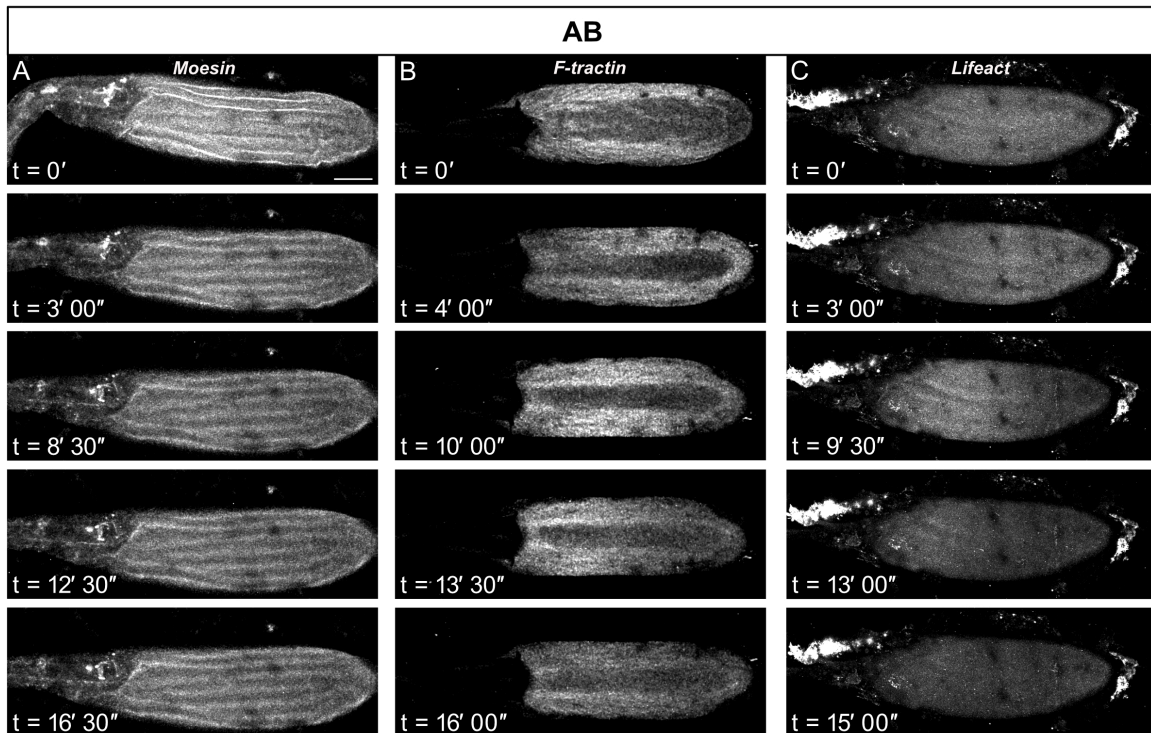
Figure 4.2. Moesin undergoes global dispersion, whilst F-tractin and Lifeact show a wavefront associated with *Drosophila* egg activation.
Mature oocyte expressing (A) GFP-Moesin, (B) UASp-F-tractin-tdTomato and and (C) UASp-Lifeact-mCherry. (A) shows the dispersion of Moesin by about t = 3′ 00″. (B) shows the initiation of the F-tractin wavefront from the posterior pole at about t = 4′ 00″ that propagates and recovers by about t = 16′ 00″. (C) shows the initiation of Lifeact wavefront from the posterior pole at t = 3′ 00″ that propagates and recovers by t = 15′ 00″. Scale bar 60µm. Maximum projection = 40µm.

4.3.4 Cortical actin dispersion is independent of the calcium wave

It is not clear whether the initial dispersion of the cortical actin is dependent on the calcium wave at *Drosophila* egg activation. To address this, mature oocytes expressing GFP-Moesin were treated with (1) AB or distilled water, previously used to cause rapid swelling and a cortical increase of calcium at egg activation (York-Andersen et al., 2015), and (2) NaCl solution (260mOsm), which results in swelling of the oocyte, but does not support the calcium wave (Chapter 3). Addition of AB or distilled water resulted in a decreased concentration of Moesin at the cortex within 3 minutes (Figure 4.3A-B). The same change in phenotype in the cortical actin was also observed when the mature oocytes were treated with NaCl solution (Figure 4.3C). These findings suggest that the cortical actin undergoes a morphological change at the onset of egg activation following the volume change of the oocyte and is independent of the calcium wave.

To investigate why the calcium wave starts at the posterior I asked whether the cortical actin is uniformly distributed across the mature oocyte. Visualisation of Moesin in the mature oocyte shows a lower concentration at the posterior pole compared to the lateral side (Figure 4.3D). To exclude the possibility that this observation might be due to the acquisition parameters, I tested the membrane marker Ressille::GFP as a negative control. Ressille showed a similar distribution at the posterior and lateral cortex with no visible decrease at the posterior pole (Figure 4.3E). These findings suggest that cortical actin organisation at the posterior pole could be a factor in the initiation of the calcium wave. It is possible that the cortical actin disperses faster at the posterior pole compared to the lateral sides, and hence results in the initiation of the calcium wave.
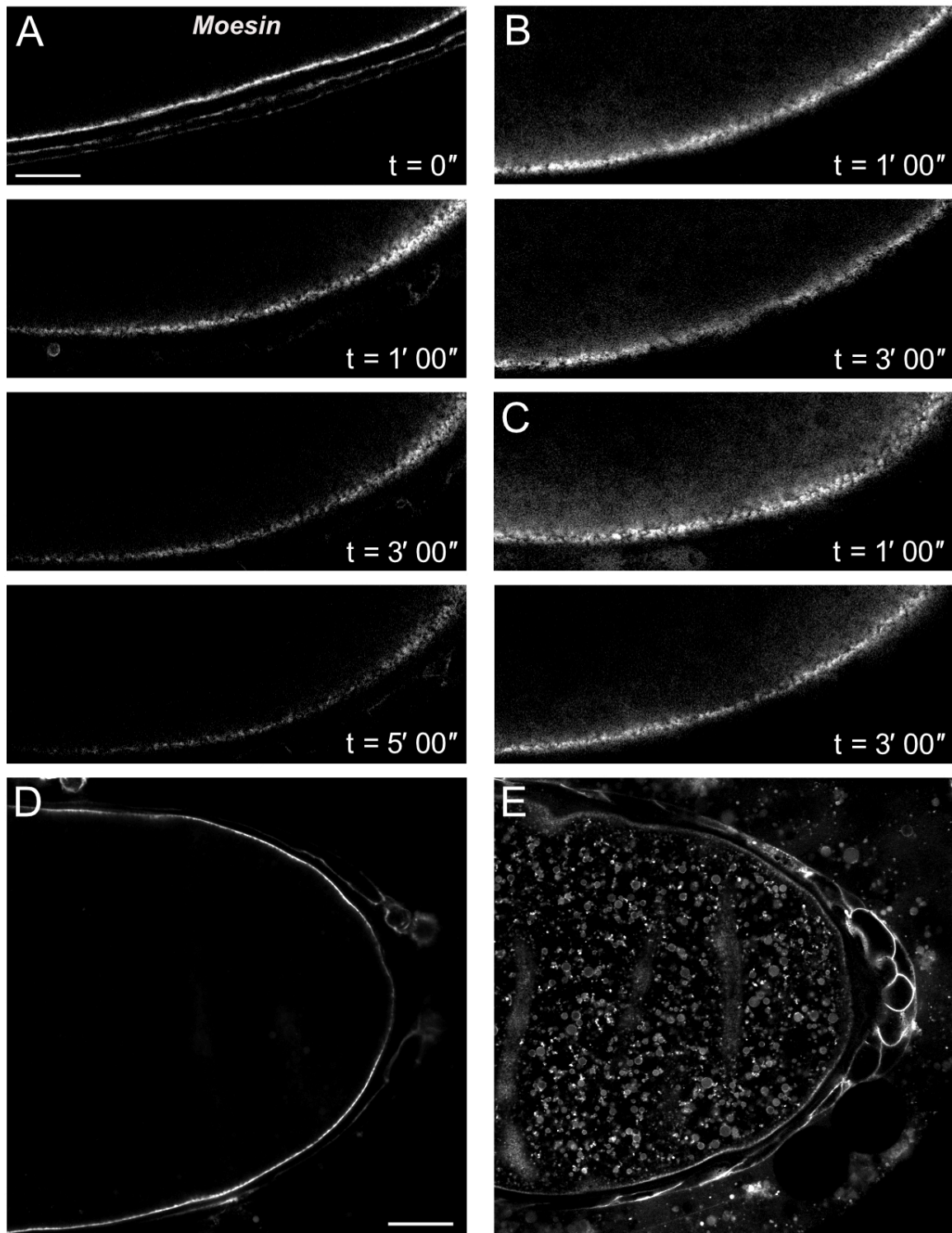
Figure 4.3. GFP-Moesin undergoes a dispersion of cortical actin at *Drosophila* egg activation.
Mature oocyte expressing GFP-Moesin, following the addition of (A) AB, (B) distilled water and (C) NaCl (50mM). (A-C) shows the lateral side next to the posterior pole. (A-C GFP-Moesin becomes more dispersed by t = 3′ 00″ following the addition of (A) AB, (B) distilled water and (C) NaCl (50mM). (D-E) shows the posterior pole of the mature oocyte before activation. (D) shows that GFP-Moesin is enriched less at the posterior pole cortex (white arrows). (E) shows membrane marker with the uniform distribution all around the cortex as a negative control. (A-C) Scale bar 20 µm. (D) Scale bar 60 µm. Single plane.

4.3.5 Calcium and actin wave dynamics at *Drosophila* egg activation

In order to test the relationship between calcium and actin at *Drosophila* egg activation, I visualised F-tractin and calcium simultaneously. Upon addition of AB, the mature oocyte showed a typical calcium wave (Figure 4.4.1A and 4.4.2A). F-tractin intensity decreased initially, concomitant with the timing of the cortical actin dispersion. This was followed by the F-tractin wavefront after 4 minutes of the initiation of the calcium wave (Figure 4.4.1C' and 4.4.2C'), which terminated by approximately 15 minutes post-initiation of the calcium wave (Figure 4.4.1G' and 4.4.2E'). The same F-actin wavefront was observed with Lifeact (data not shown). Together with my actin-only labeled experiments, these observations show that the F-actin wavefront follows the calcium wave with a similar speed and directionality.

In order to better understand the dynamics of the actin cytoskeleton and the calcium wave, I quantified mean fluorescence levels of the actin over time. One technical challenge is that the oocytes would often move out of the plane of focus after the addition of AB, leaving a black oval shape in the middle of the oocyte, when Z-stacks were made (Figure 4.4A'-G'). Therefore, I quantified the mean fluorescence intensity of the posterior and anterior poles, where t=0 was selected as the initiation of the calcium wave. The intensity of F-tractin raises with the initiation of the calcium wave, reaching a peak at 6 minutes (Figure 4.4.3A,B). This intensity then decreases to the basal levels over the subsequent 5 minutes (Figure 4.4.3A,B). The F-actin wavefront initiates on average 4 minutes after the initiation of the calcium wave. The wavefront reaches the other side of the oocyte on average by 9 minutes 30 seconds, and starts recovering within 1 minute after this. The full recovery is completed by 16 minutes 30 seconds. Excluding the delay of 4 minutes, the timings of the propagation and recovery of the calcium and actin waves are very similar.
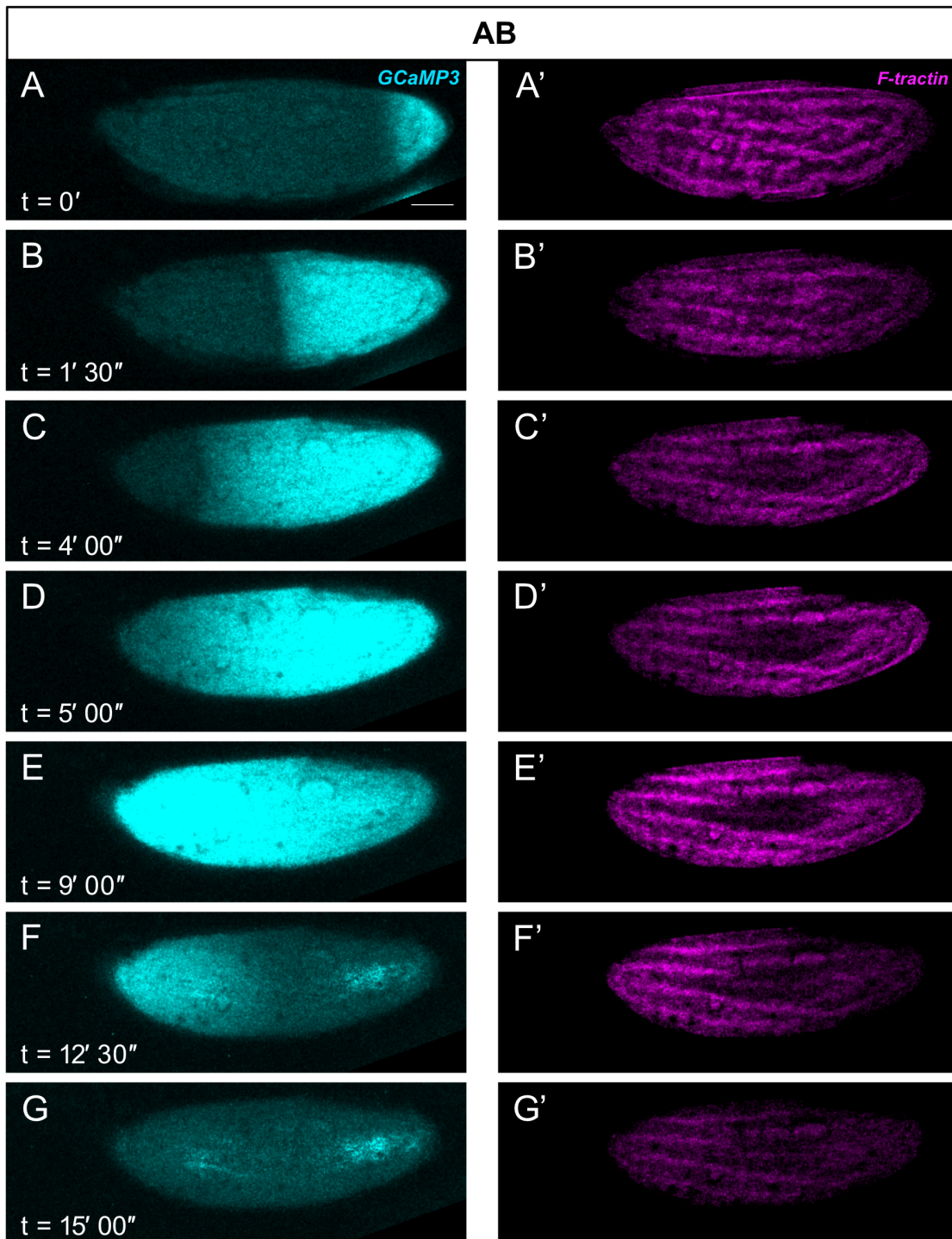
Figure 4.4.1 The Calcium wave is followed by an actin wavefront at *Drosophila* egg activation.
(A-G) Time-series of a mature oocyte co-expressing UASp-GCaMP3 (cyan) and UASp-F-tractin-tdTomato (magenta) (A'-G') imaged sequentially to exclude a possibility of the bleed-through of the channels. The calcium wave initiates from the posterior pole (A) and propagates across the oocyte (B-D). The wave recovers to the basal levels (F-G). The cortical actin disperses (B'-C') and then followed by an actin wavefront initiating from the posterior pole (D'-F'). This wavefront recovers to the basal levels (G'). Scale bar 60µm. Maximum projection = 40µm.
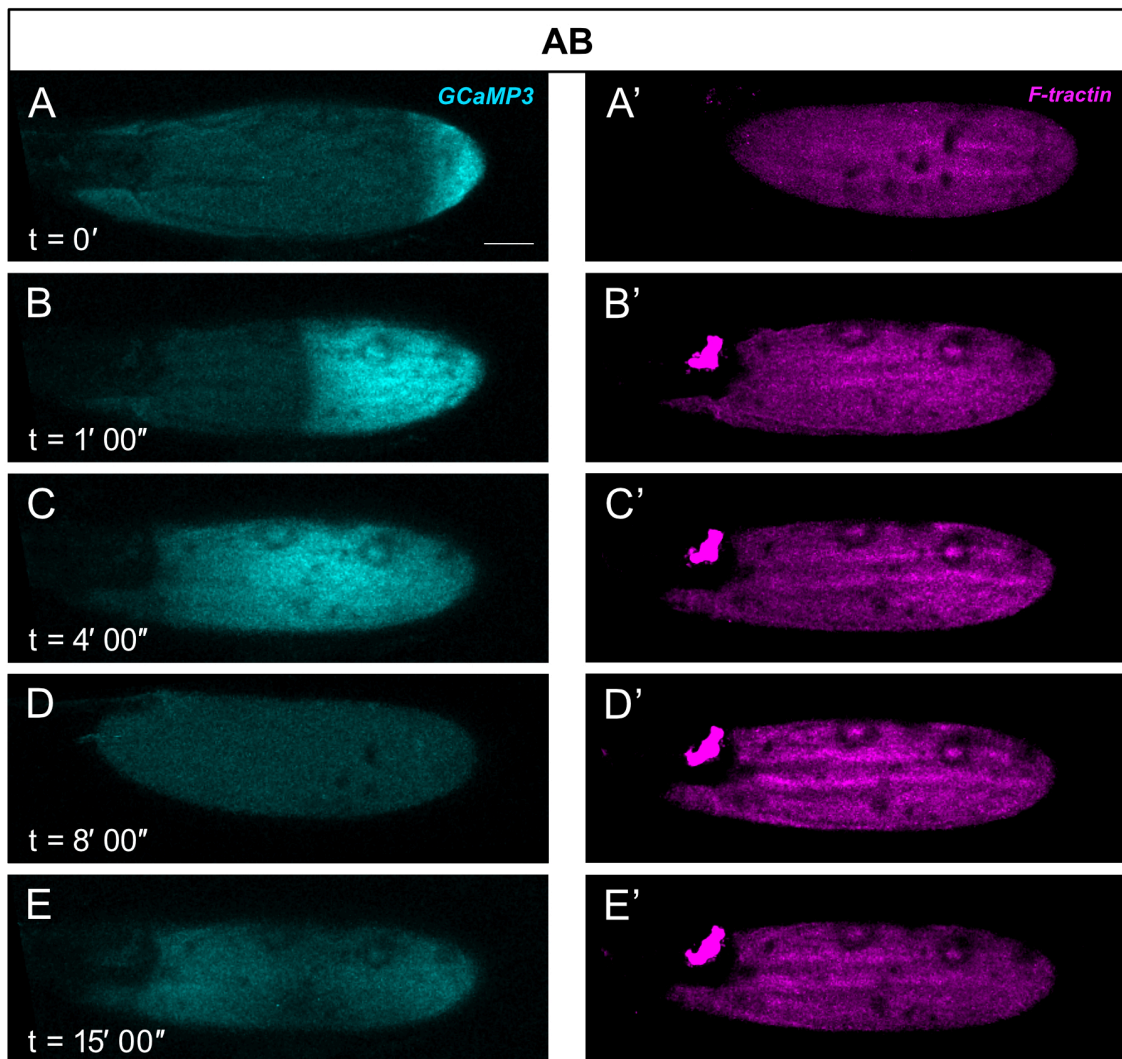
Figure 4.4.2 Calcium wave is followed by the actin wavefront at *Drosophila* egg activation.
(A-E) Time-series of a mature oocyte co-expressing UASp-GCaMP3 (cyan) and UASp-F-tractin-tdTomato (magenta) (A'-E') imaged simultaneously. The calcium wave initiates from the posterior pole (A) and propagates across the oocyte (B-D). The calcium wave recovers to the basal levels (D). The cortical actin disperses (B) and is then followed by an actin wavefront initiating from the posterior pole (C'). This wavefront recovers to the basal levels (E'). Scale bar 60µm. Maximum projection = 40µm.

A
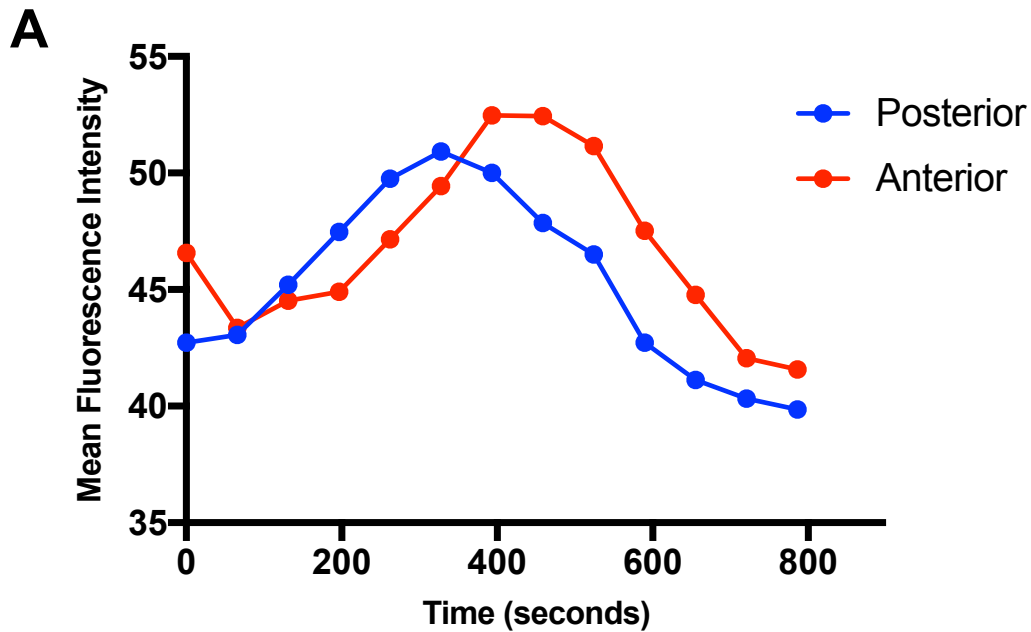
B

	Calcium wave (n=30)	F-actin wavefront (n=10)
Initiation	1 min 30 sec	4 min 00 sec
Full wave	4 min 00 sec	9 min 30 sec
Start of recovery	5 min 00 sec	10 min 30 sec
End of recovery	10 min 30 sec	16 min 30 sec

Figure 4.4.3. Graph of F-actin wavefront and average times of calcium and actin waves at *Drosophila* egg activation.
(A) Graph representing a mean fluorescence intensity of F-tractin measured over time in seconds. The sample area was the same for both anterior (red) and posterior (blue) poles. t=0 is the initiation of the calcium wave. The F-tractin shows an increase in the mean fluorescence intensity at 300-400 seconds after the initiation of the calcium wave, and then decreases after 500-600 seconds. There is a second increase in F-tractin at around 1200 seconds. The anterior line is shifted to the right of the posterior line, indicative of the F-tractin. (B) Comparison of average times of the calcium wave and the F-actin wavefront. The summary shows that the F-actin initiates on average 3 min 30 sec after the calcium wave. In both cases, the recovery starts after 1 min after both waves reach the other side of the oocyte. The recovery takes 5-6 min in both cases. The calcium wave and the F-actin wavefront are similar in dynamics.

4.3.6 F-actin wavefront initiates from the same site as the calcium wave

The calcium wave primarily initiates from the posterior pole (70%, n=50), with a few experiments showing anterior pole (20%) and lateral side (10%) initiation. It is not clear, however, if the F-actin wave initiates from the same site as the calcium wave. To test this, F-actin and calcium were visualised simultaneously in the mature oocytes, where the calcium wave initiated from the anterior pole. This revealed that the F-actin wavefront also started from the anterior pole (Figure 4.5). The same dependancy was observed with oocytes expressing F-tractin (data not shown). These findings show that the F-actin wavefront initiates and propagates in the same direction as the calcium wave, suggesting that the calcium wave plays a role in coordinating the F-actin wavefront .

To investigate the F-actin phenotype with a non-wave calcium increase, the mature oocytes were treated with distilled water. The oocytes swelled, and calcium increase initiated from all over the cortex within 1 minute (Figure 4.6A-E), and F-actin showed an increase from all over the cortex (Figure 4.6A'-E'). Interestingly, F-actin fluorescence was delayed on average by 4 minutes (Figure 4.6), the same as with the waves. This suggests that calcium initiates the changes in F-actin and points towards the mechanistic dependence of F-actin on the intracellular calcium increase.
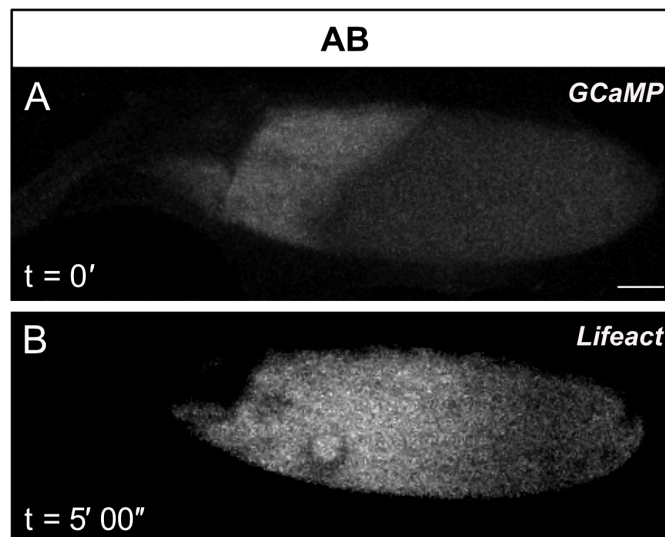
Figure 4.5. Anterior calcium wave is followed by the anterior F-actin wavefront at *Drosophila* egg activation.
(A-B) Time-series of a mature oocyte co-expressing UASp-GCaMP3 and UASp-Lifeact-mCherry. The calcium wave initiates from the anterior pole (A). The F-actin wavefront also initiates from the anterior pole following the calcium wave. Scale bar 60μm. Maximum projection = 40μm.
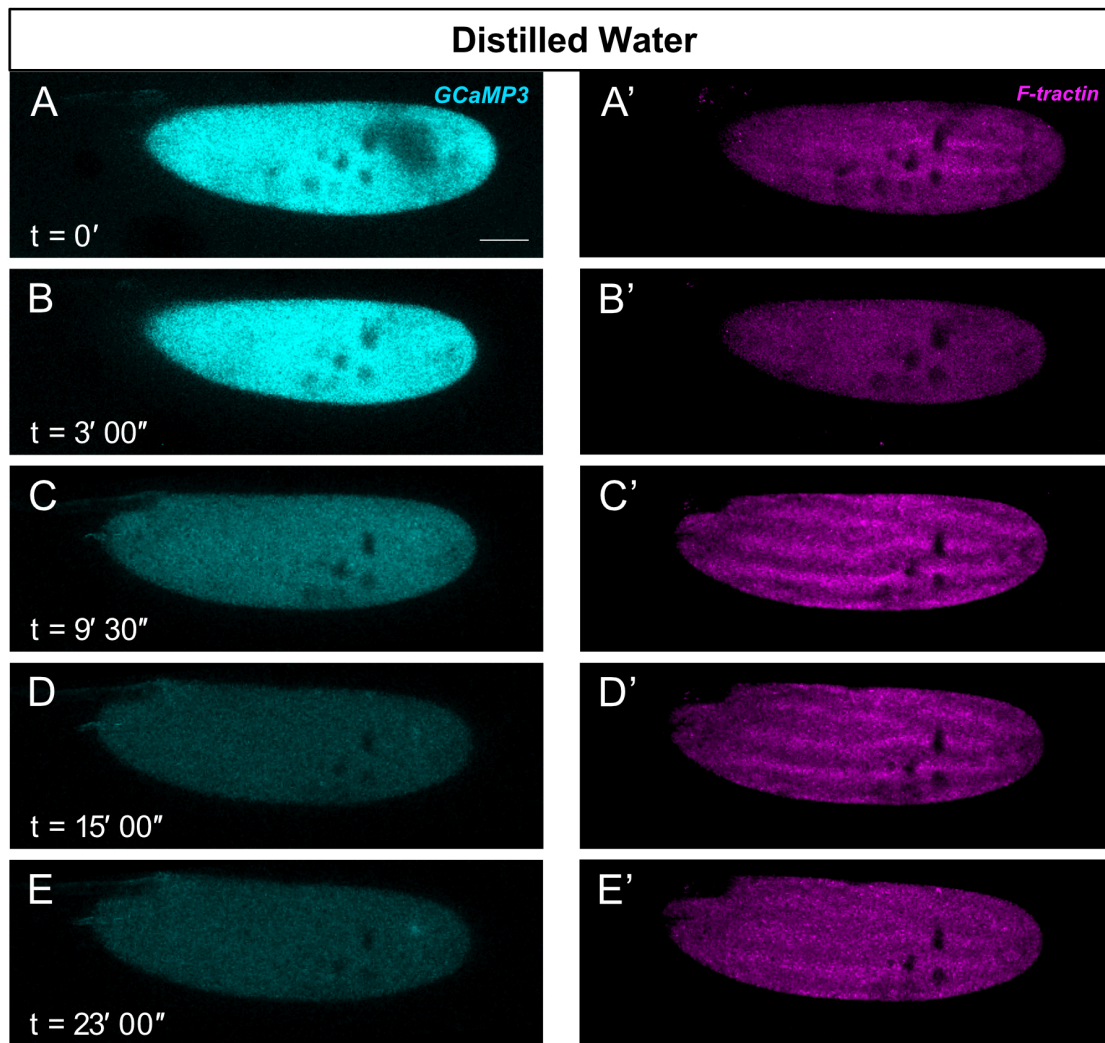
Figure 4.6. Cortical calcium increase is followed by the cortical actin increase at *Drosophila* egg activation.

(A-E) Time-series of a mature oocyte co-expressing UASp-GCaMP3 (cyan) and UASp-F-tractin-tdTomato (magenta) (A'-E'). Calcium increases from all over the cortex (A), which recovers back to the basal levels (C). The cortical actin disperses (B') and then followed by an actin cortical increase (C'), which recovers to the basal levels (E'). Scale bar 60µm. Maximum projection = 40µm.

4.3.7 F-actin wavefront is dependent on the calcium wave at egg activation

To address if a rise in calcium is required for the F-actin wavefront, the mature oocytes were treated with NaCl solution. Upon addition of NaCl, the oocytes swelled as expected and showed a drop in cortical F-actin (Figure 4.7A'-B'). However, the calcium wave and the F-actin wavefront were absent (Figure 4.7). This suggests that the F-actin wavefront requires the calcium wave in order to initiate and propagate.

My previous work has shown that the calcium wave does not occur in *Sarah* mutants, a key player in the calcium signalling pathway that inhibits calcineurin (York-Andersen et al., 2015). To genetically verify the requirement of a calcium increase for the F-actin wavefront, I visualised F-actin in a *Sarah* mutant background. Upon the addition of AB, the oocytes swelled normally, but there were no observed changes in F-actin (n=15) (Figure 4.8). This is consistent with NaCl data and supports a model where the F-actin wavefront requires an increase in intracellular calcium at *Drosophila* egg activation.
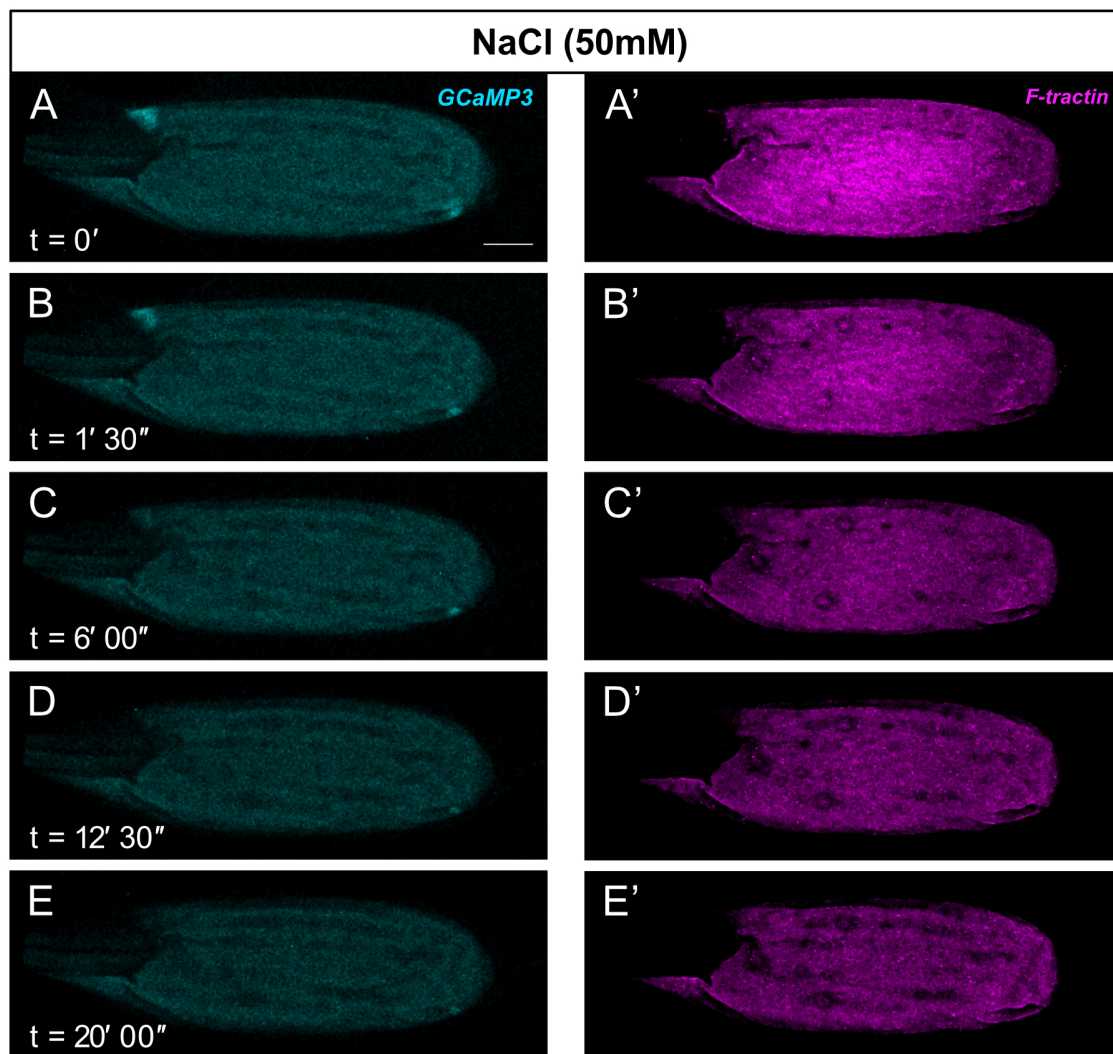
Figure 4.7. The F-actin wavefront is absent in the oocytes without a calcium increase at *Drosophila* egg activation.
(A-E) Time-series of a mature oocyte co-expressing UASp-GCaMP3 (cyan) and UASp-F-tractin-tdTomato (magenta). (A-E) The oocyte swells, but there is no change in intracellular calcium or F-actin observed. Scale bar 60µm. Maximum projection = 40µm.
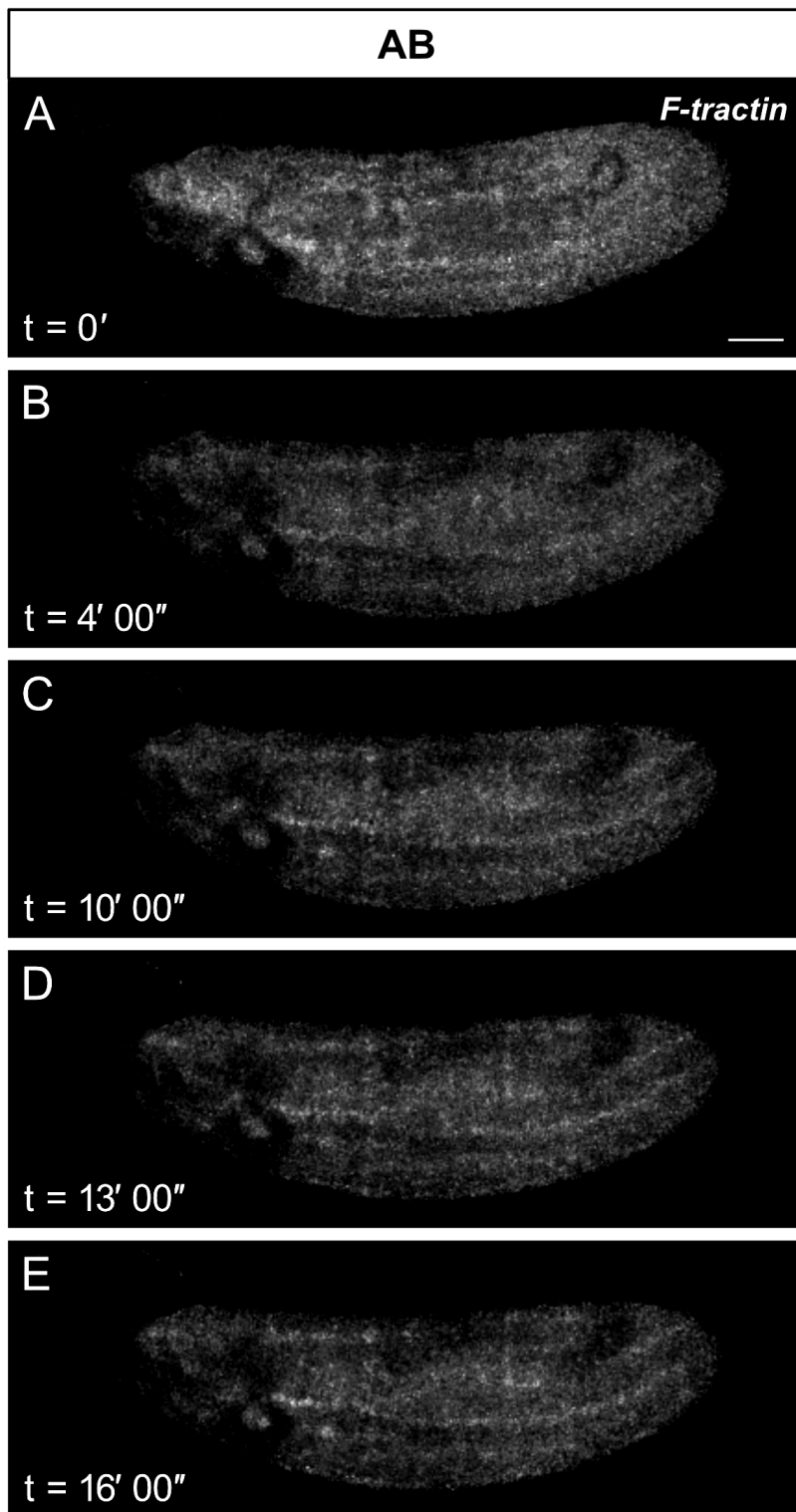
Figure 4.8. The F-actin wavefront is absent in the oocytes with *Sarah* mutant background at *Drosophila* egg activation.
(A-E) Time-series of a mature oocyte expressing and UASp-F-tractin-tdTomato. F-tractin disperses (A-B), but does not show the wavefront as in the wild-type oocytes at egg activation (C-E). The dark areas represent not displaced bubbles in oil. Scale bar 60μm. Maximum projection = 40μm.

4.3.8 Stabilisation of the actin cytoskeleton is inhibitory to the calcium wave

Calcium signalling and organisation of the actin cytoskeleton are two major cellular features that together coordinate numerous biological functions, including pollen tube growth in plants or vesicle secretion in mast cells (Cardenas et al., 2008; Wollman and Meyer, 2012; Wu et al., 2013). *Drosophila* mature oocytes provide an example, where the F-actin wavefront is dependent on the the presence of the calcium wave. However, it is not clear whether the calcium wave is also dependent on the changes in F-actin.

To address whether the dynamic changes in F-actin are required for the calcium wave, mature oocytes were incubated with AB and the actin stabilising agent Phalloidin. To ensure Phalloidin entered the eggs, I used a form conjugated to a fluorophore. Within a couple of minutes, the oocyte swelled and an increase in fluorescence intensity was observed all around the cortex (data not shown), showing that Phalloidin was in the mature oocyte. With this knowledge, I tested the effect on the calcium wave and showed a perturbed calcium wave in 68% of the oocytes (Figure 4.9) (n=35). A similar result was also observed, when the actin growing ends were capped with Cytochalasin D, resulting in the disruption of the calcium in 77% of the oocytes (n=35) (Figure 4.9). This suggests that stabilisation of the F-actin cytoskeleton is inhibitory to the the calcium wave.

To understand whether the calcium wave also requires free cytoplasmic G-actin monomers, the mature oocytes were treated with AB and Latrunculin A, which binds G-actin monomers (Yarmola et al., 2000). The experiments show that the oocytes swelled, as expected, and interestingly exhibited a full calcium wave in 72% of the cases (n=20) (Figure 4.9). This suggests that the calcium wave requires F-actin, rather than free G-actin monomers. Together, these findings point towards a model, where cortical F-actin undergoes a dynamic rearrangement to open the mechanosensitive channels to allow the calcium influx into the oocyte at egg activation.
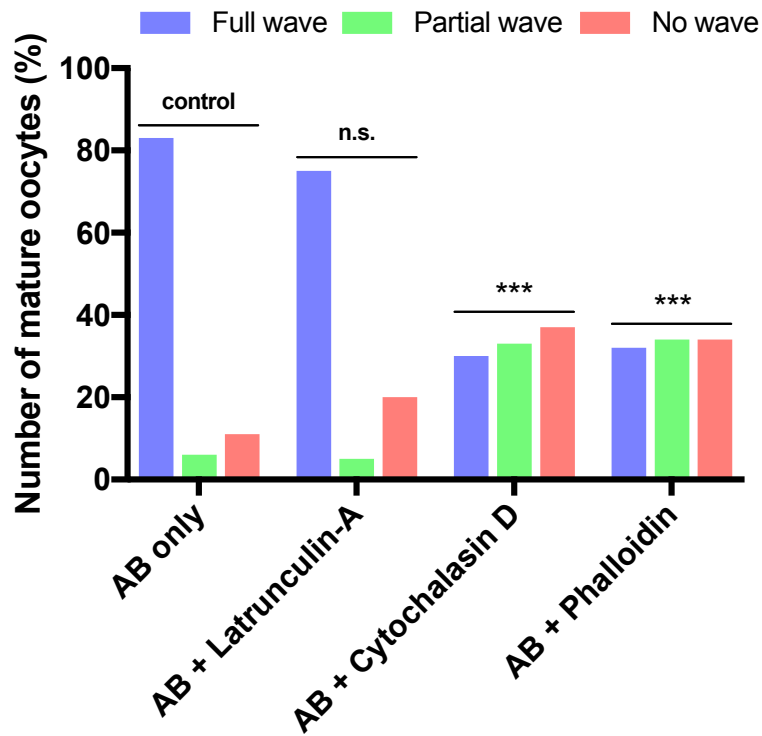
Figure 4.9. Quantification of the calcium wave phenotypes with perturbed actin cytoskeleton.
Calcium wave phenotypes are classified as a full wave (blue); partial wave (green), when a wave does not propagate across an entire oocyte; no wave (red). The mature oocytes treated with AB only exhibit 82% of the full calcium wave phenotype (control). The mature oocytes treated with AB + Latrunculin A show non-significantly different number of full waves (75%) (n=20, P=0.5). The mature oocytes treated with AB + Phallodin or AB + Cytochalasin D show a significant decrease of the full wave to approximately 35% (n=35, P=0.0001). Fisher's exact statistical analysis, P>0.05 was considered significant.

4.3.9 Cortical actin cytoskeleton is more dynamic following egg activation

To test whether cortical actin becomes more dynamic at egg activation, I performed fluorescence recovery after photobleaching (FRAP) on oocytes expressing GFP-Moesin. FRAP is a commonly used technique in cellular biology to determine the rate of redistribution of a fluorescently-tagged protein (Lippincott-Schwartz et al., 2001). The principle behind it is that a certain area is photo-bleached, and the recovery rate of the fluorophore is measured, which gives an indication of the mobility rate of proteins attached to the fluorophores.

Photo-bleaching was carried out for 15 seconds on the cortex of mature oocytes prior to or after egg activation. Prior to egg activation, GFP-Moesin started to show the recovery within 2 minutes and exhibited full recovery 12 minutes after bleaching (Figure 4.10). Following the addition of AB, the recovery after photo bleaching happened much faster in activated oocytes and was fully completed within 1 minute and 30 seconds (Figure 4.10). It was difficult to visualise the bleached area in the activated oocyte for a long time due to continuous egg swelling and movement. The mean fluorescence intensity recovery rate was compared between non-activated (blue line) and activated (red line) mature oocytes, showing that the recovery of cortical actin happens much faster in the activated oocyte (Figure 4.10C). This strongly suggests that the cortical actin becomes more dynamic following egg activation and is possibly required for the opening of the mechanosensitive channels to allow initiation and propagation of the calcium wave. This model will be further discussed in the section below.
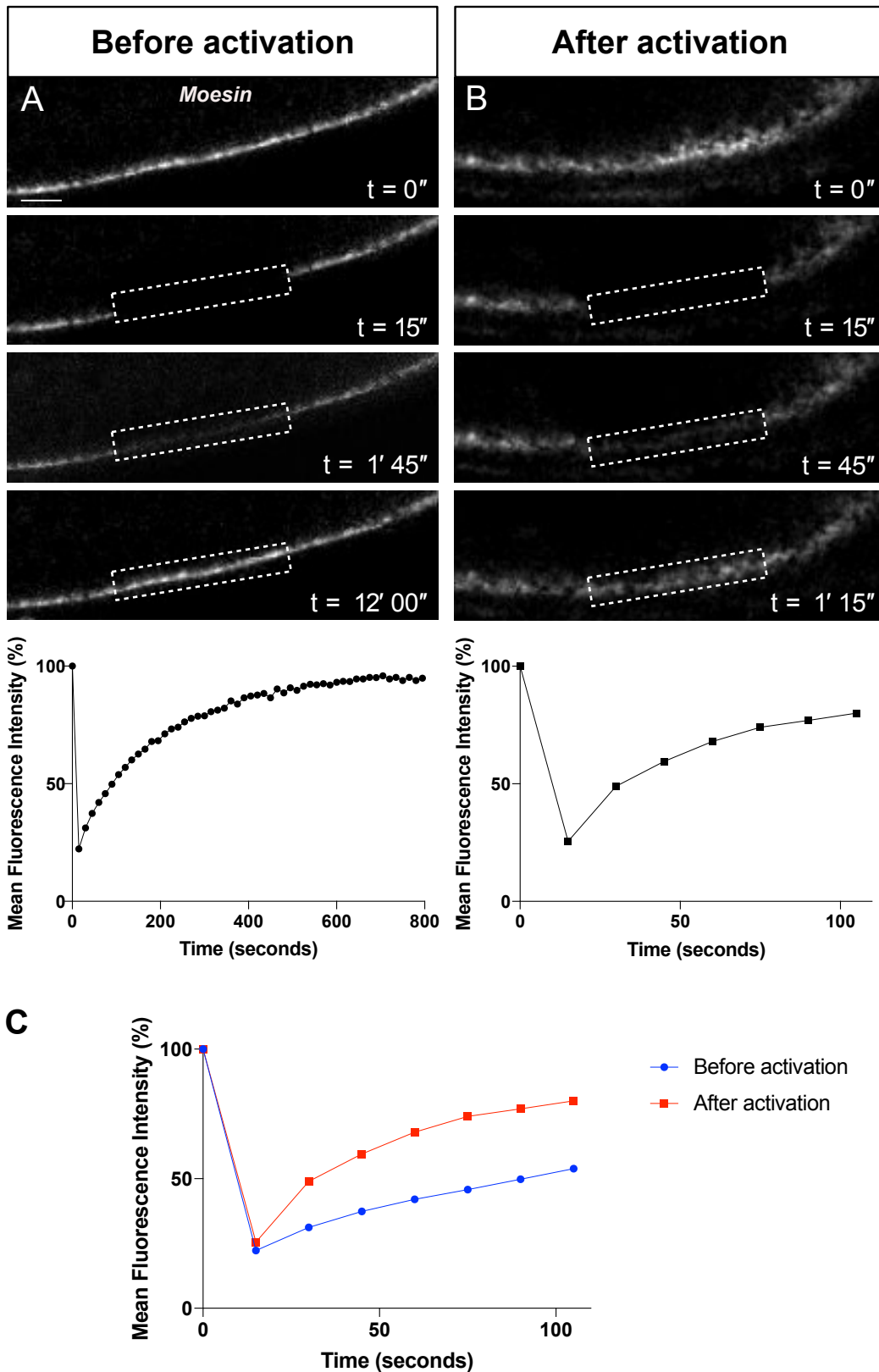
Figure 4.10. Moesin recovery after photo bleaching before and after egg activation.
Panel (A) shows GFP-Moesin prior to egg activation and panel (B) shows GFP-Moesin after egg activation. GFP-moesin is photo bleached to approximately 25% of original mean fluorescence levels for 15″. Graph (C) shows the rate of recovery of GFP-Moesin within first 100 seconds. GFP-moesin recovers to 50% within 100 seconds prior to egg activation (blue line). In comparison, GFP-moesin recovers to 75% within 100 seconds after activation (red line). GFP-moesin recovers at a faster rate after egg activation in comparison to before egg activation.

4.4 Discussion

The data from this chapter provides evidence that there are different populations of actin in the *Drosophila* mature oocyte. One of these is the cortical F-actin that forms a uniform layer at the cortex, but is less enriched at the posterior pole. The cortical F-actin disperses at the onset of egg activation becoming more dynamic following egg activation. The second actin population is the non-cortical F-actin, which shows a wavefront that initiates and propagates across the mature oocyte. The F-actin wavefront is calcium-dependent, has similar characteristics to the calcium wave and shares the same initiation pole. The calcium wave also depends on the dynamic F-actin cytoskeleton. The calcium wave does not occur when the F-actin is stabilised or not able to depolymerise. Together, these findings point towards highly co-regulated calcium and actin signalling networks in *Drosophila* mature oocytes, where actin might play an important role in the downstream events of egg activation, which will be discussed below.

4.4.1 Cortical actin as an osmotic sensor

My data has shown that the osmotic pressure acts as an initiation cue for the calcium wave at egg activation (Chapter 3). One of the cellular components that is known to mediate adequate response to the osmotic pressure is the cortical actin (reviewed in Papakonstanti and Stournaras, 2007). A change in the cortical actin architecture is a common mechanism following the osmotic change within a cell. For example, in adipocyte cells, osmotic shock results in the remodelling of the cortical actin and subsequent movement of Glut4 protein to the plasma membrane (Gual et al., 2002). In yeast, the cortical actin is thought to form so-called cortical bundles and this is proposed to be as a result of osmosensation (Gustin et al., 1998). In contrast, hypertonicity and cell shrinkage is utilised by Magnocellular neurosecretory cells. In this case, an increase in external solute concentration causes a cell to shrink and subsequently activates non-selective ion channels. The flow of positively charged ions into the cell initiates firing of action potentials across the plasma membrane. The cell shrinkage is thought to result in the reorganisation of the

cortical F-actin and the activation of a mechanosensitive channel called Trpv1. The exact mechanism of the actin structural reorganisation is not known.

The signalling pathways that connect the osmosensation and the cortical actin are still not well-understood. The osmosensitivity of the cell does depend on the intact actin as was shown in rat supraoptic nucleus neurones, where mechanosensitivity was disrupted in the presence of Cytochalasin-D (Zhang et al., 2007). One proposed mechanism is via an increase of Rho-GTP by Rho-GTPases which induces the actin polymerisation and subsequent mechanical regulation of channels (Tilly et al., 1996; Prager-Khoutorsky and Bourge, 2009). PI3K is also to be implicated, as it is one of the candidates that is directly linked to the membrane. However, how exactly it is linked to osmosensation and the actin cytoskeleton is not clear.

In *Drosophila* mature oocytes, it is also possible that cortical actin acts as an osmosensor to mediate its own remodelling in response to osmotic shock from the oviduct fluid. This would allow the oocyte to adapt and adjust to an increase in cell volume. This model would explain why Moesin becomes more dispersed within a couple of minutes of egg activation (Figure 4.3). Similarly to the aforementioned increase in Rho-GTPase or PI3K, there can be an increase or activation of signalling molecules in the mature oocyte that could facilitate remodelling of the cortical actin. After an initial dispersion, there was no further visible change in the cortical actin reorganisation in the mature oocyte or early embryo (data not shown). This suggests that the cortical actin becomes more stabilised after the initial change in volume providing a new integrity to the oocyte.

4.4.2 Cortical actin dispersion and activation of mechanosensitive channels

An alternative hypothesis is that the cortical actin reorganisation is linked to downstream processes, such as the opening of the mechanosensitive channels. These include numerous subfamilies, with TRP channels and Deg/ENaC as well-known examples. There are several models arguing as to how these channels are activated. One suggested cue is a direct mechanical stress

applied on the plasma membrane, which creates tension in the membrane, opening the channels and allowing the influx of ions (Christenen et al., 2007).

The other proposed initiation cue of the mechanosensitive channels is via the actin cytoskeleton (Christensen and Corey, 2007). This role of actin was originally shown by electrophysiological studies (Sachs 1991; Sokabe et al., 1991) where pipette suction was utilised to induce stress on the lipid bilayer. More recent work has developed a new system in cultured human umbilical vein endothelial cells, where the membrane tension was directly applied to the actin cytoskeleton by conjugating Phalloidin to fibro-nectin beads (Hayakawa et al., 2008). Once injected, these beads bound actin and induced a direct stress by electrical current (Hayakawa et al., 2008). This resulted in the activation of the mechanosensitive channels and the calcium influx, suggesting that the mechanically-stressed actin cytoskeleton is sufficient to activate some of the mechanosensitive channels.

Immunofluorescence and co-sedimentation techniques have shown that F-actin directly binds a mechanosensitive ENaC channel via the C-terminus of the alpha-subunit in cultured kidney cells (Mazzochi et al., 2006). The same channel was also implicated in osmotic sensing in the *Xenopus* oocyte (Awayda et al., 1996). Other mechanosensitive channels can bind actin indirectly via actin-binding factors, such as alpha-Actinin-2, spectrin or filamin-A (Maruoka et al., 2000; Cukovic et al., 2001; Mazzochi et al., 2006). Although it is clear that some mechanosensitive channels interact with actin in some way, it is not well-understood what causes these differences. There is not much evidence available for TRP channels' interactions with the actin cytoskeleton, other than imaging data, where TRPN1 was shown to co-localise with actin in *Xenopus* cilia of epithelial cells (Shin et al., 2005), and TRPC6 to co-localise with regulators of the actin cytoskeleton (Dryer and Reiser, 2010). Interestingly, TRP channels seem to show the polarisation in their distribution in some cells. TRPV1 and TRPV4 were shown to be independently enriched at the tip of the filopodia (Goswami and Hucno, 2007; Goswani et al., 2010).

Overall, this data suggests that the cortical actin is a suitable candidate to modulate the activity of the mechanosensitive channels and calcium influx in the

Drosophila mature oocyte at egg activation. The osmotic pressure could act by applying mechanical stress on the oocyte membrane and result in the opening of the mechanosensitive channels. Alternatively, the osmotic pressure could exert stress on the cortical actin cytoskeleton and activate channels via the actin cytoskeleton. This hypothesis is consistent with my data showing that direct pressure on the membrane can induce localised calcium response (York-Andersen et al., 2015). This response can be due to the localised actin dispersion and subsequent activation of the mechanosensitive channels.

4.4.3 Non-cortical actin wavefront role

It is hypothesised that F-actin waves are essential for the actin self re-assembly after the initial dispersion at the cortex and are thought to mediate the polymerisation of actin. For example, pharmacological depolymerisation of actin resulted in an increased number of the actin waves in Dictystelium (Bretschneider et al., 2009). A similar observation was made in fibroblasts, where the actin waves take the form of "Circular Dorsal Ruffle (CDR)", which are non-adhesive actin structures found on the dorsal side of some migrating cells (Chhabra and Higgs, 2007; Bernitt et al., 2015; Bernitt et al., 2017). In these papers, it was also argued that the wavefront of actin represents the F-actin polymerisation. Interestingly, osmotic shock has been shown to induce an actin wave in macrophages as well (O'Frenkel et al., 2001). Together, this provides other examples of how the depolymerisation of F-actin can trigger the F-actin waves. Moreover, the F-actin wave is proposed to be associated with the actin-binding factors, including Arp2/3, Myosin B, CARMIL and coronin (Bretschneider et al., 2009; Khamviwath et al., 2013). Live visualisation of these factors in *Dictyostelium* cells have shown their enrichment at the front of the F-actin wavefront (Bretschneider et al., 2009; Khamviwath et al., 2013). It is possible that the F-actin wave at *Drosophila* egg activation also has one or more of these factors associated with it.

4.4.4 Calcium and actin co-regulatory networks

Calcium predominantly regulates the actin cytoskeleton via the actin-binding factors, including myosin, profilin and villin/gelsolin (Cardenas et al., 2008). Early experiments showed that calcium regulates muscle contractions via myosin V protein, rather than directly though actin (Szent-Gyorgi et al., 1975). In this case, calcium binds troponin that, in turn, binds tropomyosin to mediate the actin-myosin contraction cycle (Lehman et al., 1994). Similarly, plants utilise the actin-myosin network for cytoplasmic streaming, and actin is again regulated by calcium signalling via myosin XI (Tominaga et al., 2012). Calcium can also control actin dynamics via profilin, an actin-binding factor, which is required for F-actin polymerisation (Vidali and Helper, 2001). Experiments with profilin show that calcium inhibits F-actin polymerisation by sequestering actin monomers and profilin subunits, which are no longer able to form the actin filaments (Kovar et al., 2000). Calcium has the same depolymerisation or severing affect on the actin cytoskeleton via villin actin-binding factor, and was shown to aid the organisation of actin in epithelial intestinal cells (Walsh et al., 1984). Therefore, calcium is able to regulate the actin cytoskeleton via the actin-binding factors.

Due to their vast number of interactions with a variety of factors, it is difficult to establish direct connections between calcium and actin networks (Veksler and Gov, 2009). The presence of calcium and actin waves and/or oscillations has been well-documented in numerous model systems. For example, the calcium oscillations were shown to result in actin oscillations in mast cells (Wollman and Meyer, 2012; Wu et al., 2013). The proposed link between the two systems is a phospholipid molecule PIP_2, which is thought to recruit an actin-binding factor WASP. The actin oscillations are proposed to result in vesicle secretion via the plasma membrane. Other possible linking candidates are FBP17 and Cdc42 that were shown to undergo oscillations in their intracellular levels at the cortex prior to actin waves in mast cells (Wu et al., 2013).

Overall, my work provides evidence of the calcium requirement for the F-actin wavefront, and vice versa. The F-actin wavefront does not occur if the calcium wave is absent. Similarly, the calcium wave is perturbed in the disrupted actin background. A possible model that the cross-talk between calcium and actin is

coordinated by the factors discussed above. One attractive hypothesis is that the initial calcium influx into the oocyte might mediate subsequent cortical actin rearrangement via profilin or villin factors.

4.4.5 The actin cytoskeleton importance in the egg activation field

The actin cytoskeleton is essential for many cellular processes, including egg activation. The rearrangement of the cortical F-actin seems to be a common feature of some eggs undergoing activation. Examples include F-actin reorganising following exposure to osmotic pressure in zebrafish oocytes, which mediates the release of the cortical granules (Hart and Collins, 1991; Becker and Hart, 1999). More recent work has shown that Aura, an actin-binding factor mediates this reorganisation of actin (Eno et al., 2016). In the mutant Aura background, the F-actin does not rearrange, and cortical granule exocytosis is inhibited.

The starfish oocytes also exhibit actin rearrangement at egg activation, which is required for the calcium influx (Kyozuka et al., 2008). The calcium wave was also shown to initiate the PIP_2 increase at the starfish cortex in a biphasic manner, whilst pharmacological inhibition of PIP_2 production results in a delayed calcium wave and disrupted actin (Chun et al., 2010). Therefore, the proposed link between the calcium and actin networks in the oocytes is PIP_2. Pharmacologically-induced calcium results in the cortical actin dispersion, which is followed by the formation of cytoplasmic F-actin bundles within the cytoplasm (Vasilev et al., 2012). The conclusion from the paper was that there are two F-actin populations in the starfish oocytes: cytoplasmic and cortical. Interestingly, the formation of F-actin bundles was observed within 5 minutes after egg activation. This timing and the presence of two actin populations seems to be similar to *Drosophila* mature oocytes.

My data provides evidence for the initial dispersion of the cortical actin, which might possibly allow the calcium influx via the mechanosensitive channels. The F-actin wavefront is a first visualisation of an actin wave in the oocyte to my knowledge. This is interesting in its own right, and might provide a mechanism

of actin repolymerisation across an entire oocyte. The polymerisation of actin might mediate the closure of the mechanosensitive channels. Future work should focus on elucidating the link between calcium and actin networks in the *Drosophila* mature oocyte, including PIP_2 and other actin-binding factors that were mentioned in this discussion.

Chapter 5

Investigating the mechanism of calcium transport at *Drosophila* egg activation

5.1 Introduction

5.1.1 Overview of the chapter

Calcium acts as an essential cellular messenger to mediate various biological functions. Cells are constantly exposed to a high extracellular calcium concentration, which is 10,000 times higher than the intracellular calcium concentration. Therefore, calcium flux must be controlled in a temporal and spatial manner utilising specialised channels, which are categorised by the activation stimuli: (1) voltage-gated; (2) mechanically-activated; (3) store-operated; and (4) ligand-activated. This introduction will summarise the mechanism of how these channels collectively regulate calcium transport, with their role at egg activation highlighted in the discussion section.

5.1.2 Voltage-gated calcium influx

Voltage-gated calcium channels are activated by changes in the membrane potential and are usually found in excitable cells (reviewed in Catterall, 2011). Purification of the voltage-gated channel complex from skeletal muscle cells indicated it was comprised of five subunits: α_1, α_2, β, γ and δ (Flockerzi et al., 1986; Takahashi et al., 1987; Award et al., 1996; Curtis and Catterall, 2002;). These studies demonstrated that the α_1 subunit is composed of six transmembrane domains and acts as a central pore to mediate the calcium influx into the cell. The γ subunit has four transmembrane domains (Jay et al., 1990). The β subunit binds the α_1 subunit via the N-terminus and does not traverse the lipid bilayer (Ruth et al., 1989), whilst both α_2 and δ are found on the extracellular side of the membrane bound via the δ subunit disulphide bonds (Gurnett et al. 1996). These subunits regulate an efficient entry of calcium ions in a voltage-dependent manner.

The voltage-gated channels were subdivided into a further five families: L, T, N, P, Q (Catterall, 2011). The L-type channels are predominantly found in excitable cells, where the calcium current is activated by a high voltage stimulus, exhibiting prolonged duration (Church and Stanley, 1996). In contrast, the short

calcium inward current is mediated by T-type voltage-gated channels which were discovered in starfish eggs at egg activation (Hagiwara et al., 1975). These become activated at a lower membrane potential compared to the L-type channels (Carbone and Lux, 1984). The final four classes of voltage-gated channels, N, R, P and Q, are primarily found in neuronal cells and are differentiated by the inhibitory affects of toxins (Mintz et al. 1992; Randall and Tsien 1995; Wang et al., 1999). The voltage-gated channels together sense a range of membrane potentials and coordinate an adequate calcium influx into the cell.

5.1.3 Ligand-operated calcium influx

Ligand binding to the receptor is another mechanism to initiate the calcium influx into the cell. In this case, the ligand binds the extracellular domain of the calcium channel resulting in the conformational change and release of calcium into the cytoplasm. Well-known examples of these receptors include the inositol 1,4,5-trisphosphate (IP_3) and ryanodine (RyR) receptors found on the ER or sarcoplasmic reticulum in muscles. These receptors are regulated by IP_3 or ryanodine ligand binding to the extracellular domain respectively.

The IP_3 receptor was originally identified and purified from the mammalian cerebellum (Maeda et al., 1988; Supathapone et al., 1988). In mammals, there are three isoforms of the IP_3 receptor IP_3R1, IP_3R2 and IP_3R3 (Taylor et al., 1999), which can form a homotetrameric or heterotetrameric receptor (Taylor and Tovey, 2010). IP_3 binding results in the conformational change in the receptor (Yoshikawa et al., 1996). It is hypothesised that IP_3 binding displaces the N-terminus suppressor domain from the channel pore and exposes the calcium binding site. Subsequent calcium binding moves the suppressor domain from the "gatekeer" domain, allowing calcium influx into the cytoplasm (Taylor et al., 2004). IP_3 initiates calcium release from the adjacent channels resulting in CICR propagation across the cell.

A similar CICR response can be mediated by the RyR (Fabiato, 1983). In comparison to the IP_3R ubiquitous expression, the RyR is more predominant in

the muscle and neuronal tissues (Bootman et al., 2012). The four RyR monomers bind together to form a homotetramer. RyR activation is regulated by ryanodine and calcium binding, but calcium is sufficient to activate the RyR on its own. Together, the IP₃R and the RyR ensure an intracellular calcium increase in a form of CICR in response to an external stimuli.

5.1.4 Store-operated calcium influx

The prolonged activation of the IP₃R and RyR can result in the depletion of the intracellular calcium stores. This depletion can activate store-operated channels, including Orai channels (Yeromin, et al., 2006). The role of Orai channels was discovered in T-cells in which mutational analysis disrupted the development and activation of these cells (Fanger, 1995; Hoth, 1995; Crabtree, 1995, Lewis, 1995; Lewis, 2001). This evidence was reinforced by the identification of the same protein using an RNAi-wide screen in *Drosophila* S2 cells (Feske et al., 2006; Peinelt, et al., 2006; Zhang et al., 2006). It was confirmed that mammals express three genes of Orai: Orai1, Orai2 and Orai3 (Moccia et al., 2015). The depletion of calcium in the ER results in an Orai-mediated calcium influx into the cytoplasm across the plasma membrane, which is coordinated by stromal-interacting molecules (STIM) (Moccia et al., 2015).

STIM was identified in *Drosophila* S2 cells (Roos et al., 2005) and in mammalian cells (Liou et al., 2005). STIM is localised to the ER membrane with its N-terminus pointing to the ER lumen (Lewis, 2011). The N-terminus has two EF-hand domains that bind calcium ions when the ER stores are full of calcium. Once calcium is released into the cytoplasm, calcium dissociates from the EF-domains, indicating the low levels of calcium within the ER lumen (Lewis, 2011). This results in STIM protein re-location within the ER closer to the plasma membrane to bind and activate Orai channels. The overexpression of both STIM and Orai1 in the mammalian cultured cells increased the inward calcium influx, indicating that Orai mediates the calcium entry from the extracellular environment (Mercer et al., 2006; Peinelt et al., 2006). The presence of STIM-Orai protein complex allows a way of detecting the calcium concentration within

the intracellular stores and refilling these stores with upregulated calcium entry from the extracellular environment.

5.1.5 Mechanically-gated calcium influx

The fourth class of calcium channels are the mechanosensitive channels, which as the name suggests, are activated by a mechanical stimuli transduced via the lipid bilayer. The transient receptor potential (TRP) channels provide a great example of the mechanosensitive channels that mediate the calcium influx in response to a variety of stimuli. Mutational and complementation analysis in the fly visual system enabled the discovery of TRP channels (Cosens and Manning, 1969; Montell et al., 1985; Montell, 2001; Montell et al., 2002). TRP channels are subdivided into a further seven families, based on sequence homology. These families include TRPC, TRPV, TRPM, TRPA,TRPP, TRPN and TRPML (Montell, 2005, Ramsey et al., 2006). The general structure of the TRP channel consists of six transmembrane spanning domains, with the pore domain formed between S5 and S6 loops. The TRP channels assemble from four subunits, which form a non-selective cation channel pore, with an exception of TRPV5 and TRPV6 channels that are selective for calcium ions.

The first activation by a mechanical stimulus was observed in *Xenopus* oocytes, which resulted in opening of TRPC1 (Methfessel et al., 1986). Mechanical stimuli also play a role in initiating TRPC3, TRV6, TRPV2 and TRPM4, which coordinate blood vessel constriction in the muscle and other tissues (Welsh et al., 2002; Earley et al., 2004; Dietrich et al., 2005). The mechanical stimuli may also be relayed indirectly via the osmotic pressure that causes the tension in the plasma membrane from inside the cell. TRPV4 and TRPV1 are examples of TRP channels that respond to external osmotic pressure in mammalian sensory neurones (Liedtke et al, 2000; Strotmann et al., 2000; Sharif Naeni et al., 2006; Ciura et al., 2011). Other potential initiation cues include nociception, taste and temperature (reviewed in Christensen and Corey, 2007). However, there is a great redundancy between the initiation cues and TRP channels, and therefore, it is difficult to place them into specific categories.

TRP channels have also been hypothesised to coordinate calcium influx via interaction with IP_3 channels. This was shown to be the case with the human channel TRP3, where the IP_3R was shown to physically bind and activate TRP in transfected cultured cells (Kiselyov et al., 1998; Kiselyov et al., 1999; Boulay et al., 1999). It is proposed that the IP_3R is able to sense the ER depletion in calcium and bind to the nearest TRP channel in the plasma membrane (Putney, 1999). Interestingly, all channels in the TRPC family are known to require PLC for their activation, suggesting a store-depletion activation mechanism (Venkatachalam et al., 2002; Montell, 2005). However, it is not quite clear whether this activation happens *in vivo*.

Interestingly, TRP channel activation has also been linked to the PIP_2 signalling pathway in fly phototransduction. It was shown that a G-protein coupled receptor (GPCR) is activated by light stimuli and results in the calcium influx via the PLC pathway. At the same time, mutations in the TRP channel results in a significant decrease in the calcium influx (Hardie and Minke, 1992; Montell, 1999). One hypothesis is that the TRP channel can be activated by the PLC hydrolysis of PIP_2, thus releasing a PIP_2 inhibitory effect on the TRP channel. This was confirmed to be the case for the TRP channels in *Drosophila* retinal cells in two independent studies: where (1) PLC hydrolysis of PIP_2 resulted in contractions of the bilayer and changes in gating of TRP channel (Hardie and Franze, 2012); and (2) depletion of PIP_2 using genetic tools resulted in the disrupted calcium influx and retinal neurodegeneration (Sengupta et al., 2013). Together, this evidence highlights a potential link between TRP channels, the phosphoinositide pathway and calcium influx. Overall, this section shows that TRP channels are suitable candidates to mediate calcium influx in response to a variety of physical and molecular stimuli.

5.1.6 Intracellular calcium removal by an electrochemical gradient

Although, calcium acts as an important second-messenger regulating various downstream processes, prolonged exposure to calcium can result in cell dysfunction and cell death (Berridge et al., 2003). Cells have evolved numerous ways to remove cytosolic calcium and bring the concentration down to basal

level of approximately 100nM. Calcium can be pumped back to the intracellular stores, such as ER or mitochondria, or to the external environment (Berridge, 2005; Clapham, 2007). As the extracellular and organelle calcium concentration is often higher than cytosolic concentration, the removal of calcium requires some form of energy.

A common mechanism to remove cytosolic calcium is through the use of a previously established electrochemical gradient of a different ion. The Na^+/Ca^{2+} exchanger (NCX) is an example of a channel that uses an electrochemical gradient of three sodium ions to pump one calcium out (Blaustein and Lederer 1999; Kang et al., 2006); as at physiological levels the extracellular sodium concentration is higher than that of intracellular sodium, this gradient can be used to export calcium in a secondary active transport mechanism (Philipson et al., 2002). NCX has low affinity for calcium ions, and hence high-capacity to coordinate rapid removal of calcium out of the cell. It is generally considered that NCX is used to guide calcium out ("forward mode"). However, NCX is also able to transport calcium into a cell ("reverse mode"), when intracellular sodium is high (Philipson et al., 2002; Jeffs et al., 2007). NCX has been shown to play a role in most cells, including heart and muscle tissues, epithelial cells and neurones (Dipolo and Beauge, 2006; Balasubramaniam et al., 2015) and has been shown to associate with some pathological conditions, such as Alzheimers disease and cardiac failure (Langenbacher et al., 2005; Henok et al., 2016). Therefore, NCX is essential for mediating calcium homeostasis and normal physiological functions.

5.1.7 Intracellular calcium removal by ATP hydrolysis

An alternative mechanism to actively remove cytosolic calcium uses ATP hydrolysis. P-type ATPases are a class of transmembrane proteins that hydrolyse ATP to facilitate ion transport across a membrane (Apell, 2004). There are two calcium P-type ATPases, which remove calcium into the ER and the external environment: sarcoendoplasmic reticulum calcium-ATPase (SERCA) and plasma membrane calcium-ATPase (PMCA). They are activated by binding of calmodulin and by phosphorylation by protein kinase A and C

(Carafoli 1991; Carafoli 1992). In contrast to the Na^+/Ca^{2+} exchanger, SERCA and PMCA have a high affinity for calcium, but low capacity, and hence these pumps are used for long-term removal of calcium (Clapham et al., 2007).

The function of SERCA has been commonly studied using a pharmacological inhibitor called Thapsigargin, which binds stoichiometrically to all SERCAs and irreversibly inhibits SERCA to remain in the calcium-free state (Lytton et al., 1991). The inhibition of SERCA by Thapsigargin was shown to activate calcium influx in an unfertilised mouse egg and to suppress repetitive calcium transients in the fertilised egg, suggesting that SERCA is required in the replenishment of calcium internal stores to support calcium oscillations in a mouse egg (Kline and Kline 1992). However, it is not clear whether SERCA is also required at *Drosophila* egg activation.

Calcium can be extruded to the extracellular environment by another calcium-ATPase, PMCA, which is essential for the control of the cytoplasmic calcium concentration (Stauffer et al., 1995). The mechanism of calcium removal for PMCA channels is similar to SERCA, except that PMCA extrudes one calcium ion per one ATP hydrolysed (Strehler and Treiman, 2004; Clapham et al., 2007). In an active form, PMCA has low calcium affinity and is inactive at the basal concentration of calcium (100nM). PMCA is activated by Calmodulin, which increases PMCA affinity for calcium (Carafoli 1992). PMCA is known to be expressed in a tissue-specific manner and has several isoforms created by alternative splicing (Strehler and Zacharias, 2001). Compared to four mammalian genes, *Drosophila* has only one gene that encodes for the PMCA protein which has been shown to play a role in the neuromuscular junction, synaptic terminals, muscle and heart tissue (Lnenicka et al., 2006; Desai-Shah et al., 2010; Desai et al., 2011). However, it is still not well-understood whether PMCA is required for the recovery at *Drosophila* egg activation.
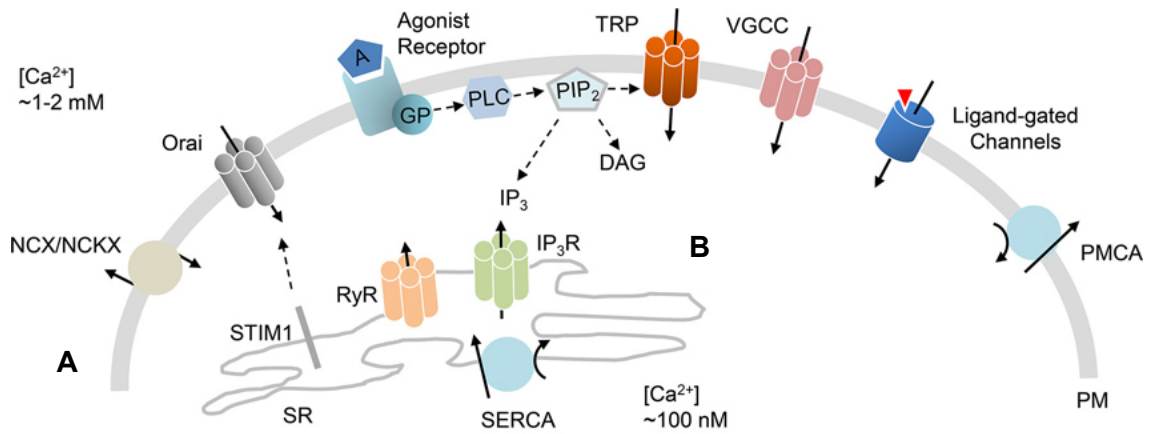
Figure 5.1. Summary diagram of the channels that mediate calcium transport. *Adapted from Harraz and Altier, Frontier Neuroscience, 2014.* (A) The channels in the plasma membrane from left to right are: (1) Na^+/Ca^{2+} exchanger (NCX); (2) Orai; (3) G-protein coupled receptor (GPCR); (4) Transient receptor potential (TRP); (5) Voltage-gated calcium channel (VGCC); (6) Ligand-gated channels; and (7) Plasma membrane calcium ATPase (PMCA). (B) Represent the endoplasmic reticulum inside the cell, starting from left with: (1) stomal-interacting molecule (STIM1); (2) ryanodine receptor (RyR); (3) IP_3 receptor (IP_3R); and (4) sarco-endoplasmic reticulum calcium ATPase (SERCA).

5.1.8 Focus of this chapter

This introduction provides an overview of the channels involved in calcium transport. In the table below I have summarised the relevant *Drosophila* homologues of these channels, and have highlighted those that are expressed in the ovarian tissue (Table 1). Due to time constraints of this project, I have selected the most likely candidates to investigate: (1) Painless; (2) Water-witch; (3) Trpm; (4) IP_3 receptor; (5) NCX; (6) SERCA (Ca-P60A); and (7) PMCA.

	Protein name	Gene name	Annotation symbol	Expression in ovarian tissue	Level of expression	Type of the channel
1	Ryanodine Receptor	rya-r44F	CG10844	NO	5 ± 1	Ligand-operated
2	Flower	fwe	CG6151	YES	147 ± 5	Ligand-operated
3	IP3 receptor	ltp-r83A	CG1063	YES	42 ± 0	Ligand-operated
4	NMDA receptor 1	nmdar1	CG2902	NO	0 ± 0	Ligand-operated
5	NMDA receptor 2	nmdar2	CG33513	NO	0 ± 0	Ligand-operated
6	Orai-1	olf186-F	CG11430	YES	362 ± 25	Store-operated
7	STIM	Stim	CG9126	YES	573 ± 5	Store-operated
8	Trpm	trpm	CG30079	YES	33 ± 1	Mechanosensitive
9	Painless	pain	CG15860	YES	15 ± 1	Mechanosensitive
10	Water-witch	wtrw	CG31284	YES	15 ± 1	Mechanosensitive
11	Ripped-pocket	rpk	CG1058	YES	904 ± 10	Mechanosensitive
12	Ca^{2+} channel α1 subunit D	Ca-α1D	CG4894	NO	0 ± 0	Voltage-gated
13	Ca^{2+}-channel α1 subunit T	Ca-α1T	CG4894	NO	0 ± 0	Voltage-gated
14	Ca^{2+}-channel-protein-β-subunit	Ca-β	CG42403	NO	1 ± 0	Voltage-gated
15	Cacophony	cac	CG43368	NO	5 ± 0	Voltage-gated
16	CG4587	CG4587	CG4587	NO	0 ± 0	Voltage-gated
17	Straightjacket	stj	CG12295	NO	2 ± 0	Voltage-gated
18	Organellar-type Ca-ATPase	Ca-P60A	CG3725	YES	543 ± 11	Calcium ATPase
19	Plasma membrane calcium ATPase	PMCA	CG2165	YES	281 ± 4	Calcium ATPase
20	Na/Ca-exchange protein	Calx	CG5685	YES	42 ± 2	NCX

Table 5.1. Summary of the possible *Drosophila* calcium influx channels and their expression levels in the ovarian tissue.
Expression levels in the ovarian tissues based on the data from Drosophila FlyAtlas.

5.2 Aims of this chapter

1. **To investigate the requirement of the mechanosensitive channels for calcium influx at *Drosophila* egg activation.**

2. **To test the requirement of the IP$_3$ channel for calcium influx at *Drosophila* egg activation.**

3. **To address the requirement of the SERCA, PMCA and Na$^+$/Ca2$^+$ exchanger for the removal of calcium at *Drosophila* egg activation.**

5.3 Results

5.3.1 Trpm and Water-witch are possibly required for the calcium influx at *Drosophila* egg activation

Drosophila expresses three TRP channels in the ovary: *Painless*, *Water-witch* and *Trpm* (*Drosophila* FlyAtlas). To address the requirement of these channels, I utilised mutant and RNAi lines to remove or knock-down the function of these genes. The first candidate I tested was Painless, which is part of the TRPA subfamily of channels. To address if Painless is required at egg activation, I tested the presence of the calcium wave in the mature oocytes expressing MyrGCaMP5 in a Painless mutant background (EP2251), which is a P-element insertion in the 5'- flanking region (Tracey et al., 2003). Upon the addition of AB, the mature oocytes swelled normally and showed the full calcium wave in 65% of the oocytes in the homozygous Painless background (n=17) (Figure 5.2) and 70% in the heterozygous background (n=10) (Figure 5.2B). This is not significantly different compared to the number of the calcium waves present in the wild-type eggs (Figure 5.2B). This suggests that Painless is likely not required for the calcium wave at *Drosophila* egg activation.

It is possible that Water-witch channels, instead, sense the change in the osmotic environment and mediate calcium influx at egg activation. To address this hypothesis, I expressed GCaMP3 in the homozygous Water-witch mutant background (EY20195), but this background was lethal. The heterozygous background of the same mutant showed the full calcium wave in 70% of the oocytes (n=10) (Figure 5.3A,D). Thus, I utilised an available RNAi knock-down line (BL51503), which is designed to reduce the Water-witch levels in somatic and germline tissues (*in vivo* fly RNAi TRiP collection). Upon the addition of AB to the mature oocytes expressing two copies of this RNAi line, the oocytes swelled as normal, but exhibited a slight, but significant decrease in the number of full calcium waves present at activation (50%, n=14, P=0.03) (Figure 5.3B,D). The expression of the Water-witch mutant with one copy of RNAi resulted in a decrease of the full calcium waves to 67% (n=9) (Figure 5.3C,D), which is not significant compared to the expression of both RNAi copies.
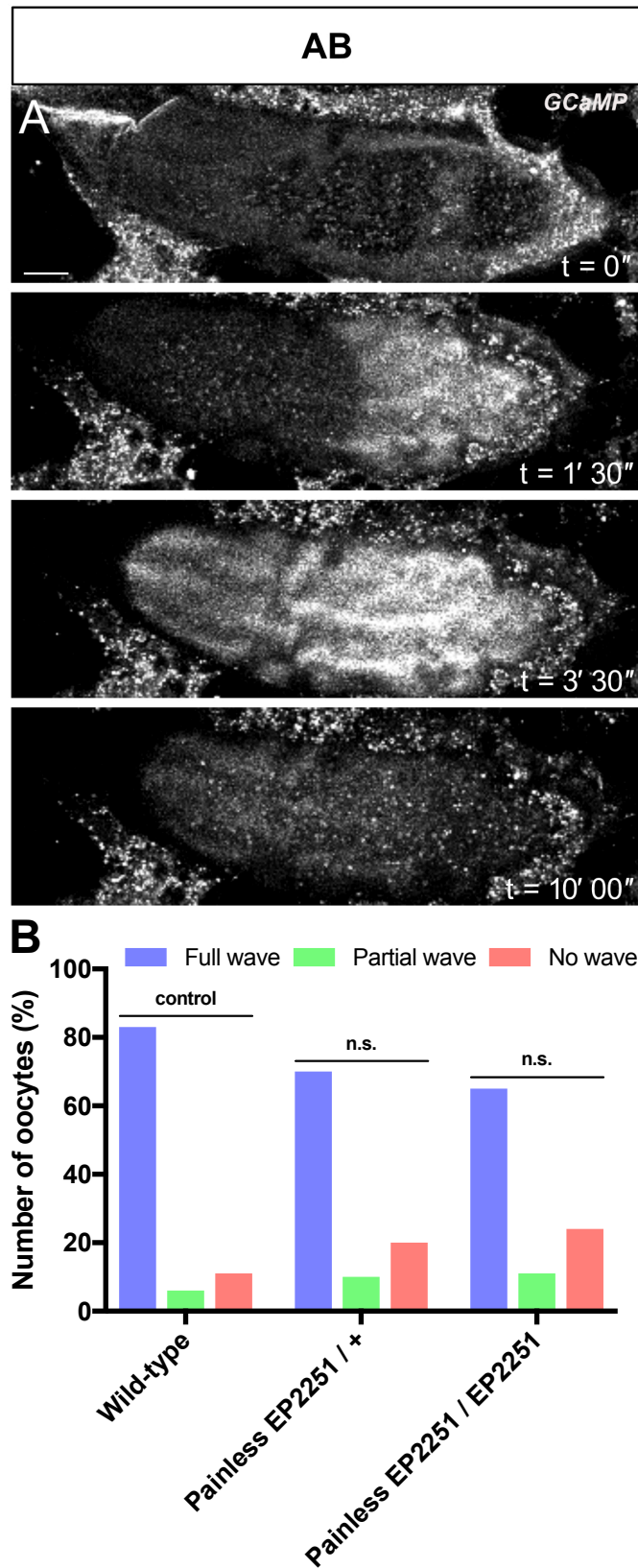
Figure 5.2. Full calcium wave is present in the Painless mutant background .
(A) Time-series of *ex vivo* mature oocyte expressing *UAS-MyrGCaMP5* following the addition of AB. The oocyte swells and shows the initiation and propagation of the calcium wave, similar to a wild-type calcium wave. The bright tissue around the egg is the ovarian tissue. Scale bar 60μm. Maximum projection = 40μm (B) Graph shows that the number of oocytes exhibiting the calcium wave is not significantly different between wild-type, heterozygous and homozygous Painless mutant (Fisher's exact statistical test).

Interestingly, the expression of two RNAi copes, or one RNAi copy with a mutant, resulted in a more rounded shape and a decrease in the length of the oocyte by 40%. These oocytes became more rounded at swelling and lifted off the slide more frequently, making imaging more challenging. Thus, the region of imaging is reduced in comparison to wild-type (Figure 5.3B and 5.3C). These findings suggest that Water-witch is likely to mediate the calcium influx at egg activation. However, it is difficult to draw a definitive conclusion, as RNAi lines do not mediate a full knock-down of the gene.

The final candidate that has been shown to be expressed in *Drosophila* ovarian tissue is Trpm (*Drosophila* Fly Atlas). To date, the role of Trpm has only been shown in calcium, magnesium and zinc ions' homeostasis (Georgiev et al., 2010; Hofmann et al., 2010). To investigate the role of Trpm in the calcium influx at *Drosophila* egg activation, I utilised a mis-expression line under the control of UASp from BDGP Gene Disruption Project (Trpm^{EY01618}) (Bellen et al., 2004). Trpm^{EY01618} is a transposon P-element insertion in the 39th splice site of which results in an imprecise deletion of three exons of *Trpm* and subsequent mis-expression of Trpm protein (Hofmann et al., 2010). I firstly expressed MyrGaMP5 in a homozygous Trpm^{EY01618} background. However, this cross turned out to be infertile. Therefore, I expressed only one copy of Trpm^{EY01618} with GCaMP. Upon the addition of AB, the mature oocytes swelled as expected, but did not show the calcium wave in any experiments (n=14) (Figure 5.4). This would suggest that Trpm might be involved in regulating the entry of calcium into the mature oocyte. Interestingly, the mammalian homolog TRPM3 was also shown to be activated by hypotonic solution of 200mOsm, and to result in an intracellular calcium increase in HEK293 cells (Grimm et al., 2003). Therefore, Trpm is the best candidate investigated in this chapter to mediate the calcium influx in response to the osmotic pressure at *Drosophila* egg activation.
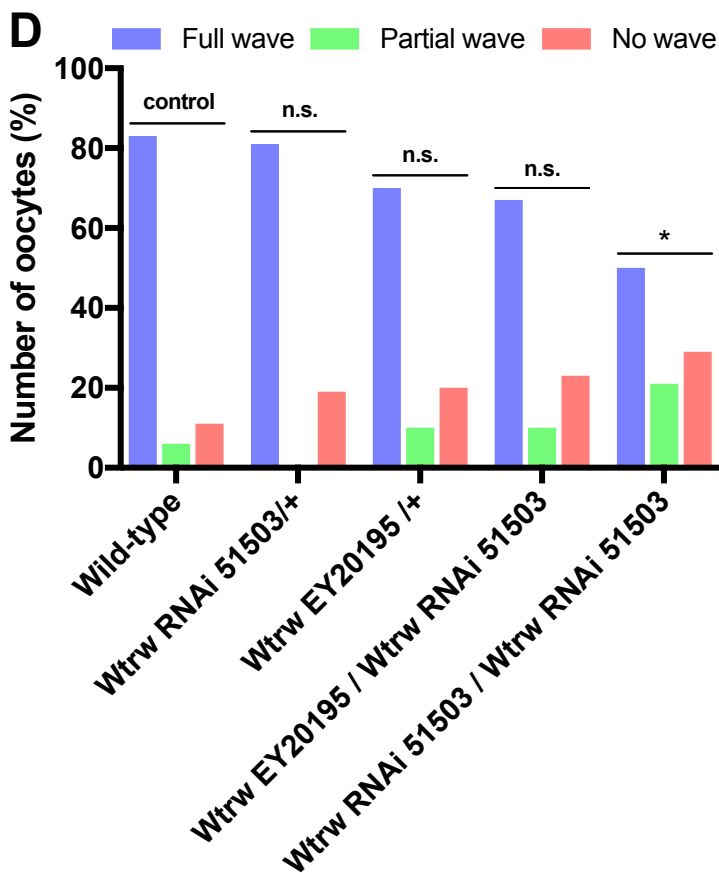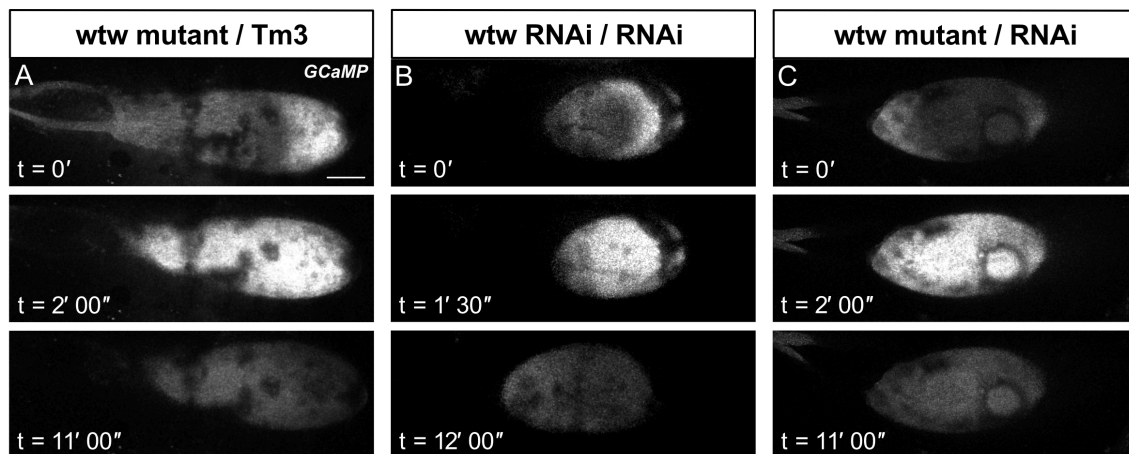
Figure 5.3. Full calcium wave is exhibited in Water-witch (Wtrw) depleted background at *Drosophila* egg activation.

(A-C) Time-series of *ex vivo* mature oocyte expressing *UAS-GCaMP3* following the addition of AB. (A-C) The oocyte swells and shows normal initiation and propagation of the calcium wave. (B-C) Water-witch RNAi background results in a reduced length of an oocyte. Upon the application of AB, the eggs were less stable on the slide, therefore the figure shows reduced area in panel B and C. (B). The dark lines or spots represent some extra tissue or bubbles. Scale bar 60µm. Maximum projection = 40µm. (D) Graph shows the number of the oocytes exhibiting the calcium wave. The significant difference is compared to the wild-type eggs expressing *GCaMP* only. Only two copies of Wtrw RNAi show a significant difference in the number of the full calcium wave present (P=0.03, Fisher's exact test).
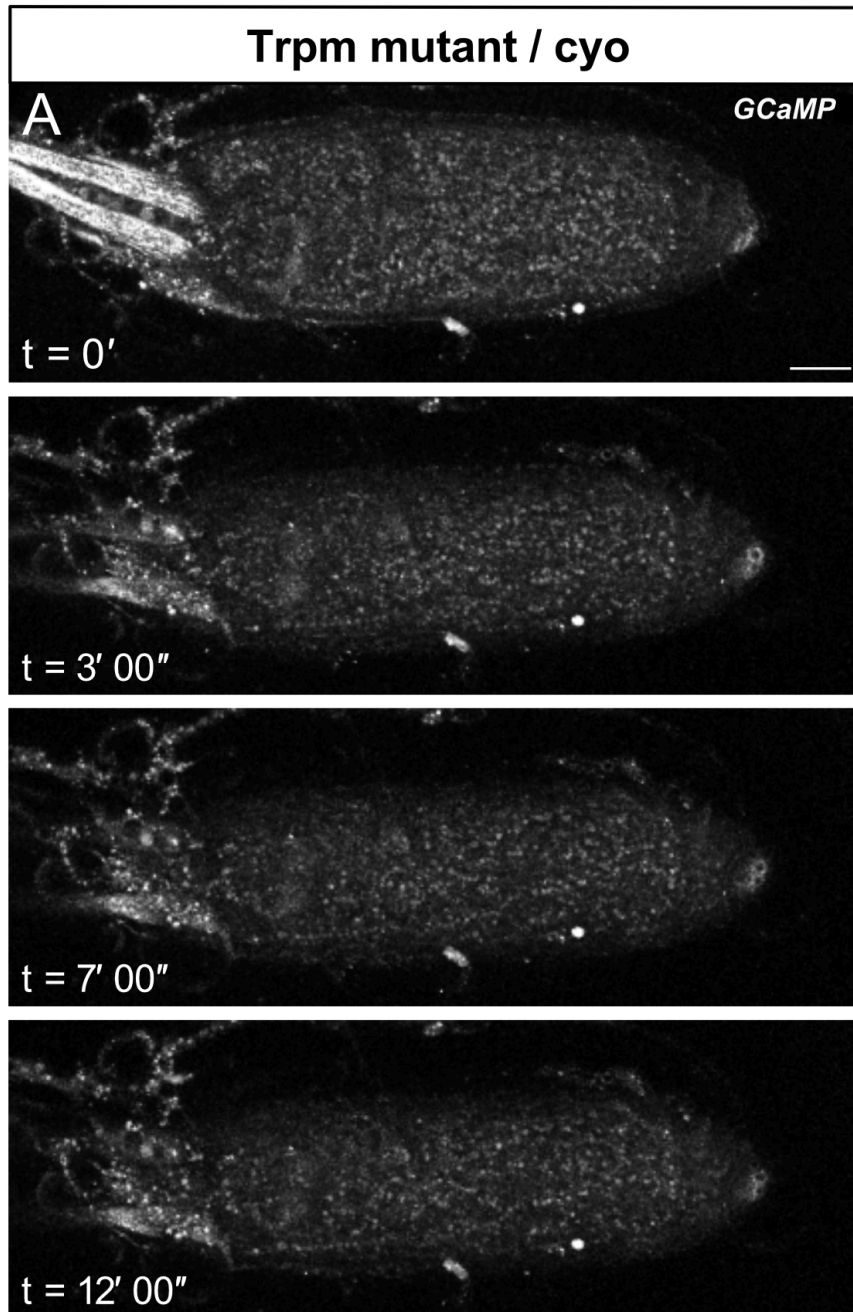
Figure 5.4. Heterozygous Trpm mutant results in no wave phenotype at egg activation .
Time-series of *ex vivo* mature oocyte expressing *UAS-MyrGCaMP5* following the addition of AB. The oocyte swells normally, but does not show the initiation or propagation of the calcium wave. Scale bar 60µm. Maximum projection = 40µm.

5.3.2 RPK mechanosensitive DEG/ENaC channel results in a cortical calcium increase at *Drosophila* egg activation

Another class of the mechanosensitive channels is DEGenerin/Epithelial Na$^+$ (DEG/ENaC) channels. These are important in transducing mechanical stimuli in many tissues, including neurones and epithelia.(Chalfie and Wolinsky, 1990; Driscoll and Chalfie, 1991; Garcia-Anoveros et al., 1995). In early development, DEG/ENaC channels have been shown to play an important role in the polyspermy block in *Xenopus* oocytes and in the blastocyst formation in mammals (Biggers and Powers, 1979; Robinson et al., 1991).

Drosophila express two members of the DEG/ENaC channels family: Pickpocket and Ripped-pocket (RPK) (Adams et al., 1998; Darboux et al., 1998). The RPK channel is specifically expressed in the oocytes from stage 5 to early embryos (Adams et al., 1998). To test whether RPK is required for egg activation, I utilised an RNAi line to knock-down RPK in somatic and germline tissues (BL39053). Upon the addition of AB to the oocytes expressing MyrGCaMP5 with two copies of RNAi, the mature oocytes exhibited the cortical calcium increase within the first 30 seconds, a lysing of the plasma membrane and a leaking of the cytoplasm in 74% of the oocytes (n=19) (Figure 5.5). This calcium phenotype is normally associated with the exposure of the oocyte to low osmolarity (Chapter 3), suggesting that RPK is required to mediate swelling of the oocyte at egg activation.
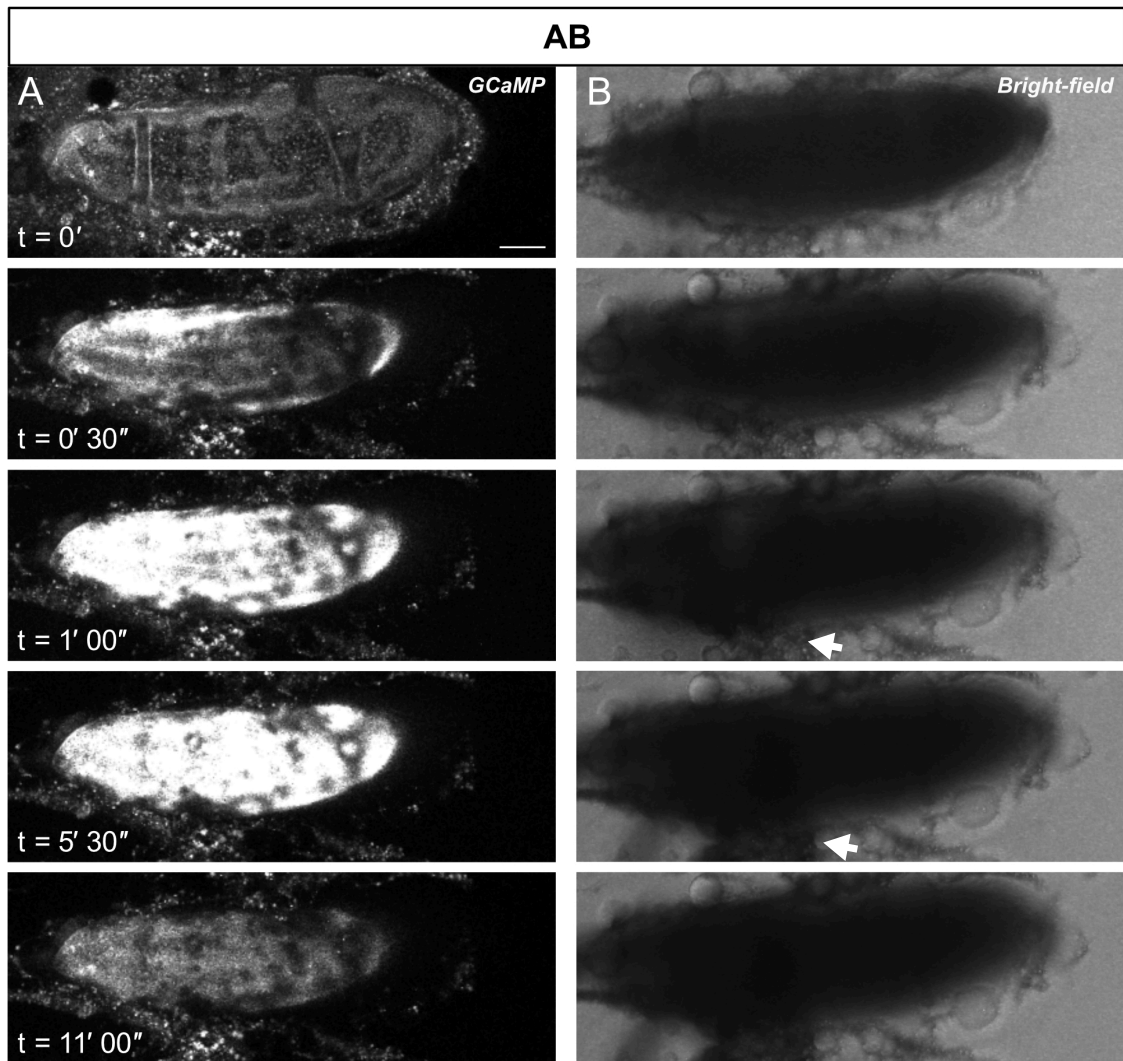
Figure 5.5. RPK knock-down results in the cortical calcium increase and a burst of the oocyte at egg activation.
(A-B) Time-series of *ex vivo* mature oocyte expressing *UAS-MyrGCaMP5* following the addition of AB. The cortical increase appears within 30 seconds of the addition of AB, which is followed by the oocyte burst (white arrow). The dark spots represent excess tissue and bubbles around the oocyte. Scale bar 60µm. Maximum projection = 40µm.

5.3.3 Possible IP$_3$ receptor requirement at *Drosophila* egg activation

The ER is a potential intracellular calcium store, which could coordinate the calcium influx via the IP$_3$ and/or RyR receptors (Berridge, 2005; Clapham, 2007). RyR is not expressed in *Drosophila* ovarian tissue (*Drosophila* Fly Atlas), and was shown not to be required for the calcium wave when inhibited with ruthenium red (Kaneuchi et al., 2015). Therefore, if the ER is essential for the *Drosophila* calcium wave, the IP$_3$ receptor is the most likely candidate to mediate the calcium influx.

To address this hypothesis, I observed the calcium wave phenotype in the IP$_3$ mutant background. I attempted to express GCaMP3 in an IP$_3$ transheterozygous mutant background, which is known to disrupt IP$_3$-mediated calcium release (BL 30740 and BL30741). Since this genotype is lethal, I investigated the mature oocytes expressing only one copy of an IP$_3$ mutant with GCaMP3 (BL 30741). Upon the addition of AB, I observed swelling and a full calcium wave in 80% of the oocytes, which was not significantly different to wild-type (n=10, P=0.6) (Figure 5.6). This does not prove that the IP$_3$ receptor is not required for the calcium wave, as the calcium wave could have been rescued by the wild-type IP$_3$ gene. Thus, to further investigate the IP$_3$ receptor requirement for the calcium wave, I utilised IP$_3$ RNAi lines expressed in the germline and somatic tissues (BL51795 and BL 51686). However, this genotype is also lethal. Therefore, it remains unclear whether the calcium wave depends on the IP$_3$-mediated pathway at *Drosophila* egg activation.
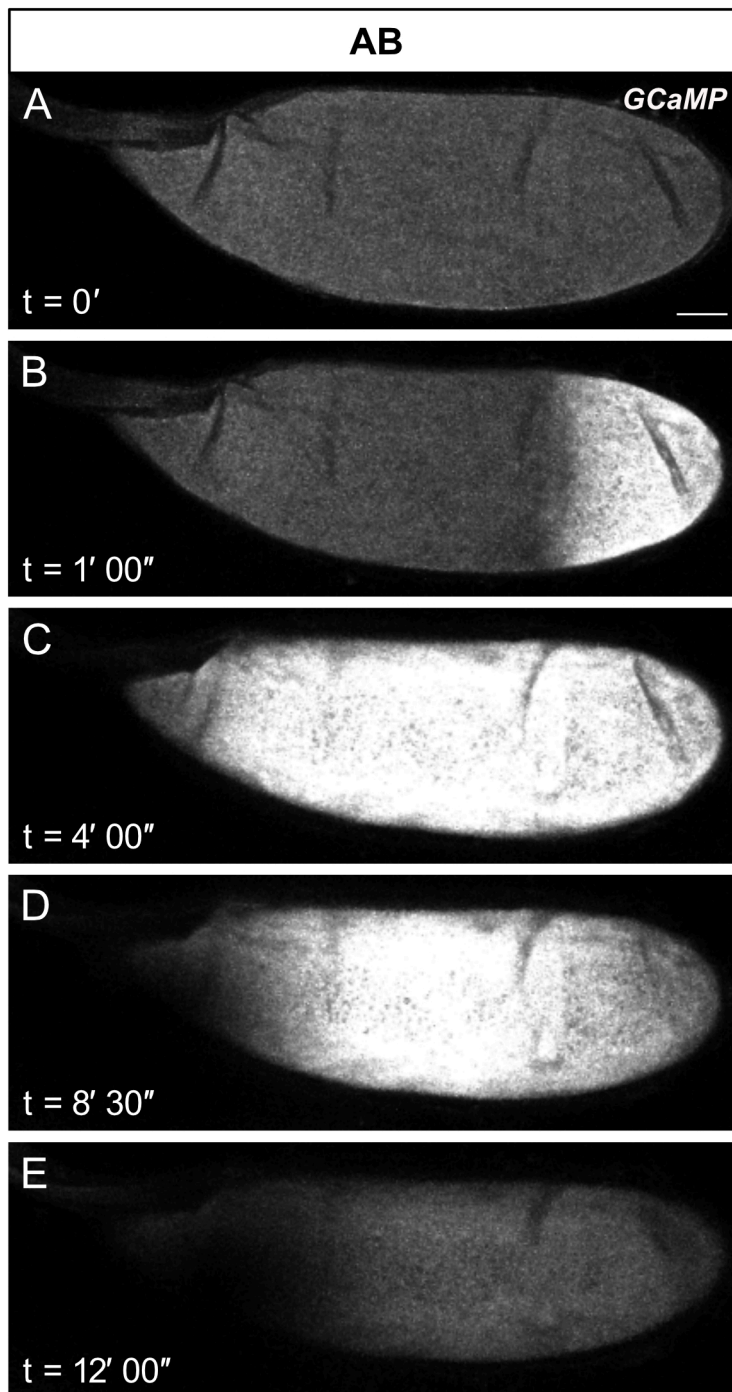
Figure 5.6. Heterozygous IP₃ mutant background displays a calcium wave at *Drosophila* egg activation.
(A-E) Time-series of *ex vivo* mature oocyte expressing *UAS-GCaMP3* following the addition of AB. The calcium wave initiates from the posterior within 1 minute of the addition of AB (B), propagates across the oocyte (C), initiates recovery at around 8 minutes 30 seconds (D) and is completed by 12 minutes (E). Scale bar 60µm. Maximum projection = 40µm.

5.3.4 Misregulation of Na$^+$/Ca^{2+} exchanger results in a reduced recovery time

It is not clear how calcium concentration is brought to the basal levels after the propagation of the calcium wave at *Drosophila* egg activation. To investigate, whether the Na$^+$/Ca^{2+} exchanger is required for the recovery of the calcium wave at *Drosophila* egg activation, the mature oocytes were incubated with LiCl (100mM, 260mOsm), a solution which increases calcium export (Flores-Soto et al., 2012). Upon addition of the solution, the calcium wave initiated within 30 seconds and displayed a "cortical increase" (Figure 5.7). This calcium increase showed a significant decrease in recovery time, which on average was observed at 3 minutes (n=6, unpaired t-test, P=0.0006) (Figure 5.11), compared to the recovery time of 5 minutes 30 seconds in wild-type conditions. This decrease in the recovery time could be as a result of LiCl reversing the direction of Na$^+$/Ca^{2+} exchanger, and pumping more calcium out, suggesting that the Na$^+$/Ca^{2+} exchanger and external sodium concentration is important for a recovery of the calcium wave at *Drosophila* egg activation.
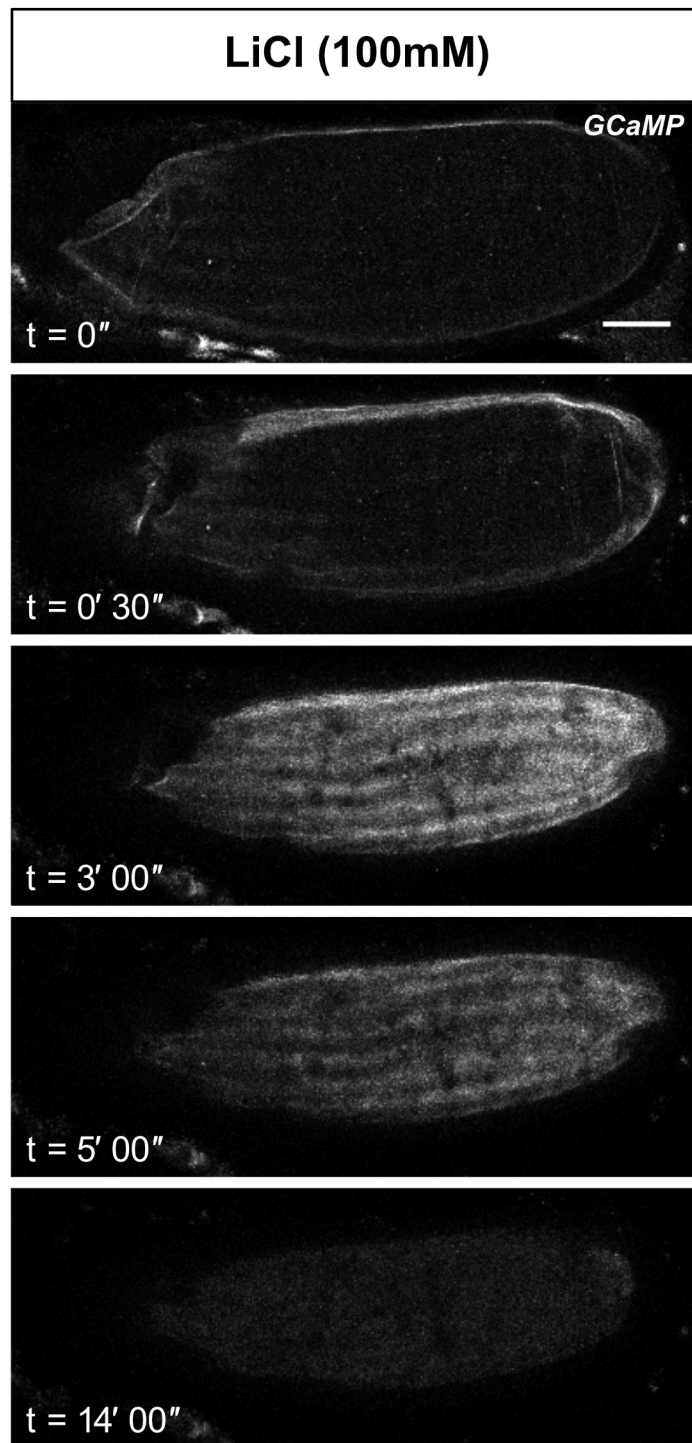
Figure 5.7. Na⁺/Ca²⁺ exchanger speeds up the entry and removal of calcium ions.
Time-series of *ex vivo* mature oocyte expressing *UAS-MyrGCaMP5* following the addition of LiCl (100mM). The oocyte swells normally and exhibits the initiation within 30 seconds, and recovery by 5 minutes. Scale bar 60μm. Maximum projection = 40μm.

5.3.5 Pharmacological inhibition and temperature-sensitive mutants of SERCA result in full recovery of the calcium wave

In order to address whether the SERCA pump facilitates the recovery of the calcium wave at *Drosophila* egg activation, I incubated stage 14 oocytes in AB and Thapsigargin (10µM). Thapsigargin is a tumour-promoting sesquiterpene lactone that binds stoichiometrically to all SERCAs and irreversibly inhibits SERCA to remain in the calcium-free state (Lytton et al., 1991). Upon activation, the oocyte exhibited the full calcium wave that initiated from the posterior pole and propagated as normal (Figure 5.8) (n=11). Recovery time was 6 minutes and 45 seconds on average, which is consistent with standard AB experiments. This suggests that SERCA is not required for recovery of the calcium wave at egg activation. Although unlikely, there is still a possibility that Thapsigargin was not able to cross the plasma membrane due to the chorion and the vitelline membrane surrounding the mature oocyte.

As an alternative approach, I tested the requirement of the SERCA pump using a temperature-sensitive mutant of SERCA CaP60A^{Kum170} (Sanyal et al., 2005). This mutant was originally generated to investigate the role of SERCA in the larval neuromuscular junctions. It was shown that 3 minutes incubation at 40°C resulted in a paralysis of the CaP60A^{Kum170} heterozygous flies (Sanyal et al., 2005). Therefore, to test the function of SERCA in the recovery of the calcium wave at *Drosophila* egg activation, I adopted a protocol from Sanyal et al., 2005 and incubated the mature oocytes, expressing CaP60A^{Kum170} and GCaMP3, for 10 min at 40°C. Upon activation, the incubated oocytes did not show any change in the recovery time of the calcium wave (data not shown). To ensure that the temperature-sensitive mutation was induced, I prolonged the incubation time to 40 minutes. This increase in the incubation time did not disrupt the morphology of the oocyte and did not cause a stress response, i.e. the formation of the P bodies aggregates (data not shown).

Upon the addition of AB, the oocytes swelled and exhibited a calcium wave with a recovery time of 7′ 43″ ± 30″ (Figure 5.9) (n=6). Even with prolonged incubation for 60 minutes, I did not observe any change in the recovery time (data not shown). As an alternative heat-shock method, I incubated whole flies,

expressing CaP60A^{Kum170} and GCaMP3, for 40 minutes in a 40°C hot-water bath. The oocytes from this fly also did not show any change in the recovery time, compared to the incubated oocytes. Interestingly, the incubation itself caused an increase in recovery time by 50% (n=7), compared to non-incubated wild-type oocytes. This would suggest that a change in temperature might be linked to the calcium recovery process in flies. Although both pharmacological and genetic approaches suggest that SERCA is not likely to play a role in removing cytosolic calcium at *Drosophila* egg activation, it is possible that heat-shock treatment did not fully disrupt stability and perdurance of SERCA protein, therefore not showing any significant difference in calcium removal from the mature oocyte. Future research should focus on developing and testing RNAi lines specific to *Drosophila* germline tissues.
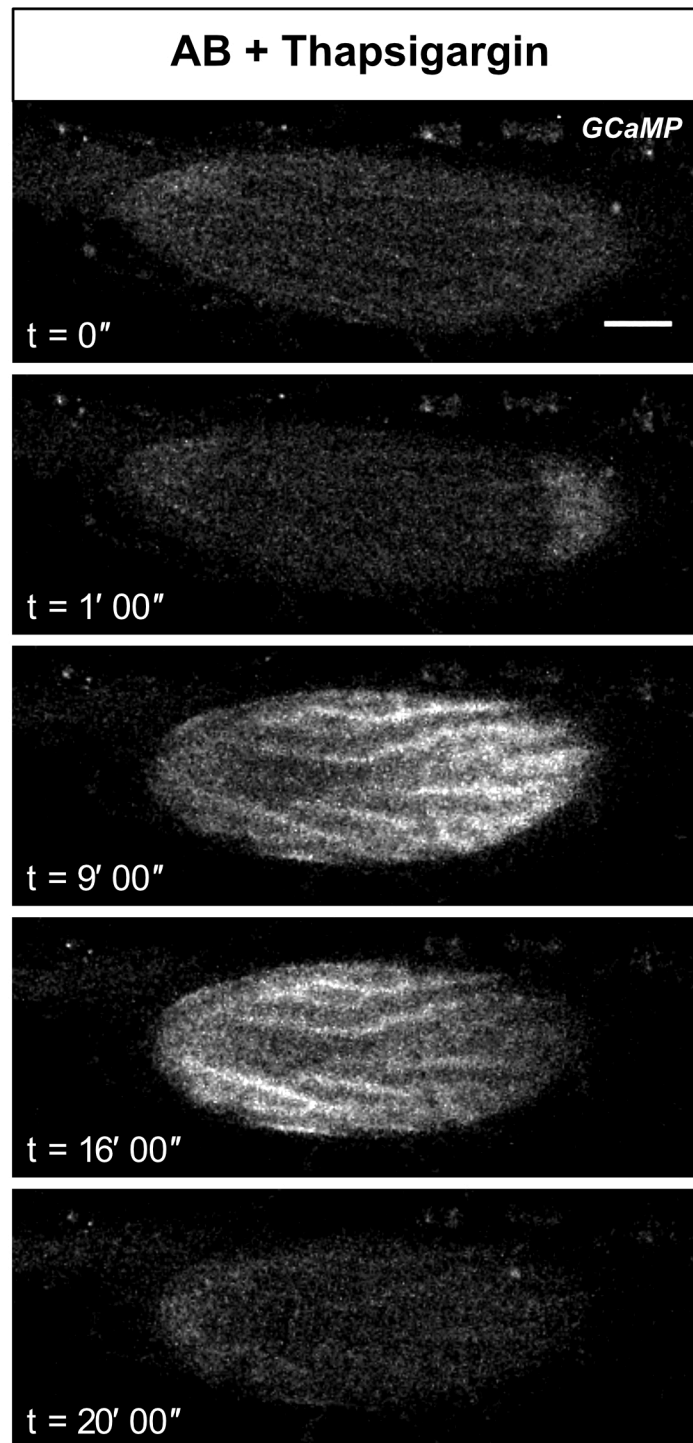
Figure 5.8. SERCA pump is not required for the recovery of the calcium wave at *Drosophila* egg activation.

Time-series of *ex vivo* mature oocyte expressing *UAS-myrGCaMP5*, following the addition of AB + Thapsigargin (10µM). The oocyte shows a calcium wave initiating from the posterior pole at 1 minute, fully propagating across entire the oocyte followed by the recovery within 20 minutes. Scale bars 60µm. Maximum projection = 40µm.
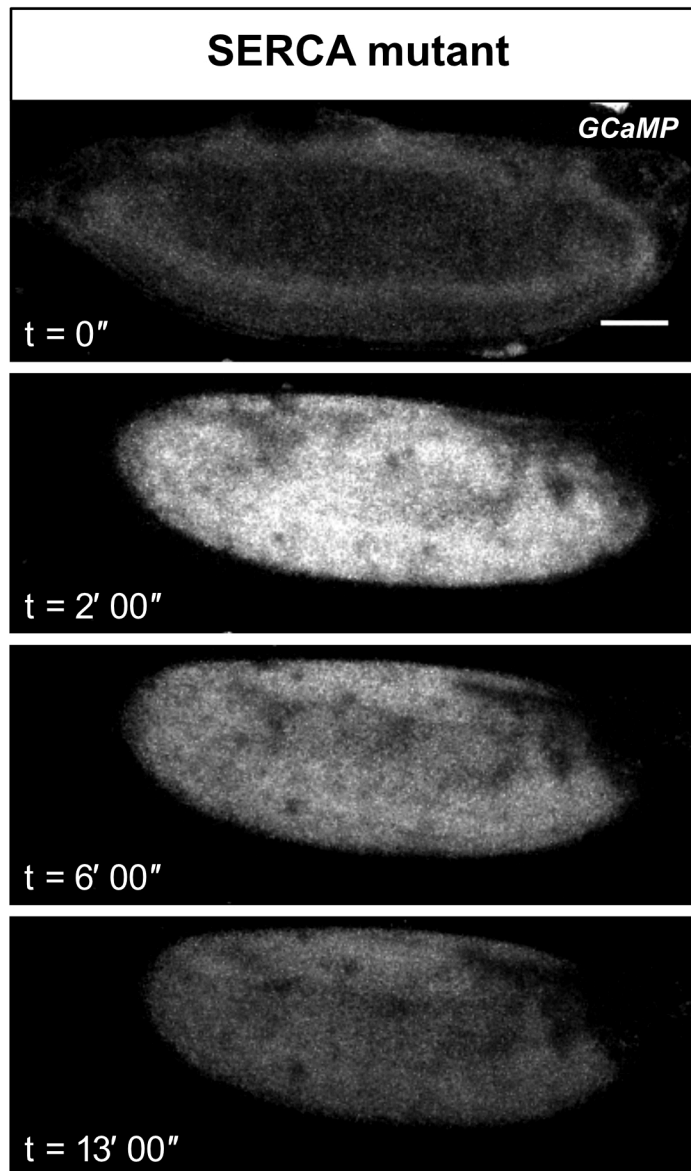
Figure 5.9 Temperature-sensitive SERCA mutation CaP60A^{Kum170} shows normal recovery of the calcium wave at *Drosophila* egg activation.
Time-series of *ex vivo* mature oocyte expressing *UAS-GCaMP3* following the addition of AB. The oocyte swells and shows the initiation and propagation of the calcium wave within 2 minutes of activation. The calcium wave recovers fully within 13 minutes. Scale bar 60μm. Maximum projection = 40μm.

5.3.6 PMCA is required for recovery of the calcium wave

To test the function of PMCA at egg activation, mature oocytes were incubated in AB with sodium orthanovanadate (10mM, 260mOsm), a commonly used ATPase inhibitor (Lajas et al., 2001). Upon activation, oocytes swelled and showed a full calcium wave, with initiation delayed to 7 minutes and a "cortical increase" (Figure 5.10). In addition, the calcium wave did not recover in 85% of the oocytes, even after 90 minutes (Figure 5.10, n=12). This suggests a requirement for PMCA for the recovery of the calcium wave at egg activation. Whilst it is possible that sodium orthanovanadate blocked the recovery of the calcium wave by inhibiting SERCA, my data suggests that SERCA is not required for the recovery. Overall, my findings point towards an ATPase as the main channel for recovery of the calcium wave at *Drosophila* egg activation, potentially pumping calcium ions to the perivitelline space. Further work should test a more specific PMCA inhibitor caloxin (Griff et al., 2012) or an RNAi to verify PMCA function in *Drosophila* mature oocytes.
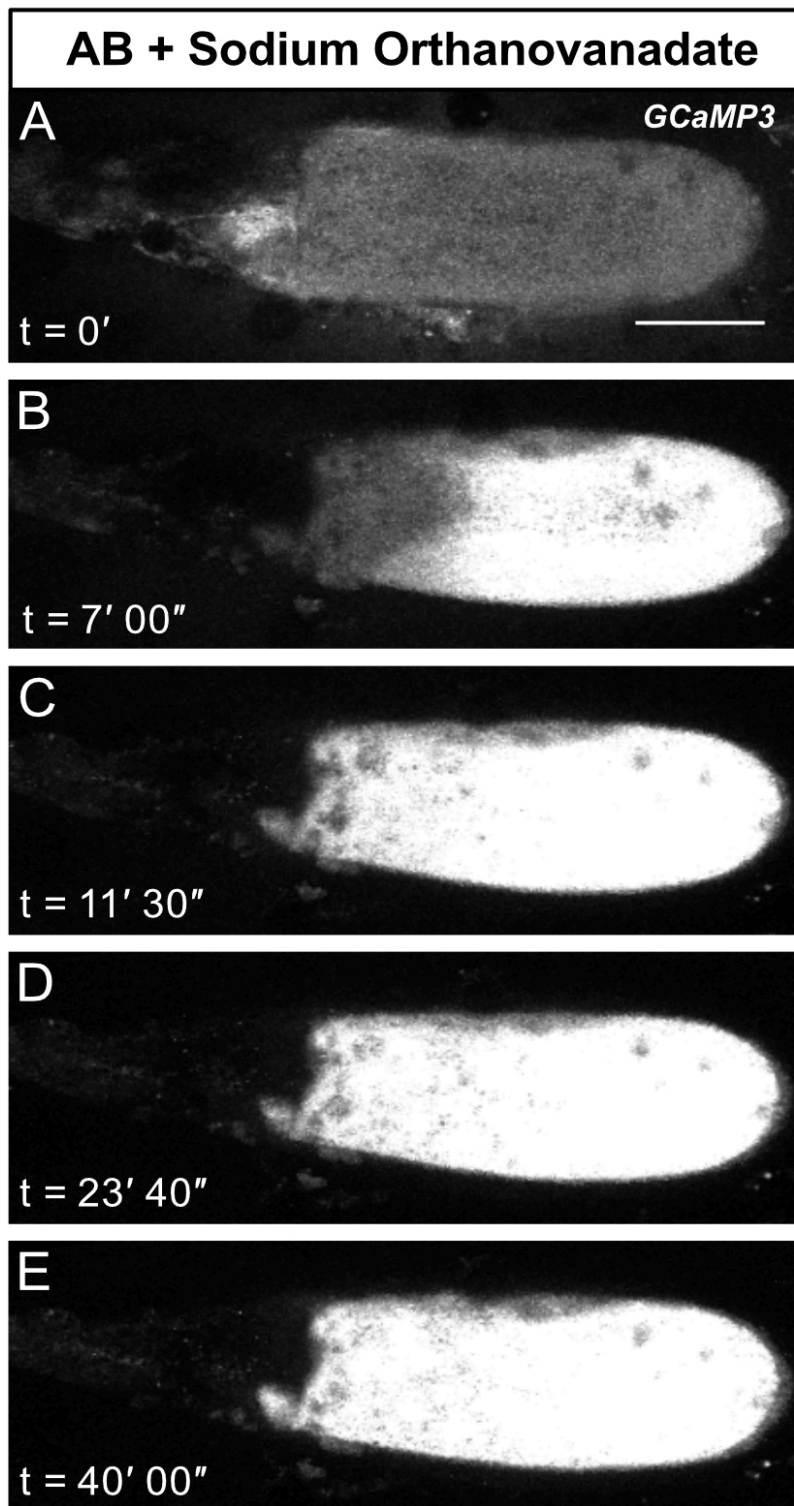
Figure 5.10 Inhibition of PMCA with sodium orthanovanadate results in a full inhibition of calcium wave recovery .
(A-E) Time-series of *ex vivo* mature oocyte expressing *UAS-GCaMP3* following the addition of AB + sodium orthanovanadate (10mM). The oocyte swells and shows a delayed initiation and propagation of the calcium wave at around 7 minutes (B). At 40 minutes, the oocytes does not show any decrease in calcium levels. Scale bar 100µm. Maximum projection = 40µm.

A
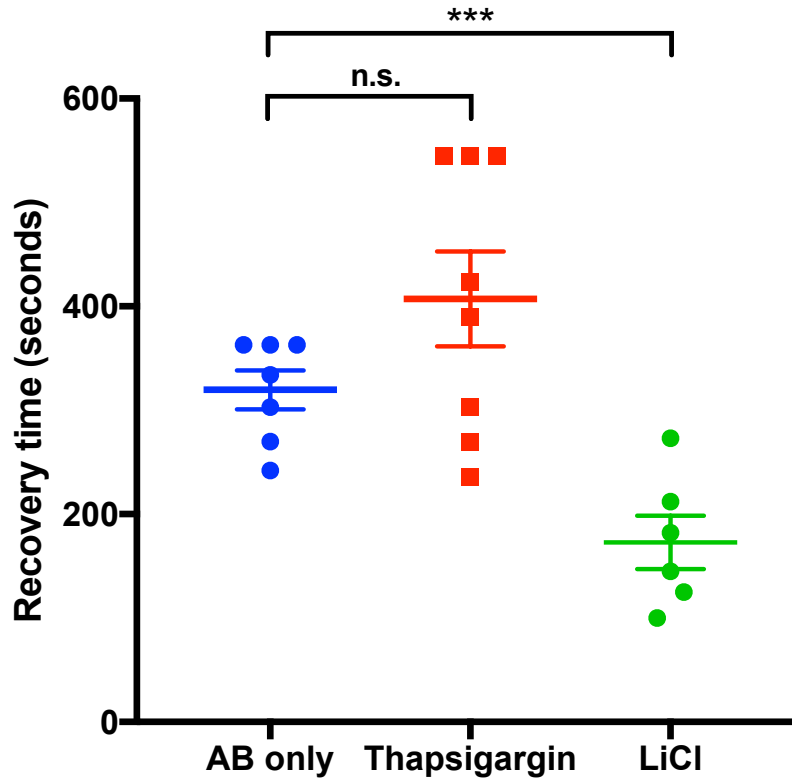
B

Incubation Solution	Percentage of oocytes that recovered	Average recovery time
AB only	100% (n=10)	5 min 25 sec
AB + Thapsigargin (10µM)	100% (n=9)	6 min 45 sec
LiCl (100mM)	100% (n=6)	2 min 50 sec
AB + Sodium orthanovanadate (10mM)	25% (n=12)	∞ (İnfinite)

Figure 5.11. Comparison of the average calcium recovery times in inhibited backgrounds.
(A) Dot plot of mean recovery time in different conditions: AB only (blue), AB + Thapsigargin (red) and LiCl (green). There is no significant difference in the recovery time in the oocytes treated with AB only or AB + Thapsigargin (p=0.12). But there is a significant decrease in the recovery time in LiCl treated oocytes compared to oocytes treated with AB only (p=0.02). AB only (n=7), AB + Thapsigargin (n=8) and LiCl (n=3). The data was analysed statistically using unpaired T-test with p<0.05 values showing significant difference. (B) Table provides a summary and quantification of the recovery times upon different pharmacological treatments. The mature oocytes treated with AB only, AB + Thapsigargin and LiCl all showed 100% recovery of the calcium wave. 85% of oocytes did not recover, when treated with AB + sodium orthanovanadate. The incubation of the mature oocytes with AB +Thapsigargin does not show a significant difference in the recovery time compared to AB only.

5.4 Discussion

The data from this chapter shows that the calcium influx depends on TRPM and Water-witch channels and RPK DEG/ENaC channels at egg activation. I provide evidence for the requirement of ATPases for the removal of intracellular calcium, most likely mediated by the PMCA pump.

5.4.1 Calcium influx at egg activation

The entry of the calcium can be mediated from the extracellular environment via voltage-gated, mechanosensitive and store-operate channels. My data shows that external calcium is not required for the calcium wave at *Drosophila* egg activation (Chapter 3). However, the calcium influx can still be coordinated via these channels from the outer perivitelline space in the mature oocyte.

5.4.1.1 The role of voltage-gated channels at egg activation

Previous work has shown that a voltage change across the lipid bilayer may play a role in regulating the calcium influx channels in worm eggs of phyla Nemertea, Mollusca and Annelida (Stricker, 1999). In these studies, the eggs were treated with potassium buffers to induce the depolarisation of the lipid bilayer. The addition of the potassium buffer caused a "cortical flash", rather than the calcium oscillations, suggesting that the voltage-change is required for calcium influx.

More specifically, L-type voltage-gated calcium channels have been shown to be implicated in the resumption of the cell in many oocytes, including mussels, ascidians and mice (Murnane et al., 1988, Dale et al., 1991, Tomkoviak et al, 1997). The T-type voltage-gated channel is also present in mouse eggs, but whether it is linked to the calcium oscillations at egg activation remains controversial, as mutant female mice are still fertile (Chen et al., 2003). However, it is not clear whether the voltage-gated calcium channels play a role in initiating the calcium influx in the *Drosophila* oocytes. It is possible that a

change in the membrane potential indirectly feeds into calcium signalling via other voltage-gated channels, including potassium and sodium channels. Therefore, I tested if there is a voltage change associated with egg activation using a genetically-encoded indicator Arclight, which did not show any visible change in fluorescence (data not shown). Further work should focus on injecting voltage indicators to clarify whether there is a change in voltage across the plasma membrane at *Drosophila* egg activation.

5.4.1.2 The role of TRP channels at egg activation

The influx of extracellular calcium can also be mediated via mechanosensitive TRP channels. The majority of findings related to the TRP channels have come from mouse oocytes. Recent work has shown the requirement of TRPV3 channel for the calcium influx in mouse eggs (Lee et al., 2016). This channel was activated by the overexpression and the application of 2-ABP (Lee et al., 2016). However, the role of TRPV3 is debatable, because another recent study has suggested the requirement of the TRPM7 channel instead of TRPV3 (Carvacho et al., 2016). TRPM7 was shown to be essential for the calcium influx at egg activation using pharmacological blockers, and important for the pre-implantation of a fertilised mouse egg (Carvacho et al., 2016). Interestingly, sperm can facilitate the influx of external calcium at the site of fertilisation by passing TRP channels to the plasma membrane of the oocyte. This was shown to be true for *C.elegans*, where the mutant for TRP3 channel failed to exhibit a calcium raise at egg activation (Takayama and Onami, 2016). Therefore, TRP channels play an important role in numerous model systems at egg activation.

My work shows that Trpm and possibly Water-witch are required for the calcium wave initiation at *Drosophila* egg activation. The common activation cues for these channels are osmotic shock or hydrostatic pressure (Grimm et al., 2003; Liu et al., 2007). These TRP channels might mediate the calcium influx in a redundant manner, therefore ensuring that a calcium increase occurs at egg activation. In *Drosophila,* a hypothesis would be that the mature oocyte is exposed to the osmotic pressure in the oviduct, resulting in the activation of Trpm and Water-witch, and a subsequent calcium influx. However, it is possible

that the RNAi lines used in this chapter might not have resulted in a complete knock-down. Therefore, it is important to keep in mind that other channels may play a role in mediating the calcium influx at *Drosophila* egg activation. Thus, future work should focus on understanding how Trpm, Water-witch and other possible candidates are activated in response to the oocyte swelling and how their activation results in the relay of the calcium influx in the form of a wavefront.

5.4.1.3 The role of store-operated channels at egg activation

Another class of calcium channels that regulate the calcium influx from the extracellular environment is the store-operated channels. Mammalian eggs undergo prolonged calcium oscillations for up to four hours at egg activation. It has been proposed that the levels of the intracellular calcium stores are maintained by the Orai/STIM complex. The original evidence for this hypothesis came from experiments that involved the treatment of mouse eggs with thapsigargin, which is known to deplete the ER (Kline and Kline, 1992; Machaty et al., 2002). This resulted in the calcium influx after adding more calcium to the external environment (Kline and Kline, 1992; Machaty et al., 2002). Further evidence highlighted the presence of Orai and STIM1 proteins in the mouse, porcine and human oocytes (Machaty et al., 2017). However, a more recent study contradicts this data by showing that the calcium influx is not affected in in the mutant backgrounds of Orai1, STIM1 or STIM2, and strongly points towards the TRPM7 requirement instead (Bernhardt et al., 2017). In *Drosophila*, Orai-1 and STIM channels are highly enriched in the ovarian tissue (Table 1) (*Drosophila* Fly Atlas). It is possible that this protein complex might mediate the calcium influx at *Drosophila* egg activation. Therefore, future work should focus on testing the function of these proteins with the mutant and RNAi lines available.

5.4.2 Calcium release by IP$_3$ receptors at egg activation

Although, the entry of calcium from the external environment plays an important role in many eggs, the release of calcium from the intracellular stores, via the IP$_3$ receptors (IP$_3$R) seems to be a predominant mechanism for the calcium influx at egg activation. The initial requirement for the phosphoinositide pathway came from studies on sea urchin oocytes, where PIP$_2$ was shown to increase at fertilisation (Turner et al., 1984). This was followed by the studies in sea urchin and golden hamster eggs, where the injection of purified IP$_3$ resulted in the calcium wave and downstream processes of egg activation (Whitaker and Irvine, 1984; Swann and Whitaker, 1986; Miyazaki et al., 1988). The later identification of the IP$_3$R structure enabled the testing of the direct role of the receptor in releasing calcium at egg activation (Furuichi et al., 1989). IP$_3$R inhibition was achieved by the application of the antagonist heparin and the injection of an IP$_3$ antibody specifically targeting the C-terminus of IP$_3$R (Miyazaki et al., 1992). The inhibition of IP$_3$R resulted in the disruption of calcium oscillations and downstream processes of egg activation (Miyazaki et al., 1992; Xu et al., 1994). Since then, IP$_3$R was shown to be essential in the calcium release in the eggs of most animals, including frogs, starfish, sea urchins, ascidians, mice and human (Parys et al. 1994; Thomas et al. 1998; Yoshida et al. 1998; Runft et al. 1999; Goud et al. 2002; Iwasaki et al. 2002). These findings in the fertilisation field highlight an essential role that IP$_3$R plays in mediating the calcium release from the ER at egg activation and fertilisation.

It is not clear whether IP$_3$R coordinates the calcium influx at *Drosophila* egg activation. My findings show that the homozygous mutant and RNAi fly lines are lethal, making it difficult to access the role of IP$_3$R in the mature oocytes. Therefore, future experiments should test the IP$_3$R function with the pharmacological antagonist heparin or the injection of antibodies against IP$_3$R into the mature oocyte. The life-time of the IP$_3$ ligand is 9/sec (Wang et al., 1995), which is much faster compared to the speed of the calcium wave (1.5μm/s) at egg activation. Therefore, it is unlikely that IP$_3$R mediates the calcium influx at egg activation, with an alternative mechanism proposed in Chapter 7.

5.4.3 Calcium removal mechanisms at egg activation

It is essential to efficiently remove calcium from the oocyte to maintain calcium homeostasis for further development of the embryo. The calcium removal can be mediated by ATPases, SERCA and PMCA, which use energy in the form of ATP to pump calcium out of the cytoplasm. Currently, there is limited evidence available on how calcium is removed from eggs after the calcium rise. For example, SERCA pumps were shown to play an important role in mouse oocytes, where SERCA was inhibited by thapsigargin blocker and resulted in the shorter calcium oscillations (Kline and Kiline, 1992). SERCA was also shown to undergo reorganisation in its redistribution in the ER in the frog oocytes, but the functional relevance of this is not yet clear (El-Jouni et al., 2005). The involvement of PMCA ATPase is also somewhat elusive, but the inhibition of PMCA was shown to prolong the calcium recovery in *Xenopus* oocytes (El-Jouni et al., 2008). Alternatively, the cells can export calcium using the inward sodium chemical gradient by Na^+/Ca^{2+} exchanger. The removal of external sodium ions can reverse the action of the exchanger and this was shown to be the case in mouse oocytes, where the calcium oscillations were faster (Pepperell et al., 1999; Carroll, 2000), a similar finding to what I observed with *Drosophila* oocytes.

My findings suggest that PMCA ATPase, rather than SERCA, is required for the recovery of the calcium wave at *Drosophila* egg activation. The calcium is likely to be pumped out into the perivitelline space, as the presence of calcium ions has been documented in early *Drosophila* embryos (Stein and Nusslein-Volhard, 1992). Further work should test a more specific PMCA inhibitor caloxin or RNAi against PMCA to verify its function at *Drosophila* egg activation.

Chapter 6

Investigating mRNA localisation in *Drosophila* embryonic hemocytes

6.1 Introduction

6.1.1 Targeted protein expression via mRNA localisation

Many biological processes require cells to mediate complex changes in response to internal and external cues. These processes include the development of the nervous system, tissue regeneration, wound healing, egg activation and fertilisation. While these are highly coordinated events, precisely how cells achieve this regulation is not fully understood.

One way in which cells can mediate complex changes is through the spatial-temporal regulation of protein expression. Asymmetric localisation of mRNA is a conserved mechanism for targeted protein expression and is required for many cellular events: in budding yeast, *ash1* mRNA is localised to the tip of the daughter cell and represses mating-type switching; in *Xenopus, vegetal1 (vg1)* mRNA is localised to the vegetal pole of an oocyte and is essential in axis determination and mesoderm signalling; in *Drosophila*, *bicoid (bcd)*, *oskar (osk)*, *gurken (grk)* and *nanos (nos)* mRNAs are localised to different regions of the oocyte and are essential for patterning the body axes (Martin and Ephrussi, 2009; Medioni et al, 2012). Moreover, in humans, misregulation or disruption of mRNA translation has been shown to be involved in Alzheimer's disease, Fragile-X syndrome and disease pathogenesis (Mus et al., 2007; Bassell et al., 2008). Although targeting of transcripts within a cell is a commonly-used process, it is still not fully understood how mRNAs are differentially localised in a cell.

mRNA undergo many events in the time from transcription to degradation. Once transcribed, an mRNA undergoes post-transcriptional splicing and is bound by numerous trans-acting factors to form a ribonucleoprotein complex (RNP) (Parton et al., 2014). It has been suggested that there are several mRNA molecules of the same species that are co-packaged in a RNP, as *oskar* mRNA was shown to multimerise in *Drosophila* oocytes (Hachet and Ephrussi, 2004; Jambor et al., 2011). However, mRNA particles are thought be individual in mammalian dendrites (Mikl et al., 2011). Subsequently, mRNAs exit nucleus via

the nuclear pores and travel to the required destination to become localised until the translation (Carmody and Wentle, 2009).

6.1.2 mRNA localisation mechanisms

There are several well-established mechanisms for RNPs localisation including diffusion-coupled local entrapment, local protection and active transport (Medioni et al., 2012). Diffusion-coupled local entrapment involves diffusion of mRNAs to the desired location and anchoring by the cytoskeleton (Medioni et al., 2012). Live imaging and pharmacological tools have shown that *nanos (nos)* mRNA diffuses to the posterior pole and becomes entrapped by actin in the *Drosophila* oocyte. Similar mechanism was observed when fluorescently labelled *Xcat2* mRNA was injected into a *Xenopus* oocyte (Chang et al., 2004). Alternatively, local protection together with degradation has been shown to be involved in localisation of *Hsp83* transcripts in *Drosophila* early embryogenesis (Ding et al., 1993). Mutant analysis have shown that *Hsp83* mRNA localisation at the posterior is lost in Smaug depleted background (Semotok et al., 2005).

The most common mechanism is active transport, where molecular motors move RNPs on polarised cytoskeletal tracks. Live imaging and immunoprecipitation analysis have shown that Kinesin-1 motor is required to transport numerous mRNAs to the plus-end of the microtubule (MT) cytoskeleton in mammalian dendrites (Kanai et al., 2004). Dynein, the minus-end-directed MT-based motor was originally shown to function in *Drosophila* embryos, where transcripts of pair-rule genes, such as *wingless*, *hairy* and *ftz*, are localised to the apical cytoplasm (Bullock and Ish-Horowicz, 2001; Wilkie and Davis, 2001; Bullock et al., 2004). In addition, colcemid disruption of microtubules together with hypomorphic Dynein mutants have highlighted the important of active transport in localisation of *bcd* mRNA (Weil et al., 2006). While the prevailing model is that RNP is transported unidirectionally by a single motor to its destination, recent research on *vg1* mRNA in *Xenopus* oocytes shows that mRNA can be transported bi-directionally using multiple types of motors (Gagnon et al., 2013). Together, these findings show that mRNAs utilise different mechanisms to ensure localisation until the translation.

6.1.3 mRNA translation

To ensure localised protein synthesis, mRNA translation is thought to be repressed during the transport. This is thought to be achieved by the binding of a repressor protein to a cis-element in the mRNA (Besse and Ephrussi, 2008; Parton et al., 2014). The classic model of eukaryotic translation involves a step-wise recruitment of trans-acting proteins, such as eIF4F factors, to cis-elements in the mRNA sequences that together initiate the translation (Jackson et al., 2010). The step that is frequently targeted by trans-regulatory translational repressors is the binding of an initiation factor eIF4G to eIF4E, where eIF4E-binding proteins compete with eIF4G binding (Besse and Ephrussi, 2008). For example, *Cup* is a *Drosophila* eIF4E-binding protein that repress translation of *oskar* mRNA by binding repressor *Bruno* at 3'-UTR. Previous work has shown that disruption of *Cup-eIF4E* interaction leads to a premature translation of *oskar* mRNA (Nakamura et al., 2004). Other mechanisms have been shown to repress translation, including regulation of polyadenine(A)-tail length or by blocking recruitment of ribosomal subunits (Castagnetti and Ephrussi, 2003; Zaessinger et al., 2006; Deng et al., 2008). Therefore, mRNA translational repression in ensured until the right time.

6.1.4 mRNA localisation in migrating cells

Migrating cells have been well-characterised and exhibit prominent structures that aid their movement. These include the lamellipodium - the leading edge; the filopodia - the membrane projections; and the retracting edge (Vicente-Manzanares et al., 2005). The lamellipodium is known to provide the force for cell movement and is filled with actin branched networks (Machesky et al., 1994; Mullins et al., 1997; Mullins et al., 1998). The branched actin is formed by the protein complex, called Arp2/3, that is in turn is regulated by another protein complex WAVE/Scar (Weaver et al., 2003). A more detailed discussion of the actin structure and the actin binding factors can be found in Chapter 4. The enrichment of actin and localisation of these factors, and many others, to the leading edge facilitates the rapid formation and turnover of the branched actin networks to coordinate directed cell movement (Bailly et al., 1999; Svitkina and

Borisy, 1999; Niggli, 2014). For example, recent study in cultured mouse neural progenitors has shown that genetic ablation of Arp2/3 results in a reduced formation of the leading edge and slower movement of the cells (Wang et al., 2016). Although actin and some actin-binding factors are enriched at the leading edge of the migrating cells, it is not well-understood whether mRNA localisation of actin or these factors in the leading edge plays a role in coordinating cell migration.
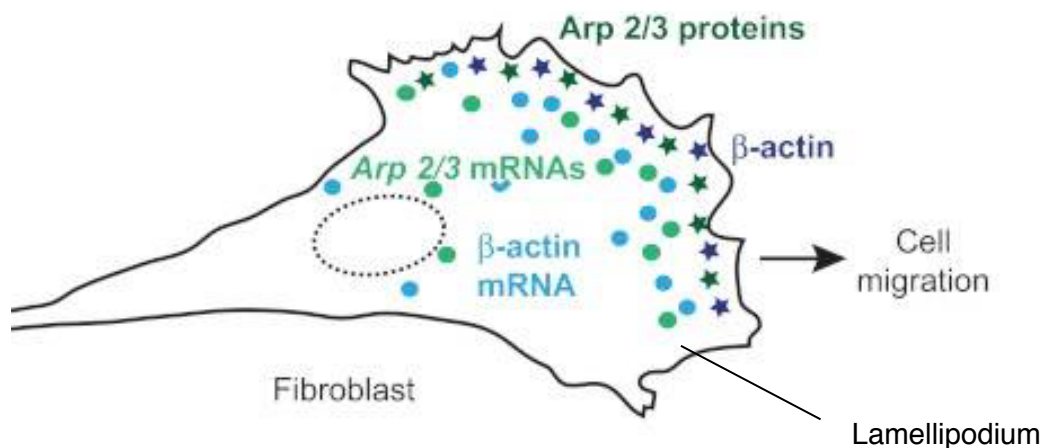
Figure 6.1. Diagram of a migrating fibroblast.
Adapted from Medioni et al., 2012. Fibroblast migrating to the right direction. Arp2/3 proteins are enriched in the leading edge (lamellipodium) of the fibroblast. Arp2/3 and *β-actin* mRNA are also localised to the leading edge of the migrating fibroblast.

Previous work has shown that *β-actin* mRNA localises to the leading edge and is required for the adequate cell movement in cultured chicken fibroblasts and myoblasts (Lawrence and Singer, 1986; Kislauskis et al., 1994; Kislauskis et al., 1997; Bassell and Singer, 2001). *β-actin* mRNA is proposed to be transported by Myosin motor proteins along the actin filaments to the leading edge, suggesting a conserved role of the cytoskeleton in transporting mRNA molecules. Once *β-actin* mRNA is transported to the required site, it is anchored by EF1α to the actin cytoskeleton (Liu et al., 2002). Transfection with the antisense oligonucleotides have shown the requirement of a zipcode sequence located in the 3'-UTR to translationally-repress *β-actin* mRNA (Kislauskis et al., 1994). Further studies using electrophoretic mobility shift assay together with the crystallography have shown that this zipcode sequence is bound by the Zipcode binding protein 1 (ZBP1), which induces morphological looping of mRNA (Farina et al., 2003; Chao et al., 2010). It is proposed that ZBP1 is phosphorylated by Src kinase, which facilitates the dissociation of ZBP1 from

the mRNA zipcode sequence, which upregulates the translation of *β*-actin mRNA (Huttelmaier et al., 2005).

Actin-binding factors have also been shown to localise with actin transcripts. The nucleating factor, a*rp2/3* mRNA, was shown by fluorescent *in situ hybridisation* to localise to the leading edge in embryonic chicken fibroblasts and Dictyostelium (Mingle et al., 2005). This localisation was suggested to require an activity of Rho, as the overexpression of the Rho resulted in the delocalisation of *arp2/3* mRNA, suggesting that this localisation requires an activity of Rho (Mingle et al., 2009).

A different study has utilised a method where fibroblasts were placed on the microporous gel and were treated with a migratory stimuli, inducing pseudopodia extensions into the gel (Mili et al., 2008). Further fractionation and microarray analysis allowed a genome-wide screen in fibroblasts, which identified many (more than 50) different mRNAs that localise to extending pseudopodia (Mili et al., 2008). Overall, these findings suggest that mRNA localisation of the actin and actin-binding factors may play a role in mediating successful cell movement in response to stimuli. While these, and other, studies show that mRNA plays a role in coordinated cell movement in tissue culture, an *in vivo* dynamic cell model has yet to be explored.

6.1.5 *Drosophila* embryonic hemocytes as a system to study cell migration

Drosophila embryonic hemocytes are a well-established system used to study coordinated cell migration, chemotaxis during inflammation and apoptotic clearance (Wood et al., 2006; Wood and Jackinto, 2007; Ratheesh et al., 2015). Hemocytes are the motile cells of the immune system that are required for embryonic development and phagocytosis of pathogens (Wood and Jackinto, 2007). Immunohistochemistry and live imaging experiments have identified that hemocytes originate from the head mesoderm at stage 10 of embryogenesis and start dispersing across the entire embryo following specific migratory routes at 0.4µm/min (Figure 6.2) (Tepass et al., 1994, Wood et al., 2006). Hemocytes

form a single line at stage 14 on the ventral side of an embryo, which is followed by alignment of the hemocytes into three parallel lines by stage 16 (Figure 6.2) (Tepass et al., 1994, Wood et al., 2006). The hemocyte migration is mediated by PDGF/Vegf-regulated ligands (Pvfs) , which were shown by *in situ hybridisation* to mimic the migratory routes of hemocytes in the embryo. Further mutant analysis have shown that Pvfs act as chemoattractants to direct hemocyte movement (Cho et al., 2002; Wood et al., 2006). Interestingly, hemocytes become highly polarised with a persistent leading edge of 20μm and increase their velocity to 1.8μm/min during lateral migration from stage 14 onwards (Wood et al., 2006), suggesting that there is a change in the morphology and dynamics of the hemocytes.
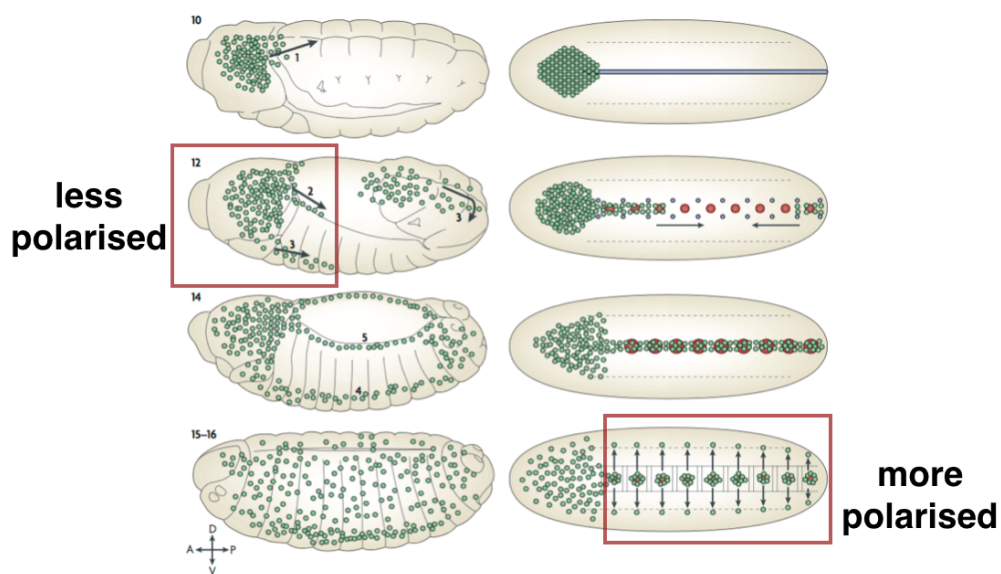
Figure 6.2. Hemocytes distribution and migratory routes at *Drosophila* embryogenesis. A*dapted from Wood and Jackinto 2007.* Left column shows hemocyte distribution from stages 10-16 of embryogenesis from the lateral-view. Right column shows hemocyte distribution from stage 10-16 of embryogenesis from the ventral view. Red boxes highlight the areas of interest for examination of mRNA localisation in hemocytes.

To sense this signal, hemocytes express the Pvr receptor that senses Pvfs ligands and is required for the migration and survival of the hemocytes (Cho et al., 2002; Sears et al., 2003). The hemocytes depleted of Pvr receptor do not undergo the migration and remain in the head mesoderm (Cho et al., 2002; Sears et al., 2003). Further mutant analysis with immunofluorescence has shown that Pvr is required for the anti-apoptotic survival of the hemocytes, and suggests that the aggregation of the hemocytes is caused by cells engulfing and clearing the apoptotic derby (Bruckner et al., 2004). As the hemocytes follow pre-determined routes within an embryo, it provides a well-characterised model system to study cell migration *in vivo*. Whilst, there has been extensive research into the mechanism of hemocyte cell movement, it is currently unknown whether mRNA localisation plays a role in mediating this movement, as in the cultured systems.

6.1.6 Selection of mRNA candidates to visualise in embryonic hemocytes

It is well-established that actin is required for cell movement and is enriched at the leading edge of hemocytes (Vicente-Manzanares et al., 2005; Zanet et al., 2009). However, it is not known which actin is required for hemocyte movement. There are six actin genes in *Drosophila*: Act5C, Act42A, Act79B, Act87E, Act57A and Act88F (Fyrberg et al., 1983). Biochemical approach with blot analysis has showed that: (1) Act42A and Act5C encode cytoplasmic and cytoskeletal actin, and are present in all developmental stages; (2) Act57A and Act87E transcripts are abundant during late embryogenesis, and correlate their expression with larval musculature differentiation; and (3) Act79B and Act88F show maximal levels of expression during mid-to-late pupal development (Crossley, 1978; Fyrberg et al., 1983). Based on this data, I selected *act42A, act87E* as experimental and *act79B* as a control in this candidate approach to investigate if actin mRNA exhibits any localisation in embryonic hemocytes. In addition, I tested the localisation of a conserved factor SCAR, which is known to regulate polymerisation of actin and is required for hemocyte movement (Mus et al., 2007; Pollitt et al., 2009; Evans et al., 2013).

6.2 Aims of this chapter

1. **To address whether transcripts of actin and/or actin-binding factor localise to the leading edge of *Drosophila* embryonic hemocytes.**

2. **To optimise fixing conditions to visualise mRNA using in situ hybridisation in *Drosophila* embryonic hemocytes.**

6.3 Results

6.3.1 Visualisation of mRNA in embryonic hemocytes

To address whether some actin and/or actin-binding factor's transcripts are enriched in hemocytes, mRNA was initially visualised using *in situ hybridisation.* Hemocytes were visualised by antibody staining against GFP expressed in hemocytes via the UAS/GAL4 system. The enrichment of mRNA was compared in hemocytes in the embryonic head region at stage 12 to the ventral side at stage 15, which are known to be more polarised and show a larger leading edge (Figure 6.2, highlighted in the red box) (Wood et al., 2006; Wood and Jackinto, 2007). The enrichment of mRNAs was used to describe the presence of visible "clumps" within hemocytes, which are bigger than four pixels. The number of hemocytes with mRNA enrichment was compared to the total number of hemocytes observed in a single plane. As *act79B* mRNA was used as a control, the enrichment level of this transcript was used to determine whether other mRNA candidates were enriched in hemocytes.

Upon visualisation, *act42A* mRNA was found to be enriched in hemocytes at both stages (Figure 6.3-6.4), while *act87E* and *act79B* did not show any enrichment at either of the stages as expected (Figure 6.5-6.8). In contrast, *SCAR* mRNA was found to be enriched in hemocytes and form five times bigger mRNA particles at stage 15 (Figure 6.10), suggesting that its activity might be unregulated in more polarised and faster hemocytes. The enrichment was quantified for all transcripts and *act42A* was found to be enriched in 77% of hemocytes at stage 12 and 79% at stage 15 (Table 6.1). *SCAR* mRNA was only enriched in 33% of hemocytes at stage 12, but in 72% at stage 15 (Table 6.1). Both *act87E* and *act79B* were present in no more than 30% hemocytes at both stages (Table 6.1). Together these findings suggest that *act42A* and *SCAR* mRNA are both enriched in hemocytes, however, it is unclear whether they show any particular localisation, such as at the leading edge.
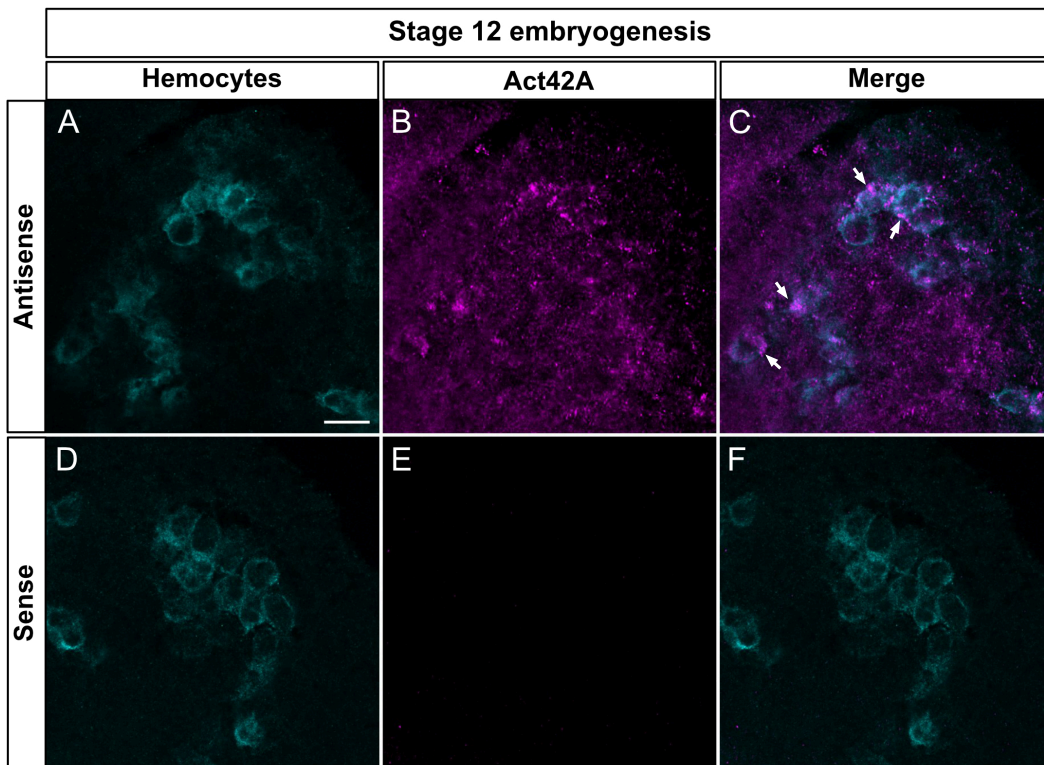
Figure 6.3. *act42A* **mRNA is enriched in hemocytes at stage 12 of embryogenesis.**
Embryos expressing UAS-GFP driven by srp-GAL4 and crq-GAL4. (A,D) Anti-GFP
antibody (cyan) shows hemocyte distribution. (B,E) *In situ hybridisation* of *act42a* mRNA
(magenta). (C,F) Merge. (B) Antisense show enrichment of *act42A* mRNA in puncta
within hemocytes, whereas sense does not. White arrows point at *act42A* mRNA
enriched in hemocytes. Single frame. Scale bar 10μm.
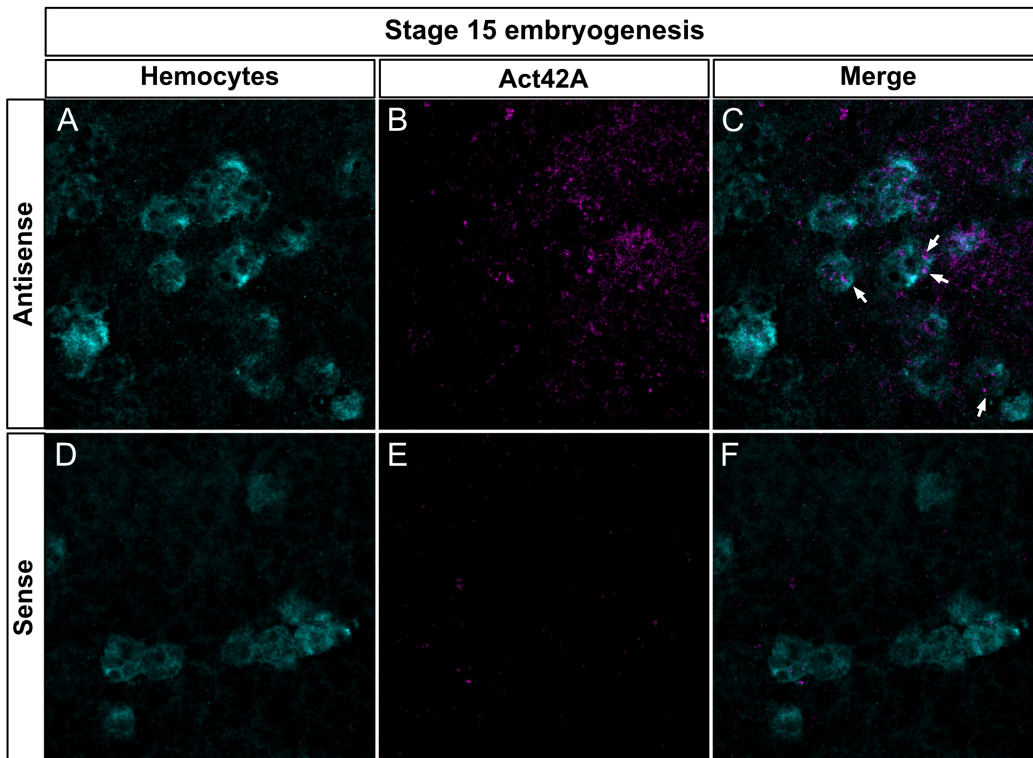
Figure 6.4. *act42A* **mRNA is enriched in hemocytes at stage 15 of embryogenesis.**
Embryos expressing UAS-GFP driven by srp-GAL4 and crq-GAL4. (A,D) Anti-GFP
antibody (cyan) shows hemocyte distribution. (B,E) *In situ hybridisation* of *act42a*
mRNA (magenta). (C,F) Merge. (B) Antisense show enrichment of *act42A* mRNA in
puncta within hemocytes, whereas sense does not. White arrows point at *act42A*
mRNA enriched in hemocytes. Single frame. Scale bar 10μm.

143
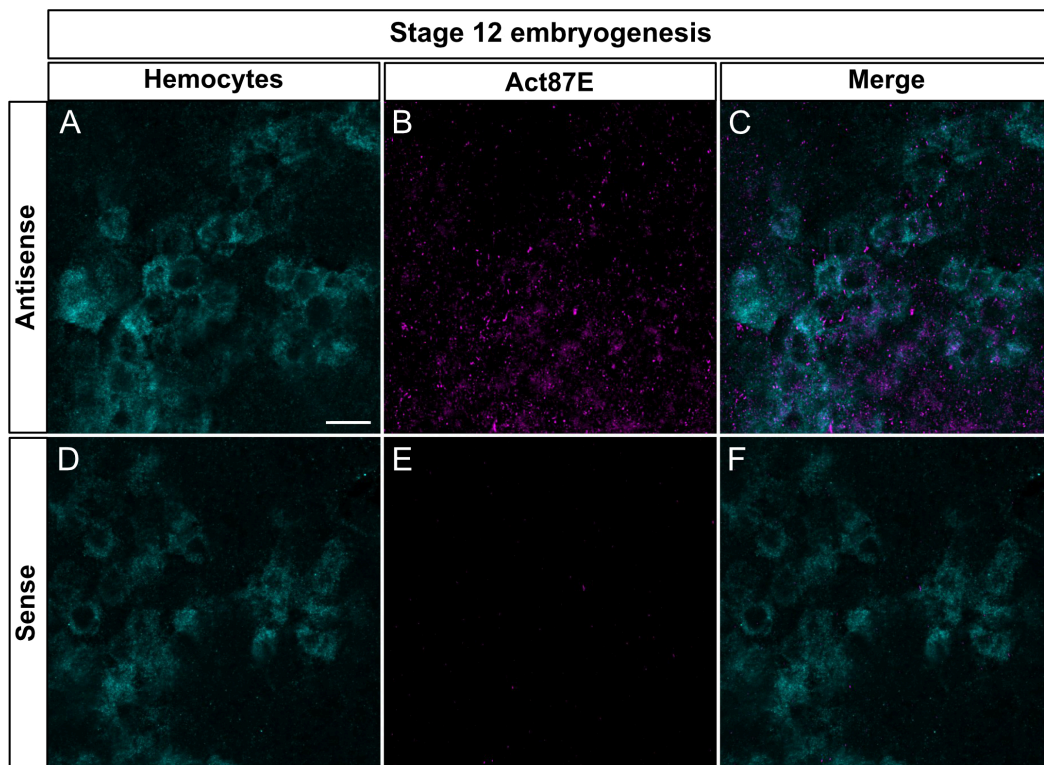
Figure 6.5.*act87E* **mRNA is not enriched in hemocytes at stage 12 of embryogenesis.**
Embryos expressing UAS-GFP driven by srp-GAL4 and crq-GAL4. (A,D) Anti-GFP antibody (cyan) shows hemocyte distribution. (B,E) *In situ hybridisation* of *act42a* mRNA (magenta). (C,F) Merge. (B) Antisense show no enrichment of *act87E* mRNA. Single frame. Scale bar 10µm.
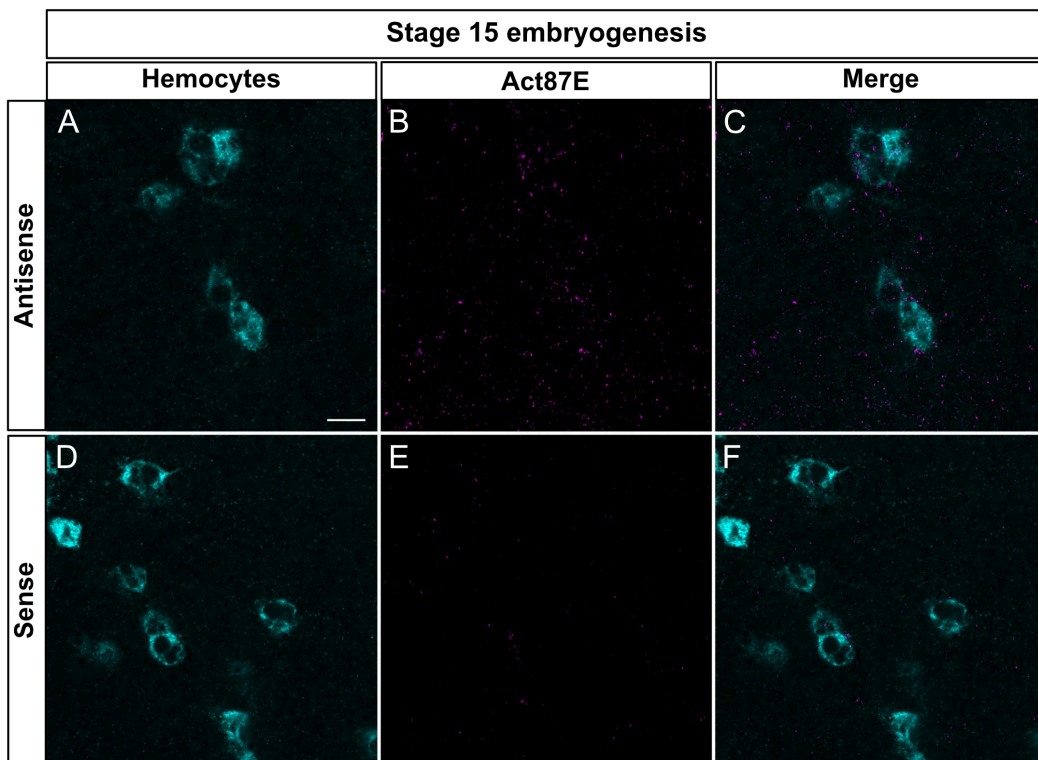
Figure 6.6.*act87E* **mRNA is not enriched in hemocytes at stage 15 of embryogenesis.**
Embryos expressing UAS-GFP driven by srp-GAL4 and crq-GAL4. (A,D) Anti-GFP antibody (cyan) shows hemocyte distribution. (B,E) *In situ hybridisation* of *act42a* mRNA (magenta). (C,F) Merge. (B) Antisense shows no enrichment of *act87E* mRNA. Single frame. Scale bar 10µm.
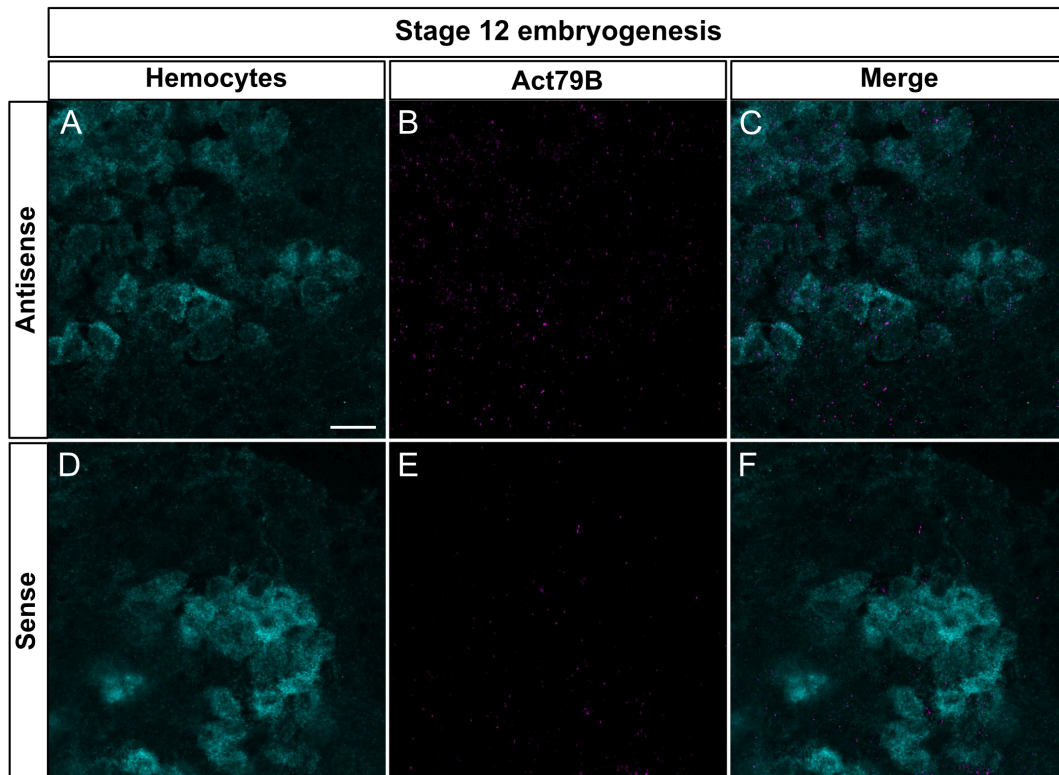
Figure 6.7.*act79B* **mRNA is not enriched in hemocytes at stage 12 of embryogenesis.** Embryos expressing UAS-GFP driven by srp-GAL4 and crq-GAL4. (A,D) Anti-GFP antibody (cyan) shows hemocyte distribution. (B,E) *In situ hybridisation* of *act79B* mRNA (magenta). (C,F) Merge. (B) Antisense shows no enrichment of *act79B* mRNA. Single frame. Scale bar 10µm.
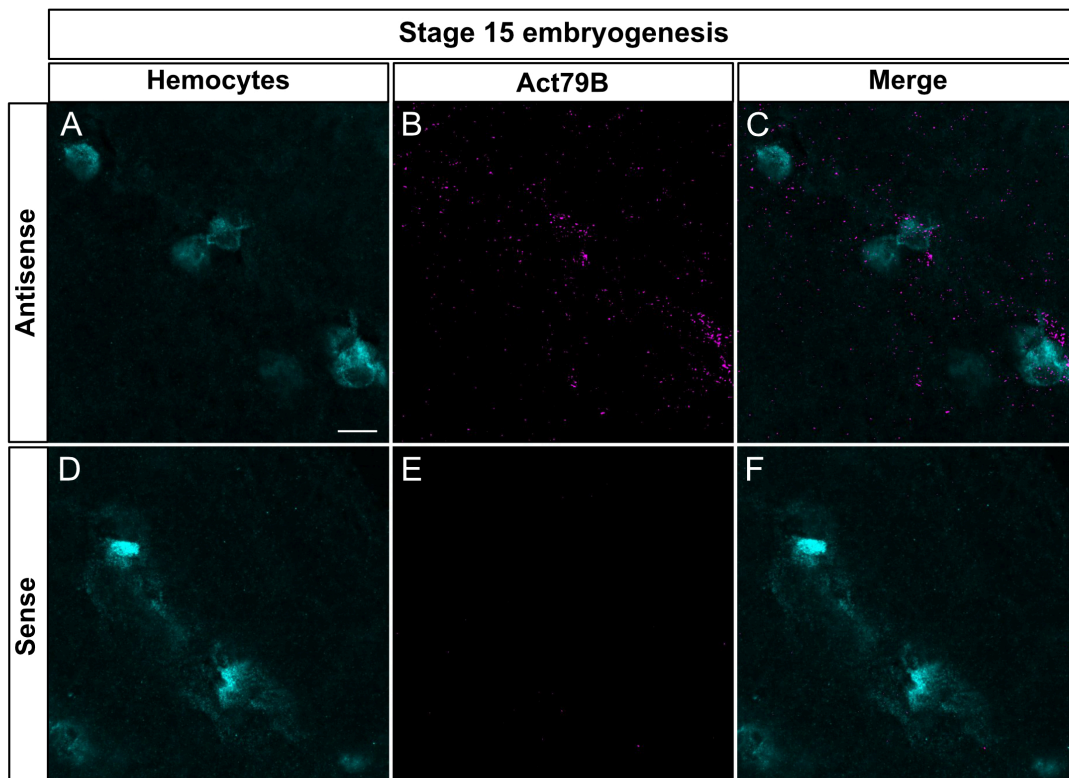
Figure 6.8.*act79B* **mRNA is not enriched in hemocytes at stage 15 of embryogenesis.** Embryos expressing UAS-GFP driven by srp-GAL4 and crq-GAL4. (A,D) Anti-GFP antibody (cyan) shows hemocyte distribution. (B,E) *In situ hybridisation* of *act79B* mRNA (magenta). (C,F) Merge. (B) Antisense shows no enrichment of *act79B* mRNA. Single frame. Scale bar 10µm.
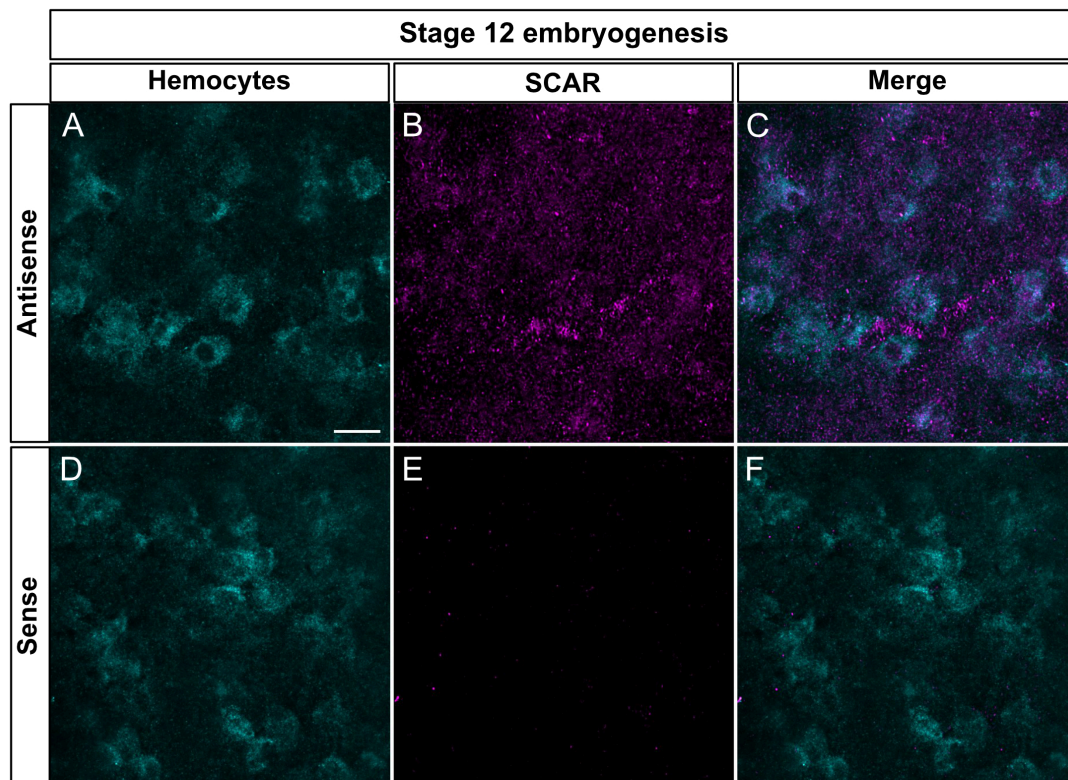
Figure 6.9. *SCAR* **mRNA is not enriched in hemocytes at stage 12 of embryogenesis.** Embryos expressing UAS-GFP driven by srp-GAL4 and crq-GAL4. (A,D) Anti-GFP antibody (cyan) shows hemocyte distribution. (B,E) *In situ hybridisation* of *SCAR* mRNA (magenta). (C,F) Merge. (B) Antisense shows no enrichment of *SCAR* mRNA. Single frame. Scale bar 10µm.
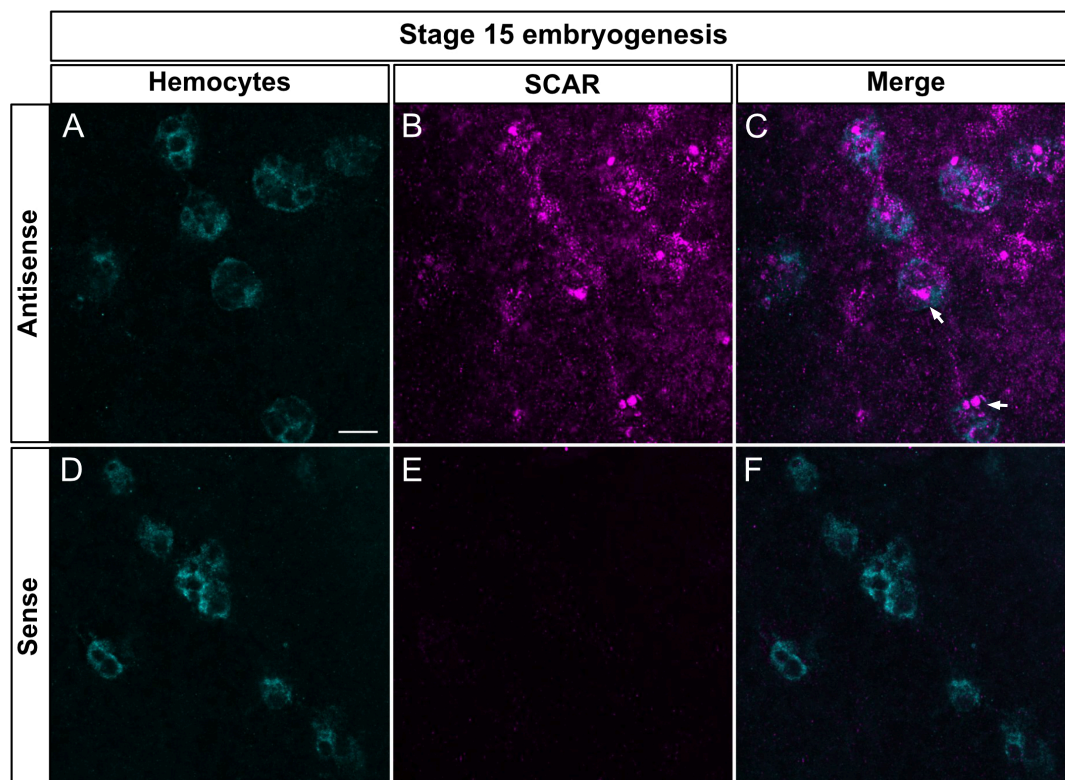
Figure 6.10. *SCAR* **mRNA is enriched in hemocytes at stage 15 of embryogenesis.** Embryos expressing UAS-GFP driven by srp-GAL4 and crq-GAL4. (A,D) Anti-GFP antibody (cyan) shows hemocyte distribution. (B,E) *In situ hybridisation* of *SCAR* mRNA (magenta). (C,F) Merge. (B) Antisense shows enrichment of *SCAR* mRNA. White arrows point at *SCAR* mRNA enriched in hemocytes. Single frame. Scale bar 10µm.

	act42A mRNA	*act87E* mRNA	*act79B* mRNA	*SCAR* mRNA
stage 12 embryogenesis	77% (n=65)	27% (n=59)	30% (n=88)	33% (n=75)
stage 15 embryogenesis	79% (n=98)	15% (n=56)	29% (n=56)	72% (n=116)

Table 6.1. Quantification of mRNA from *in situ hybridisation* data.
The percentage represents the proportion of hemocytes out of a total number of hemocytes showing an enrichment for the mRNA. *act42A* mRNA is highly enriched at stage 12 and 15. *act87E* and *act79B* mRNA show low enrichment at both stages. *SCAR* mRNA is highly enriched in hemocytes at stage 15, but less at stage 12.

6.3.2 Fixation results in a loss of the leading edge in embryonic hemocytes

Cells are highly polarised during migration with a leading edge protruding at the front of a cell (Figure 6.12A). The leading edge is driven by actin polymerisation and is thought to pull a migrating cell forward (Ananthakrishnan and Ehrlicher, 2007). *Drosophila* hemocytes have a leading edge, which extends up to 20μm from the cell body from stage 14 of embryogenesis (Wood et al., 2006). This edge was not observed during embryo fixation in the data above. Instead, hemocytes adopted a rounded and less polarised shape. With the prediction that mRNA localisation of actin would occur in the leading edge, based on fibroblasts data, I sought to preserve these structures during the *in situ hybridisation* protocol.

Previous work has shown that the addition of sucrose into fixative medium can preserve cells in neuronal tissue (Hollenbeck et al., 1987). Following a protocol from the Holt Lab (Cambridge) (Campbell and Holt, 2001), I added 15% sucrose into original 2% paraformaldehyde solution in order to fix *Drosophila* embryos. However, these conditions again did not preserve a leading edge in hemocytes. Moreover, this created a speckled-background in the cells and made it difficult to analyse hemocytes (Figure 6.12B). Another known structural preservation method is to perform the fixation protocol at 4°C (Figure 6.12C). However, this protocol also did not preserve the leading edge. Furthermore, the length of fixation was also modified from 15 minutes to 5 minutes and 1 minute in an attempt to preserve the leading edge of hemocytes. However, despite this, hemocytes remained rounded after fixation with no distinct polarisation. Further

personal communication confirmed that the loss of a leading edge in fixed tissue is a recurring problem in the field. I conclude that fixation of embryos which is required for the *in situ hybridisation* is not an optimal approach as it is difficult to establish if mRNA localises to the leading edge.
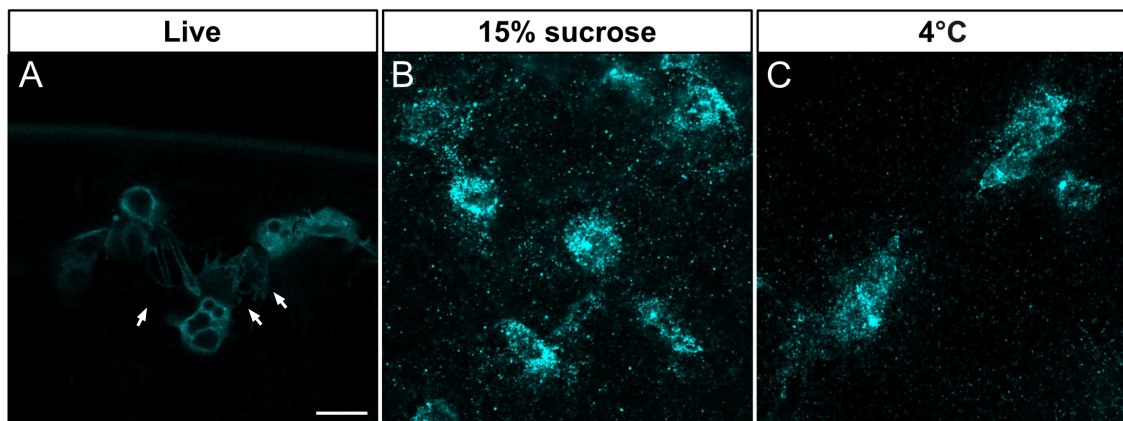
Figure 6.12. Hemocyte leading edge is lost during fixation protocol.
Stage 15 embryos expressing UAS-GFP driven by srp-GAL4 and crq-GAL4. (A) Live hemocytes. (B-C) Fixed embryos stained with anti-GFP antibody (cyan) shows hemocytes. (B) Embryos fixed with 15% sucrose, (C) embryos fixed at 4°C. Hemocyte leading edge was observed only in live hemocytes (A), but not in (B-C). White arrows are pointing at the hemocyte leading edge. Single frame. Scale bar 10µm.
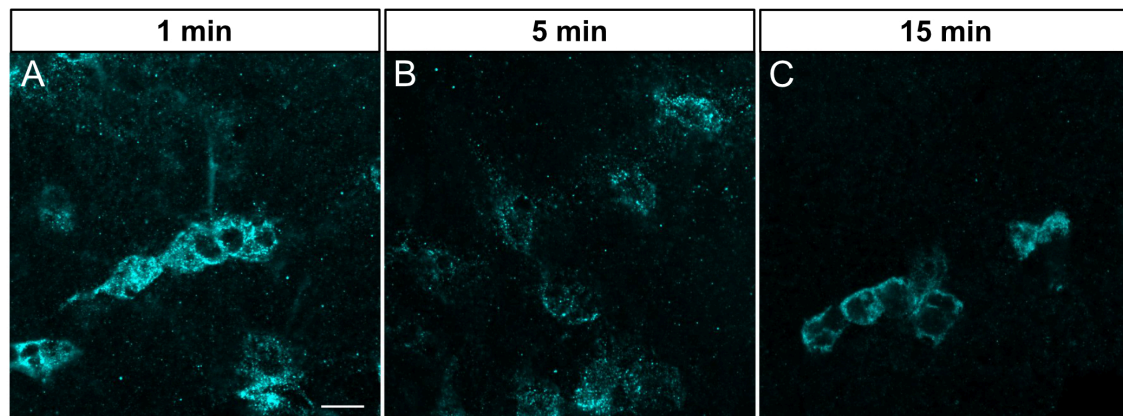
Figure 6.13. Hemocyte leading edge is lost during fixation protocol.
Stage 15 embryos expressing UAS-GFP driven by srp-GAL4 and crq-GAL4. (A-C) Fixed embryos stained with anti-GFP antibody (cyan) shows hemocytes. (A) Embryos fixed for 1min, (B) embryos fixed for 5min, (C) embryos fixed for 15min. Hemocyte leading edge was not observed at any timings (A-C). Single frame. Scale bar 10µm.

6.3.3 Visualisation of mRNA in live hemocytes with MS2-system

An alternative approach to *in situ hybridisation* is to visualise mRNA live with the MS2-system (reviewed in Weil et al., 2010). This system involves two transgenic constructs. The first is made by introducing multiple copies of the MS2 stem-loops binding sites in the 3'-UTR of mRNA of interest. The second construct expresses the MS2 coat protein fused to a fluorescent protein (Weil et al., 2010). Expression of both constructs in the same animal allows the visualisation of mRNA in living tissue, which was originally shown with *ash1* mRNA in yeast and *nanos* mRNA in flies (Bertrand et al., 1998; Forrest and Gavies, 2003; Weil et al., 2006).

As *act42A* mRNA was found to be enriched in fixed hemocytes, *act42A* mRNA was visualised in live hemocytes using the MS2-system. The fly lines were obtained from the St Johnston Lab (Cambridge), which had been developed as part of the screen in oogenesis. Although the construct was designed to be expressed in the germline with UAS/GaL4 system, I tested if it could be driven in hemocytes. I visualised *ac42A*-GFP in live hemocytes at stage 15 of embryogenesis and found that *act42A* mRNA exhibited rounded "clumps" across the entire area of the hemocyte (Figure 6.14A). To address whether *act42A* mRNA exhibits a greater localisation at the leading edge, I attempted to express an RFP marker, together with *act42*-GFP, to visualise the leading edge of the hemocytes. Unfortunately, the marker did not show any expression in the hemocytes. Recent work has designed new hemocyte markers with much brighter levels of mCherry in the hemocytes (Gyoergy et al., 2018). Future work on this project could test these markers with *act42a* MS2 lines.
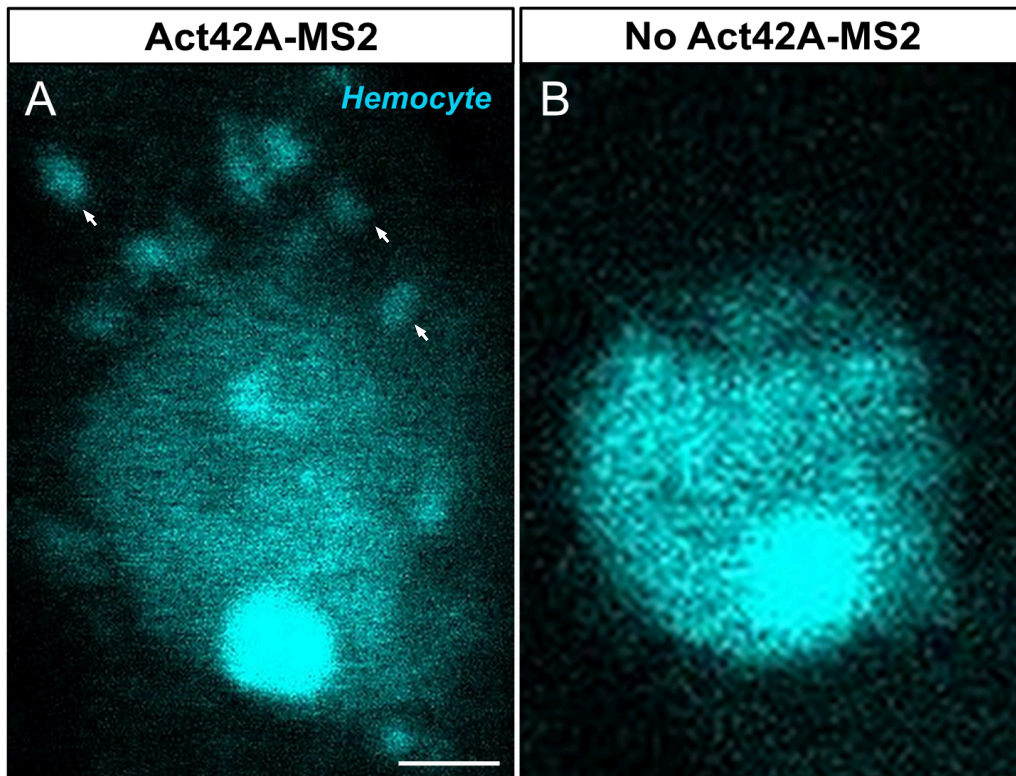
Figure 6.14. Visualisation of *act42A* mRNA in live hemocyte at stage 15.
(A) Stage 15 embryo expressing UAS-act42AMS2 and UAS-MCP-GFP driven by crq-GAL4. (B) Stage 15 embryo expressing control UAS-MCP-GFP only. (A) shows *act42A* mRNA puncta compared to the control (B). White arrows are pointing at *act42A* mRNA. Single frame. Scale bar 1μm.

6.4 Discussion

In summary, the data from this chapter shows that *act42A* mRNA is enriched in both stage 12 and 15 embryonic hemocytes, whilst *SCAR* mRNA is highly present in more polarised stage 15 hemocytes. My findings show that *in situ* hybridisation is not an optimal technique to study mRNA localisation in embryonic hemocytes. Instead, the MS2-system provides a possible suitable alternative to visualise mRNA live in *Drosophila* embryonic hemocytes.

Drosophila embryonic hemocytes could provide a suitable *in vivo* model system to study the role of mRNA localisation in cell migration. Although *in situ* hybridisation is a quicker way to visualise the transcripts in hemocytes, it results in a loss of the leading edge and it is not possible to determine whether the mRNAs show any particular localisation within a cell. Therefore, I would propose to utilise the MS2-system to visualise *act42A* and *SCAR* mRNAs in live hemocytes. Currently, there are no constructs designed for expression in hemocytes (personal communication). A different lab attempted to build the hemocyte-specific constructs to visualise some transcripts that might be involved in cell movement (personal communication). Unfortunately, these lines did not work and did not show any expression, likely due to mRNA construct issues. An alternative solution would be to use CRISPR system to guide and insert the stem-loops into the mRNAs candidates.

6.4.1 Wounding assay to study mRNA localisation in directed hemocyte migration

During hemocyte migration along the developmental routes, the hemocytes are able to detect wounds in the *Drosophila* embryo. They respond by diverting from their characteristic route and rapidly migrate towards the wound. This process allowed the design of the wounding assay, where laser ablation of an epithelial layer induces directed hemocyte migration towards the wound (Stramer et al., 2005).

Compared to migrating hemocytes, wound-induced hemocytes are considered faster and more-directed and are recruited to the site within 30 minutes of ablation (Wood et al., 2006). These hemocytes require the formation of the actin protrusions in the leading edge, as the pharmacological disruption of actin resulted in the failure of the hemocytes to reach the wound site (Wood et al., 2006). They do not depend on Pvf signalling as in the migrating hemocyte at stage 15 (Wood et al., 2006), and instead, sense and move towards hydrogen peroxide released from the wound site.

Previous work has shown that hydrogen peroxide is generated by the enzyme NADPH oxidase (DUOX) which has two EF hand domains that bind calcium, thus linking calcium and the wound-induced hemocyte migration (Moreira et al., 2010). The visualisation of calcium by genetically-encoded indicator GCaMP has shown that there is an increase in calcium in the form of a "flash" at the wound (Razzell et al., 2013). The calcium increase was shown to travel across the epithelial cells via innexins and to last up to 15 minutes (Razzell et al., 2013). The reduction in calcium levels by pharmacological agents, Thapsigargin or EGTA, significantly decreased the number of hemocytes recruited to the wound (Razzell et al., 2013). A similar finding was shown with Trpm channel knock-down, which resulted in a decrease of calcium and a reduced number of recruited hemocytes (Razzell et al., 2013). My findings from Chapter 5 have shown that Trpm is also required for the initiation and propagation of the calcium at *Drosophila* egg activation. Therefore, it is possible that the laser ablation of the outer epithelial layer in embryos results in the additional calcium influx from the extracellular space to support the propagation of a calcium wave across the epithelial cells.

I would propose to investigate mRNA localisation using the wounding assay, by ablating the ventral side of an embryo and following *act42A* or *SCAR* mRNA with MS2-system. It is possible that mRNA localisation is more prominent in the hemocyte leading edge during wound-induced migration, compared to the hemocytes at stage 15 of embryogenesis. The differences in mRNA enrichment should be compared between hemocyte populations to assess potential changes in the mechanism of mRNA transport, anchoring or localisation. In

summary, *Drosophila* embryonic hemocytes provide a suitable *in vivo* model system with the development of new tools to study directed cell migration. Further understanding of the mRNA localisation in the embryonic hemocytes should highlight some conserved similarities with vertebrate macrophages.

Chapter 7

Discussion

7.1 Summary and model for *Drosophila* egg activation

In summary, my data shows that the calcium wave associated with egg activation is initiated by osmotic pressure, which likely comes from hypotonic external fluid. The osmotic pressure is sufficient to mediate the dispersion of P bodies, a likely mechanism for the translation of maternal transcripts, and the metaphase-to-anaphase transition of the meiotic spindle, which is indicative of the resumption of the cell cycle. My data provides further evidence of a possible role for the aquaporin channels in mediating water homeostasis to withstand the osmotic pressure at *Drosophila* egg activation. Furthermore, I show that the osmotic pressure results in the dispersion of the cortical actin cytoskeleton, which is a likely mechanism leading to the activation of the mechanosensitive channels and the influx of calcium at egg activation. I show the requirement of Trpm and RPK channels in coordinating the initiation of the calcium wave, whilst eliminating the role of other calcium channels. Finally, I show that the calcium wave is followed by the non-cortical F-actin wavefront. This F-actin wavefront is calcium-dependent and exhibits similar dynamics to the calcium wave.

Together with the work of others, this data suggests a model for the mechanism of *Drosophila* egg activation (Figure 7.1). Once the female fly undergoes ovulation, the meiotically-arrested mature oocyte passes into the female oviduct. The mature oocyte is exposed to the osmotic pressure from the hypotonic oviduct fluid, which causes the oocyte to swell. The swelling results in uniform tension of the plasma membrane and the dispersion of the cortical actin. The decreased density of cortical actin at the posterior pole results in faster dispersion of this actin and initial opening of mechanosensitive channels such as Trpm via the internal domain of the channels. This results in the initial calcium influx from the perivitelline space at the posterior pole. Further increases in intracellular calcium are relayed across the oocyte by the activation of the neighbouring mechanosensitive channels via the dispersion of the cortical actin cytoskeleton at the lateral sides, resulting in the calcium wave propagation across the oocyte. The calcium wave is then followed by the F-actin wavefront, which ensures the restructuring or repolymerisation of cortical F-actin across the oocyte, deactivating the calcium influx channels. The recovery of the calcium wave is mediated by PMCA, which pumps calcium back into the

perivitelline space. Overall, a single calcium wave prepares a *Drosophila* mature oocyte to undergo successful embryogenesis, independent of fertilisation.

A Before egg activation

Ovary

Perivitelline space · RPK · NCX · Aquaporin · TRP · Oocyte cytoplasm

B 1 minute post activation

Ovary · Lateral oviduct

translation of mRNAs

Ca²⁺

resumption of the cell cycle

increased cross-linking of the chorion layer

RPK · NCX · Aquaporin · TRP

C 5 minutes post activation

Common oviduct

F-actin

Repolymerisation of actin

Closing of TRP channels

PMCA · NCX · Aquaporin · TRP

157

Figure 7.1. Model diagram summarising the events of *Drosophila* egg activation.
(A) <u>Before egg activation</u>, meiotically-arrested mature oocyte is in the posterior half of the ovary. The cortical actin (cyan blue) is found in a tight band at the plasma membrane of the oocyte. The calcium channels are in a closed formation and there is no calcium influx from the perivitelline space. (B) <u>1 minute post egg activation</u>, the mature oocyte enters the oviduct and uptakes oviduct fluid, which results in swelling (purple arrows outside the oocyte) of the oocyte promoted by aquaporin channels (blue). Subsequently, cortical actin undergoes dynamic dispersal (cyan blue dashed line and cyan arrows), resulting in the opening of the mechanosensitive channels TRP (orange), initiating calcium influx from the posterior pole. Calcium wave (blue) is propagated to the anterior pole by additional calcium influx from nearby TRP channels. Mechanosensitive RPK (yellow) and NCK (green) channels mediate sodium homeostasis. (C) <u>5 minutes post egg activation</u>, F-actin wavefront (purple) initiates from the posterior pole following the calcium wave, allowing the repolymerisation of cortical actin (cyan arrows) after the initial cortical actin dispersion and closing of TRP channels. Calcium wave recovery is mediated by PMCA transporting calcium back to the perivitelline space. Together, these events result in the processes of egg activation, such the resumption of cell cycle, translation of mRNAs and cross-linking of the chorion layer.

7.2 *Drosophila* calcium wave as a slow calcium wave

Calcium waves can be classified by how fast they traverse the cell: ultrafast, fast, slow and ultra slow (Jaffe, 2008). In most animals, calcium waves travel at 10-30 µm/sec during egg activation, which is a typical speed range for fast calcium waves (Jaffe, 2002). However, some oocytes exhibit slow calcium waves, which propagate across an egg at 0.2 - 2 µm/sec. The slow calcium waves are usually associated with a morphological change, such as indentation in the plasma membrane like furrow cleavage. For example, the first visualisation of such a wave was achieved by the injection of aequorin into medaka fish eggs undergoing furrow cleavage (Fluck et al., 1991). Similar calcium waves were also observed in the eggs of *Xenopus and* zebrafish (Muto et al., 1996; Creton et al., 1998).

Although there are numerous examples of slow calcium waves that are known to associate with developing eggs after activation, only maize eggs exhibit a slow calcium wave at egg activation (Antoine et al., 2000). This slow calcium wave was shown to propagate at 1 µm/sec (Antoine et al., 2000). It is currently unknown why maize eggs have evolved to have a slow calcium wave at egg activation. One possibility is that the maize eggs do not undergo cortical granule exocytosis to prevent polyspermy at egg activation. Thus, there might not be a need for the maize eggs to invest extra energy and cellular resources to coordinate the fast calcium wave. In contrast, ascidian oocytes display a fast

calcium wave at egg activation, but do not undergo exocytosis of cortical granules, suggesting that these two processes are not necessarily linked (Speksnijder et al., 1990). *Drosophila* oocytes do not use cortical exocytosis to prevent polyspermy. Instead, the mature oocytes ensure monospermy by the presence of a single site for sperm entry and direct competition between sperm cells (Loppin et al., 2015). Similarly to maize eggs, it is possible that *Drosophila* oocytes do not require the fast calcium wave at egg activation and instead evolved to have a slow calcium wave, which propagates at a speed of 1.5 μm/ sec.

The proposed mechanism for the slow calcium wave propagation involves the activation of the mechanosensitive channels, compared to the IP$_3$-mediated fast calcium wave (Jaffe, 2008). The opening of the mechanosensitive channels is mediated by tension in the plasma membrane and results in the influx of calcium. The slow calcium wave propagation is then coordinated by the opening of the neighbouring channels via changes in the actin cytoskeleton and myosin networks. The calcium wave associated with *Drosophila* egg activation appears to be another example of a slow calcium wave, which uses a similar mechanism for the propagation.

In *Drosophila*, the calcium wave initiates from the posterior pole upon the exposure of the oocyte to the oviduct fluid. The mature oocyte swells, which introduces tension to the plasma membrane and results in the dispersion of the actin cytoskeleton, initially at the posterior pole. Both of these are likely to act as an activation cue for the mechanosensitive channel, Trpm, and potentially other candidates (Chapter 5). The calcium wave is then relayed by the opening of the neighbouring mechanosensitive channels towards the anterior pole. It remains unclear why the slow calcium wave is beneficial to *Drosophila* oocytes at egg activation. It is possible that the slow calcium wave prepares the mature oocyte for fertilisation, creating a favourable environment for the sperm to enter the egg. Although, the oocyte does not undergo cortical granule exocytosis, egg activation results in the cross-linking and hardening of the outer shell chorion. It is possible that the slow calcium wave ensures prolonged presence of the oocyte within a female fly, in order to prepare the oocyte against the extracellular environment once deposited. Overall, it is clear that the calcium

wave at *Drosophila* egg activation presents a new example of the slow calcium wave, with more apparent similarities to plant rather than vertebrate eggs.

7.3 Plant egg activation vs *Drosophila* egg activation

Plants provide an interesting class of organisms due to the presence of double-fertilisation. Plant sperm cells are immobile and are brought into close proximity to an egg via the pollen tube. Two sperm cells are released and bind to two female gametes: the egg and central cell. The release of sperm cells from the pollen tube is thought to result in the initial events of egg activation and an increase in intracellular calcium (Denninger et al., 2014; Hamamura et al., 2014).

The first observation of a calcium increase was visualised in maize eggs, where the calcium wave was shown to take on average 24 minutes to propagate at 1.13 µm/sec and then recover (Digonnet et al., 1997; Antoine et al., 2001). Previous work has shown that the calcium wave initiates after the fusion of sperm with the oocyte and requires mechanosensitive channels for the initiation and propagation of the calcium wave (Antoine et al., 2001). In the case of *Fucus Rhizoid* zygotes, the calcium wave is induced by hypo-osmotic shock and is also dependent on mechanosensitive channels, as the treatment with gadolinium chloride causes the inhibition of the calcium influx (Taylor et al., 1996).

The mechanism of a calcium increase seems to differ in the eggs of flowering plants. For example, *Arabidopsis* oocytes exhibit a shorter calcium increase upon fertilisation, which on average lasts up to 3 minutes (Denninger et al., 2014; Hamamura et al., 2014). There are two calcium increases that have been shown to associate with *Arabidopsis* egg activation (Hamamura et al., 2014). The first calcium increase has been shown to be concomitant with the release of the pollen from the pollen tube, and the second calcium increase to correlate with the fusion of sperm with an egg (Hamamura et al., 2014). It is hypothesised that the first calcium increase is caused by the mechanical pressure generated by the pollen tube discharge (Hamamura et al., 2011).

Together, this evidence highlights many parallels between *Drosophila* and non-flowering plant egg activation. These include the propagation speed of the calcium wave, potential involvement of the mechanosensitive channels to mediate the calcium influx and the absence of cortical granule exocytosis to prevent polyspermy.

7.4 The importance of *Drosophila* egg activation and parallels with other insects

A common theme has emerged, where insect egg activation is independent of fertilisation and, instead, depends on the deformation of the oocyte's plasma membrane. Egg activation has been studied in many insects, including honeybees, mosquitos and turnip sawfly (Sawa and Oishi, 1989; Sasaki and Obara, 2002; Yamamoto et al., 2013). Many of these insects undergo parthenogenetic development, where haploid eggs develop into males.

Previous work has shown that the immersion of the oviposited mature oocytes of yellow fever mosquito into water can resume the oocyte development (Kliewer, 1961). A similar scenario was shown to occur in the oocytes of turnip sawfly and in the malaria vector mosquito, where egg activation was initiated by placing the oocytes into water (Sawa and Oishi, 1989; Yamamoto et al., 2013). It is likely that the osmotic pressure from water causes the mature oocytes to swell, stretching the plasma membrane of the oocyte, initiating an increase in intracellular calcium and resuming downstream processes of egg activation. Another form of tension can be applied on the oocyte during the passage through the insect female oviduct. Previous work has shown that the eggs of honeybees can be activated by placing them into a glass capillary tube imitating the pressure from the oviduct (Sasaki and Obara, 2002). Similar mechanical pressure from the oviduct acts as an initiation cue for egg activation in eggs of the parasitic ichneumon wasp (Went and Krause, 1973; Went and Krause, 1982). Therefore, osmotic and physical pressures seem to be predominant initiation cues of egg activation in insects.

Drosophila is currently the only example of an insect in which the mature oocytes have been shown to exhibit an increase in intracellular calcium at egg activation (York-Andersen et al., 2015; Kaneuchi et al., 2015). Future work should focus on understanding the parallels between insect, plant and mammalian mechanisms of egg activation. Understanding the conserved pathways will provide better insights on the evolution of fertilisation and egg activation, which can facilitate the development of the *in vitro* fertilisation techniques in many species. One should not forget that understanding the insect egg activation in particular may help in the discovery of an insecticide which can target egg activation as an early stage of insect development. Overall, my work has laid the foundation of the model system for studying insect egg activation, which can be used to study egg activation in Tribolium, butterfly and mosquito eggs.

Chapter 8

References

Abassi, Y.A., Carroll, D.J., Giusti, A.F., Belton, R.J., Jr., and Foltz, K.R. (2000). Evidence That Src-Type Tyrosine Kinase Activity Is Necessary for Initiation of Calcium Release at Fertilization in Sea Urchin Eggs. Dev. Biol. *218*, 206–219.

Adams, C.M., Anderson, M.G., Motto, D.G., Price, M.P., Johnson, W.A., and Welsh, M.J. (1998). Ripped pocket and pickpocket, novel Drosophila DEG/ENaC subunits expressed in early development and in mechanosensory neurons. J. Cell Biol. *140*, 143–152.

Afewerky, H.K., Lu, Y., Zhang, T., and Li, H. (2016). Roles of Sodium-Calcium Exchanger Isoform-3 toward Calcium Ion Regulation in Alzheimers Disease. Journal of Alzheimer's Disease & Parkinsonism *06*, 1–12.

Ananthakrishnan, R., and Ehrlicher, A. (2007). The forces behind cell movement. Int. J. Biol. Sci. *3*, 303–317.

Antoine, A.F., Faure, J.E., Cordeiro, S., Dumas, C., Rougier, M., and Feijó, J.A. (2000). A calcium influx is triggered and propagates in the zygote as a wavefront during in vitro fertilization of flowering plants. Proc. Natl. Acad. Sci. U.S.a. *97*, 10643–10648.

Antoine, A.F., Faure, J.E., Dumas, C., and Feijó, J.A. (2001). Differential contribution of cytoplasmic Ca2+ and Ca2+ influx to gamete fusion and egg activation in maize. Nat. Cell Biol. *3*, 1120–1123.

Apell, H.-J. (2004). How do P-type ATPases transport ions? Bioelectrochemistry *63*, 149–156.

Arbeitman, M.N. (2004). A genomic analysis of Drosophila somatic sexual differentiation and its regulation. Development *131*, 2007–2021.

Awayda, M.S. (1996). Protein kinase regulation of a cloned epithelial Na+ channel. J. Gen. Physiol. *108*, 49–65.

Ayabe, T., Kopf, G.S., and Schultz, R.M. (1995). Regulation of mouse egg activation: presence of ryanodine receptors and effects of

microinjected ryanodine and cyclic ADP ribose on uninseminated and inseminated eggs. Development *121*, 2233–2244.

Backs, J., Stein, P., Backs, T., Duncan, F.E., Grueter, C.E., McAnally, J., Qi, X., Schultz, R.M., and Olson, E.N. (2010). The gamma isoform of CaM kinase II controls mouse egg activation by regulating cell cycle resumption. Proc. Natl. Acad. Sci. U.S.a. *107*, 81–86.

Bailly, M., Macaluso, F., Cammer, M., Chan, A., Segall, J.E., and Condeelis, J.S. (1999). Relationship between Arp2/3 complex and the barbed ends of actin filaments at the leading edge of carcinoma cells after epidermal growth factor stimulation. J. Cell Biol. *145*, 331–345.

Balasubramaniam, S.L., Gopalakrishnapillai, A., Gangadharan, V., Duncan, R.L., and Barwe, S.P. (2015). Sodium-calcium exchanger 1 regulates epithelial cell migration via calcium-dependent extracellular signal-regulated kinase signaling. J. Biol. Chem. *290*, 12463–12473.

Barral, J., and Martin, P. (2011). The physical basis of active mechanosensitivity by the hair-cell bundle. Current Opinion in Otolaryngology & Head and Neck Surgery *19*, 369–375.

Bass, B.P., Tanner, E.A., Mateos San Martín, D., Blute, T., Kinser, R.D., Dolph, P.J., and McCall, K. (2009). Cell-autonomous requirement for DNaseII in nonapoptotic cell death. Cell Death Differ. *16*, 1362–1371.

Bassell, G.J., and Singer, R.H. (2001). Neuronal RNA Localization and the Cytoskeleton. In Cell Polarity and Subcellular RNA Localization, (Berlin, Heidelberg: Springer Berlin Heidelberg), pp. 41–56.

Bassell, G.J., and Warren, S.T. (2008). Fragile X syndrome: loss of local mRNA regulation alters synaptic development and function. Neuron *60*, 201–214.

Becalska, A.N., and Gavis, E.R. (2009). Lighting up mRNA localization in Drosophila oogenesis. Development *136*, 2493–2503.

Becker, K.A., and Hart, N.H. (1996). The cortical actin cytoskeleton of unactivated zebrafish eggs: Spatial organization and distribution of

filamentous actin, nonfilamentous actin, and myosin-II. Mol. Reprod. Dev. *43*, 536–547.

Becker, K.A., and Hart, N.H. (1999). Reorganization of filamentous actin and myosin-II in zebrafish eggs correlates temporally and spatially with cortical granule exocytosis. J Cell Sci. 112, 97-110.

Bement, W.M., Leda, M., Moe, A.M., Kita, A.M., Larson, M.E., Golding, A.E., Pfeuti, C., Su, K.-C., Miller, A.L., Goryachev, A.B., et al. (2015). Activator-inhibitor coupling between Rho signalling and actin assembly makes the cell cortex an excitable medium. Nat. Cell Biol. *17*, 1471–1483.

Bergsten, S.E., and Gavis, E.R. (1999). Role for mRNA localization in translational activation but not spatial restriction of nanos RNA. Development *126*, 659–669.

Bernhardt, M.L., Padilla-Banks, E., Stein, P., Zhang, Y., and Williams, C.J. (2017). Store-operated Ca2+ entry is not required for fertilization-induced Ca2+ signaling in mouse eggs. Cell Calcium *65*, 63–72.

Bernitt, E., Döbereiner, H.-G., Gov, N.S., and Yochelis, A. (2017). Fronts and waves of actin polymerization in a bistability-based mechanism of circular dorsal ruffles. Nat Commun *8*, 15863.

Bernitt, E., Koh, C.G., Gov, N., and Döbereiner, H.-G. (2015). Dynamics of actin waves on patterned substrates: a quantitative analysis of circular dorsal ruffles. PLoS ONE *10*, e0115857.

Berridge, M.J., Lipp, P., and Bootman, M.D. (2000). The versatility and universality of calcium signalling. Nat. Rev. Mol. Cell Biol. *1*, 11–21.

Berridge, M.J. (2002). The endoplasmic reticulum: a multifunctional signaling organelle. Cell Calcium *32*, 235–249.

Berridge, M.J. (2005). Unlocking the secrets of cell signaling. Annu. Rev. Physiol. *67*, 1–21.

Berridge, M.J., Bootman, M.D., and Roderick, H.L. (2003). Calcium signalling: dynamics, homeostasis and remodelling. Nat. Rev. Mol. Cell Biol. *4*, 517–529.

BERTANI, G. (1951). Studies on lysogenesis. I. The mode of phage liberation by lysogenic Escherichia coli. J. Bacteriol. *62*, 293–300.

Bertrand, E., Chartrand, P., Schaefer, M., Shenoy, S.M., Singer, R.H., and Long, R.M. (1998). Localization of ASH1 mRNA Particles in Living Yeast. Mol. Cell *2*, 437–445.

Besse, F., and Ephrussi, A. (2008). Translational control of localized mRNAs: restricting protein synthesis in space and time. Nat. Rev. Mol. Cell Biol. *9*, 971–980.

Biggers, J.D., and Powers, R. D. (1979). Sodium transport and swelling of the mammalian blastocyst: effect of amirolime. In Amiloride and Epithelial Sodium Transport, 167-179.

Blanchoin, L., and Pollard, T.D. (1999). Mechanism of interaction of Acanthamoeba actophorin (ADF/Cofilin) with actin filaments. J. Biol. Chem. *274*, 15538–15546.

Blanchoin, L., and Pollard, T.D. (2002). Hydrolysis of ATP by polymerized actin depends on the bound divalent cation but not profilin. Biochemistry *41*, 597–602.

Blanchoin, L., Boujemaa-Paterski, R., Sykes, C., and Plastino, J. (2014). Actin dynamics, architecture, and mechanics in cell motility. Physiological Reviews *94*, 235–263.

Blaustein, M.P., and Lederer, W.J. (1999). Sodium/calcium exchange: its physiological implications. Physiological Reviews *79*, 763–854.

Bolívar, J., Huynh, J.R., López-Schier, H., González, C., St Johnston, D., and González-Reyes, A. (2001). Centrosome migration into the Drosophila oocyte is independent of BicD and egl, and of the organisation of the microtubule cytoskeleton. Development *128*, 1889–1897.

Bootman, M.D. (2012). Calcium signaling. Cold Spring Harb Perspect Biol *4*, a011171–a011171.

Boulay, G., Brown, D.M., Qin, N., Jiang, M., Dietrich, A., Zhu, M.X., Chen, Z., Birnbaumer, M., Mikoshiba, K., and Birnbaumer, L. (1999). Modulation of Ca(2+) entry by polypeptides of the inositol 1,4, 5-trisphosphate receptor (IP3R) that bind transient receptor potential (TRP): evidence for roles of TRP and IP3R in store depletion-activated Ca(2+) entry. Proc. Natl. Acad. Sci. U.S.a. *96*, 14955–14960.

Breitbart, H., Cohen, G., and Rubinstein, S. (2005). Role of actin cytoskeleton in mammalian sperm capacitation and the acrosome reaction. Reproduction *129*, 263–268.

Breitsprecher, D., Kiesewetter, A.K., Linkner, J., Vinzenz, M., Stradal, T.E.B., Small, J.V., Curth, U., Dickinson, R.B., and Faix, J. (2011). Molecular mechanism of Ena/VASP-mediated actin-filament elongation. Embo J. *30*, 456–467.

Bretschneider, T., Anderson, K., Ecke, M., Müller-Taubenberger, A., Schroth-Diez, B., Ishikawa-Ankerhold, H.C., and Gerisch, G. (2009). The three-dimensional dynamics of actin waves, a model of cytoskeletal self-organization. Biophysical Journal *96*, 2888–2900.

Brucker, C., and Lipford, G.B. (1995). The human sperm acrosome reaction: physiology and regulatory mechanisms. An update. Hum. Reprod. Update *1*, 51–62.

Brückner, K., Kockel, L., Duchek, P., Luque, C.M., Rørth, P., and Perrimon, N. (2004). The PDGF/VEGF receptor controls blood cell survival in Drosophila. Dev. Cell *7*, 73–84.

Bullock, S.L., and Ish-Horowicz, D. (2001). Conserved signals and machinery for RNA transport in Drosophila oogenesis and embryogenesis. Nature 1973 244:5416 *414*, 611–616.

Bullock, S.L., Stauber, M., Prell, A., Hughes, J.R., Ish-Horowicz, D., and Schmidt-Ott, U. (2004). Differential cytoplasmic mRNA localisation

adjusts pair-rule transcription factor activity to cytoarchitecture in dipteran evolution. Development *131*, 4251–4261.

Burkel, B.M., Dassow, von, G., and Bement, W.M. (2007). Versatile fluorescent probes for actin filaments based on the actin-binding domain of utrophin. Cell Motil. Cytoskeleton *64*, 822–832.

Campbell, D.S., and Holt, C.E. (2001). Chemotropic Responses of Retinal Growth Cones Mediated by Rapid Local Protein Synthesis and Degradation. Neuron *32*, 1013–1026.

Carafoli, E. (1991). The Calcium Pumping ATPase Of The Plasma Membrane. Annu. Rev. Physiol. *53*, 531–547.

Carafoli, E. (1992). P-type ATPases. Introduction. J. Bioenerg. Biomembr. *24*, 245–247.

Carbone, E., and Lux, H.D. (1984). A low voltage-activated calcium conductance in embryonic chick sensory neurons. Biophysical Journal *46*, 413–418.

Carmody, S.R., and Wente, S.R. (2009). mRNA nuclear export at a glance. J. Cell. Sci. *122*, 1933–1937.

Carroll, D.J., Ramarao, C.S., Mehlmann, L.M., Roche, S., Terasaki, M., and Jaffe, L.A. (1997). Calcium release at fertilization in starfish eggs is mediated by phospholipase Cgamma. J. Cell Biol. *138*, 1303–1311.

Carroll, J. (2000). Na+-Ca2+ exchange in mouse oocytes: modifications in the regulation of intracellular free Ca2+ during oocyte maturation. J. Reprod. Fertil. *118*, 337–342.

Carvacho, I., Ardestani, G., Lee, H.-C., McGarvey, K., Fissore, R.A., and Lykke-Hartmann, K. (2016). TRPM7-like channels are functionally expressed in oocytes and modulate post-fertilization embryo development in mouse. Sci Rep *6*, 34236.

Castagnetti, S., and Ephrussi, A. (2003). Orb and a long poly(A) tail are required for efficient oskar translation at the posterior pole of the Drosophila oocyte. Development *130*, 835–843.

Catterall, W.A. (2011). Voltage-Gated Calcium Channels. Cold Spring Harb Perspect Biol *3*, a003947–a003947.

Cavaliere, V., Bernardi, F., Romani, P., Duchi, S., and Gargiulo, G. (2008). Building up the Drosophila eggshell: first of all the eggshell genes must be transcribed. Dev. Dyn. *237*, 2061–2072.

Cárdenas, L., Lovy-Wheeler, A., Kunkel, J.G., and Hepler, P.K. (2008). Pollen tube growth oscillations and intracellular calcium levels are reversibly modulated by actin polymerization. Plant Physiol. *146*, 1611–1621.

Celsi, F., Pizzo, P., Brini, M., Leo, S., Fotino, C., Pinton, P., and Rizzuto, R. (2009). Mitochondria, calcium and cell death: a deadly triad in neurodegeneration. Biochim. Biophys. Acta *1787*, 335–344.

Chalfie, M., and Wolinsky, E. (1990). The identification and suppression of inherited neurodegeneration in Caenorhabditis elegans. Nature 1973 244:5416 *345*, 410–416.

Chandan, G., and Tim, H. (2007). TRPV1 expression-dependent initiation and regulation of filopodia. GBM Fall Meeting Hamburg 2007 *2007*, 1900.

Chang, P., Torres, J., Lewis, R.A., Mowry, K.L., Houliston, E., and King, M.L. (2004). Localization of RNAs to the mitochondrial cloud in Xenopus oocytes through entrapment and association with endoplasmic reticulum. Mol. Biol. Cell *15*, 4669–4681.

Chang, W.-L., Liou, W., Pen, H.-C., Chou, H.-Y., Chang, Y.-W., Li, W.-H., Chiang, W., and Pai, L.-M. (2008). The gradient of Gurken, a long-range morphogen, is directly regulated by Cbl-mediated endocytosis. Development *135*, 1923–1933.

Chao, J.A., Patskovsky, Y., Patel, V., Levy, M., Almo, S.C., and Singer, R.H. (2010). ZBP1 recognition of beta-actin zipcode induces RNA looping. Genes Dev. *24*, 148–158.

Chapman, E.R., Hanson, P.I., An, S., and Jahn, R. (1995). Ca2+ regulates the interaction between synaptotagmin and syntaxin 1. J. Biol. Chem. *270*, 23667–23671.

Chen, C.-C., Lamping, K.G., Nuno, D.W., Barresi, R., Prouty, S.J., Lavoie, J.L., Cribbs, L.L., England, S.K., Sigmund, C.D., Weiss, R.M., et al. (2003). Abnormal coronary function in mice deficient in alpha1H T-type Ca2+ channels. Science *302*, 1416–1418.

Chen, Y., Song, X., Ye, S., Miao, L., Zhu, Y., Zhang, R.-G., and Ji, G. (2013). Structural insight into enhanced calcium indicator GCaMP3 and GCaMPJ to promote further improvement. Protein Cell *4*, 299–309.

Chhabra, E.S., and Higgs, H.N. (2007). The many faces of actin: matching assembly factors with cellular structures. Nat. Cell Biol. *9*, 1110–1121.

Cho, N.K., Keyes, L., Johnson, E., Heller, J., Ryner, L., Karim, F., and Krasnow, M.A. (2002). Developmental control of blood cell migration by the Drosophila VEGF pathway. Cell *108*, 865–876.

Christensen, A.P., and Corey, D.P. (2007). TRP channels in mechanosensation: direct or indirect activation? Nature Reviews Neuroscience *8*, 510–521.

Chun, J.T., Puppo, A., Vasilev, F., Gragnaniello, G., Garante, E., and Santella, L. (2010). The biphasic increase of PIP2 in the fertilized eggs of starfish: new roles in actin polymerization and Ca2+ signaling. PLoS ONE *5*, e14100.

Church, P.J., and Stanley, E.F. (1996). Single L-type calcium channel conductance with physiological levels of calcium in chick ciliary ganglion neurons. J. Physiol. (Lond.) *496*, 59–68.

Ciura, S., Liedtke, W., and Bourque, C.W. (2011). Hypertonicity sensing in organum vasculosum lamina terminalis neurons: a mechanical process involving TRPV1 but not TRPV4. J. Neurosci. *31*, 14669–14676.

Clapham, D.E. (2007). Calcium signaling. Cell *131*, 1047–1058.

Cohen, G., Rubinstein, S., Gur, Y., and Breitbart, H. (2004). Crosstalk between protein kinase A and C regulates phospholipase D and F-actin formation during sperm capacitation. Dev. Biol. *267*, 230–241.

Cooper, J.A. (1987). Effects of cytochalasin and phalloidin on actin. J. Cell Biol. *105*, 1473–1478.

COSENS, D.J., and MANNING, A. (1969). Abnormal Electroretinogram from a Drosophila Mutant. Nature 1973 244:5416 *224*, 285–287.

Créton, R., Speksnijder, J.E., and Jaffe, L.F. (1998). Patterns of free calcium in zebrafish embryos. J. Cell. Sci. *111 (Pt 12)*, 1613–1622.

Crossley, A.C. (1979). The morphology and development of the Drosophila muscular system. The Genetics and Biology of Drosophla, Vol 2b, Academic Press, 499-560.

Crossley, I., Whalley, T., and Whitaker, M. (1991). Guanosine 5'-thiotriphosphate may stimulate phosphoinositide messenger production in sea urchin eggs by a different route than the fertilizing sperm. Cell Regul. *2*, 121–133.

Cukovic, D., Ehlting, J., VanZiffle, J.A., and Douglas, C.J. (2001). Structure and evolution of 4-coumarate:coenzyme A ligase (4CL) gene families. Biol. Chem. *382*, 645–654.

Cummings, M.R., and King, R.C. (1970). Ultrastructural changes in nurse and follicle cells during late stages of oogenesis in Drosophila melanogaster. Zeitschrift FðR Zellforschung Und Mikroskopische Anatomie *110*, 1–8.

Curtis, B.M., and Catterall, W.A. (2002). Purification of the calcium antagonist receptor of the voltage-sensitive calcium channel from skeletal muscle transverse tubules. Biochemistry *23*, 2113–2118.

Dale, B., Talevi, R., and DeFelice, L.J. (1991). L-type Ca2+ currents in ascidian eggs. Exp. Cell Res. *192*, 302–306.

DAN, K. (1960). Cyto-embryology of echinoderms and amphibia. Int. Rev. Cytol. *9*, 321–367.

Darboux, I., Lingueglia, E., Pauron, D., Barbry, P., and Lazdunski, M. (1998). A new member of the amiloride-sensitive sodium channel family in Drosophila melanogaster peripheral nervous system. Biochem. Biophys. Res. Commun. *246*, 210–216.

de Cuevas, M., and Spradling, A.C. (1998). Morphogenesis of the Drosophila fusome and its implications for oocyte specification. Development *125*, 2781–2789.

De Waard, M., Gurnett, C.A., and Campbell, K.P. (1996). Structural and functional diversity of voltage-activated calcium channels. Ion Channels *4*, 41–87.

Deguchi, R., Osanai, K., and Morisawa, M. (1996). Extracellular Ca2+ entry and Ca2+ release from inositol 1,4,5-trisphosphate-sensitive stores function at fertilization in oocytes of the marine bivalve Mytilus edulis. Development *122*, 3651–3660.

Deguchi, R. (2007). Fertilization causes a single Ca2+ increase that fully depends on Ca2+ influx in oocytes of limpets (Phylum Mollusca, Class Gastropoda). Dev. Biol. *304*, 652–663.

Deng, Y., Singer, R.H., and Gu, W. (2008). Translation of ASH1 mRNA is repressed by Puf6p-Fun12p/eIF5B interaction and released by CK2 phosphorylation. Genes Dev. *22*, 1037–1050.

Denninger, P., Bleckmann, A., Lausser, A., Vogler, F., Ott, T., Ehrhardt, D.W., Frommer, W.B., Sprunck, S., Dresselhaus, T., and Grossmann, G.

(2014). Male-female communication triggers calcium signatures during fertilization in Arabidopsis. Nat Commun *5*, 4645.

Desai, S.A., and Lnenicka, G.A. (2011). Characterization of postsynaptic Ca2+ signals at the Drosophila larval NMJ. J. Neurophysiol. *106*, 710–721.

Desai-Shah, M., Papoy, A.R., Ward, M., and Cooper, R.L. (2010). Roles of the Sarcoplasmic/Endoplasmic Reticulum Ca2+-ATPase, Plasma Membrane Ca2+-ATPase and Na+/Ca2+ Exchanger in Regulation of Heart Rate in Larval Drosophila~!2010-03-10~!2010-08-13~! 2010-08-27~! The Open Physiology Journal *3*, 16–36.

Dietrich, A., Mederos Y Schnitzler, M., Kalwa, H., Storch, U., and Gudermann, T. (2005). Functional characterization and physiological relevance of the TRPC3/6/7 subfamily of cation channels. Naunyn Schmiedebergs Arch. Pharmacol. *371*, 257–265.

Digonnet, C., Aldon, D., Leduc, N., Dumas, C., and Rougier, M. (1997). First evidence of a calcium transient in flowering plants at fertilization. Development *124*, 2867–2874.

Ding, D., Parkhurst, S.M., Halsell, S.R., and Lipshitz, H.D. (1993). Dynamic Hsp83 RNA localization during Drosophila oogenesis and embryogenesis. Mol. Cell. Biol. *13*, 3773–3781.

Dipolo, R., and Beaugé, L. (2006). Sodium/Calcium Exchanger: Influence of Metabolic Regulation on Ion Carrier Interactions. Physiological Reviews *86*, 155–203.

DOANE, W.W. (1960). Completion of meiosis in uninseminated eggs of Drosophila melanogaster. Science *132*, 677–678.

Dominguez, R. (2010). Structural insights into de novo actin polymerization. Curr. Opin. Struct. Biol. *20*, 217–225.

Dominguez, R., and Holmes, K.C. (2011). Actin Structure and Function. Annual Review of Biophysics *40*, 169–186.

Driscoll, M., and Chalfie, M. (1991). The mec-4 gene is a member of a family of Caenorhabditis elegans genes that can mutate to induce neuronal degeneration. Nature 1973 244:5416 *349*, 588–593.

Dryer, S.E., and Reiser, J. (2010). TRPC6 channels and their binding partners in podocytes: role in glomerular filtration and pathophysiology. Am. J. Physiol. Renal Physiol. *299*, F689–F701.

Duncan, J.E., and Warrior, R. (2002). The cytoplasmic dynein and kinesin motors have interdependent roles in patterning the Drosophila oocyte. Curr. Biol. *12*, 1982–1991.

Dunst, S., Kazimiers, T., Zadow, von, F., Jambor, H., Sagner, A., Brankatschk, B., Mahmoud, A., Spannl, S., Tomancak, P., Eaton, S., et al. (2015). Endogenously tagged rab proteins: a resource to study membrane trafficking in Drosophila. Dev. Cell *33*, 351–365.

Dupré, A., Haccard, O., and Jessus, C. (2011). Mos in the oocyte: how to use MAPK independently of growth factors and transcription to control meiotic divisions. J Signal Transduct *2011*, 350412–350415.

Earley, S., Waldron, B.J., and Brayden, J.E. (2004). Critical role for transient receptor potential channel TRPM4 in myogenic constriction of cerebral arteries. Circ. Res. *95*, 922–929.

Edwards, K.A., Demsky, M., Montague, R.A., Weymouth, N., and Kiehart, D.P. (1997). GFP-moesin illuminates actin cytoskeleton dynamics in living tissue and demonstrates cell shape changes during morphogenesis in Drosophila. Dev. Biol. *191*, 103–117.

El-Jouni, W., Haun, S., and Machaca, K. (2008). Internalization of plasma membrane Ca2+-ATPase during Xenopus oocyte maturation. Dev. Biol. *324*, 99–107.

El-Jouni, W., Jang, B., Haun, S., and Machaca, K. (2005). Calcium signaling differentiation during Xenopus oocyte maturation. Dev. Biol. *288*, 514–525.

Endow, S.A., and Komma, D.J. (1997). Spindle dynamics during meiosis in Drosophila oocytes. J. Cell Biol. *137*, 1321–1336.

Eno, C., Solanki, B., and Pelegri, F. (2016). aura (mid1ip1l) regulates the cytoskeleton at the zebrafish egg-to-embryo transition. Development *143*, 1585–1599.

Ephrussi, A., Dickinson, L.K., and Lehmann, R. (1991). Oskar organizes the germ plasm and directs localization of the posterior determinant nanos. Cell *66*, 37–50.

Escoffier, J., Lee, H.-C., Yassine, S., Zouari, R., Martinez, G., Karaouzène, T., Coutton, C., Kherraf, Z.-E., Halouani, L., Triki, C., et al. (2016). Homozygous mutation of PLCZ1 leads to defective human oocyte activation and infertility that is not rescued by the WW-binding protein PAWP. Hum. Mol. Genet. *25*, 878–891.

Evans, I.R., Ghai, P.A., Urbančič, V., Tan, K.-L., and Wood, W. (2013). SCAR/WAVE-mediated processing of engulfed apoptotic corpses is essential for effective macrophage migration in Drosophila. Cell Death Differ. *20*, 709–720.

Fabiato, A. (1983). Calcium-induced release of calcium from the cardiac sarcoplasmic reticulum. Am. J. Physiol. *245*, C1–C14.

Fan, H.-Y., and Sun, Q.-Y. (2004). Involvement of Mitogen-Activated Protein Kinase Cascade During Oocyte Maturation and Fertilization in Mammals1. Biology of Reproduction *70*, 535–547.

Fanger, C.M., Hoth, M., Crabtree, G.R., and Lewis, R.S. (1995). Characterization of T cell mutants with defects in capacitative calcium entry: genetic evidence for the physiological roles of CRAC channels. J. Cell Biol. *131*, 655–667.

Farina, K.L., Huttelmaier, S., Musunuru, K., Darnell, R., and Singer, R.H. (2003). Two ZBP1 KH domains facilitate beta-actin mRNA localization, granule formation, and cytoskeletal attachment. J. Cell Biol. *160*, 77–87.

Feske, S., Gwack, Y., Prakriya, M., Srikanth, S., Puppel, S.-H., Tanasa, B., Hogan, P.G., Lewis, R.S., Daly, M., and Rao, A. (2006). A mutation in Orai1 causes immune deficiency by abrogating CRAC channel function. Nature 1973 244:5416 *441*, 179–185.

Fiévet, B., Louvard, D., and Arpin, M. (2007). ERM proteins in epithelial cell organization and functions. Biochimica Et Biophysica Acta (BBA) - Molecular Cell Research *1773*, 653–660.

Flockerzi, V., Oeken, H.J., and Hofmann, F. (1986). Purification of a functional receptor for calcium-channel blockers from rabbit skeletal-muscle microsomes. Eur. J. Biochem. *161*, 217–224.

Flores-Soto, E., Reyes-García, J., Sommer, B., Chavez, J., Barajas-López, C., and Montaño, L.M. (2012). PPADS, a P2X receptor antagonist, as a novel inhibitor of the reverse mode of the Na^+/Ca^{2+} exchanger in guinea pig airway smooth muscle. Eur. J. Pharmacol. *674*, 439–444.

Fluck, R., Abraham, V., Miller, A., and Galione, A. (1999). Microinjection of cyclic ADP-ribose triggers a regenerative wave of Ca2+ release and exocytosis of cortical alveoli in medaka eggs. Zygote *7*, 285–292.

Foltz, K.R., and Shilling, F.M. (2008). Recepter-mediated signal transduction and egg activation. Zygote *1*, 276–279.

Forrest, K.M., and Gavis, E.R. (2003). Live imaging of endogenous RNA reveals a diffusion and entrapment mechanism for nanos mRNA localization in Drosophila. Curr. Biol. *13*, 1159–1168.

Frenkel, O., Shani, E., Ben-Bassat, I., Brok-Simoni, F., Shinar, E., and Danon, D. (2001). Activation of human monocytes/macrophages by hypo-osmotic shock. Clin. Exp. Immunol. *124*, 103–109.

Fujimoto, S., Yoshida, N., Fukui, T., Amanai, M., Isobe, T., Itagaki, C., Izumi, T., and Perry, A.C.F. (2004). Mammalian phospholipase Cζ induces oocyte activation from the sperm perinuclear matrix. Dev. Biol. *274*, 370–383.

Fukami, K., Inanobe, S., Kanemaru, K., and Nakamura, Y. (2010). Phospholipase C is a key enzyme regulating intracellular calcium and modulating the phosphoinositide balance. Prog. Lipid Res. *49*, 429–437.

Furuichi, T., Yoshikawa, S., Miyawaki, A., Wada, K., Maeda, N., and Mikoshiba, K. (1989). Primary structure and functional expression of the inositol 1,4,5-trisphosphate-binding protein P400. Nature 1973 244:5416 *342*, 32–38.

Fyrberg, E.A., Mahaffey, J.W., Bond, B.J., and Davidson, N. (1983). Transcripts of the six Drosophila actin genes accumulate in a stage- and tissue-specific manner. Cell *33*, 115–123.

Gagnon, J.A., Kreiling, J.A., Powrie, E.A., Wood, T.R., and Mowry, K.L. (2013). Directional transport is mediated by a Dynein-dependent step in an RNA localization pathway. PLoS Biol. *11*, e1001551.

Galione, A. (1993). Cyclic ADP-ribose: a new way to control calcium. Science *259*, 325–326.

Galione, A., White, A., Willmott, N., Turner, M., Potter, B.V., and Watson, S.P. (1993). cGMP mobilizes intracellular Ca2+ in sea urchin eggs by stimulating cyclic ADP-ribose synthesis. Nature 1973 244:5416 *365*, 456–459.

Gallicano, G.I., McGaughey, R.W., and Capco, D.G. (1997). Activation of protein kinase C after fertilization is required for remodeling the mouse egg into the zygote. Mol. Reprod. Dev. *46*, 587–601.

García-Añoveros, J., Ma, C., and Chalfie, M. (1995). Regulation of Caenorhabditis elegans degenerin proteins by a putative extracellular domain. Curr. Biol. *5*, 441–448.

Georgiev, P., Okkenhaug, H., Drews, A., Wright, D., Lambert, S., Flick, M., Carta, V., Martel, C., Oberwinkler, J., and Raghu, P. (2010). TRPM channels mediate zinc homeostasis and cellular growth during Drosophila larval development. Cell Metab. *12*, 386–397.

Gilkey, J.C., Jaffe, L.F., Ridgway, E.B., and Reynolds, G.T. (1978). A free calcium wave traverses the activating egg of the medaka, Oryzias latipes. J. Cell Biol. *76*, 448–466.

Giorgi, C., Romagnoli, A., Pinton, P., and Rizzuto, R. (2008). Ca2+ signaling, mitochondria and cell death. Curr. Mol. Med. *8*, 119–130.

Glabe, C.G., and Vacquier, V.D. (1978). Egg surface glycoprotein receptor for sea urchin sperm bindin. Proc. Natl. Acad. Sci. U.S.a. *75*, 881–885.

González-Reyes, A., and St Johnston, D. (1998). The Drosophila AP axis is polarised by the cadherin-mediated positioning of the oocyte. Development *125*, 3635–3644.

González-Reyes, A., Elliott, H., and St Johnston, D. (1995). Polarization of both major body axes in Drosophila by gurken-torpedo signalling. Nature 1973 244:5416 *375*, 654–658.

Goswami, C., Rademacher, N., Smalla, K.-H., Kalscheuer, V., Ropers, H.-H., Gundelfinger, E.D., and Hucho, T. (2010). TRPV1 acts as a synaptic protein and regulates vesicle recycling. J. Cell. Sci. *123*, 2045–2057.

Goud, P.T., Goud, A.P., Leybaert, L., Van Oostveldt, P., Mikoshiba, K., Diamond, M.P., and Dhont, M. (2002). Inositol 1,4,5-trisphosphate receptor function in human oocytes: calcium responses and oocyte activation-related phenomena induced by photolytic release of InsP(3) are blocked by a specific antibody to the type I receptor. Mol. Hum. Reprod. *8*, 912–918.

Green, M.R., and Sambrook, J. (2016). Precipitation of DNA with Ethanol. Cold Spring Harbor Protocols *2016*, pdb.prot093377.

Gregor, T., Wieschaus, E.F., McGregor, A.P., Bialek, W., and Tank, D.W. (2007). Stability and nuclear dynamics of the bicoid morphogen gradient. Cell *130*, 141–152.

Griff, E.R., Kleene, N.K., and Kleene, S.J. (2012). A selective PMCA inhibitor does not prolong the electroolfactogram in mouse. PLoS ONE 7, e37148.

Grimm, C., Kraft, R., Sauerbruch, S., Schultz, G., and Harteneck, C. (2003). Molecular and functional characterization of the melastatin-related cation channel TRPM3. J. Biol. Chem. *278*, 21493–21501.

Grumet, M., and Lin, S. (1980). Reversal of profilin inhibition of actin polymerization invitro by erythrocyte cytochalasin-binding complexes and cross-linked actin nuclei. Biochem. Biophys. Res. Commun. *92*, 1327–1334.

Grumetto, L., Wilding, M., De Simone, M.L., Tosti, E., Galione, A., and Dale, B. (1997). Nitric oxide gates fertilization channels in ascidian oocytes through nicotinamide nucleotide metabolism. Biochem. Biophys. Res. Commun. *239*, 723–728.

Gual, P., Shigematsu, S., Kanzaki, M., Grémeaux, T., Gonzalez, T., Pessin, J.E., Le Marchand-Brustel, Y., and Tanti, J.-F. (2002). A Crk-II/ TC10 signaling pathway is required for osmotic shock-stimulated glucose transport. J. Biol. Chem. *277*, 43980–43986.

Gulyas, B.J., and Mattison, D.R. (1979). Degeneration of mouse oocytes in response to polycyclic aromatic hydrocarbons. Anat. Rec. *193*, 863–882.

Gundersen, G.G., Kalnoski, M.H., and Bulinski, J.C. (1984). Distinct populations of microtubules: tyrosinated and nontyrosinated alpha tubulin are distributed differently in vivo. Cell *38*, 779–789.

Gurnett, C.A., De Waard, M., and Campbell, K.P. (1996). Dual function of the voltage-dependent Ca2+ channel alpha 2 delta subunit in current stimulation and subunit interaction. Neuron *16*, 431–440.

Gustin, M.C., Albertyn, J., Alexander, M., and Davenport, K. (1998). MAP kinase pathways in the yeast Saccharomyces cerevisiae. Microbiol. Mol. Biol. Rev. *62*, 1264–1300.

Gyoergy, A., Roblek, M., Ratheesh, A., Valoskova, K., Belyaeva, V., Wachner, S., Matsubayashi, Y., Sánchez-Sánchez, B.J., Stramer, B., and Siekhaus, D.E. (2018). Tools Allowing Independent Visualization and Genetic Manipulation of Drosophila melanogaster Macrophages and Surrounding Tissues. G3 (Bethesda) *8*, 845–857.

Hachet, O., and Ephrussi, A. (2004). Splicing of oskar RNA in the nucleus is coupled to its cytoplasmic localization. Nature 1973 244:5416 *428*, 959–963.

Hagiwara, S., Ozawa, S., and Sand, O. (1975). Voltage clamp analysis of two inward current mechanisms in the egg cell membrane of a starfish. J. Gen. Physiol. *65*, 617–644.

Hall, A.C. (1995). Volume-sensitive taurine transport in bovine articular chondrocytes. J. Physiol. (Lond.) *484 (Pt 3)*, 755–766.

Hall, J.E., Brands, M.W., and Shek, E.W. (1996a). Central role of the kidney and abnormal fluid volume control in hypertension. J Hum Hypertens *10*, 633–639.

Hall, J.E., Guyton, A.C., and Brands, M.W. (1996b). Pressure-volume regulation in hypertension. Kidney Int. Suppl. *55*, S35–S41.

Hamamura, Y., Nishimaki, M., Takeuchi, H., Geitmann, A., Kurihara, D., and Higashiyama, T. (2014). Live imaging of calcium spikes during double fertilization in Arabidopsis. Nat Commun *5*, 4722.

Hamamura, Y., Saito, C., Awai, C., Kurihara, D., Miyawaki, A., Nakagawa, T., Kanaoka, M.M., Sasaki, N., Nakano, A., Berger, F., et al. (2011). Live-cell imaging reveals the dynamics of two sperm cells during double fertilization in Arabidopsis thaliana. Curr. Biol. *21*, 497–502.

Harada, K., Oita, E., and Chiba, K. (2003). Metaphase I arrest of starfish oocytes induced via the MAP kinase pathway is released by an increase of intracellular pH. Development *130*, 4581–4586.

Hardie, R.C., and Minke, B. (1992). The trp gene is essential for a light-activated Ca2+ channel in Drosophila photoreceptors. Neuron *8*, 643–651.

Harraz, O.F., and Altier, C. STIM1-mediated bidirectional regulation of Ca2+ entry through voltage-gated calcium channels (VGCC) and calcium-release activated channels (CRAC). Front. Cell. Neurosci., Feb 2014, Vol.8, 43.

Hart, N.H., and Collins, G.C. (1991). An electron-microscope and freeze-fracture study of the egg cortex of Brachydanio rerio. Zeitschrift FðR Zellforschung Und Mikroskopische Anatomie *265*, 317–328.

Haviv, L., Brill-Karniely, Y., Mahaffy, R., Backouche, F., Ben-Shaul, A., Pollard, T.D., and Bernheim-Groswasser, A. (2006). Reconstitution of the transition from lamellipodium to filopodium in a membrane-free system. Proc. Natl. Acad. Sci. U.S.a. *103*, 4906–4911.

Hayakawa, K., Tatsumi, H., and Sokabe, M. (2008). Actin stress fibers transmit and focus force to activate mechanosensitive channels. J. Cell. Sci. *121*, 496–503.

Heifetz, Y., Yu, J., and Wolfner, M.F. (2001). Ovulation triggers activation of Drosophila oocytes. Dev. Biol. *234*, 416–424.

Heytens, E., Parrington, J., Coward, K., Young, C., Lambrecht, S., Yoon, S.Y., Fissore, R.A., Hamer, R., Deane, C.M., Ruas, M., et al. (2009). Reduced amounts and abnormal forms of phospholipase C zeta (PLC) in spermatozoa from infertile men. Human Reproduction *24*, 2417–2428.

Hirai, S., and Shida, H. (1979). Shortening of microvilli during the maturation of starfish oocyte from which vitelline coat was removed. Bull. Mar. Biol. Stay. Asamushi, Tokyo Univ. 16, 161-167.

Hofmann, T., Chubanov, V., Chen, X., Dietz, A.S., Gudermann, T., and Montell, C. (2010). Drosophila TRPM channel is essential for the control of extracellular magnesium levels. PLoS ONE *5*, e10519.

Hollenbeck, P.J., and Bray, D. (1987). Rapidly transported organelles containing membrane and cytoskeletal components: their relation to axonal growth. J. Cell Biol. *105*, 2827–2835.

Holmes, K.C., Popp, D., Gebhard, W., and Kabsch, W. (1990). Atomic model of the actin filament. Nature 1973 244:5416 *347*, 44–49.

Homa, S.T., and Swann, K. (1994). Fertilization and early embryology: A cytosolic sperm factor triggers calcium oscillations and membrane hyperpolarizations in human oocytes. Human Reproduction *9*, 2356–2361.

Horner, V.L., and Wolfner, M.F. (2008a). Transitioning from egg to embryo: triggers and mechanisms of egg activation. Dev. Dyn. *237*, 527–544.

Horner, V.L., and Wolfner, M.F. (2008b). Mechanical stimulation by osmotic and hydrostatic pressure activates Drosophila oocytes in vitro in a calcium-dependent manner. Dev. Biol. *316*, 100–109.

Horner, V.L., Czank, A., Jang, J.K., Singh, N., Williams, B.C., Puro, J., Kubli, E., Hanes, S.D., McKim, K.S., Wolfner, M.F., et al. (2006). The Drosophila calcipressin sarah is required for several aspects of egg activation. Curr. Biol. *16*, 1441–1446.

Hoth, M. (1995). Calcium and barium permeation through calcium release-activated calcium (CRAC) channels. Pflugers Arch. *430*, 315–322.

Houliston, E., Carré, D., Johnston, J.A., and Sardet, C. (1993). Axis establishment and microtubule-mediated waves prior to first cleavage in Beroe ovata. Development *117*, 75–87.

Hughes, S.E., Miller, D.E., Miller, A.L., and Hawley, R.S. (2018). Female Meiosis: Synapsis, Recombination, and Segregation in Drosophila melanogaster. Genetics *208*, 875–908.

Huttelmaier, S., Zenklusen, D., Lederer, M., Dictenberg, J., Lorenz, M., Meng, X., Bassell, G.J., Condeelis, J., and Singer, R.H. (2005). Spatial

regulation of beta-actin translation by Src-dependent phosphorylation of ZBP1. Nature 1973 244:5416 *438*, 512–515.

Igusa, Y., and Miyazaki, S. (1983). Effects of altered extracellular and intracellular calcium concentration on hyperpolarizing responses of the hamster egg. J. Physiol. (Lond.) *340*, 611–632.

Ito, J., and Kashiwazaki, N. (2012). Molecular mechanism of fertilization in the pig. Animal Science Journal *83*, 669–682.

Iwasaki, H., Chiba, K., Uchiyama, T., Yoshikawa, F., Suzuki, F., Ikeda, M., Furuichi, T., and Mikoshiba, K. (2002). Molecular characterization of the starfish inositol 1,4,5-trisphosphate receptor and its role during oocyte maturation and fertilization. J. Biol. Chem. *277*, 2763–2772.

Jackson, R.J., Hellen, C.U.T., and Pestova, T.V. (2010). The mechanism of eukaryotic translation initiation and principles of its regulation. Nat. Rev. Mol. Cell Biol. *11*, 113–127.

Jaffe, L. (2002). On the conservation of fast calcium wave speeds. Cell Calcium *32*, 217–229.

Jaffe, L.A., Giusti, A.F., Carroll, D.J., and Foltz, K.R. (2001). Ca2+ signalling during fertilization of echinoderm eggs. Semin. Cell Dev. Biol. *12*, 45–51.

Jaffe, L.F. (2008). Calcium waves. Philos. Trans. R. Soc. Lond., B, Biol. Sci. *363*, 1311–1316.

Jambor, H., Brunel, C., and Ephrussi, A. (2011). Dimerization of oskar 3' UTRs promotes hitchhiking for RNA localization in the Drosophila oocyte. Rna *17*, 2049–2057.

Januschke, J., Gervais, L., Gillet, L., Keryer, G., Bornens, M., and Guichet, A. (2006). The centrosome-nucleus complex and microtubule organization in the Drosophila oocyte. Development *133*, 129–139.

Jay, S.D., Ellis, S.B., McCue, A.F., Williams, M.E., Vedvick, T.S., Harpold, M.M., and Campbell, K.P. (1990). Primary structure of the gamma

subunit of the DHP-sensitive calcium channel from skeletal muscle. Science *248*, 490–492.

Jeffs, G.J., Meloni, B.P., Bakker, A.J., and Knuckey, N.W. (2007). The role of the Na(+)/Ca(2+) exchanger (NCX) in neurons following ischaemia. J Clin Neurosci *14*, 507–514.

Johnson, H.W., and Schell, M.J. (2009). Neuronal IP3 3-kinase is an F-actin-bundling protein: role in dendritic targeting and regulation of spine morphology. Mol. Biol. Cell *20*, 5166–5180.

Jones, K.T., and Nixon, V.L. (2000). Sperm-Induced Ca2+ Oscillations in Mouse Oocytes and Eggs Can Be Mimicked by Photolysis of Caged Inositol 1,4,5-Trisphosphate: Evidence to Support a Continuous Low Level Production of Inositol 1,4,5-Trisphosphate during Mammalian Fertilization. Dev. Biol. *225*, 1–12.

Kabsch, W., Mannherz, H.G., Suck, D., Pai, E.F., and Holmes, K.C. (1990). Atomic structure of the actin:DNase I complex. Nature 1973 244:5416 *347*, 37–44.

Kaji, K., Oda, S., Shikano, T., Ohnuki, T., Uematsu, Y., Sakagami, J., Tada, N., Miyazaki, S., and Kudo, A. (2000). The gamete fusion process is defective in eggs of Cd9-deficient mice. Nat. Genet. *24*, 279–282.

Kambysellis, M.P., Starmer, T., Smathers, G., and Heed, W.B. (1980). Studies of Oogenesis in Natural Populations of Drosophilidae. II. Significance of Microclimatic Changes on Oogenesis of Drosophila mimica. The American Naturalist *115*, 67–91.

Kanai, A. (2004). [Transcriptome and non-coding RNAs: so many mRNA-like non-coding RNAs are really functional?]. Tanpakushitsu Kakusan Koso *49*, 2521–2528.

Kaneuchi, T., Wolfner, M.F., and Aigaki, T. (2015). A calcium rise occurs as activating Drosophila eggs move through the female reproductive tract. Mol. Reprod. Dev. *82*, 501–501.

KANG, T.M., STECIUK, M., and HILGEMANN, D.W. (2006). Sodium-Calcium Exchange Stoichiometry. Annals of the New York Academy of Sciences *976*, 142–151.

Khamviwath, V., Hu, J., and Othmer, H.G. (2013). A continuum model of actin waves in Dictyostelium discoideum. PLoS ONE *8*, e64272.

Kiehart, D.P., Crawford, J.M., and Montague, R.A. (2007). Collection, dechorionation, and preparation of Drosophila embryos for quantitative microinjection. CSH Protoc *2007*, pdb.prot4717–pdb.prot4717.

Kim-Ha, J., Smith, J.L., and Macdonald, P.M. (1991). oskar mRNA is localized to the posterior pole of the Drosophila oocyte. Cell *66*, 23–35.

King, R.C. (1970). The meiotic behavior of the Drosophila oocyte. Int. Rev. Cytol. *28*, 125–168.

Kinsey, W.H., Wu, W., and Macgregor, E. (2003). Activation of Src-family PTK activity at fertilization: role of the SH2 domain. Dev. Biol. *264*, 255–262.

Kirilly, D., and Xie, T. (2007). The Drosophila ovary: an active stem cell community. Cell Research *17*, 15–25.

Kiselyov, K., Mignery, G.A., Zhu, M.X., and Muallem, S. (1999). The N-terminal domain of the IP3 receptor gates store-operated hTrp3 channels. Mol. Cell *4*, 423–429.

Kiselyov, K., Xu, X., Mozhayeva, G., Kuo, T., Pessah, I., Mignery, G., Zhu, X., Birnbaumer, L., and Muallem, S. (1998). Functional interaction between InsP3 receptors and store-operated Htrp3 channels. Nature 1973 244:5416 *396*, 478–482.

Kishimoto, T. (1998). Cell cycle arrest and release in starfish oocytes and eggs. Semin. Cell Dev. Biol. *9*, 549–557.

Kislauskis, E.H., Zhu, X., and Singer, R.H. (1994). Sequences responsible for intracellular localization of beta-actin messenger RNA also affect cell phenotype. J. Cell Biol. *127*, 441–451.

186

Kislauskis, E.H., Zhu, X., and Singer, R.H. (1997). beta-Actin messenger RNA localization and protein synthesis augment cell motility. J. Cell Biol. *136*, 1263–1270.

Kliewer, J.W. (1961). Weight and Hatchability of Aedes aegypti Eggs (Diptera: Culicidae)1. Annals of the Entomological Society of America *54*, 912–917.

Kline, D., and Kline, J.T. (1992). Repetitive calcium transients and the role of calcium in exocytosis and cell cycle activation in the mouse egg. Dev. Biol. *149*, 80–89.

Knott, J.G., Kurokawa, M., Fissore, R.A., Schultz, R.M., and Williams, C.J. (2005). Transgenic RNA interference reveals role for mouse sperm phospholipase Czeta in triggering Ca2+ oscillations during fertilization. Biology of Reproduction *72*, 992–996.

Koch, E.A., and King, R.C. (1966). The origin and early differentiation of the egg chamber of Drosophila melanogaster. Journal of Morphology *119*, 283–303.

Kouchi, Z., Fukami, K., Shikano, T., Oda, S., Nakamura, Y., Takenawa, T., and MIYAZAKI, S. (2004). Recombinant phospholipase Czeta has high Ca2+ sensitivity and induces Ca2+ oscillations in mouse eggs. J. Biol. Chem. *279*, 10408–10412.

Kovar, D.R., Staiger, C.J., Weaver, E.A., and McCurdy, D.W. (2000). AtFim1 is an actin filament crosslinking protein from Arabidopsis thaliana. Plant J. *24*, 625–636.

Kubiak, J.Z., Weber, M., de Pennart, H., Winston, N.J., and Maro, B. (1993). The metaphase II arrest in mouse oocytes is controlled through microtubule-dependent destruction of cyclin B in the presence of CSF. Embo J. *12*, 3773–3778.

Kuo, R.C., Baxter, G.T., Thompson, S.H., Stricker, S.A., Patton, C., Bonaventura, J., and Epel, D. (2000). NO is necessary and sufficient for egg activation at fertilization. Nature 1973 244:5416 *406*, 633–636.

Kültz, D., Madhany, S., and Burg, M.B. (1998). Hyperosmolality Causes Growth Arrest of Murine Kidney Cells. J. Biol. Chem. *273*, 13645–13651.

Kyozuka, K., Chun, J.T., Puppo, A., Gragnaniello, G., Garante, E., and Santella, L. (2008). Actin cytoskeleton modulates calcium signaling during maturation of starfish oocytes. Dev. Biol. *320*, 426–435.

LaFleur, G.J., Horiuchi, Y., and Wessel, G.M. (1998). Sea urchin ovoperoxidase: oocyte-specific member of a heme-dependent peroxidase superfamily that functions in the block to polyspermy. Mech. Dev. *70*, 77–89.

Lajas, A.I., Sierra, V., Camello, P.J., Salido, G.M., and Pariente, J.A. (2001). Vanadate inhibits the calcium extrusion in rat pancreatic acinar cells. Cell. Signal. *13*, 451–456.

Langenbacher, A.D., Dong, Y., Shu, X., Choi, J., Nicoll, D.A., Goldhaber, J.I., Philipson, K.D., and Chen, J.-N. (2005). Mutation in sodium-calcium exchanger 1 (NCX1) causes cardiac fibrillation in zebrafish. Proc. Natl. Acad. Sci. U.S.a. *102*, 17699–17704.

las Heras, de, M.A., Valcarcel, A., Pérez, L.J., and Moses, D.F. (1997). Actin localization in ram spermatozoa: effect of freezing/thawing, capacitation and calcium ionophore-induced acrosomal exocytosis. Tissue Cell *29*, 47–53.

Lasko, P. (2012). mRNA localization and translational control in Drosophila oogenesis. Cold Spring Harb Perspect Biol *4*, a012294–a012294.

LAWRENCE, J. (1986). Intracellular localization of messenger RNAs for cytoskeletal proteins. Cell *45*, 407–415.

Lee, H.C., Aarhus, R., and Walseth, T.F. (1993). Calcium mobilization by dual receptors during fertilization of sea urchin eggs. Science *261*, 352–355.

Lee, H.-C., Yoon, S.-Y., Lykke-Hartmann, K., Fissore, R.A., and Carvacho, I. (2016). TRPV3 channels mediate Ca²⁺ influx induced by 2-APB in mouse eggs. Cell Calcium *59*, 21–31.

Lee, T., and Luo, L. (1999). Mosaic Analysis with a Repressible Cell Marker for Studies of Gene Function in Neuronal Morphogenesis. Neuron *22*, 451–461.

Leguia, M., Conner, S., Berg, L., and Wessel, G.M. (2006). Synaptotagmin I is involved in the regulation of cortical granule exocytosis in the sea urchin. Mol. Reprod. Dev. *73*, 895–905.

Lehman, W., Craig, R., and Vibert, P. (1994). Ca(2+)-induced tropomyosin movement in Limulus thin filaments revealed by three-dimensional reconstruction. Nature 1973 244:5416 *368*, 65–67.

Lelkes, P.I., Friedman, J.E., Rosenheck, K., and Oplatka, A. (1986). Destabilization of actin filaments as a requirement for the secretion of catecholamines from permeabilized chromaffin cells. FEBS Lett. *208*, 357–363.

LeMosy, E.K., and Hashimoto, C. (2000). The Nudel Protease of Drosophila Is Required for Eggshell Biogenesis in Addition to Embryonic Patterning. Dev. Biol. *217*, 352–361.

Lewis, R.S. (2001). Calcium signaling mechanisms in T lymphocytes. Annu. Rev. Immunol. *19*, 497–521.

Lécuyer, E., Parthasarathy, N., and Krause, H.M. (2008). Fluorescent In Situ Hybridization Protocols in Drosophila Embryos and Tissues. In Drosophila, (Totowa, NJ: Humana Press), pp. 289–302.

Li, J. (1994). Egg chorion tanning in Aedes aegypti mosquito. Comp. Biochem. Physiol. a Physiol. *109*, 835–843.

Li, J.S., and Li, J. (2006). Major chorion proteins and their crosslinking during chorion hardening in Aedes aegypti mosquitoes. Insect Biochem. Mol. Biol. *36*, 954–964.

Liedtke, W., Choe, Y., Martí-Renom, M.A., Bell, A.M., Denis, C.S., Sali, A., Hudspeth, A.J., Friedman, J.M., and Heller, S. (2000). Vanilloid receptor-related osmotically activated channel (VR-OAC), a candidate vertebrate osmoreceptor. Cell *103*, 525–535.

Lim, D., Lange, K., and Santella, L. (2002). Activation of oocytes by latrunculin A. Faseb J. *16*, 1050–1056.

Lin, C.C., Love, H.D., Gushue, J.N., Bergeron, J.J., and Ostermann, J. (1999). ER/Golgi intermediates acquire Golgi enzymes by brefeldin A-sensitive retrograde transport in vitro. J. Cell Biol. *147*, 1457–1472.

Lin, H., and Spradling, A.C. (1993). Germline Stem Cell Division and Egg Chamber Development in Transplanted Drosophila Germaria. Dev. Biol. *159*, 140–152.

Lin, H., and Spradling, A.C. (1995). Fusome asymmetry and oocyte determination inDrosophila. Developmental Genetics *16*, 6–12.

Lindsay, L.L., Hertzler, P.L., and Clark, W.H. (1992). Extracellular Mg2+ induces an intracellular Ca2+ wave during oocyte activation in the marine shrimp Sicyonia ingentis. Dev. Biol. *152*, 94–102.

Liou, J., Kim, M.L., Heo, W.D., Jones, J.T., Myers, J.W., Ferrell, J.E., and Meyer, T. (2005). STIM is a Ca2+ sensor essential for Ca2+-store-depletion-triggered Ca2+ influx. Curr. Biol. *15*, 1235–1241.

Lippincott-Schwartz, J., Altan-Bonnet, N., and Patterson, G.H. (2003). Photobleaching and photoactivation: following protein dynamics in living cells. Nat. Cell Biol. *Suppl*, S7–S14.

Lipshitz, H.D. (2009). Follow the mRNA: a new model for Bicoid gradient formation. Nat. Rev. Mol. Cell Biol. *10*, 509–512.

Liu, G., Grant, W.M., Persky, D., Latham, V.M., Singer, R.H., and Condeelis, J. (2002). Interactions of elongation factor 1alpha with F-actin and beta-actin mRNA: implications for anchoring mRNA in cell protrusions. Mol. Biol. Cell *13*, 579–592.

Liu, L., Li, Y., Wang, R., Yin, C., Dong, Q., Hing, H., Kim, C., and Welsh, M.J. (2007). Drosophila hygrosensation requires the TRP channels water witch and nanchung. Nature 1973 244:5416 *450*, 294–298.

Liu, M. (2011). The biology and dynamics of mammalian cortical granules. Reproductive Biology and Endocrinology *9*, 149.

Lnenicka, G.A., Grizzaffi, J., Lee, B., and Rumpal, N. (2006). Ca2+ dynamics along identified synaptic terminals in Drosophila larvae. J. Neurosci. *26*, 12283–12293.

Loitto, V.M., Karlsson, T., and Magnusson, K.-E. (2009). Water flux in cell motility: expanding the mechanisms of membrane protrusion. Cell Motil. Cytoskeleton *66*, 237–247.

Longo, F.J., Woerner, M., Chiba, K., and Hoshi, M. (1995). Cortical changes in starfish (Asterina pectinifera) oocytes during 1-methyladenine-induced maturation and fertilisation/activation. Zygote *3*, 225–239.

Loppin, B., Dubruille, R., and Horard, B. (2015). The intimate genetics of Drosophila fertilization. Open Biol *5*, 150076.

Lorca, T., Cruzalegui, F.H., Fesquet, D., Cavadore, J.C., Méry, J., Means, A., and Dorée, M. (1993). Calmodulin-dependent protein kinase II mediates inactivation of MPF and CSF upon fertilization of Xenopus eggs. Nature 1973 244:5416 *366*, 270–273.

Lye, C.M., Naylor, H.W., and Sanson, B. (2014). Subcellular localisations of the CPTI collection of YFP-tagged proteins in Drosophila embryos. Development *141*, 4006–4017.

Lytton, J., Westlin, M., and Hanley, M.R. (1991). Thapsigargin inhibits the sarcoplasmic or endoplasmic reticulum Ca-ATPase family of calcium pumps. J. Biol. Chem. *266*, 17067–17071.

Ma, H., Li, B., and Tsien, R.W. (2015). Distinct roles of multiple isoforms of CaMKII in signaling to the nucleus. Biochimica Et Biophysica Acta (BBA) - Molecular Cell Research *1853*, 1953–1957.

Ma, T., Song, Y., Gillespie, A., Carlson, E.J., Epstein, C.J., and Verkman, A.S. (1999). Defective secretion of saliva in transgenic mice lacking aquaporin-5 water channels. J. Biol. Chem. *274*, 20071–20074.

Macháty, Z., Ramsoondar, J.J., Bonk, A.J., Bondioli, K.R., and Prather, R.S. (2002). Capacitative calcium entry mechanism in porcine oocytes. Biology of Reproduction *66*, 667–674.

Macháty, Z., Wang, C., Lee, K., and Zhang, L. (2017). Fertility: Store-Operated Ca2+ Entry in Germ Cells: Role in Egg Activation. Adv. Exp. Med. Biol. *993*, 577–593.

Machesky, L.M., Atkinson, S.J., Ampe, C., Vandekerckhove, J., and Pollard, T.D. (1994). Purification of a cortical complex containing two unconventional actins from Acanthamoeba by affinity chromatography on profilin-agarose. J. Cell Biol. *127*, 107–115.

MacLean-Fletcher, S., and Pollard, T.D. (1980). Identification of a factor in conventional muscle actin preparations which inhibits actin filament self-association. Biochem. Biophys. Res. Commun. *96*, 18–27.

MacLeod, R.J., and Hamilton, J.R. (1999). Increases in intracellular pH and Ca(2+) are essential for K(+) channel activation after modest "physiological" swelling in villus epithelial cells. J. Membr. Biol. *172*, 47–58.

Maeda, N., Niinobe, M., Nakahira, K., and Mikoshiba, K. (1988). Purification and characterization of P400 protein, a glycoprotein characteristic of Purkinje cell, from mouse cerebellum. J. Neurochem. *51*, 1724–1730.

Magni, F., Sarto, C., Ticozzi, D., Soldi, M., Bosso, N., Mocarelli, P., and Kienle, M.G. (2006). Proteomic knowledge of human aquaporins. Proteomics *6*, 5637–5649.

Mahowald, A.P., Goralski, T.J., and Caulton, J.H. (1983). In vitro activation of Drosophila eggs. Dev. Biol. *98*, 437–445.

Malcuit, C., Kurokawa, M., and Fissore, R.A. (2006). Calcium oscillations and mammalian egg activation. J. Cell. Physiol. *206*, 565–573.

Margaritis, L.H. (1985). The egg-shell of Drosophila melanogaster III. Covalent crosslinking of the chorion proteins involves endogenous hydrogen peroxide. Tissue Cell *17*, 553–559.

Margaritis, L.H., Kafatos, F.C., and Petri, W.H. (1980). The eggshell of Drosophila melanogaster. I. Fine structure of the layers and regions of the wild-type eggshell. J. Cell. Sci. *43*, 1–35.

Markoulaki, S., Matson, S., and Ducibella, T. (2004). Fertilization stimulates long-lasting oscillations of CaMKII activity in mouse eggs. Dev. Biol. *272*, 15–25.

Martin, K.C., and Ephrussi, A. (2009). mRNA localization: gene expression in the spatial dimension. Cell *136*, 719–730.

Maruoka, N.D., Steele, D.F., Au, B.P., Dan, P., Zhang, X., Moore, E.D., and Fedida, D. (2000). alpha-actinin-2 couples to cardiac Kv1.5 channels, regulating current density and channel localization in HEK cells. FEBS Lett. *473*, 188–194.

Maruyama, R., Velarde, N.V., Klancer, R., Gordon, S., Kadandale, P., Parry, J.M., Hang, J.S., Rubin, J., Stewart-Michaelis, A., Schweinsberg, P., et al. (2007). EGG-3 regulates cell-surface and cortex rearrangements during egg activation in Caenorhabditis elegans. Curr. Biol. *17*, 1555–1560.

Mazzochi, C., Benos, D.J., and Smith, P.R. (2006). Interaction of epithelial ion channels with the actin-based cytoskeleton. Am. J. Physiol. Renal Physiol. *291*, F1113–F1122.

McAvey, B.A., Wortzman, G.B., Williams, C.J., and Evans, J.P. (2002). Involvement of calcium signaling and the actin cytoskeleton in the membrane block to polyspermy in mouse eggs. Biology of Reproduction *67*, 1342–1352.

McCall, K. (2004). Eggs over easy: cell death in the Drosophila ovary. Dev. Biol. *274*, 3–14.

Medioni, C., Mowry, K., and Besse, F. (2012). Principles and roles of mRNA localization in animal development. Development *139*, 3263–3276.

Mehlmann, L.M., and Jaffe, L.A. (2005). SH2 domain-mediated activation of an SRC family kinase is not required to initiate Ca2+ release at fertilization in mouse eggs. Reproduction *129*, 557–564.

Mehlmann, L.M., Carpenter, G., Rhee, S.G., and Jaffe, L.A. (1998). SH2 Domain-Mediated Activation of Phospholipase Cγ Is Not Required to Initiate Ca2+Release at Fertilization of Mouse Eggs. Dev. Biol. *203*, 221–232.

Meldolesi, J., and Pozzan, T. (1998). The endoplasmic reticulum Ca2+ store: a view from the lumen. Trends Biochem. Sci. *23*, 10–14.

Melom, J.E., and Littleton, J.T. (2013). Mutation of a NCKX eliminates glial microdomain calcium oscillations and enhances seizure susceptibility. J. Neurosci. *33*, 1169–1178.

Mercer, J.C., Dehaven, W.I., Smyth, J.T., Wedel, B., Boyles, R.R., Bird, G.S., and Putney, J.W. (2006). Large store-operated calcium selective currents due to co-expression of Orai1 or Orai2 with the intracellular calcium sensor, Stim1. J. Biol. Chem. *281*, 24979–24990.

Methfessel, C., Witzemann, V., Takahashi, T., Mishina, M., Numa, S., and Sakmann, B. (1986). Patch clamp measurements on Xenopus laevis oocytes: currents through endogenous channels and implanted acetylcholine receptor and sodium channels. Pflugers Arch. *407*, 577–588.

Micklem, D.R., Adams, J., Grünert, S., and St Johnston, D. (2000). Distinct roles of two conserved Staufen domains in oskar mRNA localization and translation. Embo J. *19*, 1366–1377.

Mikl, M., Vendra, G., and Kiebler, M.A. (2011). Independent localization of MAP2, CaMKIIα and β-actin RNAs in low copy numbers. EMBO Rep. *12*, 1077–1084.

Mili, S., Moissoglu, K., and Macara, I.G. (2008). Genome-wide screen reveals APC-associated RNAs enriched in cell protrusions. Nature 1973 244:5416 *453*, 115–119.

Mindrinos, M.N., Petri, W.H., Galanopoulos, V.K., Lombard, M.F., and Margaritis, L.H. (1980). Crosslinking of theDrosophila chorion involves a peroxidase. Wilhelm Roux' Archiv *189*, 187–196.

Mingle, L.A. (2005). Localization of all seven messenger RNAs for the actin-polymerization nucleator Arp2/3 complex in the protrusions of fibroblasts. J. Cell. Sci. *118*, 2425–2433.

Mingle, L.A., Bonamy, G., Barroso, M., Liao, G., and Liu, G. (2009). LPA-induced mutually exclusive subcellular localization of active RhoA and Arp2 mRNA revealed by sequential FRET and FISH. Histochemistry and Cell Biology *132*, 47–58.

Mintz, I.M., Adams, M.E., and Bean, B.P. (1992). P-type calcium channels in rat central and peripheral neurons. Neuron *9*, 85–95.

Missiaen, L., Van Acker, K., Van Baelen, K., Raeymaekers, L., Wuytack, F., Parys, J.B., De Smedt, H., Vanoevelen, J., Dode, L., Rizzuto, R., et al. (2004). Calcium release from the Golgi apparatus and the endoplasmic reticulum in HeLa cells stably expressing targeted aequorin to these compartments. Cell Calcium *36*, 479–487.

Miyazaki, S. (1988). Inositol 1,4,5-trisphosphate-induced calcium release and guanine nucleotide-binding protein-mediated periodic calcium rises in golden hamster eggs. J. Cell Biol. *106*, 345–353.

Miyazaki, S. (1995). Calcium signalling during mammalian fertilization. Ciba Found. Symp. *188*, 235–47–discussion247–51.

Miyazaki, S., Hashimoto, N., Yoshimoto, Y., Kishimoto, T., Igusa, Y., and Hiramoto, Y. (1986). Temporal and spatial dynamics of the periodic

increase in intracellular free calcium at fertilization of golden hamster eggs. Dev. Biol. *118*, 259–267.

Miyazaki, S., Shirakawa, H., Nakada, K., Honda, Y., Yuzaki, M., Nakade, S., and Mikoshiba, K. (1992). Antibody to the inositol trisphosphate receptor blocks thimerosal-enhanced Ca(2+)-induced Ca2+ release and Ca2+ oscillations in hamster eggs. FEBS Lett. *309*, 180–184.

Moccia, F., Zuccolo, E., Soda, T., Tanzi, F., Guerra, G., Mapelli, L., Lodola, F., and D'Angelo, E. (2015). Stim and Orai proteins in neuronal Ca2+ signaling and excitability. Frontiers in Cellular Neuroscience *9*.

Mochida, S., and Hunt, T. (2007). Calcineurin is required to release Xenopus egg extracts from meiotic M phase. Nature 1973 244:5416 *449*, 336–340.

Montell, C. (2001). Physiology, phylogeny, and functions of the TRP superfamily of cation channels. Sci. STKE *2001*, re1–re1.

Montell, C., Jones, K., Hafen, E., and Rubin, G. (1985). Rescue of the Drosophila phototransduction mutation trp by germline transformation. Science *230*, 1040–1043.

Montell, C. (2005). Drosophila TRP channels. Pflugers Arch. *451*, 19–28.

Montell, C., Birnbaumer, L., Flockerzi, V., Bindels, R.J., Bruford, E.A., Caterina, M.J., Clapham, D.E., Harteneck, C., Heller, S., Julius, D., et al. (2002). A unified nomenclature for the superfamily of TRP cation channels. Mol. Cell *9*, 229–231.

Montell, D.J., Rorth, P., and Spradling, A.C. (1992). slow border cells, a locus required for a developmentally regulated cell migration during oogenesis, encodes Drosophila C/EBP. Cell *71*, 51–62.

Montell, D.J., Yoon, W.H., and Starz-Gaiano, M. (2012). Group choreography: mechanisms orchestrating the collective movement of border cells. Nat. Rev. Mol. Cell Biol. *13*, 631–645.

Moore, J.D., Kirk, J.A., and Hunt, T. (2003). Unmasking the S-phase-promoting potential of cyclin B1. Science *300*, 987–990.

Moreira, S., Stramer, B., Evans, I., Wood, W., and Martin, P. (2010). Prioritization of competing damage and developmental signals by migrating macrophages in the Drosophila embryo. Curr. Biol. *20*, 464–470.

Muallem, S., Kwiatkowska, K., Xu, X., and Yin, H.L. (1995). Actin filament disassembly is a sufficient final trigger for exocytosis in nonexcitable cells. J. Cell Biol. *128*, 589–598.

Mullins, R.D., Heuser, J.A., and Pollard, T.D. (1998). The interaction of Arp2/3 complex with actin: nucleation, high affinity pointed end capping, and formation of branching networks of filaments. Proc. Natl. Acad. Sci. U.S.a. *95*, 6181–6186.

Mullins, R.D., Stafford, W.F., and Pollard, T.D. (1997). Structure, subunit topology, and actin-binding activity of the Arp2/3 complex from Acanthamoeba. J. Cell Biol. *136*, 331–343.

Murnane, J.M., De Felice, L.J., Cohen, J. (1988). Development of iconic currents in mouse oocyte. J Cell Biol., 107, 4664.

Mus, E., Hof, P.R., and Tiedge, H. (2007). Dendritic BC200 RNA in aging and in Alzheimer's disease. Proc. Natl. Acad. Sci. U.S.a. *104*, 10679–10684.

Muto, A., Kume, S., Inoue, T., Okano, H., and Mikoshiba, K. (1996). Calcium waves along the cleavage furrows in cleavage-stage Xenopus embryos and its inhibition by heparin. J. Cell Biol. *135*, 181–190.

NAKADA, K., MIZUNO, J., SHIRAISHI, K., ENDO, K., and MIYAZAKI, S. (1995). Initiation, Persistence, and Cessation of the Series of Intracellular Ca2+ Responses during Fertilization of Bovine Eggs. Journal of Reproduction and Development *41*, 77–84.

Nakai, J., Ohkura, M., and Imoto, K. (2001). A high signal-to-noise Ca(2+) probe composed of a single green fluorescent protein. Nat. Biotechnol. *19*, 137–141.

Nakamura, A., Amikura, R., Hanyu, K., and Kobayashi, S. (2001). Me31B silences translation of oocyte-localizing RNAs through the formation of cytoplasmic RNP complex during Drosophila oogenesis. Development *128*, 3233–3242.

Nakamura, A., Sato, K., and Hanyu-Nakamura, K. (2004). Drosophila Cup Is an eIF4E Binding Protein that Associates with Bruno and Regulates oskar mRNA Translation in Oogenesis. Dev. Cell *6*, 69–78.

Neuman-Silberberg, F.S., and Schüpbach, T. (1993). The Drosophila dorsoventral patterning gene gurken produces a dorsally localized RNA and encodes a TGF alpha-like protein. Cell *75*, 165–174.

Niggli, V. (2014). Insights into the mechanism for dictating polarity in migrating T-cells. Int Rev Cell Mol Biol *312*, 201–270.

Nomikos, M., Elgmati, K., Theodoridou, M., Georgilis, A., Gonzalez-Garcia, J.R., Nounesis, G., Swann, K., and Lai, F.A. (2011). Novel regulation of PLCζ activity via its XY-linker. Biochem. J. *438*, 427–432.

Nomikos, M., Sanders, J.R., Parthimos, D., Buntwal, L., Calver, B.L., Stamatiadis, P., Smith, A., Clue, M., Sideratou, Z., Swann, K., et al. (2015). Essential Role of the EF-hand Domain in Targeting Sperm Phospholipase Cζ to Membrane Phosphatidylinositol 4,5-Bisphosphate (PIP2). J. Biol. Chem. *290*, 29519–29530.

Nomikos, M., Yu, Y., Elgmati, K., Theodoridou, M., Campbell, K., Vassilakopoulou, V., Zikos, C., Livaniou, E., Amso, N., Nounesis, G., et al. (2013). Phospholipase Cζ rescues failed oocyte activation in a prototype of male factor infertility. Fertil. Steril. *99*, 76–85.

O'Connor, E.R., and Kimelberg, H.K. (1993). Role of calcium in astrocyte volume regulation and in the release of ions and amino acids. J. Neurosci. *13*, 2638–2650.

Oda, S., Tomioka, M., and Iino, Y. (2011). Neuronal plasticity regulated by the insulin-like signaling pathway underlies salt chemotaxis learning in Caenorhabditis elegans. J. Neurophysiol. *106*, 301–308.

Page, A.W., and Orr-Weaver, T.L. (1997). Activation of the meiotic divisions in Drosophila oocytes. Dev. Biol. *183*, 195–207.

Page, S.L., and Hawley, R.S. (2001). c(3)G encodes a Drosophila synaptonemal complex protein. Genes Dev. *15*, 3130–3143.

Papadopoulos, M.C., Saadoun, S., and Verkman, A.S. (2008). Aquaporins and cell migration. Pflugers Arch. *456*, 693–700.

Papakonstanti, E.A., and Stournaras, C. (2007). Actin cytoskeleton architecture and signaling in osmosensing. Meth. Enzymol. *428*, 227–240.

Parton, R.M., Davidson, A., Davis, I., and Weil, T.T. (2014). Subcellular mRNA localisation at a glance. J. Cell. Sci. *127*, 2127–2133.

Parys, J.B., McPherson, S.M., Mathews, L., Campbell, K.P., and Longo, F.J. (1994). Presence of inositol 1,4,5-trisphosphate receptor, calreticulin, and calsequestrin in eggs of sea urchins and Xenopus laevis. Dev. Biol. *161*, 466–476.

Pavlov, D., Muhlrad, A., Cooper, J., Wear, M., and Reisler, E. (2007). Actin filament severing by cofilin. J. Mol. Biol. *365*, 1350–1358.

Peinelt, C., Vig, M., Koomoa, D.L., Beck, A., Nadler, M.J.S., Koblan-Huberson, M., Lis, A., Fleig, A., Penner, R., and Kinet, J.-P. (2006). Amplification of CRAC current by STIM1 and CRACM1 (Orai1). Nat. Cell Biol. *8*, 771–773.

Pelletán, L.E., Suhaiman, L., Vaquer, C.C., Bustos, M.A., De Blas, G.A., Vitale, N., Mayorga, L.S., and Belmonte, S.A. (2015). ADP ribosylation factor 6 (ARF6) promotes acrosomal exocytosis by modulating lipid turnover and Rab3A activation. J. Biol. Chem. *290*, 9823–9841.

Pepperell, J.R., Kommineni, K., Buradagunta, S., Smith, P.J., and Keefe, D.L. (1999). Transmembrane regulation of intracellular calcium by a plasma membrane sodium/calcium exchanger in mouse ova. Biology of Reproduction *60*, 1137–1143.

Peri, F., Bökel, C., and Roth, S. (1999). Local Gurken signaling and dynamic MAPK activation during Drosophila oogenesis. Mech. Dev. *81*, 75–88.

Pesin, J.A., and Orr-Weaver, T.L. (2007). Developmental role and regulation of cortex, a meiosis-specific anaphase-promoting complex/cyclosome activator. PLoS Genet. *3*, e202.

Peterson, J.S., and McCall, K. (2013). Combined Inhibition of Autophagy and Caspases Fails to Prevent Developmental Nurse Cell Death in the Drosophila melanogaster Ovary. PLoS ONE *8*, e76046.

Philipson, K.D. (2002). Na(+)-Ca(2+) exchange: three new tools. Circ. Res. *90*, 118–119.

Pinton, P., Pozzan, T., and Rizzuto, R. (1998). The Golgi apparatus is an inositol 1,4,5-trisphosphate-sensitive Ca2+ store, with functional properties distinct from those of the endoplasmic reticulum. Embo J. *17*, 5298–5308.

Pizzo, P., Lissandron, V., Capitanio, P., and Pozzan, T. (2011). Ca(2+) signalling in the Golgi apparatus. Cell Calcium *50*, 184–192.

Pollard, T.D. (1983). Measurement of rate constants for actin filament elongation in solution. Anal. Biochem. *134*, 406–412.

Pollard, T.D., Blanchoin, L., and Mullins, R.D. (2000). Molecular mechanisms controlling actin filament dynamics in nonmuscle cells. Annu Rev Biophys Biomol Struct *29*, 545–576.

Pollitt, A.Y., and Insall, R.H. (2009). WASP and SCAR/WAVE proteins: the drivers of actin assembly. J. Cell. Sci. *122*, 2575–2578.

Prager-Khoutorsky, M., and Spira, M.E. (2009). Neurite retraction and regrowth regulated by membrane retrieval, membrane supply, and actin dynamics. Brain Research *1251*, 65–79.

Puppo, A., Chun, J.T., Gragnaniello, G., Garante, E., and Santella, L. (2008). Alteration of the cortical actin cytoskeleton deregulates Ca2+ signaling, monospermic fertilization, and sperm entry. PLoS ONE *3*, e3588.

Putney, J.W. (1999). TRP, inositol 1,4,5-trisphosphate receptors, and capacitative calcium entry. Proc. Natl. Acad. Sci. U.S.a. *96*, 14669–14671.

Ramsey, I.S., Delling, M., and Clapham, D.E. (2006). An introduction to TRP channels. Annu. Rev. Physiol. *68*, 619–647.

Randall, A., and Tsien, R.W. (1995). Pharmacological dissection of multiple types of Ca2+ channel currents in rat cerebellar granule neurons. J. Neurosci. *15*, 2995–3012.

Ratheesh, A., Belyaeva, V., and Siekhaus, D.E. (2015). Drosophila immune cell migration and adhesion during embryonic development and larval immune responses. Curr. Opin. Cell Biol. *36*, 71–79.

Rauzi, M., Lenne, P.-F., and Lecuit, T. (2010). Planar polarized actomyosin contractile flows control epithelial junction remodelling. Nature 1973 244:5416 *468*, 1110–1114.

Razzell, W., Evans, I.R., Martin, P., and Wood, W. (2013). Calcium flashes orchestrate the wound inflammatory response through DUOX activation and hydrogen peroxide release. Curr. Biol. *23*, 424–429.

Resnick, T.D., Dej, K.J., Xiang, Y., Hawley, R.S., Ahn, C., and Orr-Weaver, T.L. (2009). Mutations in the chromosomal passenger complex and the condensin complex differentially affect synaptonemal complex disassembly and metaphase I configuration in Drosophila female meiosis. Genetics *181*, 875–887.

Riedl, J., Crevenna, A.H., Kessenbrock, K., Yu, J.H., Neukirchen, D., Bista, M., Bradke, F., Jenne, D., Holak, T.A., Werb, Z., et al. (2008). Lifeact: a versatile marker to visualize F-actin. Nat. Methods *5*, 605–607.

Robinson, D.H., Bubien, J.K., Smith, P.R., and Benos, D.J. (1991). Epithelial sodium conductance in rabbit preimplantation trophectodermal cells. Dev. Biol. *147*, 313–321.

Rogers, N.T., Hobson, E., Pickering, S., Lai, F.A., Braude, P., and Swann, K. (2004). Phospholipase Czeta causes Ca2+ oscillations and parthenogenetic activation of human oocytes. Reproduction *128*, 697–702.

Rongo, C., Gavis, E.R., and Lehmann, R. (1995). Localization of oskar RNA regulates oskar translation and requires Oskar protein. Development *121*, 2737–2746.

Roos, J., DiGregorio, P.J., Yeromin, A.V., Ohlsen, K., Lioudyno, M., Zhang, S., Safrina, O., Kozak, J.A., Wagner, S.L., Cahalan, M.D., et al. (2005). STIM1, an essential and conserved component of store-operated Ca2+ channel function. J. Cell Biol. *169*, 435–445.

Ross, P.J., Rodriguez, R.M., Iager, A.E., Beyhan, Z., Wang, K., Ragina, N.P., Yoon, S.-Y., Fissore, R.A., and Cibelli, J.B. (2009). Activation of bovine somatic cell nuclear transfer embryos by PLCZ cRNA injection. Reproduction *137*, 427–437.

Runft, L.L., Watras, J., and Jaffe, L.A. (1999). Calcium release at fertilization of Xenopus eggs requires type I IP(3) receptors, but not SH2 domain-mediated activation of PLCgamma or G(q)-mediated activation of PLCbeta. Dev. Biol. *214*, 399–411.

Runft, L.L., Carroll, D.J., Gillett, J., Giusti, A.F., O'Neill, F.J., and Foltz, K.R. (2004). Identification of a starfish egg PLC-gamma that regulates Ca2+ release at fertilization. Dev. Biol. *269*, 220–236.

Runft, L.L., Jaffe, L.A., and Mehlmann, L.M. (2002). Egg activation at fertilization: where it all begins. Dev. Biol. *245*, 237–254.

Russo, G.L., Kyozuka, K., Antonazzo, L., Tosti, E., and Dale, B. (1996). Maturation promoting factor in ascidian oocytes is regulated by different intracellular signals at meiosis I and II. Development *122*, 1995–2003.

Ruth, P., Röhrkasten, A., Biel, M., Bosse, E., Regulla, S., Meyer, H.E., Flockerzi, V., and Hofmann, F. (1989). Primary structure of the beta subunit of the DHP-sensitive calcium channel from skeletal muscle. Science *245*, 1115–1118.

Saadoun, S., Papadopoulos, M.C., Hara-Chikuma, M., and Verkman, A.S. (2005). Impairment of angiogenesis and cell migration by targeted aquaporin-1 gene disruption. Nature 1973 244:5416 *434*, 786–792.

SACHS, F., SIGURDSON, W., RUKNUDIN, A., and BOWMAN, C. (1991). Single-Channel Mechanosensitive Currents. Science 800–801.

Santella, L., De Riso, L., Gragnaniello, G., and Kyozuka, K. (1999). Cortical granule translocation during maturation of starfish oocytes requires cytoskeletal rearrangement triggered by InsP3-mediated Ca2+ release. Exp. Cell Res. *248*, 567–574.

Sanyal, S., Jennings, T., Dowse, H., and Ramaswami, M. (2006). Conditional mutations in SERCA, the Sarco-endoplasmic reticulum Ca2+-ATPase, alter heart rate and rhythmicity in Drosophila. J. Comp. Physiol. B, Biochem. Syst. Environ. Physiol. *176*, 253–263.

Sartain, C.V., and Wolfner, M.F. (2013). Calcium and egg activation in Drosophila. Cell Calcium *53*, 10–15.

Sasaki, K., and Obara, Y. (2002). Egg activation and timing of sperm acceptance by an egg in honeybees (Apis mellifera L.). Insectes Sociaux *49*, 234–240.

Satoh, Y., Sato, H., Kunitomo, H., Fei, X., Hashimoto, K., and Iino, Y. (2014). Regulation of experience-dependent bidirectional chemotaxis by a neural circuit switch in Caenorhabditis elegans. J. Neurosci. *34*, 15631–15637.

Sauer, H., Ritgen, J., Hescheler, J., and Wartenberg, M. (1998). Hypotonic Ca2+ signaling and volume regulation in proliferating and quiescent cells from multicellular spheroids. J. Cell. Physiol. *175*, 129–140.

Saunders, C.M., Larman, M.G., Parrington, J., Cox, L.J., Royse, J., Blayney, L.M., Swann, K., and Lai, F.A. (2002). PLC zeta: a sperm-specific trigger of Ca(2+) oscillations in eggs and embryo development. Development *129*, 3533–3544.

Saxton, W.M. (2001). Microtubules, motors, and mRNA localization mechanisms: watching fluorescent messages move. Cell *107*, 707–710.

Schatten, G., and Hülser, D. (1983). Timing the early events during sea urchin fertilization. Dev. Biol. *100*, 244–248.

Schell, M.J., Erneux, C., and Irvine, R.F. (2001). Inositol 1,4,5-trisphosphate 3-kinase A associates with F-actin and dendritic spines via its N terminus. J. Biol. Chem. *276*, 37537–37546.

Schnermann, J., Chou, C.L., Ma, T., Traynor, T., Knepper, M.A., and Verkman, A.S. (1998). Defective proximal tubular fluid reabsorption in transgenic aquaporin-1 null mice. Proc. Natl. Acad. Sci. U.S.a. *95*, 9660–9664.

SCHUEL, H. (1985). Functions of Egg Cortical Granules. In Biology of Fertilization, (Elsevier), pp. 1–43.

Sears, H.C., Kennedy, C.J., and Garrity, P.A. (2003). Macrophage-mediated corpse engulfment is required for normal Drosophila CNS morphogenesis. Development *130*, 3557–3565.

Semotok, J.L., Cooperstock, R.L., Pinder, B.D., Vari, H.K., Lipshitz, H.D., and Smibert, C.A. (2005). Smaug recruits the CCR4/POP2/NOT deadenylase complex to trigger maternal transcript localization in the early Drosophila embryo. Curr. Biol. *15*, 284–294.

Sengupta, S., Barber, T.R., Xia, H., Ready, D.F., and Hardie, R.C. (2013). Depletion of PtdIns(4,5)P$_2$ underlies retinal degeneration in Drosophila trp mutants. J. Cell. Sci. *126*, 1247–1259.

SHAPIRO, B.M., SOMERS, C.E., and WEIDMAN, P.J. (1989). Extracellular Remodeling during Fertilization. In The Cell Biology of Fertilization, (Elsevier), pp. 251–276.

Sharif Naeini, R., Witty, M.-F., Séguéla, P., and Bourque, C.W. (2006). An N-terminal variant of Trpv1 channel is required for osmosensory transduction. Nat. Neurosci. *9*, 93–98.

Shearer, J., De Nadai, C., Emily-Fenouil, F., Gache, C., Whitaker, M., and Ciapa, B. (1999). Role of phospholipase Cgamma at fertilization and during mitosis in sea urchin eggs and embryos. Development *126*, 2273–2284.

Shen, M.R., Chou, C.Y., Browning, J.A., Wilkins, R.J., and Ellory, J.C. (2001). Human cervical cancer cells use Ca2+ signalling, protein tyrosine phosphorylation and MAP kinase in regulatory volume decrease. J. Physiol. (Lond.) *537*, 347–362.

Shin, J.-B., Adams, D., Paukert, M., Siba, M., Sidi, S., Levin, M., Gillespie, P.G., and Gründer, S. (2005). Xenopus TRPN1 (NOMPC) localizes to microtubule-based cilia in epithelial cells, including inner-ear hair cells. Proc. Natl. Acad. Sci. U.S.a. *102*, 12572–12577.

Sokabe, M., SACHS, F., and Jing, Z.Q. (1991). Quantitative video microscopy of patch clamped membranes stress, strain, capacitance, and stretch channel activation. Biophysical Journal *59*, 722–728.

Spirov, A., Fahmy, K., Schneider, M., Frei, E., Noll, M., and Baumgartner, S. (2009). Formation of the bicoid morphogen gradient: an mRNA gradient dictates the protein gradient. Development *136*, 605–614.

Spracklen, A.J., Fagan, T.N., Lovander, K.E., and Tootle, T.L. (2014a). The pros and cons of common actin labeling tools for visualizing actin dynamics during Drosophila oogenesis. Dev. Biol. *393*, 209–226.

Spracklen, A.J., Kelpsch, D.J., Chen, X., Spracklen, C.N., and Tootle, T.L. (2014b). Prostaglandins temporally regulate cytoplasmic actin bundle formation during Drosophila oogenesis. Mol. Biol. Cell *25*, 397–411.

Spudich, A. (1979). Actin in triton-treated cortical preparations of unfertilized and fertilized sea urchin eggs. J. Cell Biol. *82*, 212–226.

St Johnston, D., Driever, W., Berleth, T., Richstein, S., Nusslein-Volhard, C. (1989). Multi steps in the localisation of bicoid to the anterior pole of the Drosophila oocyte. Dev. 107: 13-19.

Stauffer, T.P., Guerini, D., and Carafoli, E. (1995). Tissue distribution of the four gene products of the plasma membrane Ca2+ pump. A study using specific antibodies. J. Biol. Chem. *270*, 12184–12190.

Stein, D., and Nüsslein-Volhard, C. (1992). Multiple extracellular activities in Drosophila egg perivitelline fluid are required for establishment of embryonic dorsal-ventral polarity. Cell *68*, 429–440.

Stice, S.L., and Robl, J.M. (1990). Activation of mammalian oocytes by a factor obtained from rabbit sperm. Mol. Reprod. Dev. *25*, 272–280.

Stramer, B., Wood, W., Galko, M.J., Redd, M.J., Jacinto, A., Parkhurst, S.M., and Martin, P. (2005). Live imaging of wound inflammation in Drosophila embryos reveals key roles for small GTPases during in vivo cell migration. J. Cell Biol. *168*, 567–573.

Strehler, E.E., and Zacharias, D.A. (2001). Role of alternative splicing in generating isoform diversity among plasma membrane calcium pumps. Physiological Reviews *81*, 21–50.

Strehler, E.E., and Treiman, M. (2004). Calcium pumps of plasma membrane and cell interior. Curr. Mol. Med. *4*, 323–335.

Stricker, S.A. (1996). Repetitive calcium waves induced by fertilization in the nemertean worm Cerebratulus lacteus. Dev. Biol. *176*, 243–263.

Stricker, S.A. (1999). Comparative biology of calcium signaling during fertilization and egg activation in animals. Dev. Biol. *211*, 157–176.

Strotmann, R., Harteneck, C., Nunnenmacher, K., Schultz, G., and Plant, T.D. (2000). OTRPC4, a nonselective cation channel that confers sensitivity to extracellular osmolarity. Nat. Cell Biol. *2*, 695–702.

Summers, R.G., and Hylander, B.L. (1975). Species-specificity of acrosome reaction and primary gamete binding in echinoids. Exp. Cell Res. *96*, 63–68.

Supattapone, S.,P.F. Worley, J.M. Baraban, and S.H.Snyder. (1988). Solubilization, purification, and characterisation of an inositol triphosphate. J. Biol. Chem. 263:1530-1534.

Surroca, A., and Wolff, D. (2000). Inositol 1,4,5-trisphosphate but not ryanodine-receptor agonists induces calcium release from rat liver Golgi apparatus membrane vesicles. J. Membr. Biol. *177*, 243–249.

Suzanne, M., Perrimon, N., and Noselli, S. (2001). The Drosophila JNK pathway controls the morphogenesis of the egg dorsal appendages and micropyle. Dev. Biol. *237*, 282–294.

Svitkina, T.M., and Borisy, G.G. (1999). Arp2/3 Complex and Actin Depolymerizing Factor/Cofilin in Dendritic Organization and Treadmilling of Actin Filament Array in Lamellipodia. J. Cell Biol. *145*, 1009–1026.

Swan, A., and Schüpbach, T. (2007). The Cdc20 (Fzy)/Cdh1-related protein, Cort, cooperates with Fzy in cyclin destruction and anaphase progression in meiosis I and II in Drosophila. Development *134*, 891–899.

Swann, K. (1990). A cytosolic sperm factor stimulates repetitive calcium increases and mimics fertilization in hamster eggs. Development *110*, 1295–1302.

Swann, K. (1996). Soluble sperm factors and Ca2+ release in eggs at fertilization. Rev. Reprod. *1*, 33–39.

Swann, K., and Whitaker, M. (1986). The part played by inositol trisphosphate and calcium in the propagation of the fertilization wave in sea urchin eggs. J. Cell Biol. *103*, 2333–2342.

Szent-Györgyi, A.G. (1975). Calcium regulation of muscle contraction. Biophysical Journal *15*, 707–723.

Tadros, W., and Lipshitz, H.D. (2005). Setting the stage for development: mRNA translation and stability during oocyte maturation and egg activation in Drosophila. Dev. Dyn. *232*, 593–608.

Tadros, W., Goldman, A.L., Babak, T., Menzies, F., Vardy, L., Orr-Weaver, T., Hughes, T.R., Westwood, J.T., Smibert, C.A., and Lipshitz, H.D. (2007). SMAUG is a major regulator of maternal mRNA destabilization in Drosophila and its translation is activated by the PAN GU kinase. Dev. Cell *12*, 143–155.

Tahara, M., Tasaka, K., Masumoto, N., Mammoto, A., Ikebuchi, Y., and Miyake, A. (1996). Dynamics of cortical granule exocytosis at fertilization in living mouse eggs. Am. J. Physiol. *270*, C1354–C1361.

Takahashi, M., and Catterall, W.A. (1987). Dihydropyridine-sensitive calcium channels in cardiac and skeletal muscle membranes: studies with antibodies against the alpha subunits. Biochemistry *26*, 5518–5526.

Takayama, J., and Onami, S. (2016). The Sperm TRP-3 Channel Mediates the Onset of a Ca 2+ Wave in the Fertilized C. elegans Oocyte. Cell Reports *15*, 625–637.

Takeo, S., Tsuda, M., Akahori, S., Matsuo, T., and Aigaki, T. (2006). The calcineurin regulator sra plays an essential role in female meiosis in Drosophila. Curr. Biol. *16*, 1435–1440.

Tatone, C., Delle Monache, S., Iorio, R., Caserta, D., Di Cola, M., and Colonna, R. (2002). Possible role for Ca(2+) calmodulin-dependent protein kinase II as an effector of the fertilization Ca(2+) signal in mouse oocyte activation. Mol. Hum. Reprod. *8*, 750–757.

Taylor, A.R., Manison, N., Fernandez, C., Wood, J., and Brownlee, C. (1996). Spatial Organization of Calcium Signaling Involved in Cell Volume Control in the Fucus Rhizoid. Plant Cell *8*, 2015–2031.

Taylor, C.W., Genazzani, A.A., and Morris, S.A. (1999). Expression of inositol trisphosphate receptors. Cell Calcium *26*, 237–251.

Taylor, C.W., and Tovey, S.C. (2010). IP(3) receptors: toward understanding their activation. Cold Spring Harb Perspect Biol *2*, a004010–a004010.

Taylor, C.W., da Fonseca, P.C.A., and Morris, E.P. (2004). IP(3) receptors: the search for structure. Trends Biochem. Sci. *29*, 210–219.

Tepass, U., Fessler, L.I., Aziz, A., and Hartenstein, V. (1994). Embryonic origin of hemocytes and their relationship to cell death in Drosophila. Development *120*, 1829–1837.

Terasaki, M. (1996). Actin filament translocations in sea urchin eggs. Cell Motil. Cytoskeleton *34*, 48–56.

Tesarik, J., Sousa, M., and Testart, J. (1994). Human oocyte activation after intracytoplasmic sperm injection. Human Reproduction *9*, 511–518.

Thomas, T.W., Eckberg, W.R., Dubé, F., and Galione, A. (1998). Mechanisms of calcium release and sequestration in eggs of Chaetopterus pergamentaceus. Cell Calcium *24*, 285–292.

Tilly, B.C., Edixhoven, M.J., Tertoolen, L.G., Morii, N., Saitoh, Y., Narumiya, S., and de Jonge, H.R. (1996). Activation of the osmo-sensitive chloride conductance involves P21rho and is accompanied by a transient reorganization of the F-actin cytoskeleton. Mol. Biol. Cell *7*, 1419–1427.

Tilney, L.G. (1980). Actin, microvilli, and the fertilization cone of sea urchin eggs. J. Cell Biol. *87*, 771–782.

Tojo, K., and Machida, R. (1998). Early embryonic development of the mayfly Ephemera japonica McLachlan (Insecta: Ephemeroptera, Ephemeridae). Journal of Morphology *238*, 327–335.

Tominaga, M., Kojima, H., Yokota, E., Nakamori, R., Anson, M., Shimmen, T., and Oiwa, K. (2012). Calcium-induced mechanical change

in the neck domain alters the activity of plant myosin XI. J. Biol. Chem. *287*, 30711–30718.

Tomkowiak, M., Guerrier, P., and Krantic, S. (1997). Meiosis reinitiation of mussel oocytes involves L-type voltage-gated calcium channel. Journal of Cellular Biochemistry *64*, 152–160.

Tracey, W.D., Wilson, R.I., Laurent, G., and Benzer, S. (2003). painless, a Drosophila gene essential for nociception. Cell *113*, 261–273.

Trcek, T., Grosch, M., York, A., Shroff, H., Lionnet, T., and Lehmann, R. (2015). Drosophila germ granules are structured and contain homotypic mRNA clusters. Nat Commun *6*, 7962.

Trifaró, J.M., Rodríguez Del Castillo, A., and Vitale, M.L. (1992). Dynamic changes in chromaffin cell cytoskeleton as prelude to exocytosis. Mol. Neurobiol. *6*, 339–358.

Tucker, W.C., and Chapman, E.R. (2002). Role of synaptotagmin in Ca2+-triggered exocytosis. Biochem. J. *366*, 1–13.

Turner, P.R., Jaffe, L.A., and Fein, A. (1986). Regulation of cortical vesicle exocytosis in sea urchin eggs by inositol 1,4,5-trisphosphate and GTP-binding protein. J. Cell Biol. *102*, 70–76.

Turner, P.R., Sheetz, M.P., and Jaffe, L.A. (1984). Fertilization increases the polyphosphoinositide content of sea urchin eggs. Nature 1973 244:5416 *310*, 414–415.

Turunen, O., Wahlström, T., and Vaheri, A. (1994). Ezrin has a COOH-terminal actin-binding site that is conserved in the ezrin protein family. J. Cell Biol. *126*, 1445–1453.

Van Baelen, K., Vanoevelen, J., Callewaert, G., Parys, J.B., De Smedt, H., Raeymaekers, L., Rizzuto, R., Missiaen, L., and Wuytack, F. (2003). The contribution of the SPCA1 Ca2+ pump to the Ca2+ accumulation in the Golgi apparatus of HeLa cells assessed via RNA-mediated interference. Biochem. Biophys. Res. Commun. *306*, 430–436.

van der Meer, J.M., and Jaffe, L.F. (1983). Elemental composition of the perivitelline fluid in early Drosophila embryos. Dev. Biol. *95*, 249–252.

Vanzo, N.F., and Ephrussi, A. (2002). Oskar anchoring restricts pole plasm formation to the posterior of the Drosophila oocyte. Development *129*, 3705–3714.

Vasilev, F., Chun, J.T., Gragnaniello, G., Garante, E., and Santella, L. (2012). Effects of ionomycin on egg activation and early development in starfish. PLoS ONE *7*, e39231.

Veksler, A., and Gov, N.S. (2009). Calcium-Actin Waves and Oscillations of Cellular Membranes. Biophysical Journal *97*, 1558–1568.

Venkatachalam, K., van Rossum, D.B., Patterson, R.L., Ma, H.-T., and Gill, D.L. (2002). The cellular and molecular basis of store-operated calcium entry. Nat. Cell Biol. *4*, E263–E272.

Verkman, A.S. (2011). Aquaporins at a glance. J. Cell. Sci. *124*, 2107–2112.

Verkman, A.S., Anderson, M.O., and Papadopoulos, M.C. (2014). Aquaporins: important but elusive drug targets. Nat Rev Drug Discov *13*, 259–277.

Vicente-Manzanares, M., Webb, D.J., and Horwitz, A.R. (2005). Cell migration at a glance. J. Cell. Sci. *118*, 4917–4919.

Vidali, L., and Hepler, P.K. (2001). Actin and pollen tube growth. Protoplasma *215*, 64–76.

Vignjevic, D., Yarar, D., Welch, M.D., Peloquin, J., Svitkina, T., and Borisy, G.G. (2003). Formation of filopodia-like bundles in vitro from a dendritic network. J. Cell Biol. *160*, 951–962.

Vitale, M.L., Rodríguez Del Castillo, A., Tchakarov, L., and Trifaró, J.M. (1991). Cortical filamentous actin disassembly and scinderin redistribution during chromaffin cell stimulation precede exocytosis, a phenomenon not exhibited by gelsolin. J. Cell Biol. *113*, 1057–1067.

Walsh, T.P., Weber, A., Davis, K., Bonder, E., and Mooseker, M. (1984). Calcium dependence of villin-induced actin depolymerization. Biochemistry *23*, 6099–6102.

Wang, G., Dayanithi, G., Newcomb, R., and Lemos, J.R. (1999). An R-type Ca(2+) current in neurohypophysial terminals preferentially regulates oxytocin secretion. J. Neurosci. *19*, 9235–9241.

Wang, P.-S., Chou, F.-S., Ramachandran, S., Xia, S., Chen, H.-Y., Guo, F., Suraneni, P., Maher, B.J., and Li, R. (2016). Crucial roles of the Arp2/3 complex during mammalian corticogenesis. Development *143*, 2741–2752.

Wang, S.S., Alousi, A.A., and Thompson, S.H. (1995). The lifetime of inositol 1,4,5-trisphosphate in single cells. J. Gen. Physiol. *105,* 149–171.

Wang, Y., and Riechmann, V. (2007). The Role of the Actomyosin Cytoskeleton in Coordination of Tissue Growth during Drosophila Oogenesis. Current Biology *17*, 1349–1355.

Ward, E.J., and Berg, C.A. (2005). Juxtaposition between two cell types is necessary for dorsal appendage tube formation. Mech. Dev. *122*, 241–255.

Waring, G.L. (2000). Morphogenesis of the eggshell in Drosophila. Int. Rev. Cytol. *198*, 67–108.

Wassarman, P., Chen, J., Cohen, N., Litscher, E., Liu, C., Qi, H., and Williams, Z. (1999). Structure and function of the mammalian egg zona pellucida. J. Exp. Zool. *285*, 251–258.

Watanabe, Y.,Yokota, H., K. and Hatakeyama, M. (1999) Artificial parthenogenesis in the dragonfly, *Stylurus oculatus* (Odonata). Proc Arthropod Embryol Soc Jpn 34, 31-32.

Weaver, A.M., Young, M.E., Lee, W.-L., and Cooper, J.A. (2003). Integration of signals to the Arp2/3 complex. Curr. Opin. Cell Biol. *15*, 23–30.

Weil, T.T. (2014). mRNA localization in the Drosophila germline. RNA Biol *11*, 1010–1018.

Weil, T.T., Forrest, K.M., and Gavis, E.R. (2006). Localization of bicoid mRNA in late oocytes is maintained by continual active transport. Dev. Cell *11*, 251–262.

Weil, T.T., Parton, R.M., and Davis, I. (2010a). Making the message clear: visualizing mRNA localization. Trends Cell Biol. *20*, 380–390.

Weil, T.T., Parton, R.M., Herpers, B., Soetaert, J., Veenendaal, T., Xanthakis, D., Dobbie, I.M., Halstead, J.M., Hayashi, R., Rabouille, C., et al. (2012). Drosophila patterning is established by differential association of mRNAs with P bodies. Nat. Cell Biol. *14*, 1305–1313.

Weil, T.T., Parton, R., Davis, I., and Gavis, E.R. (2008). Changes in bicoid mRNA anchoring highlight conserved mechanisms during the oocyte-to-embryo transition. Curr. Biol. *18*, 1055–1061.

Weil, T.T., Xanthakis, D., Parton, R., Dobbie, I., Rabouille, C., Gavis, E.R., and Davis, I. (2010b). Distinguishing direct from indirect roles for bicoid mRNA localization factors. Development *137*, 169–176.

Welsh, D.G., Morielli, A.D., Nelson, M.T., and Brayden, J.E. (2002). Transient receptor potential channels regulate myogenic tone of resistance arteries. Circ. Res. *90*, 248–250.

Went, D.F., and KRAUSE, G. (1973). Normal Development of Mechanically Activated, Unlaid Eggs of an Endo-parasitic Hymenopteran. Nature 1973 244:5416 *244*, 454–455.

Went, D.F., and KRAUSE, G. (1974). Alteration of egg architecture and egg activation in an endoparasitic Hymenopteran as a result of natural or imitated oviposition. W. Roux' Archiv F. Entwicklungsmechanik *175*, 173–184.

Went, D.F. (1982). EGG ACTIVATION AND PARTHENOGENETIC REPRODUCTION IN INSECTS. Biological Reviews *57*, 319–344.

Weskamp, M., Seidl, W., and Grissmer, S. (2000). Characterization of the increase in [Ca(2+)](i) during hypotonic shock and the involvement of Ca(2+)-activated K(+) channels in the regulatory volume decrease in human osteoblast-like cells. J. Membr. Biol. *178*, 11–20.

Whitaker, M. (2006). Calcium at Fertilization and in Early Development. Physiological Reviews *86*, 25–88.

Whitaker, M. (2008). Calcium signalling in early embryos. Philos. Trans. R. Soc. Lond., B, Biol. Sci. *363*, 1401–1418.

Whitaker, M., and Irvine, R.F. (1984). Inositol 1,4,5-trisphosphate microinjection activates sea urchin eggs. Nature 1973 244:5416 *312*, 636–639.

Wilding, M., and Dale, B. (1998). Soluble extracts from ascidian spermatozoa trigger intracellular calcium release independently of the activation of the ADP ribose channel. Zygote *6*, 149–154.

Wilkie, G.S., and Davis, I. (2001). Drosophila wingless and Pair-Rule Transcripts Localize Apically by Dynein-Mediated Transport of RNA Particles. Cell *105*, 209–219.

Willmott, N., Sethi, J.K., Walseth, T.F., Lee, H.C., White, A.M., and Galione, A. (1996). Nitric oxide-induced mobilization of intracellular calcium via the cyclic ADP-ribose signaling pathway. J. Biol. Chem. *271*, 3699–3705.

Wollman, R., and Meyer, T. (2012). Coordinated oscillations in cortical actin and Ca2+ correlate with cycles of vesicle secretion. Nat. Cell Biol. *14*, 1261–1269.

Wood, W., and Jacinto, A. (2007). Drosophila melanogaster embryonic haemocytes: masters of multitasking. Nat. Rev. Mol. Cell Biol. *8*, 542–551.

Wood, W., Faria, C., and Jacinto, A. (2006). Distinct mechanisms regulate hemocyte chemotaxis during development and wound healing in Drosophila melanogaster. J. Cell Biol. *173*, 405–416.

Woodrum, D.T., Rich, S.A., and Pollard, T.D. (1975). Evidence for biased bidirectional polymerization of actin filaments using heavy meromyosin prepared by an improved method. J. Cell Biol. *67*, 231–237.

Wu, M., Wu, X., and De Camilli, P. (2013). Calcium oscillations-coupled conversion of actin travelling waves to standing oscillations. Proc. Natl. Acad. Sci. U.S.a. *110*, 1339–1344.

Wu, X., Tanwar, P.S., and Raftery, L.A. (2008). Drosophila follicle cells: morphogenesis in an eggshell. Semin. Cell Dev. Biol. *19*, 271–282.

Wyrick, R.E., Nishihara, T., and Hedrick, J.L. (1974). Agglutination of jelly coat and cortical granule components and the block to polyspermy in the amphibian Xenopus laevis. Proc. Natl. Acad. Sci. U.S.a. *71*, 2067–2071.

Xiang, Y., Takeo, S., Florens, L., Hughes, S.E., Huo, L.-J., Gilliland, W.D., Swanson, S.K., Teeter, K., Schwartz, J.W., Washburn, M.P., et al. (2007). The inhibition of polo kinase by matrimony maintains G2 arrest in the meiotic cell cycle. PLoS Biol. *5*, e323.

Xu, Z., Kopf, G.S., and Schultz, R.M. (1994). Involvement of inositol 1,4,5-trisphosphate-mediated Ca2+ release in early and late events of mouse egg activation. Development *120*, 1851–1859.

Yamamoto, D.S., Hatakeyama, M., and Matsuoka, H. (2013). Artificial activation of mature unfertilized eggs in the malaria vector mosquito, Anopheles stephensi (Diptera, Culicidae). Journal of Experimental Biology *216*, 2960–2966.

Yang, Y., Liu, N., He, Y., Liu, Y., Ge, L., Zou, L., Song, S., Xiong, W., and Liu, X. (2018). Improved calcium sensor GCaMP-X overcomes the calcium channel perturbations induced by the calmodulin in GCaMP. Nat Commun *9*, 1504.

Yeromin, A.V., Zhang, S.L., Jiang, W., Yu, Y., Safrina, O., and Cahalan, M.D. (2006). Molecular identification of the CRAC channel by altered ion selectivity in a mutant of Orai. Nature 1973 244:5416 *443*, 226–229.

York-Andersen, A.H., Parton, R.M., Bi, C.J., Bromley, C.L., Davis, I., and Weil, T.T. (2015). A single and rapid calcium wave at egg activation in Drosophila. Biol Open *4*, 553–560.

Yoshida, M., Sensui, N., Inoue, T., Morisawa, M., and Mikoshiba, K. (1998). Role of two series of Ca2+ oscillations in activation of ascidian eggs. Dev. Biol. *203*, 122–133.

Yoshikawa, F., Morita, M., Monkawa, T., Michikawa, T., Furuichi, T., and Mikoshiba, K. (1996). Mutational analysis of the ligand binding site of the inositol 1,4,5-trisphosphate receptor. J. Biol. Chem. *271*, 18277–18284.

Yoshimoto, A., Nakanishi, K., Anzai, T., and Komine, S. (1990). Effects of inositol 1,4,5-trisphosphate on calcium release from the endoplasmic reticulum and Golgi apparatus in mouse mammary epithelial cells: a comparison during pregnancy and lactation. Cell Biochem. Funct. *8*, 191–198.

Yu, Y., Nomikos, M., Theodoridou, M., Nounesis, G., Lai, F.A., and Swann, K. (2012). PLCζ causes Ca(2+) oscillations in mouse eggs by targeting intracellular and not plasma membrane PI(4,5)P(2). Mol. Biol. Cell *23*, 371–380.

Zaessinger, S., Busseau, I., and Simonelig, M. (2006). Oskar allows nanos mRNA translation in Drosophila embryos by preventing its deadenylation by Smaug/CCR4. Development *133*, 4573–4583.

Zhang, S.L., Yeromin, A.V., Zhang, X.H.-F., Yu, Y., Safrina, O., Penna, A., Roos, J., Stauderman, K.A., and Cahalan, M.D. (2006). Genome-wide RNAi screen of Ca(2+) influx identifies genes that regulate Ca(2+) release-activated Ca(2+) channel activity. Proc. Natl. Acad. Sci. U.S.a. *103*, 9357–9362.

Zhang, Z., Kindrat, A.N., Sharif-Naeini, R., and Bourque, C.W. (2007). Actin Filaments Mediate Mechanical Gating during Osmosensory Transduction in Rat Supraoptic Nucleus Neurons. J. Neurosci. *27*, 4008–4013.

Zhao, T., Graham, O.S., Raposo, A., and St Johnston, D. (2012). Growing Microtubules Push the Oocyte Nucleus to Polarize the Drosophila Dorsal-Ventral Axis. Science *336*, 999–1003.

Zimyanin, V.L., Belaya, K., Pecreaux, J., Gilchrist, M.J., Clark, A., Davis, I., and St Johnston, D. (2008). In vivo imaging of oskar mRNA transport reveals the mechanism of posterior localization. Cell *134*, 843–853.

Zweifach, A., and Lewis, R.S. (1995). Slow calcium-dependent inactivation of depletion-activated calcium current. Store-dependent and -independent mechanisms. J. Biol. Chem. *270*, 14445–14451.

http://www.smasupportuk.org.uk/blog/research/plastin-3-is-a-potential-therapeutic-target-for-sma (Adapted for figure 4.1).

http://flyatlas.org/atlas.cgi (Drosophila Fly Atlas)

http://www.fruitfly.org/EST/gold_collection.shtml (Drosophila Gold Collection)

http://www.discoveryandinnovation.com/BIOL202/notes/lecture21.html (Adapted for figure 3.2).

https://fgr.hms.harvard.edu/fly-in-vivo-rnai (in vivo fly RNAi (TRiP))